AN INVESTIGATION OF THE BIOLOGY AND CHEMISTRY OF THE CHINESE MEDICINAL PLANT, *Amorphophallus konjac*

MELINDA CHUA FUI YEE BSc (Hons)

A thesis submitted in partial fulfilment of the
requirements of the University of Wolverhampton
for the degree of Doctor of Philosophy

September, 2011

Signature……..

Date……..

Contents Page

List of Tables

List of Figures

Acknowledgements

This PhD programme has been financially supported by a PhD studentship awarded by the Research Centre in Applied Sciences (RCAS), University of Wolverhampton.

My greatest thanks is to my director of studies, Dr. Timothy C. Baldwin, whose positive and encouraging nature has been an inspiration throughout, and I thank him for his advice, help and support throughout this project.

I also deeply appreciate the support and guidance provided by my second supervisor Professor Trevor Hocking, who supervised the plant experiments and provided many valuable comments on drafts of this thesis.

I thank Professor Kelvin Chan for providing some of the initial corm materials and for his advice on TCM aspect of the project; Dr. Christopher Perry for his guidance and advice with aspects of the chemistry component of the project. I also appreciate the help of Dr. Malcolm Inman, who assisted with the light microscopy; Mr. Paul Stanley and staff of the Electron Microscope Centre, University of Birmingham, for use of their TEM facilities. I am grateful to Professor Peter Williams and Dr. Ian Ratcliffe of the Centre for Water Soluble Polymers, Glyndwr University for use of their laboratory facilities; Mr. Robert Hooton who assisted with the cultivation of the konjac and Professor HuaChun Guo and Dr. Yaqiong Zhang for providing corm materials and for their hospitality during my two visits to Yunnan

Agricultural University. Special thanks also go to Dr. Habib Khan for his sincere advice and guidance throughout my PhD.

Lastly, I wish to thank my parents for their love, support and encouragement during my years of study in the UK. I couldn't have achieved all these without my beloved family.

Abstract

Konjac glucomannan (KGM), the main biologically active constituent of konjac flour extracted from corms of *Amorphophallus konjac* (konjac), can be used to prepare functional foods and may also have potential as a pharmaceutical product to combat obesity. The current study employed three experimental approaches to study the biology and chemistry of konjac, namely (1) glasshouse experiments to study the morphogenesis, growth and productivity of konjac plants, (2) a histological and immunocytochemical investigation of the localisation and developmental regulation of the deposition and metabolism of KGM in developing corm tissues, and (3) a comparative study of methodologies for the extraction and analysis of KGM.

The current data demonstrated a morphological and functional separation between the ventral and dorsal regions of corms. The ventral region appeared to function as a source during the initial period of shoot development, while the dorsal region appeared to operate as a sink after the development of mature canopy. Once the corm reached maturity, both an inflorescence and a leaf were produced within a single season. It has also been demonstrated that the age of the 'mother' corm is an important factor affecting the quality of offsets produced.

An anti-mannan antiserum detected a temporally regulated pattern of mannan epitope production within glucomannan idioblasts in developing corm tissues, with increased expression as the corm approached maturity/dormancy. The current observations also suggest that the mobilization of KGM initiates at the periphery of the corm and proceeds inwards towards the centre of the corm.

Compositional analysis showed that the purified konjac flour (PKF) produced using a modified extraction procedure contained 92% glucomannan, with a weight average molecular weight (M_w), polydispersity index (PDI) and degree of acetylation

(DA) of 9.5 ± 0.6 x 10^5 $gmol^{-1}$, 1.2 and 2.8 wt. %. These data, plus Fourier-transform infrared spectral (FTIR) and zero shear viscosity analyses of the extract (PKF) were all consistent with the literature. Comparison of three existing methodologies for the quantitative analysis of the KGM content, namely 3,5-dinitrosalicylic acid (3,5-DNS), phenol-sulphuric acid and enzymatic colorimetric assays; indicated that the 3,5-DNS colorimetric assay was the most reproducible and accurate method, with a linear correlation coefficient of 0.997 and recoveries between 97% and 103% across three spiking levels of starch.

In summary, this study has provided a better understanding of aspects of the biology and cultivation of *A. konjac* and has also produced methodologies which can be used as the basis for an improved good laboratory practice (GLP) for the commercial extraction and analysis of this multifunctional natural polymer.

Abbreviations

A	amyloplast
ADP	adenosine diphosphate
ADP-Glc	ADP-D-glucose
AG	arabinogalactan
AGP	arabinogalactan protein
ANOVA	analysis of variance
ap	apical bud
ATP	adenosine triphosphate
Ces	cellulose synthase
CKF	crude konjac flour
CMA	Chinese Ministry of Agriculture
Csl	cellulose synthase-like
CslA	cellulose synthase-like family A
CW	cell wall
DA	degree of acetylation
DAP	days after planting
DC	daughter corm
DI	deionised
DI	druse idioblast
3,5-DNS	3,5-dinitrosalicylic acid
dr	dried roots
EST	expressed sequence tags
fb	flower bud
FCS	foetal calf serum
FDA	Food and Drug Administration
FEV	final extraction volume
Fru-6-P	fructose-6-phosphate
FSA	Food Safety Authority
FTIR	Fourier transform infrared
GDP	guanine diphosphate
GDP-Glc	GDP-D-glucose
GDP-Man	GDP-D-mannose

GI	glucomannan idioblasts
Glc-1-P	glucose-1-phosphate
Glc-6-P	glucose-6-phosphate
GLP	good laboratory practice
GOPOD	glucose oxidase/peroxidase
GPC	gel-permeation chromatography
IR	infrared
KGM	konjac glucomannan
lb	leaf bud
LM	light microscope
LSD	least significant differences
LVKF	low-viscosity konjac flour
MALLS	multi angle laser light scattering
Man-1-P	mannose-1-phosphate
Man-6-P	mannose-6-phosphate
Max	maximum
MC	mother corm
ML	middle lamella
M_n	number-average molecular weight
M_w	weight-average molecular weight
Mz	z-average molecular weight
NADP	nicotinamide adenine dinucleotide phosphate
nd	node
NDP	nucleoside diphosphate
NKF	nutraceutical grade konjac flour
NMP	nucleoside monophosphate
of	offset
PC	parenchyma cell
PDI	polydispersity index
PHP	potassium hydrogen phthalate
PKF	purified konjac flour
PM	plasma membrane
RChl	relative chlorophyll
RI	raphide idioblasts

RI	refractive index
RSD	relative standard deviation
SD	standard deviation
SEM	scanning electron microscope
stn	stolon
TCM	traditional Chinese medicine
TEM	transmission electron microscope
UDP	uridine diphosphate
UDP-Glc	UDP-D-glucose
USDA	U.S. Department of Agriculture
VB	vascular bundle
Vig	vigorous
WFS	World of Food Science
WIPO	World Intellectual Property Organization
wt	weight

Chapter one: General introduction

1.1. Introduction to *Amorphophallus konjac*

Plants of the genus *Amorphophallus* have a long history of use in tropical and subtropical Asia as a food source and as a traditional Chinese medicine (TCM) (Liu *et al*., 1998). They are perennial plants with an underground stem in the form of a corm and a highly dissected umbrella-shaped leaf blade (Hetterscheid and Ittenbach, 1996; Bown, 2000). One of the best known is *Amorphophallus konjac* (synonym *A. rivieri*, konjac, devil's tongue, snake palm or voodoo lily) which has been cultivated in China for more than 2000 years (Liu *et al*., 1998; Long, 1998). Whole corm extracts of this species have been used as a TCM for the treatment of asthma, cough, hernias, breast pain, burns and skin disorders (Niwa *et al*., 2000; Xu *et al*., 2001). Moreover, the corm tissues are known to be a valuable source of glucomannan, a soluble, non-cellulosic polysaccharide (Takigami, 2000; Edison, 2010; Parry, 2010). Traditionally, this polysaccharide (which has no calorific content) is extracted from corm tissues and is used to produce flour from which foodstuffs (e.g. noodles) are prepared (Long, 1998). In addition to its use to prepare functional foods, a purified version of this flour may also have potential as a nutraceutical, or pharmaceutical product for use in the treatment of obesity (Kraemer *et al*., 2007), obesity-related dyslipidemia (Gallaher *et al*., 2000; Keithley and Swanson, 2005; Vasques *et al*., 2008) and diabetes (Vuksan *et al*., 1999, 2000, 2001) in countries where these are increasingly important medical problems, such as the U.K. (Leeds, 2010).

Currently, konjac is grown in China, Japan, Korea, Indonesia and Thailand with a total crude flour production exceeding 25,000 tonnes (Parry, 2010). China and Japan are the largest producers of konjac flour and account for 60% and 28%,

respectively of global production (Xu *et al*., 2001; Liu, 2004). Around half the flour produced in China is exported (Liu, 2004) and approximately 400 factories are devoted to the production of konjac flour and related goods (En, 2008). The main growing regions in China are in the mountainous areas of Yunnan, Sichuan, Guizhou, Hubei, Guangxi and Shaanxi provinces (Edison, 2010). Yunnan is the 'richest' Chinese province in terms of *Amorphophallus*, with 15 of the 23 indigenous species being native to this province (Long, 1998). As the global consumption and market price of konjac flour has steadily increased over the past 10 years (Figure 1.1), konjac is now regarded by the Chinese government as an important cash crop which has great potential in both domestic and overseas markets including Japan, Taiwan, Thailand, Korea, Malaysia and Singapore (WFS, 2003; Parry, 2010). Since the mid 1990s, with the help of provincial governments and local companies, konjac has been planted as a cash crop in mountainous regions of Southern China, to combat rural poverty among local farmers (WFS, 2003).

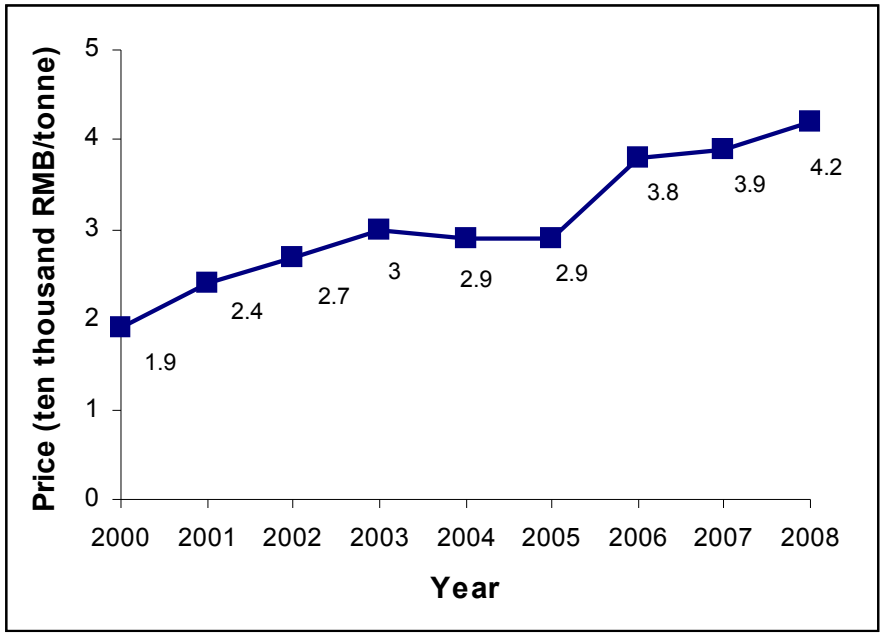

Figure 1.1 Market price of konjac flour in China (2000 - 2008) (Zhang, 2009).

Despite the fact that konjac is a widely used foodstuff and traditional medicine in the Orient, consumption in the West is relatively limited. A major challenge to the global usage of this versatile and useful foodstuff/nutraceutical is a lack of detailed information on the productivity, biosynthesis and analysis/quality assurance for both cost-effective production and safe use within the appropriate regulatory frameworks (US, UK or EU), for the various products to be brought to market. To date, the majority of literature regarding konjac glucomannan (KGM) has focused on the structural, physicochemical and pharmacological properties of this substance and to a lesser extent on the morphogenesis, cultivation, molecular biology of the crop itself and the processing chemistry of KGM. Therefore, a more detailed understanding of the science which underpins the use of konjac from cultivation to the commercialization of finished products as well as corm productivity, accumulation and metabolism of KGM is essential for further improvement of the commercial potential of this crop.

1.2. Botanical background

The genus *Amorphophallus* belongs to the family Araceae (Aroids), subfamily Aroideae and tribe Thomsonieae. It comprises of approximately 200 herbaceous species and is distributed in both tropical and subtropical regions of the palaeotropics, including Africa, Madagascar, India, continental South East Asia, Melanesia and North East Australia (Hetterscheid and Ittenbach, 1996; Sedayu *et al*., 2010). They are lowland plants that grow in tropical and seasonal forest margins, in open woodlands and in humus deposits on limestone areas (Hetterscheid, 1994; Mayo, *et al*., 1997).

As well as having beautifully patterned petioles and fine floral details, they also produce some of the most fascinating inflorescences in the family (Figure 1.2). The inflorescence of *Amorphophallus titanum* from Western Sumatra is one of the largest known inflorescences, reaching 3 m or more in height (Mayo *et al*., 1997).

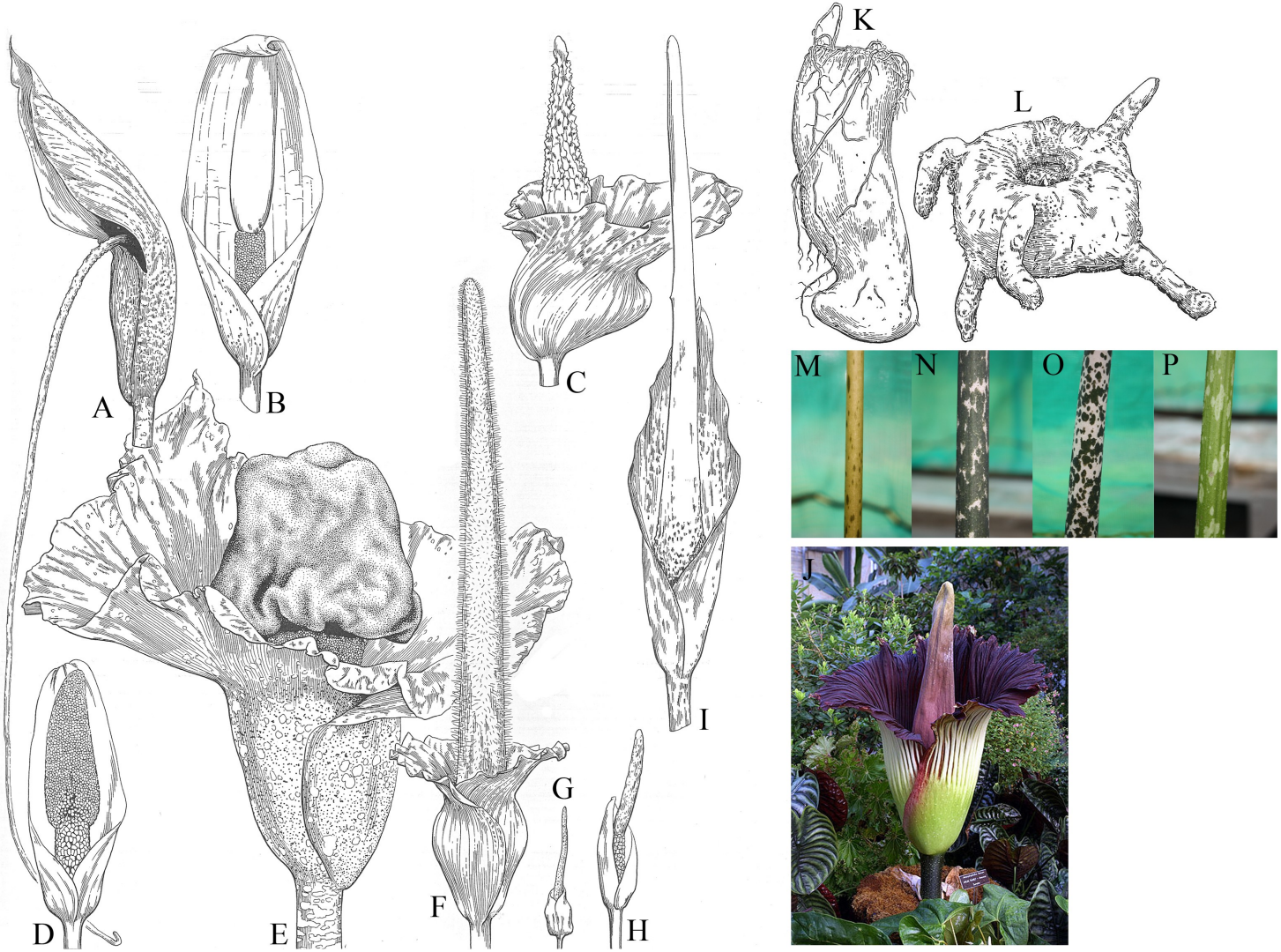
A
B
C
D
E
F
G
H
I
K
L
M
N
O
P
J

Figure 1.2 Different types of inflorescences (A - J), tubers (K, L) and petioles (M - P) of *Amorphophallus* species (A - I, K, L: adapted from Mayo *et al*., 1997; J: adapted from U.S. Botanic Garden, 2003; M - P: photographs taken from plants grown under glasshouse conditions at the Crop Technology Unit, University of Wolverhampton). **(A)** *A. krausei* x 1/6, **(B)** *A. albus* x 1/6, **(C)** *A. sumawongii* x 1/6, **(D)** *A. paeoniifolius* x 1/3, **(E)** *A. hirtus* x 1/16, **(F)** *A. pusillus* x 1/12, **(G)** *A. pygmaeus* x 1/3, **(H)** *A. gomboczianus* x 1/3, **(I)** *A. konjac* x 1/12, **(J)** *A. titanum*, **(K)** elongated tuber x 1/6, **(L)** globose corm x 1/6, **(M)** *A. albus*, **(N)** *A. konjac*, **(O)** *A. krausei*, **(P)** *A. paeoniifolius*.

As in other related genera within the Araceae family, such as *Arisaema*, *Dracontium*, and *Typhonium*, most species develop a subterranean corm or fleshy rhizome, which serves as a storage organ (Boyce, 1993; Mayo *et al*., 1997). *Amorphophallus* species produce leaves singly from the top of the corm, usually 1 - 2 m in height. Leaves are tripartite and divided into numerous pinnatisect segments (O'Hair and Asokan, 1986; Hetterscheid and Ittenbach, 1996; Hejnowicz and Barthlott, 2005) with all the branches bunched up like an inside-out umbrella (Bown, 2000).

On maturity, an inflorescence composed of a unisexual flower-bearing protuberance (the spadix) and a petal-like leaf (the spathe) is developed (O'Hair and Asokan, 1986; Mayo *et al*., 1997; Bown, 2000). On the spadix, the male and female flowers occur in separate zones. Female flowers form the basal zone and are each reduced to a pistil. Above this zone is a zone of highly reduced male flowers which exist as a group of stamens and often, one or several zones of sterile flowers and a smooth, tail-like sterile appendage (Mayo *et al*., 1997). The production of an appendage by unisexual-flowered species is unique in the plant world (Bown, 2000) and the name of the genus "*Amorphophallus*" derived from Greek (*amorphos*, "shapeless"; *phallos*, "penis") refers to the shape of the prominent spadix (Mayo *et al*., 1997; Bown, 2000; Liu, 2004).

The spathe has a convoluted lower portion which forms a chamber round the flowers and may serve as a trap, or mating arena to detain pollinators during the consecutive opening of female and male flowers (Kite *et al*., 1998; Bown, 2000). During anthesis, the sterile flowers of most species (except *A. albispathus*, *A. odoratus*, *A. yuloensis* and *A. manta*) release a pungent pheromone (odour) (Hetterscheid and Ittenbach, 1996; Kite and Hetterscheid, 1997) which has been

described as “a mixture of rotting fish and burnt sugar” to attract insect pollinators (Bown, 2000). It has been reported that these odours are compounds of ammonia, amines, amino acids as well as skatole and indole, which are rarely found in higher plants (Chen and Meeuse, 1971). After successful pollination, the female flowers develop into colourful berries, each containing one to three seeds (Bown, 2000).

To date, corms of 20 *Amorphophallus* species (Table 1.1) are recorded as edible (Liu, 2004). Several of which have been used in times of famine, but only two are significant as crops. One of which is *A. konjac*, the other is *A. paeoniifolius* (syn. *A. campanulatus*) (O’Hair and Asokan, 1986; Mayo *et al*., 1997; Bown, 2000; Liu, 2004) which produces a starch-rich corm and is commonly used as food in tropical Asia, especially India, where the species is widely cultivated (Mayo *et al*., 1997; Ravi *et al*., 2009). Species such as *A. albus*, *A. kachinensis*, *A. krausei* and *A. yuloensis* which have traditionally been used as food, medicine and fodder by ethnic groups in Southern China have also been recently considered as important alternative sources of glucomannan (Liu, 2004).

Table 1.1 Edible *Amorphophallus* species and their area(s) of distribution (Liu, 2004).

Species	Distribution
A. aphyllus	Senegal and Sudan
A. dracotioides	From Madagascar to Polynesia
A. harmandii	Ivory Coast
A. paeoniifolius	Cambodia, Vietnam and India
A. prainii	Thailand and Indonesia (Eastern Kalimantan)
A. titanum	Indonesia (Sumatra) and Burma
A. variabilis	Philippines, Indonesia (Java) and Malaysia
A. oncophyllus	South East Asia
A. bulbifer	India and Indonesia (Java)
A. corrugatus	China (Guangxi and Yunnan provinces) and Thailand
A. kachinensis	China (Yunnan province), Burma, Thailand and Laos
A. kiusianus	Eastern China, Taiwan, Southern Japan
A. krausei	China (Yunnan province), Burma, Northern Thailand
A. konjac	China, Japan, Vietnam, Indonesia, Philippines
A. tonkinensis	China (Yunnan province), Vietnam
A. yunnanensis	China (Yunnan province), Thailand, Laos and Vietnam
A. albus	China (Sichuan and Yunnan provinces)
A. odoratus	China (Hong Kong)
A. nanus	China (Yunnan province)
A. yuloensis	China (Yunnan province)

1.3. The biology and chemistry of *A. konjac*

1.3.1. Origin, distribution and ecology

A. konjac is endemic to the tropical rain forests in South East Asia. It is distributed throughout the Himalayas, Indochina (Myanmar, Thailand, Cambodia, Laos and Vietnam), Japan, Philippines, South West (Yunnan province) and North West (Shanxi, Ningxia and Gansu provinces) China (Liu, 2004). This species can be found at forest margins, deciduous woodlands, limestone areas, most commonly in undisturbed secondary forest, at 600 to 2500 m above sea level (Hetterscheid, 1994; Mayo, *et al*., 1997; Liu, 2004).

1.3.2. Morphology

A. konjac is a herbaceous, perennial monocotyledon, growing from an underground stem in the form of a corm (Figure 1.3) up to 30 cm in diameter (Mayo *et al*., 1997; Bown, 2000). The corm is globose, possessing an apical bud at the central area of the dorsal surface from which the shoot develops (Liu, 2004). Below the apical bud, there are 8 - 12 nodes from which the "daughter" corm develops through elongation and enlargement of these nodes. Buds held by nodes closer to the apical bud differentiate into cataphylls, whilst those further away may develop into rhizomatous offsets and roots (Liu, 2004). Two types of roots are produced: 1) fine, fibrous roots for water and nutrient uptake, and 2) thick, contractile adventitious roots which help support and position the corm at an appropriate level in the soil (Bown, 2000; Liu, 2004).

The apical bud is enclosed by layers of cataphylls (bract-like modified leaves) which serve to protect the developing shoot from soil impedance, both underground and as it emerges (Liu, 2004). The protective cataphylls elongate concomitantly with leaf (or inflorescence) development and dry out as the leaf matures (Liu, 2004), after which they are shed.

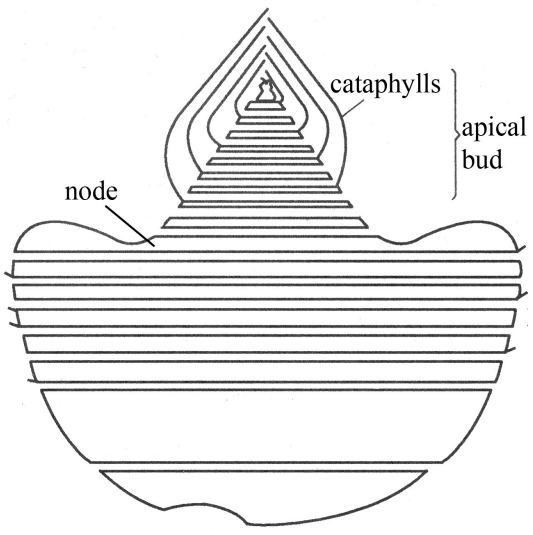

Figure 1.3 Sketch of the corm of *A. konjac* (adapted from Liu, 2004).

A. konjac produces a solitary leaf supported by a smooth, densely spotted pink-white petiole up to 1 m in length (Mayo *et al*., 1997; Bown, 2000). One of the common names of *A. konjac*, "snake palm", is derived from the pattern on its petiole, resembling the body of a snake (Hetterscheid, 1994). The leaf is tripartite and divided into numerous pinnatisect, pointed and elliptic leaflets, measures 3 - 10 cm long and 2 - 6 cm wide (Figure 1.4) (O'Hair and Asokan, 1986; Bown, 2000). Moreover, it has been shown that the length of petiole, leaf area and number of leaflets increase with increasing corm age (Table 1.2) (Liu, 2004).

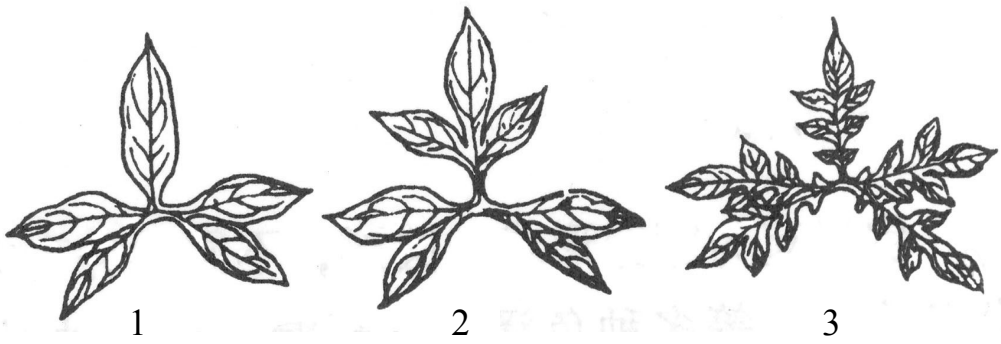

Figure 1.4 Sketch of the leaves produced by *A. konjac* plants of varying age (adapted from Liu, 2004). **(1)** one-year-old plant, **(2)** two-year-old plant, **(3)** three-year-old plant.

Table 1.2 The size of leaf produced by *A. konjac* plants of varying age (Liu, 2004).

Corm age (years)	Petiole length (cm)	Leaf area (dm^2)	Number of leaflets
1	19	5.6	80
2	47	41.9	267
3	67	90.9	430
4	83	173.5	538

The inflorescence is borne on a peduncle (up to 1 m in length) which produces a similar appearance to the petiole in terms of colour and patterning (Mayo *et al*., 1997). The most conspicuous part of the inflorescence is the spathe (a modified leaf).

This is an erect, broadly triangular, wavy margined, funnel-shaped bract of 10 - 60 cm long and 10 - 55 cm wide (Bown, 2000). The spathe has a rough, dull brown-green outer surface with black-green spots; whilst the interior is maroon-brown. The flowers are unisexual and tightly packed on a maroon, narrowly conic spadix which protrudes from the spathe, measuring 15 - 110 cm long. As mentioned previously, the sexes are segregated into distinct zones (Figure 1.5). The female flowers occur within the lowest portion of the spathe (floral chamber), whilst the male flowers locate within the upper spathe blade, followed by a tail-like sterile appendage (Mayo *et al*., 1997).

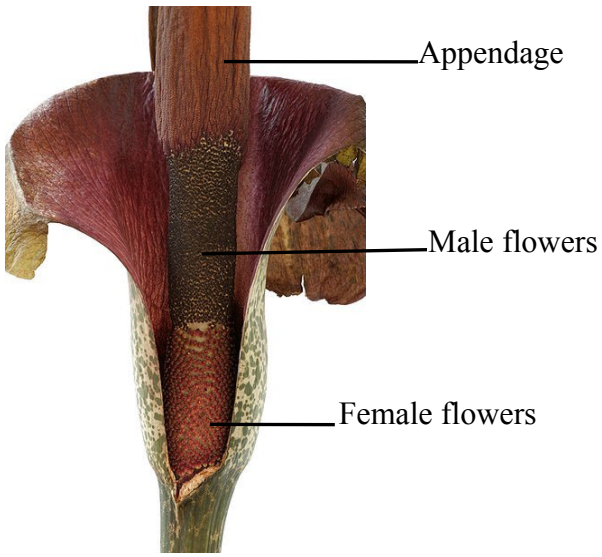

Figure 1.5 Interior of the floral chamber of *A. konjac* inflorescence, showing tightly packed female and male flowers on the spadix (adapted from Hetterscheid and Ittenbach, 1996).

1.3.3. Growth and development

A. konjac grows well in shady environments (Mayo *et al*., 1997) with free-draining, humus-rich soils of pH 6.5 - 7.5 (Hetterscheid and Ittenbach, 1996; Bown, 2000; Follett and Douglas, 2002). It is one of the hardiest *Amorphophallus* species and can grow in seasonal temperatures ranging between 5 and 43 °C, with an optimum temperature range of 20 - 25 °C (Imai and Coleman, 1983; Hetterscheid

and Ittenbach, 1996; Douglas *et al*., 2005). The shade-loving nature and tolerance to higher temperatures of this species are believed to be related to its original habitat, which is thought to have been the floor of tropical rain forests in South East Asia (Imai and Coleman, 1983).

Except for a few evergreen species (e.g. *A. arnautovii* and *A. pingbianensis*) (Hetterscheid and Ittenbach, 1996), all *Amorphophallus* species have a distinct dormancy period, which affects the planting and harvesting cycle (O'Hair and Asokan, 1986). Most often, konjac is planted in spring (March/April) and attains maturity after 6 - 7 months (October/November). During this time, the foliage dies back and the plant over winters as a dormant corm for about 6 months, before re-emerging the following spring (Bown, 2000; Follett and Douglas, 2002).

The minimum temperature required to break dormancy is 14 °C. In temperate climates when this temperature is reached (during the spring), the shoot apical meristem is activated, followed by leaf bud emergence which usually takes place in May (Liu, 2004). A fasciculate compound leaf subsequently emerges from the surrounding cataphylls. Liu (2004) reported that leaf development in konjac takes 45 - 65 days (Figure 1.6) and the rate of leaf expansion is affected by the growing temperature, age and size of corm.

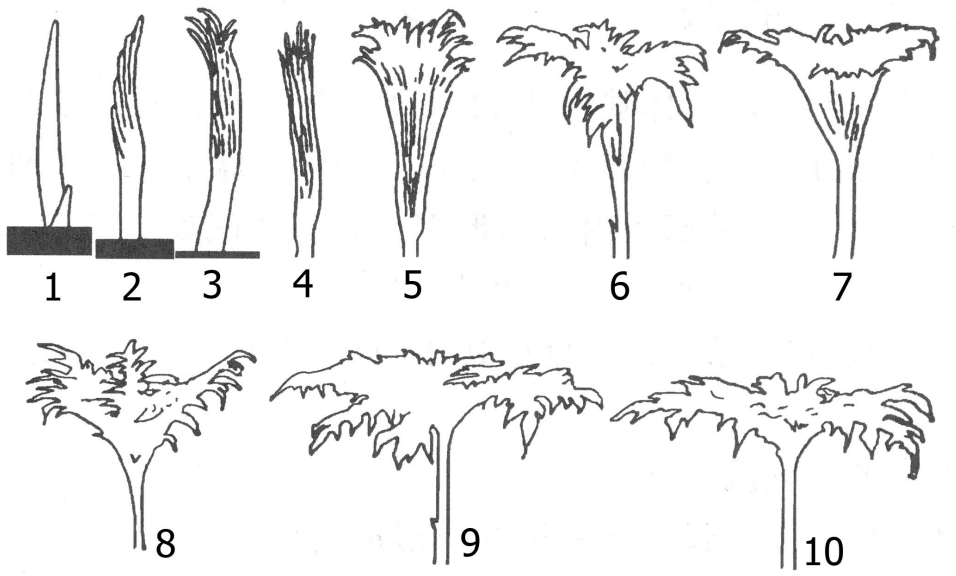

Figure 1.6 Various stages of leaf development in *A. konjac* (adapted from Liu, 2004). **(1)** Leaf bud (enclosed with cataphylls) emergence. **(2)** Cataphylls rupture, with the emergence of folded leaflets. **(3)** Full emergence of leaflets. **(4)** Petiole elongation. **(5)** Leaflets unfolding. **(6)** Midrib expansion. **(7)** Expansion of the lower part of midribs, forming a funnel-shaped leaf canopy. **(8)** Continuous leaf expansion, forming a Y-shaped leaf canopy. **(9)** Further leaf expansion, forming a T-shaped leaf canopy. **(10)** Mature leaf canopy.

During the course of leaf development, an internal bud is formed within the abscission layer at the base of petiole (Figure 1.7). The internal bud later develops into an apical bud, from which the leaf of the subsequent growing season initiates (Liu, 2004). However, it has been reported that, typically, during the third or fourth growing season, the internal bud no longer differentiates into a leaf bud. Instead, a flower bud forms thus completing the reproductive life cycle (Imai and Coleman, 1983; Sun *et al*., 1995; Liu, 2004). According to Sun *et al*. (1995), once the apical flower bud has emerged, none of the lateral leaf buds germinate due to strong apical dominance, suggesting that the inflorescence and leaf of a plant never grow concurrently. However, if the flower bud is removed before emergence, one of the lateral buds may develop into a leaf during that season.

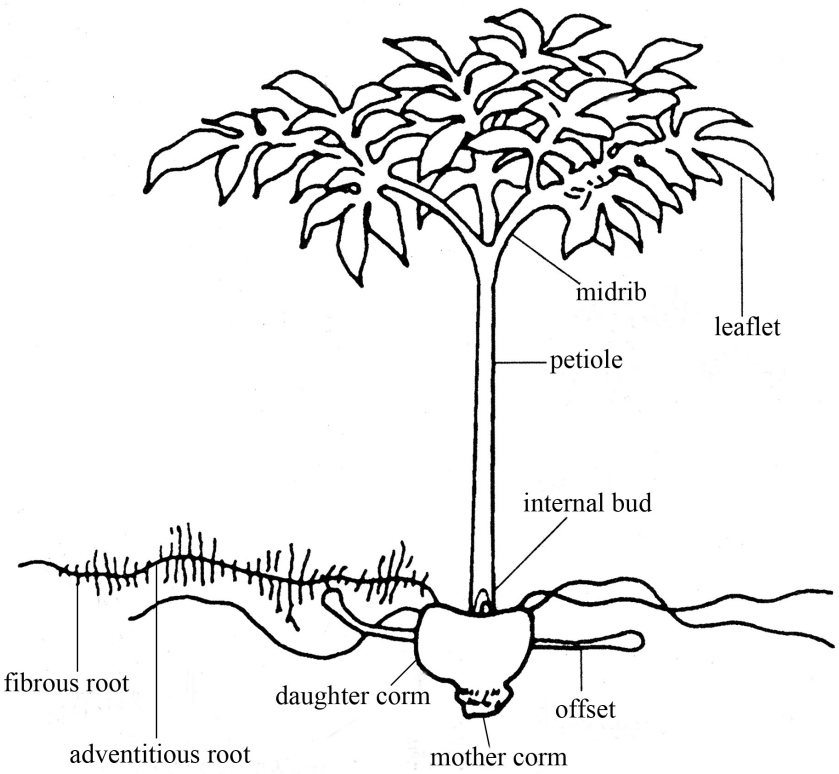

Figure 1.7 Morphology of a mature plant of *A. konjac* (adapted from Liu, 2004). During the course of leaf development, the "mother" corm (first generation) degenerates, with the formation of a "daughter" corm (second generation) on top of the degenerating "mother" corm. Meanwhile, an internal bud (third generation), from which the shoot of the subsequent growing season initiates, is formed within the abscission layer at the base of petiole.

The minimum temperature required for root formation after dormancy is 10 - 12 °C. As this temperature is slightly lower than is required for apical bud germination (14 °C), the growth and development of the roots take place earlier than the apical bud, approximately 15 days after planting (Liu, 2004). Root development initiates from the root apical meristems located below the apical bud of the "mother" corm. These apical meristems differentiate into root caps and procambium, of which the root caps extend horizontally to form thick, fleshy contractile adventitious roots. The roots extend vertically down into the soil, anchoring the corm which until this stage is rootless and unstable. Once the corm is in a firm position, the feeding roots start to develop. These roots are short-lived and are quickly replaced in an ongoing

process of root turnover. Following the growth and development of rhizomatous offsets beginning in early July, roots start to form around the offset. The adventitious roots formed around the offsets have a slower rate of extension and appear to be finer with less feeding roots produced (Liu, 2004). After the mature leaf canopy has developed towards the end of growing season (mid August), the formation of new roots gradually decreases. The feeding roots start to wither and the central core tissue inside the spongy contractile roots begins to contract. The "daughter" corm is then pulled more deeply into the soil, bringing it to approximately the same depth as the "mother" corm at the beginning of the growth period (Liu, 2004).

1.3.4. Chemical composition of konjac corms

The chemical composition of a developing konjac corm changes throughout the growing season (Table 1.3). On maturation, the dry matter of fresh corms contain 49 - 60% glucomannan, 10 - 30% starch, 2.6 - 7% inorganic elements (aluminium, calcium, chromium, cobalt, iron, magnesium, manganese, phosphorus, potassium, selenium, silicon, sodium, tin and zinc), 5 - 14% crude protein, 3 - 5% soluble sugars (sucrose, mannose, fructose and glucose), 3.4 - 5.3% ash and a small amount of alkaloids (trigonelline) and saponin (USDA, 2004; Li *et al*., 2005). Organic compounds such as β-carotene, choline, niacin, riboflavin and thiamine (USDA, 2004) as well as serotonin and its derivatives, *i.e*. *cis-N-(p*-Coumaroyl) serotonin and *trans-N-(p*-Coumaroyl) serotonin, have also been identified (Niwa *et al*., 2000).

The composition of mature corms varies with species, origin and growing conditions. Of the *Amorphophallus* species cultivated in China, only *A. konjac*, *A. albus* and *A. krausei* have glucomannan as their main storage polysaccharide (Table 1.4) (Liu, 2004).

Table 1.3 Changes in the main compositions (% dry weight) of konjac corms throughout a growing season (Liu *et al*., 1998).

Time (date/month)		10/05	30/05	30/06	10/07	30/07	10/08	30/08	10/09	30/09	10/10	30/10
Days after planting		0	20	50	60	80	90	110	130	140	150	170
Fresh weight (g)	MC	65.0	58.5	10.7								
	DC			6.7	17.5	50.0	81.0	152.0	234.0	365.0	408.0	382.0
Glucomannan (%)	MC	51.5	41.9	7.2								
	DC			24.3	36.7	50.9	51.8	56.0	55.3	54.3	54.5	53.2
Starch (%)	MC	10.5	7.5	1.0								
	DC			1.3	8.3	10.9	10.7	10.6	10.8	10.5	10.9	10.7
Soluble sugar (%)	MC	4.8	5.6	6.8								
	DC			6.9	8.7	6.4	6.2	5.8	5.4	4.9	5.2	4.8
Protein (%)	MC	8.9	11.8	6.5								
	DC			13.4	7.1	6.0	5.6	5.0	5.8	7.0	7.5	8.0

N.B. MC = “mother” corm, DC = “daughter” corm.

Table 1.4 Carbohydrate content (% dry weight) of corms of *Amorphophallus* species from different origins (Liu, 2004).

Species	Origin	Water *	Glucomannan	Starch	Soluble sugar
A. konjac	Sichuan	78.9	58.8	12.3	2.9
	Chongqing	79.3	59	12.9	2.7
	Guizhou	80.3	58.3	12.7	2.7
	Yunnan	78.5	54.4	16.2	3.8
	Hubei	78.2	54.6	17.3	3.2
	Guangxi	78.7	55.1	14.1	3.4
	Jiangxi	81.8	52.2	19.8	2.9
	Fujian	81	52.1	20.1	3.5
A. albus	Sichuan	78.6	59.3	11.5	1.5
A. yuloensis	Yunnan	-	33.7	38.8	5.5
A. kachinensis	Yunnan	-	39.8	46.1	8.3
A. krausei	Yunnan	-	28.5	21	7.6
A. paeoniifolius	India	-	-	35 - 70	-

* Percentage fresh weight.
- Data not available.

1.3.5. Traditional and contemporary uses of konjac corms

Konjac was first listed as a Chinese medicinal herb in the "*Shen Nong Materia Medica*" as early as 206 B.C. during the Western Han Dynasty. According to the ancient Chinese pharmacopoeia, "Ben Cao Gang Mu", konjac is a toxic, pungent and cold-natured herb (Xu *et al*., 2001). Traditionally, corms are washed, peeled, sliced, dried and ground to produce konjac flour which is consumed in the form of cake (or gel) after boiling the flour with plant ash. In TCM, the therapeutic effects of extracts from konjac corms have partially been ascribed to its pungent and toxic principles with the functions of detoxification, tumour-suppression, blood stasis alleviation and phlegm liquefaction (Niwa *et al*., 2000; Xu *et al*., 2001). For more than 2000 years, konjac gel has been used for the treatment of asthma, coughs, hernias, breast pain, burns as well as haematological and skin disorders. Konjac flour has also been consumed as a functional food in the form of noodles, tofu and snacks (Wootton *et*

al., 1993; Long, 1998; Bown, 2000; Douglas *et al*., 2005), or as konjac curd, which is tasteless and is usually braised with meat in traditional Chinese cuisine. In addition to the use of the flour derived from the corm, the leaves of the konjac plant are used as a natural insect repellent and as animal fodder by the indigenous people in Southern China (Long, 1998).

In Japanese cuisine, konjac flour is pounded with lime and water into a gelatinous grey cake ("konnyaku"), a key ingredient in Japanese noodles ("shirataki") and cuisines such as "sukiyaki" and "gyudon" (Bown, 2000). Outside Asia, konjac is grown as an ornamental due to its beautiful compound foliage and marbled petioles (Follett and Douglas, 2002).

Much of the recent interest in the use of konjac stems from its potential use as a dietary fibre. The term dietary fibre, classified as soluble or insoluble, is described as the endogenous component of plant material in the diet that is resistant to human digestive enzymes (McCleary, 2003). The main biologically-active constituent in the konjac corms is a soluble fibre which primarily consists of the non-cellulosic polysaccharide, glucomannan (Takigami, 2000; Edison, 2010; Parry, 2010). As β-1,4 linkages of KGM cannot be hydrolysed by salivary and pancreatic amylase, KGM passes into the colon unchanged and is fermented by colonic bacteria (Keithley and Swanson, 2005). A highly purified form of KGM has been used in the treatment of obesity (Kraemer *et al*., 2007), obesity-related dyslipidemia (Gallaher *et al*., 2000; Keithley and Swanson, 2005; Vasques *et al*., 2008) and diabetes (Vuksan *et al*., 1999, 2000, 2001) by its action as a satiety agent (Sood *et al*., 2008). It has been marketed as such in capsule form, as a drink mix and in food products in China and neighbouring countries. The potential use of KGM as a prebiotic (Chen *et al*., 2005,

2006, 2008; Al-ghazzewi *et al*., 2007; Elamir *et al*., 2008; Wang *et al*., 2008) and as an immunomodulator (Onishi *et al*., 2007a, b) has also been suggested.

In addition, the unique rheological and gelling properties of KGM are widely employed in emulsifier and stabiliser products for the food, drink, cosmetic and pharmaceutical industries. Since 1994, KGM has been approved as a food additive by the U.S. Food and Drug Administration (FDA) (Takigami, 2000; Zhang *et al*., 2005). In 1996, it was also passed as a binder in meat and poultry products by the U.S. Department of Agriculture (USDA). In Europe, KGM has been given an E425 agreement number by the European Food Safety Authority (FSA, 2007). Moreover, KGM has been used in controlled drug delivery systems (Alvarez-Mancenido *et al*., 2008; Alonso-Sande *et al*., 2009) and in the production of absorbent materials such as disposable nappies and sanitary towels (Kok *et al*., 2009).

To summarise, konjac is used traditionally in the Orient as a TCM and as a functional food. The current usage of konjac in the West is mainly in the food and nutraceutical industries; where KGM extracted from the corms is used as a food additive and in the development of dietary supplements (Chua *et al*., 2010).

1.4. Localisation and biosynthesis of KGM

Polysaccharides containing β-1,4-mannosyl residues (referred to as mannan, mannan epitopes or mannan polysaccharides in this thesis) such as mannans, glucomannans, galactomannans and galactoglucomannans, are commonly found as cell wall components in both angiosperms and gymnosperms (Pettolino *et al*., 2001; Handford *et al*., 2003; Liepman *et al*., 2007). As a non-commelinoid monocot, *A. konjac* has type I cell wall. The most widely accepted model of this wall type is of a cellulose microfibrillar network cross-linked in a matrix of complex, non-cellulosic

polysaccharides which generally include pectic polysaccharides, xyloglucans and heteroxylans as major constituents, and heteromannans as minor constituents (Bacic *et al*., 1988; Brett and Waldron, 1996; Albersheim *et al*., 2010). The cell wall provides mechanical support to individual cells by defining plant cell and organ shape (Taiz and Zeiger, 2010), acts as a primary barrier against pathogen attack, mechanical injury and other environmental stress (Dhugga, 2005; Taiz and Zeiger, 2010) and is involved in intercellular signalling events which directs plant growth and development (Cheung *et al*., 2000; Freshour *et al*., 2003). Moreover, substantial evidence has been presented that the spatial and temporal control of cell wall deposition plays an important role(s) in the biology of plant cells, particularly in their development and differentiation (Knox, 1995; Carpita *et al*., 2001; Liepman *et al*., 2007; Goubet *et al*., 2009).

The mannan family of hemicellulosic polysaccharides contain a β-1,4-linked mannan backbone (Liepman *et al*., 2007; Moreira and Filho, 2008). In glucomannan, the mannose residues are interspersed by β-1,4-linked glucose, whereas single galactosyl residues are α-1,6-linked to the mannan backbone in galactomannan. Galactoglucomannans have a similar backbone to glucomannans, but some of the mannose residues bear α-D-Gal*p* and β-D-Gal*p*(1→2)-α-D-Gal*p* side chains at O6 (Rose, 2003; Moreira and Filho, 2008).

Mannan polysaccharides are a widespread component of secondary walls (Brett and Waldron, 1996; Maeda *et al*., 2000; Samuels *et al*., 2002). In *Arabidopsis thaliana*, mannans have been immunolocalized to the thickened secondary cell walls of xylem and interfascicular fibres (Handford *et al*., 2003). Mannans also constitute a significant percentage of total monosaccharide in *A. thaliana* inflorescence stems, which contain vascular cells and fibres with thickened secondary cell walls (Zhong

et al., 2005; Brown *et al*., 2005; Harholt *et al*., 2006). Furthermore, crystalline mannans appear to take the place of cellulose as the primary structural polysaccharide in some algal species (Frei and Preston, 1968; Preston, 1968). Both glucomannans and galactoglucomannans are components of the lignified walls of woody tissues in coniferous gymnosperms, where they serve as structural polymers (Matheson, 1990). Galactoglucomannans have also been identified in tissue-cultured tobacco (*Niciotiana plumbaginifolia*) cells (Sims and Bacic, 1995), blackberry (*Rubus fructicosus*) (Cartier *et al*., 1988) and kiwi fruit (*Actinidia deliciosa*) (Schroder *et al*., 2001).

In addition to its function as a structural polymer, the mannan family has long been recognised as a major group of cell wall storage polysaccharides and has been found in the endosperms of a variety of plant species (Reid and Edwards, 1995; Edwards *et al*., 2004). Glucomannans found in the Araceae, Liliaceae and Iridaceae, and galactomannans found in Leguminosae and Palmae serve as plant carbohydrate reserves (Reid, 1985) and may perform a role in cellular water-retention due to the presence of numerous hydrophilic galactose side-chains (Reid and Bewley, 1979; Brett and Waldron, 1996).

As mentioned previously, glucomannan is deposited within the underground corm tissues of *A. konjac*, where it serves as carbohydrate reserve. KGM is composed of β-1,4-linked D-glucose and D-mannose residues as the main chain, with branches through β-1,6-glucosyl units. The degree of branching is estimated at approximately 3 for every 32 sugar units. It consists of mannose and glucose units in a molar ratio of 1.6:1 and the acetyl groups along the KGM backbone are located, on average, every 9 - 19 sugar units at the C-6 (Kato and Matsuda, 1969; Shimahara *et al*., 1975; Maeda *et al*., 1980).

According to Takigami and colleagues, who studied the tissue structure of two-year-old corms of konjac using the scanning electron microscope (SEM); KGM granules accumulate in egg-shaped idioblasts within the parenchyma and the size and frequency of these idioblasts increases with distance from the epidermis, reaching ~ 650 μm in diameter at the central region of the corm (Takigami *et al*., 1997). Starch, cellulose, ash and nitrogen-containing materials (including proteins) are present in the parenchyma cells surrounding the idioblasts within the corm (Takigami *et al*., 1997; Zhao *et al*., 2010). In addition, calcium oxalate is deposited in needle-shaped raphide crystals (Takigami *et al*., 1997) and in multi-crystal druses (cluster crystals) (Prychid *et al*., 2008) which can be found in the glucomannan idioblasts and the surrounding parenchyma (Takigami *et al*., 1997). Table 1.5 shows the physical characteristics of glucomannan idioblasts compared with surrounding parenchyma cells (Zhao *et al*., 2010).

Table 1.5 Differences between a glucomannan idioblast and parenchyma cell within the fresh corm tissues (Zhao *et al*., 2010).

	Glucomannan idioblast	Parenchyma cell
Main constituent	Glucomannan	Starch
Hardness	High	Low, easily break to dust
Granule	Single granule	Agglomerated granules
Diameter (μm)	150 - 650	10 - 50
Water solubility	Soluble	Insoluble in cold water

Regarding biosynthesis of non-cellulosic polysaccharides, cellulose synthase–like (*Csl*) genes, belonging to a cellulose synthase (CesA) superfamily within the glycosyltransferase family 2 (Suzuki *et al*., 2006) are hypothesised to be promising candidates for encoding Golgi-localised β-glycan synthases that catalyze the assembly of β-linked backbones of non-cellulosic polysaccharides in plant cell walls. Like the CesA proteins, the Csl proteins contain the D, D, D, Q/RXXRW motif, a

diagnostic feature of processive glycosyltransferases (Albersheim *et al*., 2010). It has been reported that there are at least ten *CesA* genes in *A. thaliana* (*AtCesA1 - 10*) (Pear *et al*., 1996; Richmond and Somerville, 2000; Scheible *et al*., 2001), twelve in rice (*Oryza sativa*) (Richmond and Somerville, 2000), at least nine in maize (*Zea mays*) (Holland *et al*., 2000; Dhugga, 2001) and eight in barley (*Hordeum vulgare*) (HvCesA1 - 8) (Burton *et al*., 2004). Complete genome sequencing also revealed the presence of at least 30 *Csl* genes in *Arabidopsis* and 37 in rice (*Oryza sativa*) (Dhugga, 2005). Based on predicted protein sequences, these genes were grouped into six families (*AtCslA* - *AtCslE*, and *AtCslG*) in *Arabidopsis* (Richmond and Somerville, 2000) and two further families (*OsCslAF* and *OsCslAH*) in rice (Hazen *et al*., 2002).

The only *Csl* gene for which a specific function has been defined is *CslA*, which catalyses glucomannan synthase reactions (Liepman *et al*., 2007; Goubet *et al*., 2009). Liepman *et al*. (2007) reported that CslA protein from *Arabidopsis* catalyzed mannan and glucomannan synthase activity in *Drosophila* Schneider 2 cells. In another investigation, Suzuki *et al*. (2006) discovered a highly expressed xylem-specific *CslA* gene in black cottonwood (*Populus trichocarpa*) (*PtCslA1*) which encodes glucomannan synthase, suggesting its key role for the synthesis of wood glucomannan. More recently, Goubet *et al*. (2009) demonstrated that CslA2, CslA3 and CslA9 proteins are responsible for the glucomannan synthesis in *Arabidopsis* stems *in vivo*. To date, *CslA* gene sequences have been observed in over 100 species, including mosses and gymnosperm, as well as angiosperms (Liepman *et al*., 2007).

Photosynthesis is the ultimate source of the sugars incorporated into cell wall polysaccharides. Newly synthesized sugars are often stored transiently in starch,

fructans or oligosaccharides in photosynthetic or storage tissues (Taiz and Zeiger, 2010). Subsequently these storage polymers are converted into sucrose, raffinose or stachyose sugars for transport to their destinations, where they are converted via a series of reactions to hexose monophosphate, and then usually to nucleoside diphosphate sugars (NDP-sugars) (Rose, 2003; Konishi *et al*., 2007; Albersheim *et al*., 2010). Uridine and to a lesser extent, guanine are the principle nucleosides of the NDP-sugars used in the biosynthesis of plant cell walls; adenosine is used in starch synthesis (Seifert, 2004; Albersheim *et al*., 2010). Both UDP and GDP-sugar are produced in the cytoplasm, whilst ADP-sugar is made in plastid (Reiter, 2008).

The starting material for the synthesis of most NDP-sugars is a pool of five hexose monophosphates, including glucose-1-phosphate (Glc-1-P), glucose-6-phosphate (Glc-6-P), fructose-6-phosphate (Fru-6-P), mannose-6-phosphate (Man-6-P) and mannose-1-phosphate (Man-1-P), which are produced and maintained in rapid equilibrium by a combination of phosphoglycomutases and 6-phosphate isomerases (Albersheim *et al*., 2010). NDP-sugars can be formed either directly from Glc-1-P or Man-1-P by pyrophosphorylases, or through subsequent enzyme-mediated NDP-sugar interconversions (Reiter, 2008).

The cytoplasmically generated NDP-sugar molecules are transported into the lumen of the Golgi cisternae by means of an antiport system, exchanging nucleoside monophosphate (NMP) for specific NDP-sugars (Reyes and Orellana, 2008). The glycosyltransferase transfers the sugar from the NDP-sugar molecule to the oligosaccharide chain and NDP is released into the cisternal lumen (Lerouxel *et al*., 2006). The NDP is then hydrolyzed by a phosphatase in the membrane into NMP and Pi, which return through separate carriers to the cytoplasm, where they can be recycled (Rose, 2003; Albersheim *et al*., 2010).

Recently, Gille *et al*. (2011) studied the molecular biosynthesis of glucomannan in a developing corm of *A. konjac* which was harvested 17 weeks after planting. It has been proposed that the CslA3 protein is responsible for the synthesis of the glucomannan polysaccharides in *A. konjac*. However, with the active site of this enzyme remains unclear. The proposed KGM biosynthetic pathway (Figure 1.8) is as follows: Sucrose is first converted into the hexose phosphate pool by transformation into fructose and UDP-glucose, followed by the feeding of glucose into the hexose phosphate pool through UDP-D-glucose pyrophosphorylase. Glc-1-P is further converted into ADP-D-glucose, which is then utilised by starch synthase to produce starch. Phosphoglucomutase, an equilibrium enzyme, diverts Glu-1-P from the starch biosynthetic pathway to the synthesis of GDP-D-mannose. In relation to the synthesis of GDP-D-glucose, two pathways have been proposed. The first pathway involves the conversion of Glc-1-P to GDP-D-glucose via a GDP-D-glucose pyrophosphorylase, whilst the second would entail a GDP-D-mannose-2-epimerase converting GDP-D-mannose into GDP-D-glucose (Reiter, 2008). According to these authors, however, no orthologs to any genes concerned have been found within the EST collection database of the developing corm.

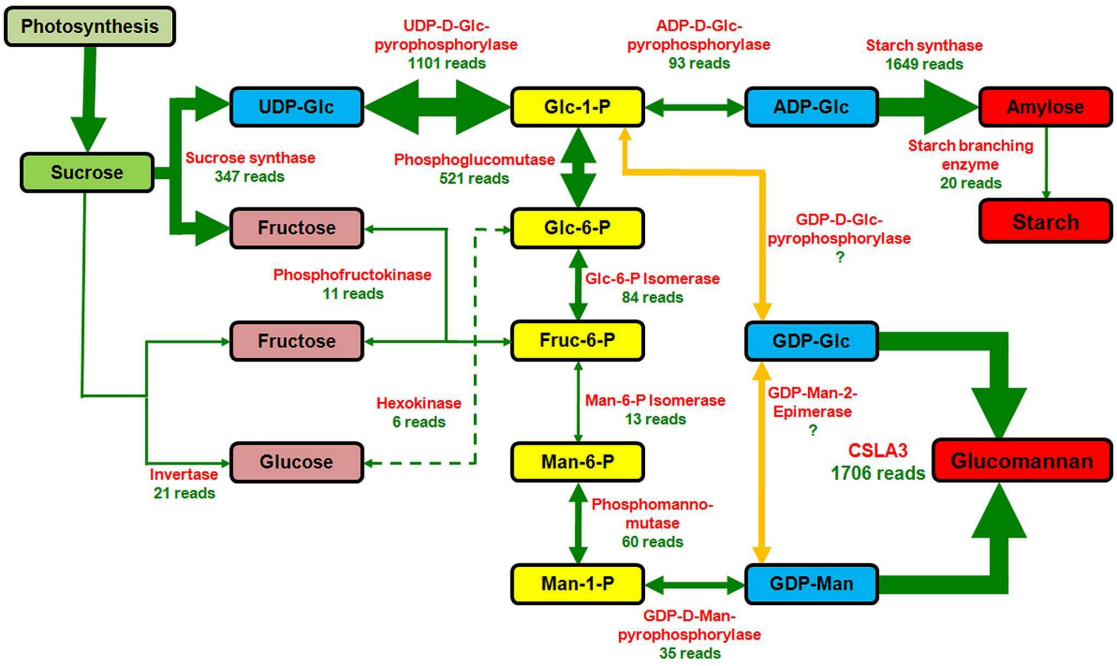

Figure 1.8 Proposed glucomannan and starch biosynthesis pathway in corm of *A. konjac* based on the established expressed sequence tags (EST) database (adapted from Gille *et al*., 2011). Red, the necessary converting enzymes found in the EST data. Green, the number of EST reads. UDP-glc, UDP-D-glucose; Glc-1-P, glucose-1-phosphate; glc-6-P, glucose-6-phosphate; Fruc-6-P, fructose-6-phosphate; Man-6-P, mannose-6-phosphate; Man-1-P, mannose-1-phosphate; GDP-Man, GDP-D-mannose; GDP-Glc, GDP-D-glucose; ADP-Glc, ADP-D-glucose, CSLA3, cellulose synthase-like family A member 3.

1.5. Cultivation (agronomy) of konjac to improve corm yield

A. konjac can be propagated by seed or vegetative divisions. For commercial cultivation, konjac is vegetatively propagated from corms and offsets (Follett and Douglas, 2002; Edison, 2010). Offsets attached to the "mother" corm are severed at harvest, and planted 10 - 15 cm deep to prevent roots developed at the dorsal region of the corm from drying out during a dry spring (Follett and Douglas, 2002). Propagation from seed, on the other hand, is not common as it is extremely hard for the seeds of konjac to germinate under natural conditions (O'Hair and Asokan, 1986). In Southern China, however, indigenous people facilitate artificial

germination by eliminating the mature seed coats, followed by mixing with moist sand in the ratio of 1:4, before covering with a layer of thick soil (Long, 1998).

Most cultural practices for edible aroids are the result of empirical knowledge collected by untold generations of farmers. Practices based on scientific research are a recent event (O'Hair and Asokan, 1986). In Japan, a traditional konjac cropping system ("Jinenjo system") which has been in use for over 100 years, involves continuous planting of offsets and older corms as a natural community on sloping ground (wooded areas) (Figure 1.9). Konjac plants are mulched heavily with grain straw, barley or wild herbs and have been intercropped with Paulownia (*Paulownia tomentosa*) to protect the plants from direct sunlight (Kurihara, 1979; Douglas *et al*., 2006). In late autumn, only older corms are harvested for sale, the remainder are left in the fields to continue growing the following season (Kurihara, 1979). Corms produced under such cropping system are reported to be of high quality (*i.e.* high glucomannan content) and remarkably free from pests and diseases (Kurihara, 1979).

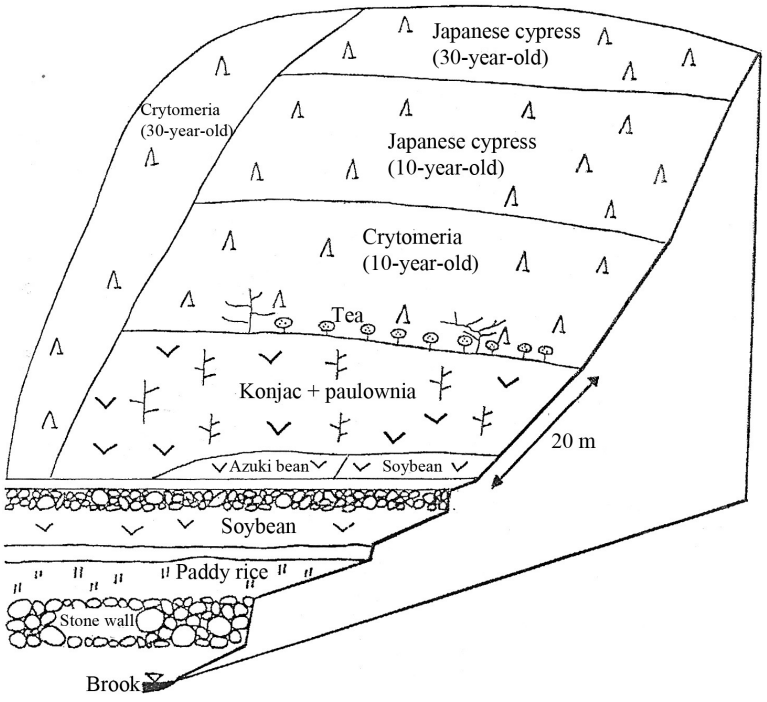

Figure 1.9 Sketch of a typical "Jinenjo" field in Japan (adapted from Kurihara, 1979).

Under modern (intensive) cropping systems ("Uedama system"), however, corms are grouped by age and planted separately without intercropping with shade plants (Kurihara, 1979; Douglas *et al*., 2006). Typically, offsets are propagated at a high planting density for one year in order to establish propagation material for subsequent growing seasons (Douglas *et al*., 2005). After harvesting, older corms are sold and the remainder are stored in groups subdivided by age in ventilated warehouses over the winter months, for planting the following spring (Kurihara, 1979; Follett and Douglas, 2002; Douglas *et al*., 2006). Although the corm yields were reported to be higher under such cultural practice compared to the "Jinenjo" cultivation method, various problems such as increases in soil diseases and pests, growth retardation as a result of continuous cropping and reductions in corm quality, have been encountered under this cropping system (Kurihara, 1979). The major diseases affecting the crop are the bacterial soft rot erwinia (*Erwinia carotovora*) and fungal diseases such as fusarium (*Fusarium solani*) and pythium (*Pythium* species) (Follett and Douglas, 2002; Edison, 2010). Due to the scarcity of suitable land for konjac production, soils are often fumigated prior to re-planting, although crop rotation is the preferred option to control such soil-borne diseases. Moreover, winter barley is grown as a companion plant to konjac in early spring to reduce infection. By midsummer, barley is cut to form mulch which prevents soil splash onto the konjac, thus reducing the risk of infection from soil-borne rots (Follett and Douglas, 2002).

Over the past 30 years, the agronomy of konjac has been investigated, with most of the earlier work by the Japanese focussed on the traditional "Jinenjo" cropping system, in order to improve konjac production under modern management techniques (Kurihara, 1979). To date, five cultivars of konjac have been grown in

Japan, including Zairai (originated in Japan), Shina (originated in China), Haruna-kuro, Akagi-ohdama and Miyogi-yutaka. The latter three are hybrids, resulting from the cross-fertilization of Zairai and Shina. The Haruna-kuro and Akagi-ohdama cultivars constitute ~ 90% of the total Japanese corm production (Takigami and Phillips, 1996; Takigami, 2000).

Outside Asia, konjac has recently been studied as a potential new crop in the Waikato region of New Zealand (Follett and Douglas, 2002; Douglas *et al*., 2005; Douglas *et al*., 2006). Studies have focussed on the effects of shading, planting density, size of propagules and fertilizer on konjac production.

Earlier research conducted in the 1980s has shown that corm yields are generally increased by shading, but with contradictory evidence that up to 70% shade could either reduce, or increase yield (Miura and Osada, 1981; Seo *et al*., 1988). Miura and Osada (1981) found that corm weight was increased by 70% and 43% under 50% and 70% shade respectively, compared to plants grown without shade. Similar findings were reported by Seo *et al*. (1988) who said that corm yields were increased by 35% under 75% shade level, but with only a 20% increase under 50% shade. More recently, Douglas *et al*. (2005) reported that corm yield was increased by 45% and 70% under 30% and 70% shade respectively, using corms as propagation material. However, shading has no significant effect on corm yield when offsets were used as propagules (Douglas *et al*., 2005).

At a cellular level, the leaf anatomy of konjac plants grown under full sunlight, 30%, 50% and 70% shade was studied by Inaba (1984). According to this author, the thickness of the upper and lower epidermis, as well as the palisade and spongy mesophyll in leaflets decreased with decreasing light intensity. In addition, the total palisade cell surface area per unit leaf area decreased with decreasing light intensity

and the intercellular spaces in palisade tissue were larger in leaves developed under shade, than in those without shade. In the same year, Inaba and Chonan (1984) examined the ultrastructure of chloroplasts from plants grown under full sunlight, 50% and 70% shade. They demonstrated that the green area of leaves grown at full sunlight began to decrease from 40 days after leaf expansion, compared to leaves grown under the shade which maintained the fully expanded area for three months. Moreover, chloroplasts from plants grown at full sunlight had poorly organized grana consisting of 2 - 5 overlapping thylakoids, which began to separate two weeks after leaf expansion. By contrast, chloroplasts from plants grown at both 50% and 70% shade contained well-developed grana with more than 10 overlapping thylakoids, which remained intact for three months after leaf expansion. However, chloroplasts from plants grown at 50% shade were observed to contain more starch grains than those at 70% shade. Therefore, it has been concluded that the higher corm yields for plants grown under shaded conditions could be attributed to their higher photosynthetic rates (Miura and Osada, 1981; Inaba, 1984), lower respiratory activities (Miura and Osada, 1981) and delayed chloroplast senescence (Inaba and Chonan, 1984).

It has been shown that the size of corms used to establish a konjac crop has a large effect on the resultant yield (Miura and Watanabe, 1985; Follett and Douglas, 2002). Miura and Watanabe (1985) demonstrated that corm fresh weight and the number of offsets produced are positively correlated with the size of the planted corm. It has also been shown that the resultant yield is higher if corms of 300 - 500 g are planted (Long, 1995). Douglas *et al*. (2006) reported that crop yield after two growing seasons was increased by 9.8 g for every gram increase (x 10 factor) in planted corm weight of between 6.6 g - 260 g. The same group also devised an

equation ($\sqrt{number\ of\ offset\ produced} = -2.42 + log_{10}(harvested\ corm\ weight) \times 2.538$) to demonstrate the positive correlation between the harvested corm fresh weight and the number of offsets produced after two growing seasons. From the graph generated from this equation, a steep rise in offset production of up to ~ 40 from a harvested corm weight of 1 kg and below are observed, but in general, there was no increase in offset production above this corm weight (Follett and Douglas, 2002).

Planting densities vary considerably from one location to another depending on the size of propagule, cultivar, local custom and intended use (O'Hair and Asokan, 1986). Yield is usually higher as planting densities increase; however, production inputs such as fertilizer, water, as well as pest and disease control must be greater at high planting densities. Generally, individual plant weights decline under high planting densities due to the greater competition for space and light (Holliday, 1960; O'Hair and Asokan, 1986). A better understanding of the interaction between the size of propagule and planting density is therefore essential for investigating and optimizing corm yield and quality of konjac. In Japan, corms are planted in 1 - 1.2 m spaced rows with intra-row spacing adjusted to be three times the diameter of the planted corms (Douglas *et al*., 2005). In New Zealand, Douglas *et al*. (2006) conducted a trial in which corms with a mean weight of 55 g were planted at a uniform row width of 0.5 m and intra-row spacing of 0.7 (28570 plants/ha), 0.5 (40000 plants/ha) and 0.3 m (66670 plants/ha) for two consecutive years. Although increasing planting densities increased yield, it has been suggested that the planting densities used were too low to maximise yield, as no significant differences in individual corm weights were observed between each density treatment.

Fertilizers are generally applied both as basal and side dressings during the growth season and the application rate is dependent upon the soil type and nutrient level. Application of side dressing is recommended at one month after planting and best done in conjunction with soil mounding (Follett and Douglas, 2002). Research in Korea has shown the highest corm yields were produced with an application of 140:44:116 kg/ha NPK fertiliser (Lee *et al*., 1992). It has also been reported that crops in Japan are fertilised with 100 - 150 kg/ha NPK fertiliser, but with no details on the formulation (Douglas *et al*., 2005). A trial conducted by Douglas *et al*. (2005) in New Zealand has examined the effects of nitrogen (0, 75 and 150 kg/ha) and potassium (0, 100 and 200 kg/ha) fertiliser, with or without lime (3 t/ha) application on corm production. Lime application gave an 87% increase in total (corms and offsets) yield and also increased offset production. Application of potassium fertiliser (100 kg/ha) alone increased the total yield by three fold, but there was a strong depressive effect of nitrogen when applied in conjunction with potassium. These findings suggest that potassium has a critical role in corm development, while konjac may be adversely sensitive to predominantly nitrogen based fertiliser (Douglas *et al*., 2005).

1.6. Harvesting and processing of corms for konjac flour and KGM production

Time of harvest is an important factor affecting both the corm yield and quality. It has been shown that the glucomannan content of corms changes throughout the growing season and is highest just before the foliage dies off, prior to dormancy (Table 1.3) (Liu *et al*., 1998; Bown, 2000). Early harvesting before complete maturation of the corm may prevent it from initiating dormancy and biomass in the

foliage from partitioning into the corm, which in turn may hinder the terminal growth of the corm (Bown, 2000).

As mentioned previously, in Japan, older corms are harvested for sale in late autumn; the remainder are either left in the fields to continue growing the following season, or are stored in groups subdivided by age in aerated warehouses over the winter months (Kurihara, 1979; Follett *et al*., 2002; Douglas *et al*., 2006). In Southern China, corms may be left all year in the field (Kurihara, 1979) and are usually harvested for domestic use when they weigh ~ 200 g (may occur after one year of growth), or are left for 2 - 3 years and harvested at ~ 2 kg for commercial processing (Douglas *et al*., 2005). Whether or not konjac needs to be grown for one or more years to achieve a marketable crop is dependent on the size and quality of the planted corm. Typically in Japan, two-year-old corms are processed into flour, but for KGM production, the corms may be grown a further year to increase the glucomannan content (Takigami and Phillips, 1996; Takigami, 2000; WFS, 2003; Douglas *et al*., 2006).

Konjac flour has traditionally been prepared from fresh corms using a dry processing method. The sliced corms are first skewered onto bamboo sticks and dried by placing under the sun, or on a heated brick bed (Takigami and Phillips, 1996; Takigami, 2000; Zhao *et al*., 2010). The dried chips ("Arako" in Japanese) are then milled to flour using a mortar operated by a water wheel, followed by wind sifting to separate impurities such as starch from the glucomannan granules (Takigami and Phillips, 1996; Takigami, 2000; Parry, 2010). To date, the drying procedure is performed via hot air currents, generated either directly by coal burning, or indirectly through heat transmission from coal burning in order to avoid direct contact of sulphur dioxide fumes with the corm slices (WFS, 2003). Since the whole process

only involves drying and mechanical separation, it is hence known as “dry processing”. The milling operation breaks up starch granules, celluloses, ashes and nitrogen-containing materials which are present in the parenchyma cells (Takigami *et al*., 1997; Shi *et al*., 1998), into fine, ash-like powder, while KGM granules which are larger and harder remain unbroken. These differences in size and weight between the KGM and starch granules (Table 1.5), thus allow them to be isolated mechanically, via cyclonic separation and sifting (Liu, 2004; Zhao *et al*., 2010). The flour obtained using such methods has been classified as “common konjac flour” (“Seiko” in Japanese”) by the Chinese Ministry of Agriculture (Liu *et al*., 2002). It has a light brown colour, fish-like smell and a slightly acrid taste (Takigami and Phillips, 1996; WFS, 2003). Moreover, the purity of “common konjac flour” is low (consisting 60 - 70% glucomannan) and is used in making vegetarian foods such as noodles and fabricated meat pieces for culinary purposes (WFS, 2003). Micro-fine powder (“Tobiko” in Japanese) which consists mainly of starch, protein, ash and nitrogenous materials, on the other hand, is collected as a by-product and is commonly known as “konjac starch” (Takigami, 2000; WFS, 2003).

During November 2008, my supervisors and I made a visit to a konjac field and a processing factory (Fuyuan Golden Field Agricultural Products Company Ltd.) in Fuyuan County of Yunnan Province, one of the major konjac production areas in China (Edison, 2010). It was observed that the procedures employed by this factory for the production of “common konjac flour” (Figure 1.10) are similar to those previously described. After harvesting, two and three-years-old corms were brought to a storehouse and inspected for any damage, rotting or other disease symptoms. Disease-free corms were subsequently transported to a washing apparatus by conveyer belts and washed to remove dirt and soil. The cleaned corms were then

sliced into chips of 2 - 3 mm in thickness, prior to drying in a hot air drier. The dried chips were subsequently milled (40 – 60 mesh), followed by sieving to isolate the glucomannan granules from the freshly milled flour to form the “common konjac flour”.

Figure 1.10 Various stages of the production of "common konjac flour" from fresh corms. Photographs taken during a personal visit to Fuyuan Golden Field Agricultural Products Company Ltd, Yunnan Province, P.R. China in November 2008. **(1)** Selection of disease-free corms for flour production. **(2)** The corms are transported to a washing apparatus by conveyer belts and are washed to remove dirt and soil. **(3)** The corms are sliced into chips of 2 - 3 mm in thickness. **(4)** The fresh chips are dried in a hot air drier to remove moisture. **(5)** The dried chips are milled to produce crude konjac flour. **(6)** Removal of micro-fine powder (*i.e.* impurities) from the crude flour via sieving.

As mentioned previously, “common konjac flour” produced via the “dry processing” method contains 60 - 70% glucomannan and the low purity of this flour was shown to be due to considerable quantities of micro-fine powder (*i.e.* impurities) which remain adhered to the surface of the glucomannan granules after sifting, as observed by Takigami (2000) under SEM. In recent decades, various methods have been developed for the purification of konjac flour with the use of chemicals or organic solvents for KGM extraction and have collectively been known as “wet processing”.

To date, the most common form of “wet processing” of konjac flour involves alcohol (ethanol) precipitation of KGM (Takigami, 2000; WFS, 2003; Parry, 2010). Considerable success in producing high quality purified konjac flour which retains the physicochemical properties of KGM have been reported by Sugiyama *et al*. (1972) and Ogasawara *et al*. (1987) using this method. The working principle and procedures involved in both Ogasawara’s and Sugiyama’s methods are similar (Sugiyama *et al*., 1972; Ogasawara *et al*., 1987; WIPO, 1993), with differences in the duration of ethanol extraction and hydration treatment of konjac flour. In both methods, the konjac flour was stirred continuously (3 - 10 days) in different ethanol concentrations ranging from 50 - 100% (v/v) to remove soluble starch and low molecular weight sugars (D-fructose and D-mannose), followed by oven-drying (60 - 90 °C) of the resultant flour before being hydrated (3 - 12 h) to form a sol. As the sol produced was highly viscous, it was diluted up to 10 fold before being dialysed (72 h). The dialyzed solution was subsequently freeze-dried to form purified konjac flour. Using the Bertrand method, the total reducing sugar content of the purified flour produced using the Sugiyama’s method was shown to be 95% as D-glucose

(Sugiyama *et al*., 1972). The detail protocols for both methodologies are shown in Figure 1.11 and 1.12.

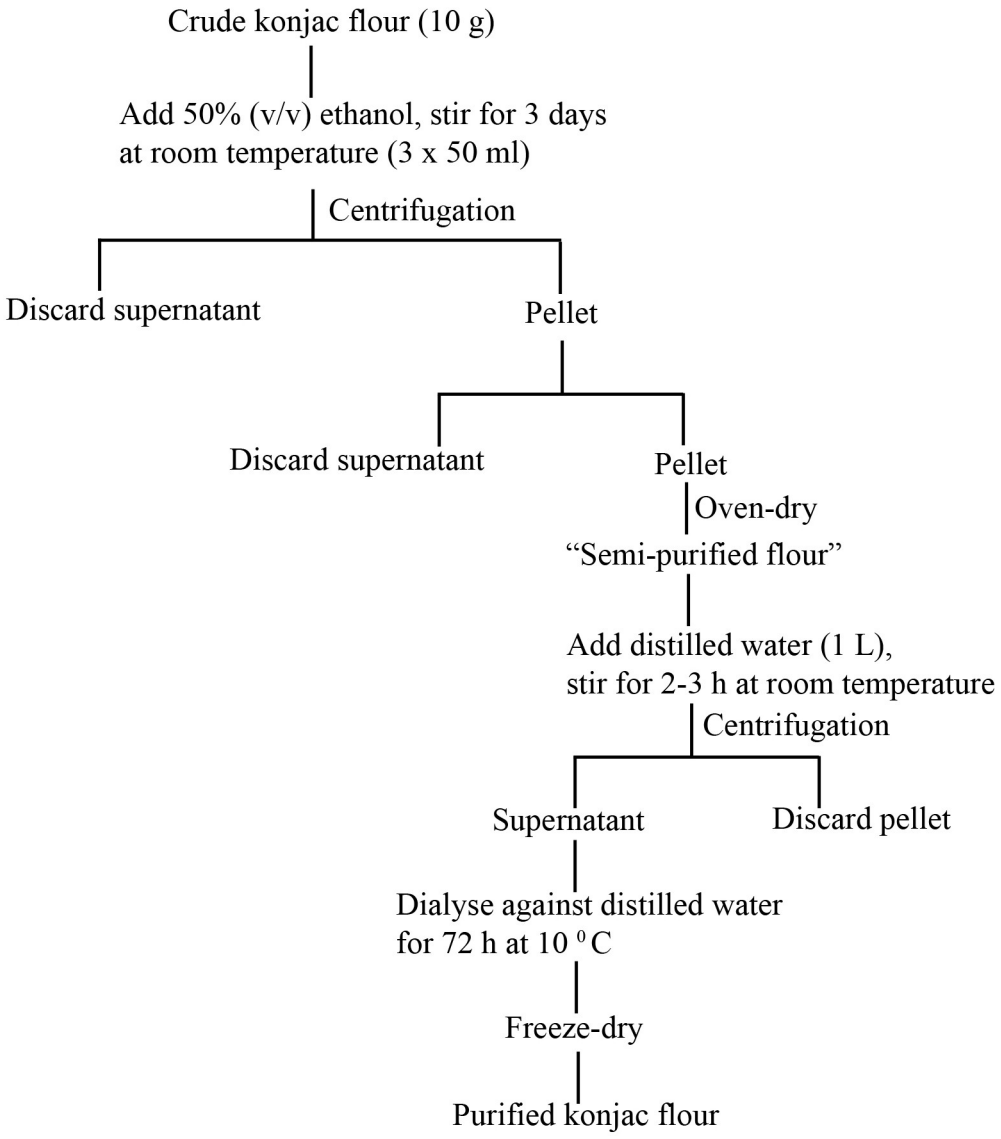

Figure 1.11 Protocol for the extraction and purification of konjac flour established by Sugiyama *et al*. (1972).

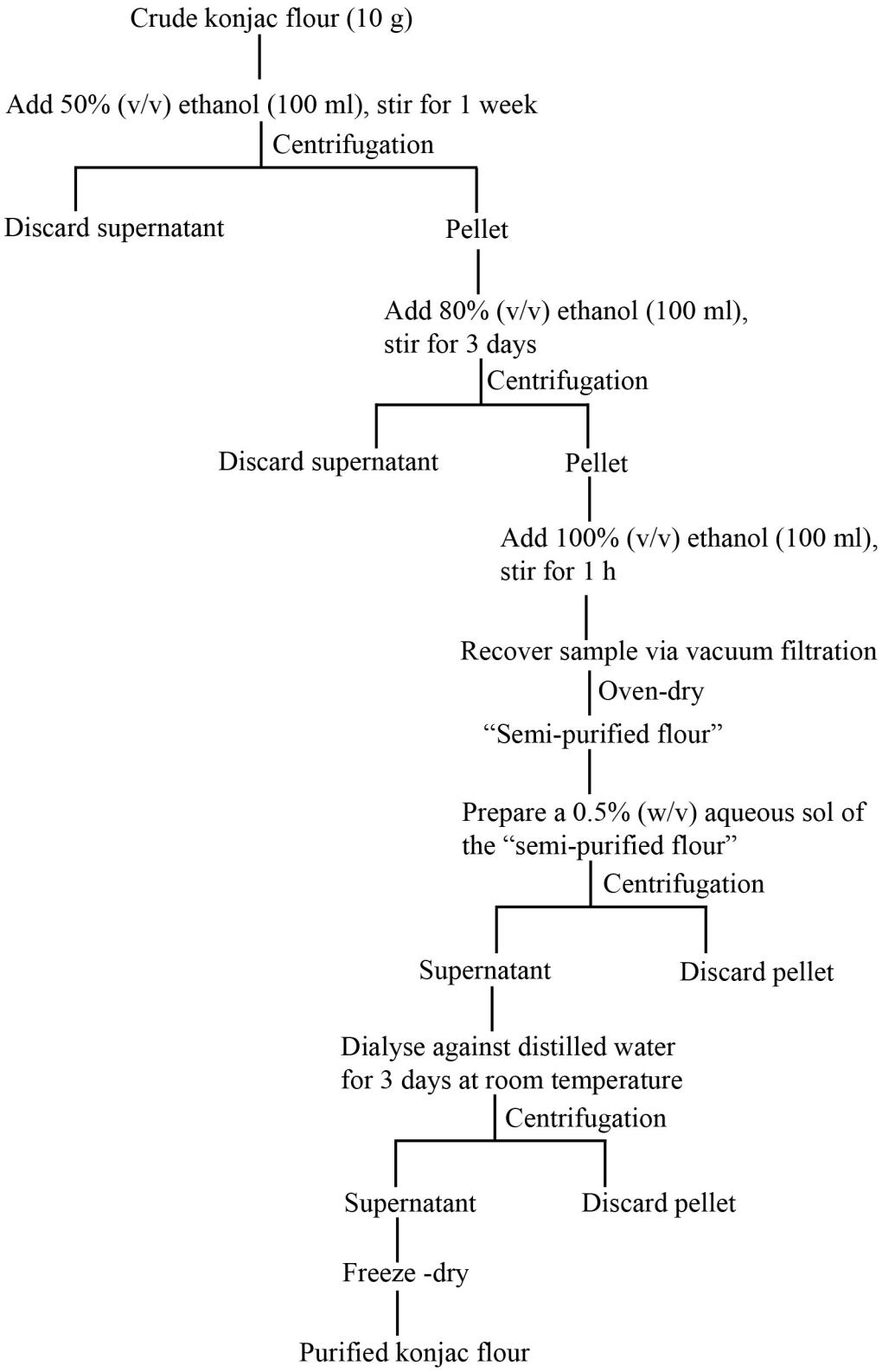

Figure 1.12 Protocol for the extraction and purification of konjac flour established by Ogasawara *et al*. (1987).

Wootton *et al*. (1993) described a purification method using 2-propanol which enabled carotene to be produced as a side-product. This method involves peeling and slicing of fresh corms, followed by extraction with 2-propanol (5 x 10 ml) and filtration to separate the 2-propanol extract from insolubles, consisting mainly of glucomannan and starch. In this protocol, 2-propanol was used as it had been shown to dissolve carotenes present in the fresh corms, which could later be dried to produce a pure side-product. Starch present in the insoluble corm extract was removed by hydrolysis with *Bacillus licheniformis* α-amylases. This was performed by heating the extract at 75 - 80 °C until all the starch was gelatinised and then cooled to 40 °C, prior to the addition of hydrolysing enzyme. After the enzymatic treatment, the samples were heated in a microwave oven for 3 min to inactivate any remaining enzyme, followed by centrifugation to remove the insoluble impurities. The samples were subsequently dialysed and freeze-dried to form the purified konjac flour, which was shown to exhibit high water-solubility and good gelling properties.

In addition to the previously described methods, treating an aqueous sol of crude konjac flour with salt (aluminium sulphate, dicalcium phosphate, calcium phosphate or magnesium phosphate) at pH 10 or below to extract impurities has been disclosed in the Japanese patent 58-165758 and 59-227267 (WIPO, 1993). Both methods are characterized by the consecutive steps of: 1) preparing an aqueous sol of crude konjac flour (consisting glucomannan and insoluble impurities), 2) treating the sol with an extraction salt, 3) removing and discarding the insoluble impurities from the sol, 4) forming a glucomannan precipitate by treating the remaining aqueous sol with one or more water miscible coagulating agents (methanol, ethanol or 2-propanol), or water miscible polar organic solvents (acetone or ethylethyl ketone) and 5) isolation and drying of the glucomannan precipitate to form the purified

konjac flour. The individual steps and conditions of this method may be varied somewhat. The extraction salt may be added to the water either before, or after the aqueous dispersal of the crude konjac flour. In order to speed up this process, water is preferably heated to 85 - 90 °C. Furthermore, the most effective extraction salt and coagulant has been found to be aluminium sulphate and isopropyl alcohol, respectively. It has also been shown that the coagulant: glucomannan volume ratio of 2 - 3:1 is sufficient to recover glucomannan from the remaining aqueous sol (WIPO, 1993).

1.7. Regulatory status of konjac flour/konjac glucomannan

The detailed standards for the classification of konjac flour established by the Chinese Ministry of Agriculture, the European Commission and the U.S. Food Chemicals Codex are shown in Table 1.6. At present, there is no worldwide agreed regulatory standard for konjac flour, or KGM. Without such an agreed standard, KGM products are currently introduced to the general public as dietary supplements, functional foods, nutraceuticals or prescription herbal medicines, depending on the licensing policy established by the countries concerned.

For regulatory purposes, konjac flour with 60 - 75% glucomannan has been generally classified as “konjac flour”, “common konjac flour” or “konjac gum” (Table 1.6a), while those with > 85% glucomannan have been classified as “KGM” or “purified konjac flour” (Table 1.6b) (Byrne, 2001; Liu *et al*., 2002; U.S. Food Chemicals Codex, 2003). Moreover, the Chinese Ministry of Agriculture has sub-classified the “common” and “purified konjac flour” into 2 or 3 different grades, based upon the glucomannan, sulphur dioxide and moisture content of the flour (Liu

et al., 2002). The European Commission has also drawn a distinction between "konjac gum" and "KGM" (Byrne, 2001). Below are the definitions of each:

"*Konjac gum is a water-soluble hydrocolloid obtained from the konjac flour by aqueous extraction. Konjac flour is the unpurified raw product from the root of the perennial plant Amorphophallus konjac. The main component of konjac gum is the water-soluble high-molecular-weight polysaccharide glucomannan (more than 75%), which consists of D-mannose and D-glucose units at a molar ration of 1.6:1.0, connected by β-(1-4)-glycosidic bonds. Shorter side chains are attached through β-(1-3)-glycosidic bonds, and acetyl groups occur at random at a ratio of about 1 group per 9 to 19 sugar units. The main component, glucomannan, has an average molecular weight of 200 000 to 2 000 000*."

"*Konjac glucomannan is a water-soluble hydrocolloid obtained from konjac flour by washing with water-containing ethanol. Konjac flour is the unpurified raw product from the tuber of the perennial plant Amorphophallus konjac. The main component is the water-soluble high-molecular-weight polysaccharide glucomannan (more than 95% on a dry weight basis), which consists of D-mannose and D-glucose units at a molar ratio of 1.6:1.0, connected by β-(1-4)-glycosidic bonds with a branch at about each 50th or 60th unit. About each 19th sugar residue is acetylated. The main component, glucomannan, has an average molecular weight of 500 000 to 2 000 000*."

The definition of konjac flour given by the U.S. Food Chemicals Codex (2003) is: "*Konjac flour occurs as a cream to light tan powder. It is a hydrocolloidal polysaccharide obtained from the tubers of various species of Amorphophallus. Konjac Flour is a high molecular weight, non-ionic glucomannan primarily consisting of mannose and glucose at a respective molar ratio of approximately*

1.6:1.0. It is a slightly branched polysaccharide connected by β-1,4 linkages and has an average molecular weight of 200 to 2000 kDa. Acetyl groups along the glucomannan backbone contribute to solubility properties and are located, on average, every 9 to 19 sugar units. Konjac Flour is dispersible in hot or cold water and forms a highly viscous solution with a pH between 4.0 and 7.0. Solubility is increased by heat and mechanical agitation. Addition of mild alkali to the solution results in the formation of a heat-stable gel that resists melting, even under extended heating conditions."

Therefore, harmonization of monographic standards is needed to assess and ensure the quality of existing and future KGM products (Chan *et al*., 2009; Chua *et al*., 2010).

Table 1.6 Standards (% w/w) for the classification of konjac flour/KGM (Byrne, 2001; Liu *et al*., 2002; U.S. Food Chemicals Codex, 2003).

(a) Common konjac flour/ konjac gum/ konjac flour

	Chinese Ministry of Agriculture (common konjac flour)			European Commission (konjac gum)	U.S. Food Chemicals Codex (konjac flour)
	Top grade	First grade	Second grade		
Glucomannan (%)	70	65	60	> 75	> 75
Sulphur dioxide (g/kg)	1.6	1.8	2.0		
Loss on drying (%)	11.0	12.0	13.0	< 12	< 15
Total ash	4.5	4.5	5.0	< 5	< 5
Arsenic (mg/kg)	3.0	3.0	3.0	< 3	< 3
Lead (mg/kg)	1.0	1.0	1.0	< 2	< 2
Starch (%)	-	-	-	< 3	
Protein (%)	-	-	-	< 3	< 8

(b) Purified konjac flour/ konjac glucomannan

	Chinese Ministry of Agriculture (purified konjac flour)		European Commission (konjac glucomannan)
	Top grade	First grade	
Glucomannan (%)	90	85	> 95
Sulphur dioxide (g/kg)	0.3	0.5	< 0.004
Loss on drying (%)	10.0	10.0	< 8
Total ash	3.0	3.0	< 2
Arsenic (mg/kg)	2.0	2.0	
Lead (mg/kg)	1.0	1.0	< 1
Starch (%)	-	-	< 1
Protein (%)	-	-	< 1.5

1.8. Quantitative determination of KGM content

Glucomannan content is a key indicator for evaluating the quality of konjac flour (Byrne, 2001; Liu *et al*., 2002; U.S. Food Chemicals Codex, 2003). Two methods have been commonly used for the determination of glucomannan content. The first is the mannose-hydrazone method, and the second is the colorimetric method, which includes phenol-sulphuric acid (Dubois *et al*., 1956), 3,5-dinitrosalicylic acid (3,5-DNS) (Lindsay, 1973; Liu *et al*., 2002) and enzymatic colorimetric assays. The following are the descriptions of the working principles and established protocols for each of these methods.

1.8.1. Mannose-hydrazone method

The mannose-hydrazone method was first employed by the Japanese to determine the glucomannan content in corms of different *Amorphophallus* species (Ohtsuki, 1967). In this method, D-mannose sugars produced as a result of KGM acid hydrolysis are reacted with benz-hydrazine to form an insoluble precipitate, namely mannose-hydrazone ($C_6H_{12}O_6 + C_6H_5NH{\cdot}NH_2 \rightarrow C_6H_{12}O_5N{\cdot}NHC_6H_5 + H_2O$). Completion of this reaction, is then followed by isolation of the insoluble precipitate via filtering through a pre-weighed filter apparatus (Buchner funnel), washings of isolated precipitate with organic solvent, drying and weighing of the Buchner funnel after filtration. By subtracting the weight of the Buchner funnel before and after filtration, the amount of D-mannose sugars in the konjac flour sample is deduced. The glucomannan content is determined based upon the D-mannose to D-glucose ratio of KGM molecules in the sample analysed.

The optimal protocol for this methodology has been established by Wang *et al*. (2001) and is shown schematically in Figure 1.13.

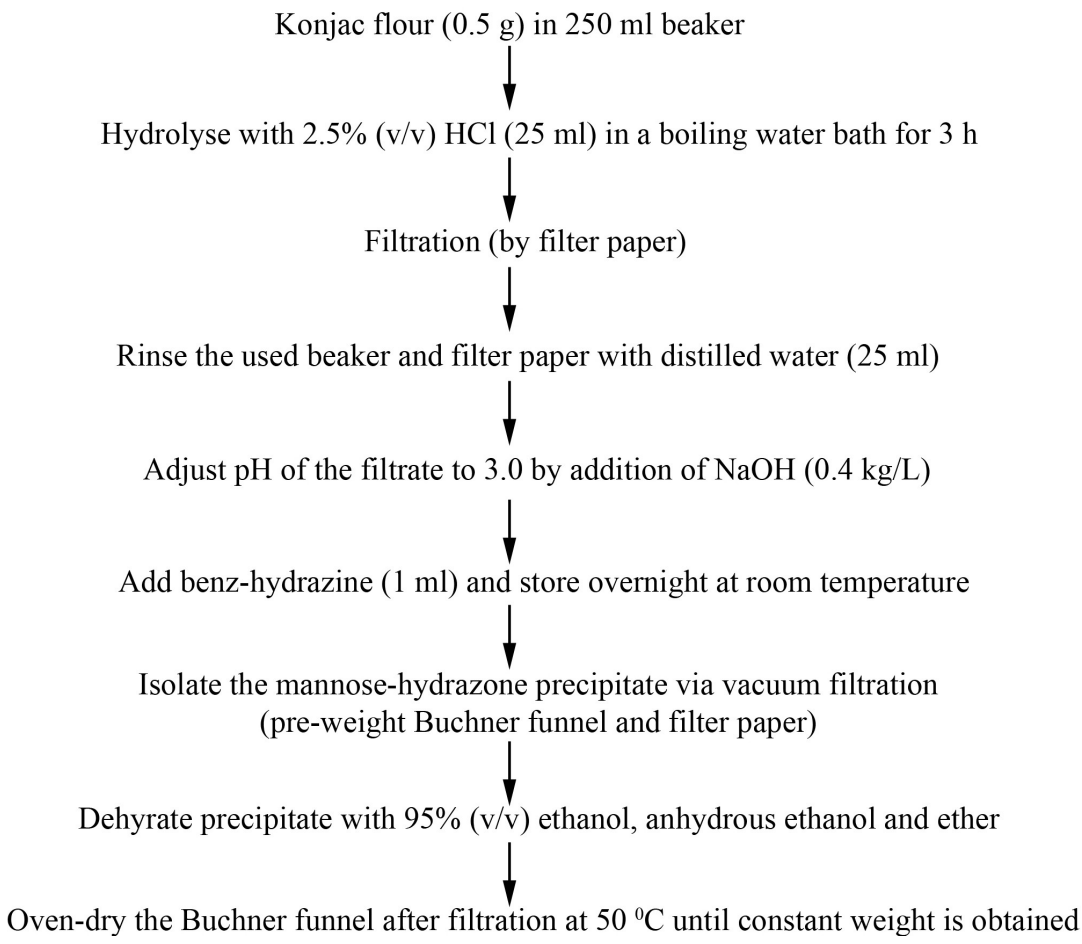

Figure 1.13 Protocol for the mannose-hydrazone method established by Wang *et al.* (2001).

1.8.2. Phenol-sulphuric acid colorimetric assay

Simple sugars, oligosaccharides, polysaccharides and their derivatives, including the methyl ethers with free or potentially free reducing groups (C=O), give an orange-yellow colour when treated with phenol and concentrated sulphuric acid. The colour intensity produced at a constant phenol concentration is proportional to the amount of sugar present (Dubois *et al*., 1956).

By use of this phenol-sulphuric acid reaction, Dubois *et al*. (1956) developed a method to determine submicro amounts of sugars and related substances. It has been reported that in conjunction with paper partition chromatography, this method is also

useful for the determination of the composition of polysaccharides and their methyl derivatives. In this method, the colorimetric reaction is performed by placing sugar solution (2 ml) into a colorimetric tube, followed by the addition of 5% (w/w) phenol reagent (1 ml). Concentrated sulphuric acid (5 ml) is then delivered rapidly into the tube with the stream of acid being directed against the liquid surface, rather than against the side of the tube in order to obtain good mixing. The tube is allowed to stand 10 min at room temperature and mixed prior to incubation at 25 - 30 °C for 10 - 20 min in a water bath. The absorbance of the characteristic yellow-orange colour is then measured at 480 nm for hexoses and 490 nm for pentoses and uronic acids. Blanks are prepared by substituting distilled water for the sugar solution. The amount of sugar may then be determined by reference to a standard curve which is constructed for the particular sugar under examination.

1.8.3. 3,5-dinitrosalicylic acid (3,5-DNS) colorimetric assay

The 3,5-DNS reagent was first used by Sumner (1925) for the determination of sugar in diabetic urine (Sumner and Howell, 1935). It was also used for the analysis of reducing sugars in syrups, fruit products and potatoes (Lindsay, 1973). More recently, this method was employed by the Chinese Ministry of Agriculture (Liu *et al*., 2002) for the determination of glucomannan content in konjac flour (Figure 1.14).

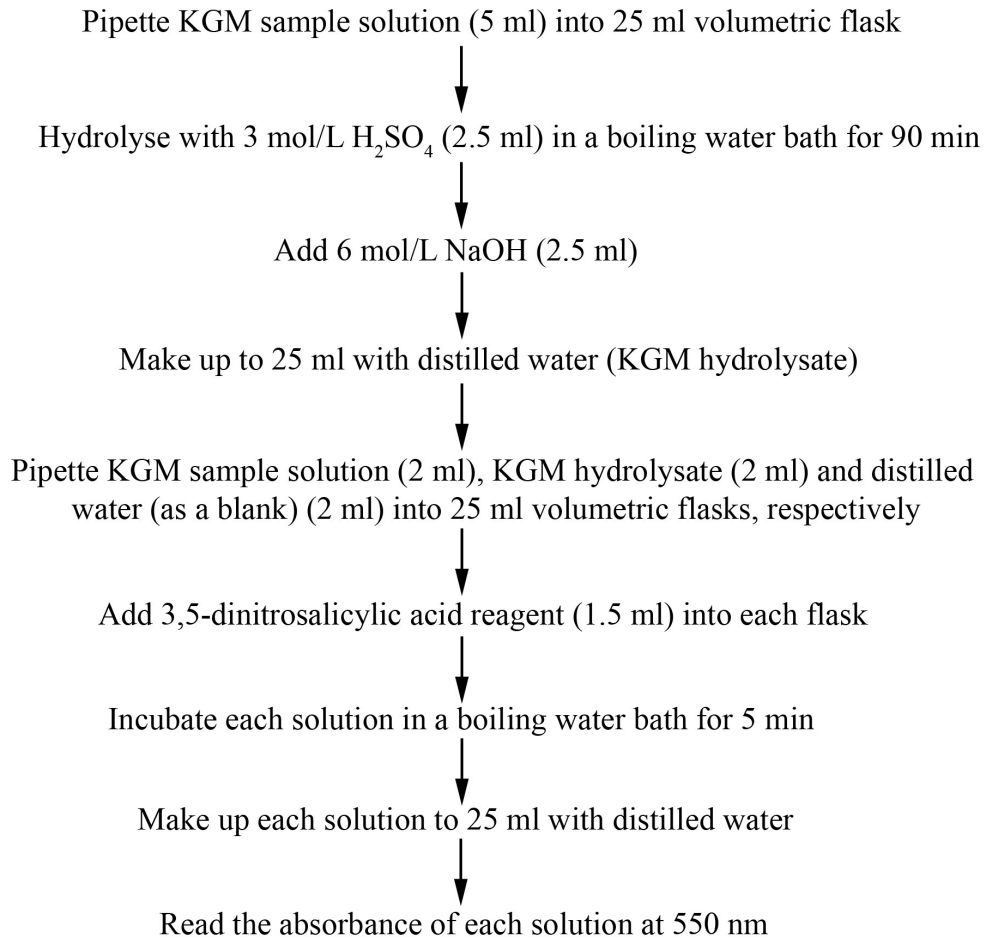

Figure 1.14 3,5-dinitrosalicylic acid colorimetric assay established by the Chinese Ministry of Agriculture (Liu *et al*., 2002)**.**

Reducing sugars, D-glucose and D-mannose, produced as a result of the acid hydrolysis of glucomannan, react with 3,5-DNS under alkaline conditions to form a brownish red amino-compound. This reaction involves the oxidation of aldehyde groups present in the reducing sugars to carboxyl groups, and simultaneously the reduction of 3,5-DNS to 3-amino-5-nitrosalicylic acid. The colour intensity of the amino compound produced is positively correlated to the amount of reducing sugars (Liu *et al*., 2002), which can be determined by measuring the absorbance at 550 nm. The 3,5-DNS reagent is composed of dinitrosalicylic acid, potassium sodium tartrate (Rochelle salt), phenol, sodium bisulfite and sodium hydroxide. Rochelle salt is

introduced to prevent the reagent from dissolving oxygen (as dissolved oxygen can interfere with glucose oxidation); phenol, to increase the colour intensity produced; and bisulfite, to stabilize the colour obtained in the presence of phenol. The alkali is required for the reducing action of sugars on dinitrosalicylic acid (Miller, 1959).

1.8.4. Enzymatic colorimetric assay

In 2004, the Megazyme International Ireland Limited developed an assay kit which determines the content of glucomannan in konjac flour (catalogue number: K-GLUM, see Appendix 1). The quantification of KGM using this kit is based on several enzyme reactions which are specific for KGM and its breakdown products (Figure 1.15). Free D-glucose, D-mannose or D-fructose in the flour extract are removed by aqueous ethanol (80% v/v) washing during the sample preparation steps. The first enzymatic reaction involves depolymerisation of acetylated-glucomannan by endo-β-mannanase to produce acetylated glucomanno-oligosaccharides. After depolymerisation into acetylated glucomano-oligosaccharides, the oligosaccharides are deacetylated by treatment at high pH. The resulting glucomanno-oligosaccharides are quantitatively hydrolysed to D-glucose (D-Glc) and D-mannose (D-Man) by the combined action of β-glucosidase and β-mannosidase. D-glucose and D-mannose are then phosphorylated by the enzyme hexokinase and adenosine-5-triphosphate (ATP) to glucose-6-phosphate (Glc-6-P) and mannose-6-phosphate (Man-6-P) respectively, with the simultaneous formation of adenosine-5-diphosphate. In the presence of enzyme Glc-6-P dehydrogenase, Glc-6-P is oxidized by nicotinamide-adenine dinucleotide phosphate ($NADP^+$) to gluconate-6-phosphate with the formation of reduced NADP (NADPH). The amount of NADPH formed in this reaction is stoichiometric with the amount of D-glucose. It is the NADPH which is measured by

the increase in absorbance at 340 nm. On completion of the reaction, Man-6-P is converted to fructose-6-phosphate and then to Glc-6-P by the sequential action of phosphomannose isomerase and phosphoglucose isomerase. Glc-6-P reacts in turn with $NADP^+$ forming gluconate-6-phosphate and NADPH, leading to further rise in absorbance that is stoichiometric with the amount of D-mannose.

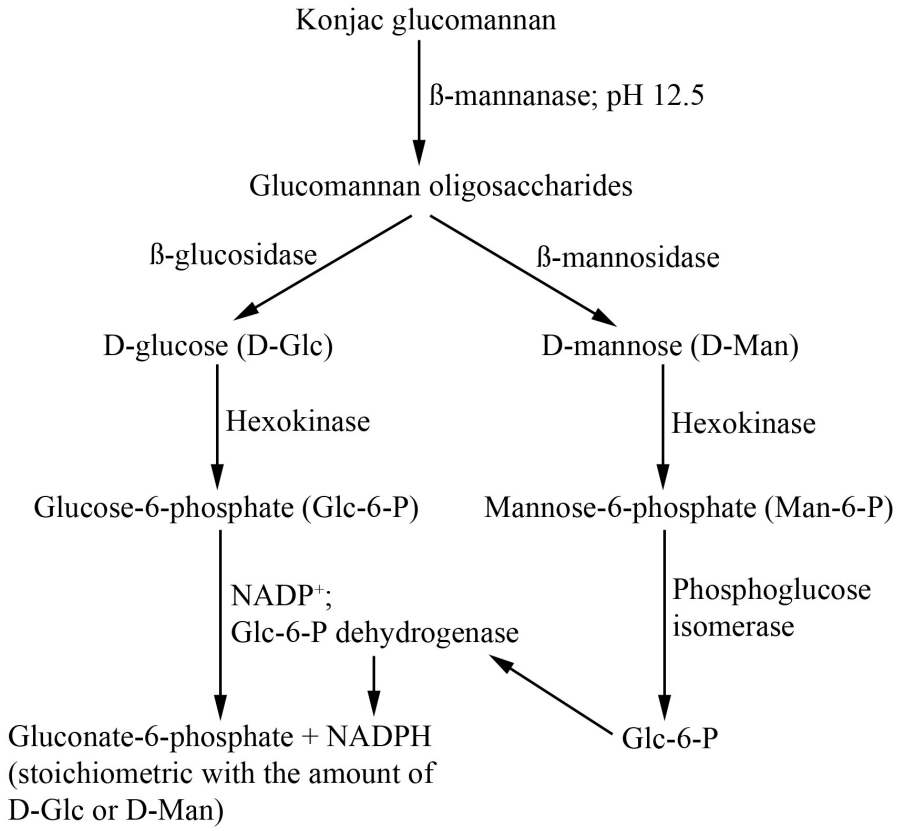

Figure 1.15 Enzymatic colorimetric assay established by the Megazyme International Ireland Limited, Ireland.

1.9. Aims and objectives of the current study

1. To study the morphogenesis and growth patterns of different-aged konjac plants grown under semi-controlled conditions, leading to an improved understanding of the growth and development of this species. The vegetative and reproductive growth cycles, as well as the morphological changes in both corm and offset structures at various developmental stages, including dormancy, were studied. In addition, an immunocytochemical analysis was performed to investigate the localisation of KGM within the glucomannan idioblasts (Takigami *et al*., 1997) and the developmental regulation of the deposition and metabolism of this storage polysaccharide in developing corm tissues. The immunoctyochemical investigation was performed at both the light microscope (LM) and transmission electron microscope (TEM) level using a well-characterised anti-mannan/glucomannan antiserum (Handford *et al*., 2003; Chen *et al*., 2006) on corms harvested at various developmental stages.

2. To assess the productivity of different propagation materials. For this purpose, the overall growth patterns and yields of both corm (one, three, four and five years-old) and offset materials were recorded and quantitatively compared for two consecutive growing seasons, *i.e.* 2009 and 2010. Moreover, the productivity of offsets produced by corms of different age was also compared.

3. To compare methodologies for the purification and analysis of KGM, to assist in the establishment of KGM monographic standards. Two extraction and purification methodologies were developed based on the working principles of both Sugiyama's (Sugiyama *et al*., 1972) and Ogasawara's (Ogasawara *et al*., 1987) methods. The yield, structure (degree of acetylation), composition

(glucomannan, starch and protein content) and physicochemical properties (molecular weight distribution and zero-shear viscosity) of the resultant purified konjac flours were then analysed. In addition, 3,5-DNS (Liu *et al*., 2002), phenol-sulphuric acid (Dubois *et al*., 1956) and enzymatic (purchased from Megazyme International Ireland Limited, Ireland) colorimetric assays were compared to identify the most appropriate method, with reference to reproducibility, precision and accuracy.

Chapter two: A morphological, histological and immunocytochemical investigation of growth and development in *A. konjac*

2.1. Introduction

A. konjac is a semi-shade, perennial, C_3 crop commercially cultivated in China and Japan (Imai and Coleman, 1983; Follett and Douglas, 2002; Douglas *et al*., 2006). Most often, konjac is planted in spring (March/April) and attains maturity after 6 - 7 months (October/November). In November, the foliage dies back and the plant over winters as a dormant corm for about 6 months, before re-emerging the following spring (Bown, 2000; Follett and Douglas, 2002). Typically, konjac plants do not complete a reproductive cycle, until they are at least four or five years-old (Imai and Coleman, 1983; Sun *et al*., 1995; Liu, 2004).

Wang and Liu (1990), who studied the growth and development of konjac plants throughout the vegetative growth cycle, observed that two months after planting (early July), reserve carbohydrates (*i.e.* glucomannan and starch) stored in the planted ("mother") corm were completely mobilized for early shoot development and the initiation of the "daughter" corm which formed on top of the degenerating "mother" corm (Figure 2.1). During this early phase of growth, the corm fresh weight was reduced by 1/60 of the total fresh weight on a daily basis. Upon leaflet emergence, the "mother" corm was completely degenerated and usually became detached from the "daughter" corm. At this time, the dry weight of the "daughter" corm was shown to constitute 7% of the final dry weight of the total plant recorded at the end of growing season.

From July to early August, vigorous leaf development took place, associated with the enlargement of the "daughter" corm via photosynthetic assimilates partitioned from the foliage. Moreover, during this active period of shoot development, the glucomannan and starch content in the corm were shown to increase by 110% and 690%, respectively. The highest net assimilation rate was recorded between mid August and late September, by which time the foliage was fully developed and mature. A daily gain of ~ 0.8 g in dry matter content of the "daughter" corm was recorded throughout this period, which appeared to be a critical stage influencing the yield and quality of the resultant mature corm. Towards the end of September, both the fresh and dry weight of the "daughter" corm was shown to constitute 63% and 50%, respectively of the total plant weight. From October onwards, the leaf gradually senesced, with the shoot subsequently detached from the underground corm structure, marking the beginning of the dormant period.

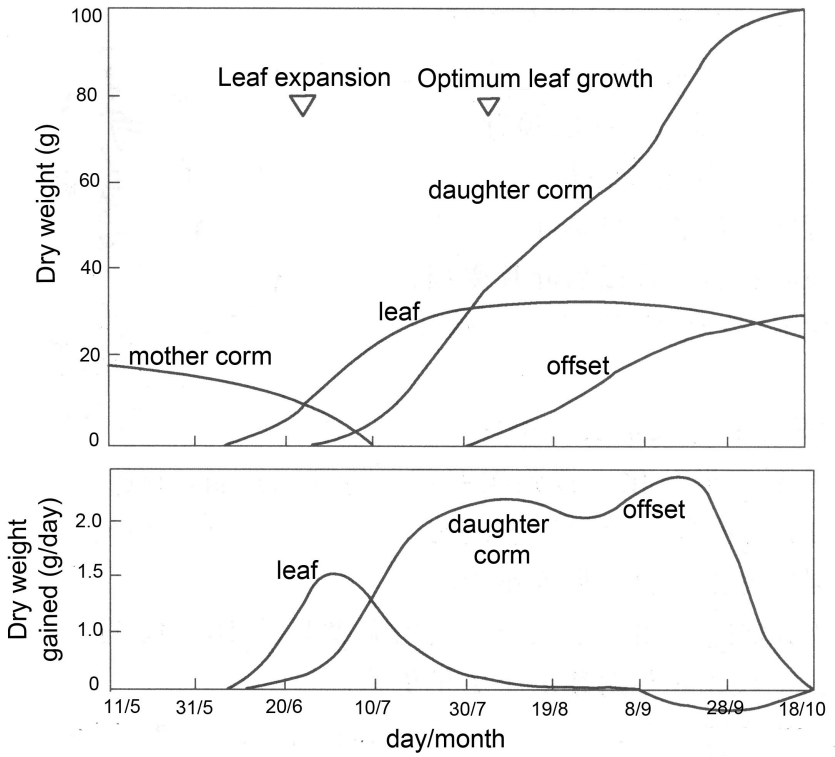

Figure 2.1 Changes in dry weight of different organs of *A. konjac* throughout a vegetative growth cycle (adapted from Wang and Liu, 1990).

To date, there have been few descriptions of morphogenesis in konjac plants grown under semi-controlled conditions. Moreover, there are no published reports of plant development from offsets, compared to full-size corms. At a cellular level, it has long been recognized that the corm tissues of konjac are a valuable source of glucomannan, a soluble, non-cellulosic polysaccharide (Liu *et al*., 1998; Bown, 2000; Takigami, 2000; Chua *et al*., 2010). However, studies of the cell biology of the developing corm tissue of this species are very limited. Previous studies have focussed primarily on the anatomy of the glucomannan idioblast and its surrounding parenchyma cells within the dormant corm tissues (Wakabayashi, 1957; Takigami *et al*., 1997; Shi *et al*., 1998). The detailed localisation of konjac glucomannan (KGM) within the idioblasts and the developmental regulation of the deposition and metabolism of this storage polysaccharide throughout a vegetative growth cycle have not been described previously.

In the current study, based on the preliminary observations reported by Wang and Liu (1990), corms and offsets were harvested at six stages of development, namely 1) dormancy, 2) leaf bud emergence, 3) leaf bud elongation, 4) leaflet emergence, 5) leaf expansion and 6) shoot senescence, to study the morphogenesis of underground plant structures in detail at each stage. Immunocytochemical analyses using an anti-mannan antiserum (Handford *et al*., 2003) were also performed on these samples to investigate the localisation and developmental regulation of KGM deposition in the developing corm tissues.

Moreover, corms of different ages and the growth potential of offsets from these different aged corms were compared, in order to assess the productivity of different propagation materials. Offsets provide a rapid means of propagule

multiplication if they can deliver growth rates that would be acceptable for agricultural production.

Therefore, the objectives of this component of my research were 1) to describe and analyse the morphogenesis of konjac plants under semi-controlled conditions, 2) to investigate the localisation and developmental regulation of KGM deposition and metabolism in corm tissues, 3) to compare the growth potential of different aged propagation materials and 4) to compare the growth and productivity of offsets produced by corms of different age.

2.2. Materials and methods

2.2.1. Propagation of plant materials

As described in section 1.5, konjac can be propagated either by seed or vegetative divisions. Establishment of plant material from seed was unsuitable for the current study as it is not used for commercial cultivation due to its high genetic variability (Edison, 2010). Vegetative propagation from corms or offsets is considered the most suitable option due to its potential to produce large numbers of plants from original stock and their subsequent rapid growth, and as such is used for commercial cultivation in both China and Japan (Liu *et al*., 1998; Long, 1998; Follett and Douglas, 2002; WFS, 2003; Douglas *et al*., 2005, 2006).

Konjac material comprising one, three, four and five-year-old corms obtained from Guangxi Province, P. R. China; and offsets purchased from the "Desert to Jungle Nursery", Somerset, UK was planted out in pots and grown in a shaded glasshouse (Cambridge Glasshouse Company Ltd, Cambridge) during March 2008 (Table 2.1). In November 2008, corms and offsets of this material were harvested. From the harvested material, 6 corms (*red font*) and 12 offsets (*pink font*) with

similar weights (74 ± 0.9 g and 3.1 ± 0.0 g, respectively) were selected for morphogenic and immunocytochemical analyses in the subsequent growing season (2009).

In addition, 8 corms (*i.e.* 2 x one-year-old, 4 x two-year-old, 1 x four-year-old and 1 x five-year-old) and 45 offsets (*green font*) were chosen for quantitative analyses during both the 2009 and 2010 growing seasons. Offsets were selected on the basis of their "mother" corm age, which was classified into one, two and ≥ four-year-old groups (Table 2.1). Each age group comprised of 15 offsets with a mean weight of 2.7 - 3.0 g at planting. Corm and offset materials propagated each season were labelled using a specific code system (Figure 2.2), which are used throughout this thesis for brevity.

Table 2.1 Data on propagules (corms and offsets) selected as experimental material at the end of the 2008 growing season. (a) Planting weight and age of propagules collected in 2008, and the number of offsets produced at the end of the growing season. (**b**) Planting weight of experimental propagules in March 2009.

		(a) 2008 growing season			**(b)** 2009 growing season		
Corm label	Origin	Age (years)	Planting wt. (g)	No. of offsets produced	Corm planting wt. (g)	Age (years)	Offset planting wt. (g)
AK3	China	3	444.2	8	**725.2**	4	5.3, **4.6**, **1.6**, 7.6, 6.0, 5.7, 5.8, **3.1**
AK4	China	4	484.5	4	**1092.1**	5	**2.2**, **4.5**, **4.4**, **1.5**
AK8	China	3	430.3	9	KGM analysis	4	**3.5**, **4.1**, **3.8**, 2.3, **1.8**, **2.7**, **2.0**, **2.3**, **1.9**
AK14	China	1	18.2	5	**74.0**	2	7.0, **3.1**, **2.8**, **2.5**, 2.1
AK15	China	1	15.7	4	**88.8**	2	4.3, 4.4, **3.6**, 1.8
AK16	China	1	14.5	6	KGM analysis	2	9.9, **3.6**, **3.1**, 4.3, **3.3**, **3.0**
AK17	China	1	17.1	4	**113.3**	2	**3.9**, **3.5**, **2.2**, 2.1
AK18	China	1	19.4	3	**112.9**	2	5.1, **3.2**, **2.6**
AK19	China	1	21.8	4	**109.1**	2	5.0, **3.7**, 1.8, 1.4
AK20	China	1	13.9	5	KGM analysis	2	5.4, 3.0, 2.9, **2.3**, 0.6
AK21	China	1	9.7	6	**72.3**	2	4.4, 4.3, **2.8**, **2.3**, 1.1, 0.3
AK22	China	1	10.5	6	KGM analysis	2	11.6, 6.8, **3.0**, **2.3**, 1.7, 1.1
AKD1-2	UK	0	3.2	7	Rotten	1	4.1, **3.5**, **2.1**, 2.1, 1.6, **2.8**, 6.9
AKD1/1	UK	0	3.3	5	**73.0**	1	**3.0**, **3.0**, 2.1, 1.6, 1.0
AKD1/2	UK	0	3.2	6	**74.2**	1	**3.1**, **3.1**, **3.1**, **3.0**, 2.0, 2.1
AKD1/3	UK	0	4.4	5	**73.5**	1	**3.7**, **3.1**, **2.8**, **2.5**, 1.8
AKD1/4	UK	0	2.9	7	**74.7**	1	**3.6**, **3.1**, **2.7**, **2.5**, **2.3**, **2.3**, 1.6
AKR1	UK	0	n/a	3	**26.7**	1	**2.7**, **2.3**, 1.1
AKR2	UK	0	n/a	3	**35.8**	1	**2.9**, **2.2**, 1.6

N.B. Green font: corm (8) and offset (45) materials used for quantitative analyses during the 2009 and 2010 growing seasons.
Blue font: corm materials (4) taken for KGM studies (trial experiments) at the end of the 2008 growing season.
Red font: corm materials (6) selected for morphogenic and immunocytochemical analyses during the 2009 growing season.
Pink font: offset materials (12) selected for morphogenic studies during the 2009 growing season.

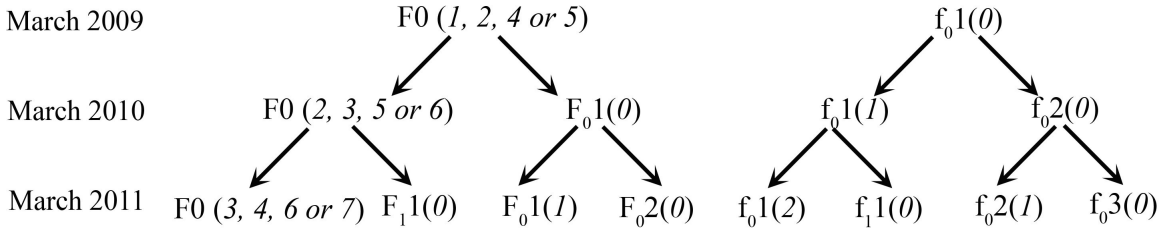

Figure 2.2 Labelling of corm and offset materials used for quantitative analyses during the 2009 and 2010 growing seasons. Corms and offsets planted in March 2009 were referred to as F0 and $f_0$1, respectively. The age of propagated material in each year is shown in parentheses. The offsets produced during each season were regarded as 0-year-old materials. F = "mother" corm line; f = offset line.

2.2.2. Glasshouse conditions

The glasshouse (33'4'' long x 15'6'' wide) used for this study is located at the Crop Technology Unit, University of Wolverhampton. As indicated in section 1.3.3, konjac is a shade-loving species and previous research has shown that konjac grown under 50% shade produces a higher corm yield than without shade (Miura and Osada, 1981; Douglas *et al*., 2005). In the current study, 50% Sarlon shade cloth was installed at the glasshouse, as shown in Plate 2.1, throughout the 2009 and 2010 growing seasons. The temperature and humidity (Table 2.2) were recorded using a thermohygrograph (Casella London) installed in the glasshouse.

Table 2.2 Temperature and humidity recorded in the Cambridge glasshouse throughout the (a) 2009 and (b) 2010 growing seasons (March - October).

(a) 2009 growing season

	Temperature (°C)		Humidity (%)	
Month	Minimum	Maximum	Minimum	Maximum
March	15.3	25.8	31.8	88.4
April	15.7	26.8	32.1	89.3
May	16.8	28.4	31.1	90.4
June	18.6	30.3	30.3	86.7
July	17.1	30.6	29.8	88.3
August	16.9	30.5	33.1	90.9
September	15.6	30.5	31.2	91.7
October	16.9	28.5	30.7	88.3
Mean ± SD	17 ± 1.0	29 ± 2.0	31 ± 1.0	89 ± 2.0

(b) 2010 growing season

	Temperature (°C)		Humidity (%)	
Month	Minimum	Maximum	Minimum	Maximum
March	15.1	26.2	31.9	89.3
April	15.8	27.1	31.3	90.8
May	16.2	28.9	30.8	86.4
June	17.5	31.5	30.4	89.2
July	18.1	31.8	31.8	90.5
August	17.8	32.1	32.8	91.5
September	16.2	31.2	32.0	89.6
October	16.0	29.8	31.2	90.5
Mean ± SD	17 ± 1.0	30 ± 2.0	32 ± 1.0	90 ± 2.0

2.2.3. Potting

All corm and offset materials were planted on 17th March for both the 2009 and 2010 growing seasons, except for the two oldest corms, AK3 and AK4 (Table 2.1), which were sown two weeks earlier due to their apical buds having developed faster than the other material. Konjac materials were planted in a compost consisting of 2 parts loam (EJ Godwin Peat Industries Ltd, Somerset, UK), 2 parts fine bark, 2 parts medium bark (EJ Godwin Peat Industries Ltd, Somerset, UK), 2 parts coir, 1

part perlite (William Sinclair Horticulture Ltd, Lincoln, UK) and 1 part grit (William Sinclair Horticulture Ltd, Lincoln, UK) (Hetterscheid and Ittenbach, 1996). As most of the roots develop from the upper corm surface (Lobin *et al*., 2007), the size of pot used was approximately 2.5 times larger than the corm diameter. This allowed the roots to grow into the surrounding compost. "Mother" corms (F0) were planted in 10 L pots, whilst offsets with weight < 1.5 g were planted in 0.5 L pots; 1.5 - 3.5 g in 1 L pots; 3.5 - 5.0 g in 1.5 L pots; 5.0 - 7.0 g in 2 L pots and > 7 g in 3 L pots. The pots were placed on free draining benches (Plate 2.1) and were watered thoroughly after planting.

2.2.4. Watering and feeding

Plants were watered twice a week and watering was stopped when they started to senesce (Plate 2.2). During the 2009 growing season, liquid fertilizer (N:P:K 20:20:20) containing trace elements (boron 0.02%, copper 0.01%, iron 0.20%, manganese 0.02%, molybdenum 0.002% and zinc 0.05%) (Chempak, Essex, UK) was applied every fortnight after leaflet emergence, until the onset of leaf chlorosis. However, during the 2010 season, NPK fertilizer was applied once after leaflet emergence. While not originally intended by the research team, this incident did allow comparison of plant growth with and without fertilizer.

2.2.5. Harvesting and storage

The optimum time for harvesting of konjac is after above ground senescence, when most of the photosynthetic assimilates are translocated to the corm (Liu *et al*., 1998; Bown, 2000). In the current study, corms were harvested from the end of October to early November in both growing seasons, after detachment of the above

ground plant structures from the corm (Stage 4; Plate 2.2), except for those which were selected for the morphogenic and immunocytochemical analyses (Table 2.1). For the later, corms and offsets were harvested at six developmental stages (one corm and two offsets for each stage), namely 1) dormancy, 2) leaf bud emergence, 3) leaf bud elongation, 4) leaflet emergence, 5) leaf expansion and 6) shoot senescence during the 2009 growing season. The morphological changes in underground structures at each developmental stage were examined via close observations, with changes in fresh weight and diameter since planting being recorded at each harvest. Immunocytochemical analyses (see section 2.2.8) were performed on corm material of each developmental stage and the dormant corm tissue was also viewed under a scanning electron microscope (SEM) (Zeiss 1530 VP FE-SEM, Carl Zeiss, USA). For the scanning electron microscopy, fresh corm samples were frozen (cryofixation) immediately after removal, in their native, hydrated state by liquid nitrogen and were subsequently visualised on a peltier cold-stage attached to the SEM.

At harvest, pots were emptied, the surrounding compost and dead roots were removed from the corm complex and any offsets attached to the "mother" corm were carefully removed with secateurs. Corm, offset and above ground plant materials (petiole and leaf) were weighed for each individual plant immediately after harvesting and the number of offsets recorded. The harvested material was stored in open containers in the glasshouse during the dormant period (November - March) (Plate 2.3). The dry weight of harvested plant materials were obtained after air-drying for approximately 5 months in the glasshouse.

2.2.6. Measurement of plant growth and development

Plant growth and development was assessed by non-destructive methods during the 2009 and 2010 growing seasons. Measurements concentrated on the above ground components, which included petiole length, leaf width and relative chlorophyll (RChl) content. These measurements were made once or twice a week, and the time span of vegetative growth from leaf bud emergence to shoot senescence was also recorded. Moreover, to construct the reproductive growth curve for the inflorescences produced by the AK3 and AK4 corms, the length of each flower bud was measured every two days until anthesis, with the timings of flower bud emergence, anthesis and senescence of the inflorescences being recorded.

For the measurement of morphological traits, petiole length was measured from the soil surface to the point of leaf spread; leaf width was measured across the widest leaf spread.

The relative chlorophyll (RChl) content was determined *in situ* using a Minolta SPAD-502 meter (Minolta Camera Co, Ltd), which measures the absorbance of infra red (IR) light passing through a leaf. The meter was composed of an IR source and a detector, which clamped together, thereby enclosing the leaf (Plate 2.4). Prior to use, the meter was calibrated by measurement of a known standard provided by Minolta. Readings were recorded on a scale between 0 to 100 RChl units, indicating increasing RChl content. Profiles of RChl units were made by sampling 10 (for F0) and 6 (for F_0 and f_0) randomly selected leaflets of a plant from which a mean value per plant was calculated.

2.2.7. Statistical analysis

Data were subjected to analysis of variance (ANOVA) using the "SPSS 16.0" computer software. The differences between means were compared by Least Significant Differences (LSD) at 5% level of probability ($P < 0.05$).

2.2.8. Construction of corm tissue maps and immunocytochemical analyses of corm tissues by light and transmission electron microscopy

2.2.8.1. Fixation, embedding and sectioning of corm material

Preparation of fixative

All steps of fixative preparation were performed in a fume-hood. To prepare 50 ml fixative, paraformaldehyde powder (2.0 g) was added into l X phosphate-buffered saline (PBS; 40 ml; pH 7.2) in a screw-topped bottle, which was pre-warmed in a 60 °C water bath. Drops of 1 M NaOH were then slowly added to the solution until all of the powder had dissolved. The bottle was shaken vigorously for 30 s, releasing the pressure every 5 to 10 s, and cooled on ice. The pH of the solution was then adjusted to 7 by addition of 1 M sulphuric acid. Subsequently, 25% (v/v) EM-quality glutaraldehyde (2 ml) was added into the bottle, followed by 0.1 M $CaCl_2$ (1 ml), sucrose (0.5 g) and 5% (v/v) Triton X-100 (1 ml), to increase the penetrability of the fixative. The solution was then made up to 50 ml by addition of 1 X PBS (pH 7.2) and was mixed thoroughly before being stored on ice. The constituents in the freshly made fixative and 10 X PBS (pH 7.2) stock solution are shown in Table 2.3 and Table 2.4. The fixative was made fresh immediately prior to fixation of plant tissues and was kept on ice.

Table 2.3 Constituents of the fixative.

Chemical	Concentration
Formaldehyde (freshly made from paraformaldehyde)	4% (v/v)
Glutaraldehyde (EM quality)	1% (v/v)
Triton X-100	0.1% (v/v)
$CaCl_2$	2 mM
Sucrose	1% (w/v)
1 X PBS (pH 7.2)	Add to 50 ml

Table 2.4 Constituents of 10 X PBS stock buffer (pH 7.2).

Chemical	Amount
NaCl	8 g
KCl	0.20 g
Na_2HPO_4	1.44 g
KH_2PO_4	0.24 g
Deionised water	Add to 1000 ml (adjusted to pH 7.2)

All manipulations of the tissue samples were performed under a well-ventilated fume hood and the samples were constantly agitated to enhance penetration of chemical solutions. All solutions were carefully introduced and removed with disposable, sterile, plastic Pasteur pipettes to avoid tissue shrinkage and too ensure preservation of cell structures as close to the natural state as possible.

Fixation

As mentioned in section 1.4, the tissue structure of dormant corms was previously observed using SEM by Takigami and colleagues at 0.5, 2.5 and 7.5 cm (mid-point of the corm) from the epidermis (Takigami *et al*., 1997). In the current study, in order to further investigate the localisation of KGM and the developmental regulation of the deposition and metabolism of this storage polysaccharide, three tissue samples were removed at each of three positions from cross sections of

cleaned corms; as shown in Figure 2.3, using a single-sided razor blade. The tissue samples were subsequently cut into 1 mm cubes whilst immersed in freshly prepared, ice-cold fixative, on top of a glass Petri dish containing ice, placed in an ice bucket. Samples were then transferred into fixative via a sterile, plastic Pasteur pipette into labelled glass vials containing ice-cold fixative. Subsequently, samples were incubated in fixative overnight at 4 °C with gentle rotation (Rotator, RT731, Agar Scientific, Essex, UK). During the fixation process, properly fixed tissues sank to the bottom of the vials.

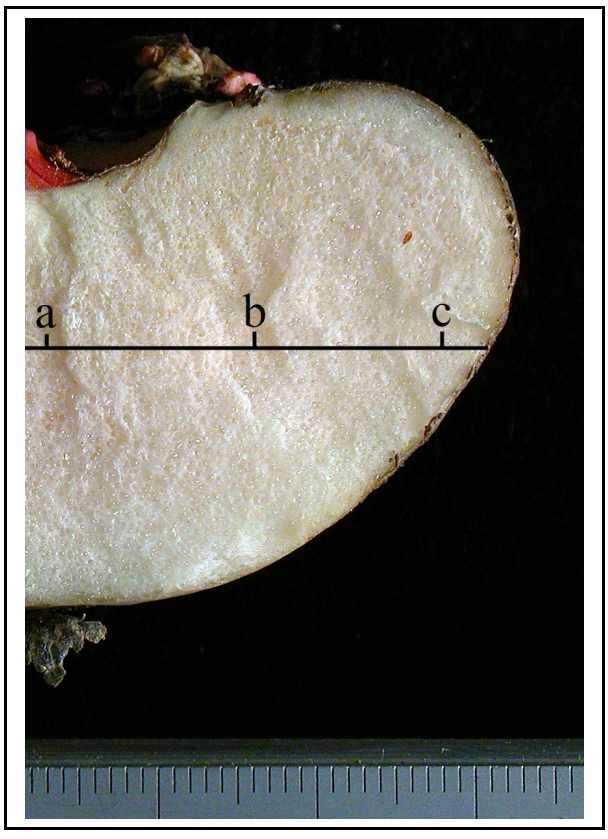

Figure 2.3 Cross section of a one-year-old corm, showing locations (*i.e.* a - c) from which tissue samples (*n* = 3) were removed for fixation and resin-embedding. (a) Mid-point of the corm, **(b)** a point approximately equidistant from the mid-point and the epidermis, **(c)** a point close to the epidermis.

Dehydration

Fixed samples were dehydrated for 60 min in each of the following percentages of absolute ethanol/deionised water: 10, 30, 50, 70, 90, 100 and 100% (v/v). Dehydration was carried out at room temperature with gentle agitation and each grade of the solution was changed every 30 min.

Embedding in L.R. White resin

Dehydrated tissues were infiltrated in a series of mixed solutions of absolute ethanol and L.R. White resin (Agar Scientific, Essex, UK; medium grade): (1) 3:1 mixture of 100% absolute ethanol : L.R. White resin for 2 h; (2) 1:1 mixture of 100% absolute ethanol : L.R. White resin overnight; (3) 1:3 mixture of 100% absolute ethanol : L.R. White resin for 8 h and (4) 100% L.R. White resin for 36 h with the solution being changed every 12 h. All infiltration steps were performed at room temperature with gentle agitation. Finally, each dehydrated corm tissue sample was embedded in a gelatine capsule (Agar Scientific, Essex, UK) filled with pure L.R. White resin and subsequently polymerised in a 50 °C oven for 8 h.

N.B. The L.R. White resin used for these procedures was stored at 4 °C and was left to equilibrate to room temperature prior to embedding.

Sectioning

Samples were cut from polymerised resin blocks using a hacksaw and the block surface was trimmed to give a trapezoid shape using a single-sided razor blade under an optic light source (Meta Scientific Ltd). For light microscopy (LM), semi-thin sections (1 μm) were manually cut on a Reichert-Jung Ultracut E ultramicrotome (Reichert-Jung, Vienna, Austria) using freshly made glass knives (LKB7801A Knife maker). Floating sections were collected, and transferred onto

droplets of sterile distilled water on polysine-coated glass slides (Agar Scientific, Essex, UK). The sample slides were then briefly dried on a 50 ºC hotplate until the water evaporated, followed by oven-drying at 50 ºC overnight.

For transmission electron microscopy (TEM), the sample block was first manually cut using a freshly made glass knife set at 1 μm for LM examination. LM sections were then stained with toluidine blue and viewed to identify areas of interest before reducing the size of the block face using a single-sided razor blade. The microtome was then switched to automatic cutting and sections were cut from the reduced block face at 60 - 90 nm in thickness using a diamond knife (Micro Star Technologies, Huntsville, USA) at a speed of 1 mms^{-1}. After the desired number of sections had been cut, the ribbon floating on the distilled water in the trough of the diamond knife was gently moved away from the cutting edge. Sections were grouped together in the middle of the trough using a single-hair brush. To expand the sections, a piece of filter paper was dipped into chloroform and held by a forceps close to, but not in contact with the sections for 6 s. Gold grids (200 mesh) (Agar Scientific, Essex, UK) were pre-coated with 0.5% (w/v) solution of Formvar in chloroform on the dull side. Each grid was held by watchmakers forceps and was lowered onto the sections which were then collected onto the Formvar-coated side of the grid. Each grid was then placed on filter paper with the section side uppermost and left to dry in a covered plastic Petri dish. Dried grids were subsequently stored at room temperature in a plastic, labelled grid holder.

2.2.8.2. Construction of corm tissue maps

Sections of corm tissues harvested at a variety of developmental stages embedded in L.R. White resin, as described previously, were cut at 1 μm using a Reichert-Jung Ultracut E ultramicrotome (Reichert-Jung, Vienna, Austria) and stained for 30 s with 1% toluidine blue, in 1% (w/v) sodium borate. Sections were examined under a bright field microscope and photographic images were taken under a Nikon 'Eclipse' ME600 microscope (Nikon Corporation, Japan). Cell outlines of the tissues were subsequently traced, by drawing onto a transparent laminating sheet placed on top of the images. The traces were then scanned on a photo scanner (HP ScanJet G2710, USA) to derive tissue map images at positions a, b and c (Figure 2.3) at each of the selected developmental stages.

2.2.8.3. Immunolabelling for light microscopy

For light microscopy, 1 μm sections were transferred to polysine-coated glass microscope slides (Agar Scientific, Essex, UK). Regions of the slides which contained sections were then circled using a hydrophobic pen and the slides were placed in a humidity chamber (Agar Scientific, Essex, UK). Sections were subsequently incubated in 0.1 M Na_2CO_3 for 30 min, then washed thoroughly with 1 X PBS buffer in order to expose any acetylated mannan epitopes (Handford *et al*., 2003). All sections were blocked in 10% (w/v) foetal calf serum (FCS), 2% bovine serum albumin in 1 X PBS, pH 7.2 for 30 min at room temperature to mask non-specific binding sites. Blocking buffer was then removed with filter paper before incubating the samples with the rabbit polyclonal anti-mannan antiserum (provided by Professor Paul Dupree, University of Cambridge), diluted 1:100 in blocking buffer at 4 °C overnight. The anti-mannan antiserum recognises β-1,4-mannosyl epitopes present within mannan, galactomannan and glucomannan (Handford *et al*.,

2003). Negative controls were performed by omitting the primary antibody. After being rinsed in blocking buffer (10 x 10 min), sections were incubated with the secondary antibody, *i.e.* Cy3-conjugated AffiniPure goat anti-rabbit IgG (H+L) antiserum (Jackson ImmunoResearch Laboratories, West Grove, PA, USA), diluted 1:100 in blocking buffer for 1 h at room temperature in total darkness. After being extensively washed in blocking buffer (10 x 10 min) and several rinses in 1 X PBS, followed by sterile deionised (DI) water, slides were shaken dry and mounted with an aqueous anti-fading mounting medium (Fluoromount, Sera Laboratories Ltd, Sussex, UK). Samples were then covered by coverslips, sealed with nail varnish and viewed under a Nikon ME600 Eclipse fluorescence microscope (Nikon Corporation, Japan). Live images were captured on the computer screen using a SPOT RT colour camera (Diagnostic Instruments Inc., Michigan, USA) accompanied with compatible software.

2.2.8.4. Immunolabelling for transmission electron microscopy

For transmission electron microscopy, ultra-thin sections were collected onto formvar-coated gold grids (200 mesh) (Agar Scientific, Essex, UK). Sections on TEM grids were pre-treated with 0.1 M Na_2CO_3 for 30 min for mannan epitope detection, followed by being rinsed thoroughly in DI water. After excess DI water was removed from the grid with filter paper, sections were incubated with the primary antibody (rabbit polyclonal anti-mannan antiserum) in blocking buffer at 4 ^{o}C overnight and washed extensively by being transferred through 8 drops of blocking buffer. Excess solution was removed from the grid with filter paper between each transfer. Negative controls were performed by omitting the primary antibody. Sections were then treated with secondary antibody, *i.e.* 12 nm colloidal

Gold-AffiniPure goat anti-rabbit IgG (H+L) antiserum (Jackson ImmunoResearch Laboratories, West Grove, PA, USA) at room temperature for 1 h in a humidity chamber. Secondary antibody was removed from the grid with filter paper. Sections were washed extensively by being transferred through 8 drops of blocking buffer. Excess solution was removed from the grid with filter paper between each transfer. The grid was transferred through 8 drops of DI water, excess DI water was removed from the grid with filter paper between each transfer. Sections were then stained with 2% (w/v) aqueous uranyl acetate (filtered through 0.2 μm filter) for 45 min at 37 ^{o}C in a humidity chamber. Grids were washed thoroughly by rinsing in ultra pure water three times. Excess solution was removed from the grid with filter paper between each transfer. Sections were stained with Reynolds lead citrate (filtered through 0.2 μm filter) for 7 min at room temperature. Grids were washed thoroughly by rinsing in 1 N NaOH once and ultra pure water three times. Grids were then dried by blotting onto filter paper and stored. Sections were viewed under a JEOL 1200EX transmission electron microscope (JEOL, Tokyo, Japan) at an accelerating voltage of 80 kV.

Plate 2.1 *A. konjac* plants growing in the Cambridge glasshouse, Crop Technology Unit, University of Wolverhampton.

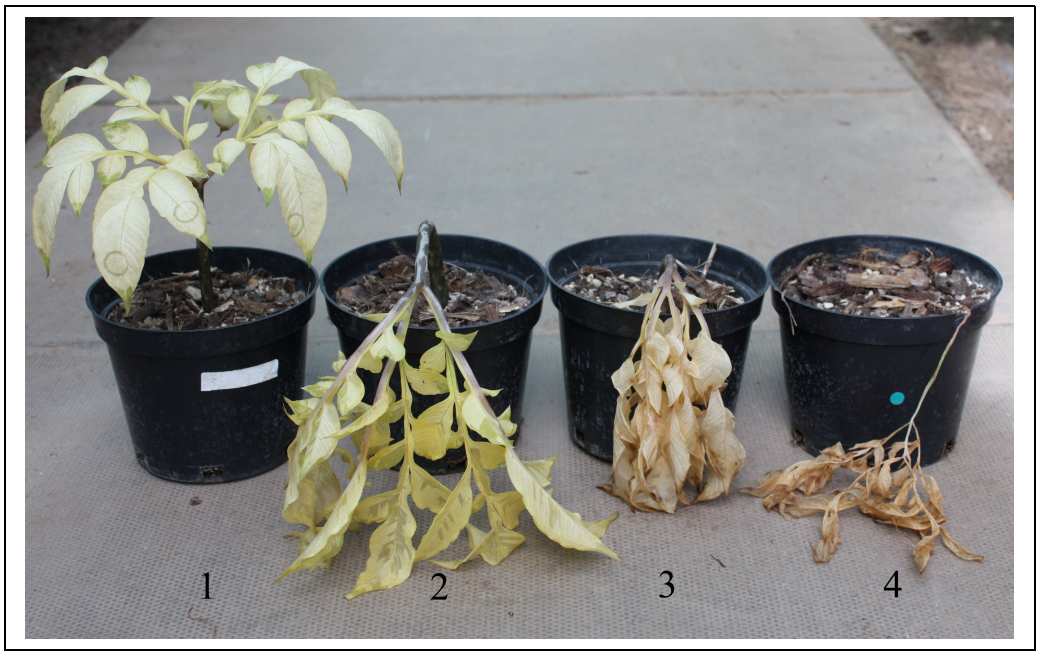

Plate 2.2 Developmental stages of konjac shoot senescence. (1) Stage 1: leaf chlorosis (defined as leaf giving a SPAD reading of zero). **(2)** Stage 2: collapse of petiole. **(3)** Stage 3: dying off of petiole and leaf. **(4)** Stage 4: detachment of petiole from corm**.**

Plate 2.3 Storage of corm and offset materials in open containers in the glasshouse over the dormant period (November - March).

Plate 2.4 Minolta SPAD-502 meter for determination of relative chlorophyll content. Whilst taking measurements of relative chlorophyll content, the head (composed of an IR source and detector) was closed to enclose the leaf material being analysed.

2.3. Results

2.3.1. Vegetative and reproductive growth cycles of *A. konjac*

During the 2009 and 2010 growing seasons, two distinct growth cycles, vegetative and reproductive, were observed in the konjac plants (Figure 2.4).

Apart from the two oldest "mother" (F0) corms, *i.e.* AK3 and AK4, each corm and offset started a vegetative cycle in both seasons by producing a leaf bud ~ 8 - 10 weeks after potting (mid to late May). The leaf bud then proceeded to elongate and leaflets subsequently emerged from the enclosed cataphylls a few days later. During the period late July to early August, the leaf canopy expanded to its full size and then senesced by the end of September. The corm then entered into a dormant phase for 5 to 6 months during the winter months, before the re-emergence of a leaf bud the following spring.

For AK3 and AK4, however, both floral and vegetative life cycles were observed during the growing season in both 2009 and 2010. Each corm first initiated a reproductive cycle (producing an inflorescence from a flower bud), followed by a vegetative cycle, with a leaf canopy being produced once the inflorescence had senesced (Figure 2.4g). For both AK3 and AK4, the winter dormant periods were observed to be considerably shorter, as the flower buds emerged 2 to 3 months before the leaf buds produced by younger corms. A latent period of approximately 2 months was also observed after the senescence of the inflorescence (Figure 2.4f), prior to leaf bud emergence.

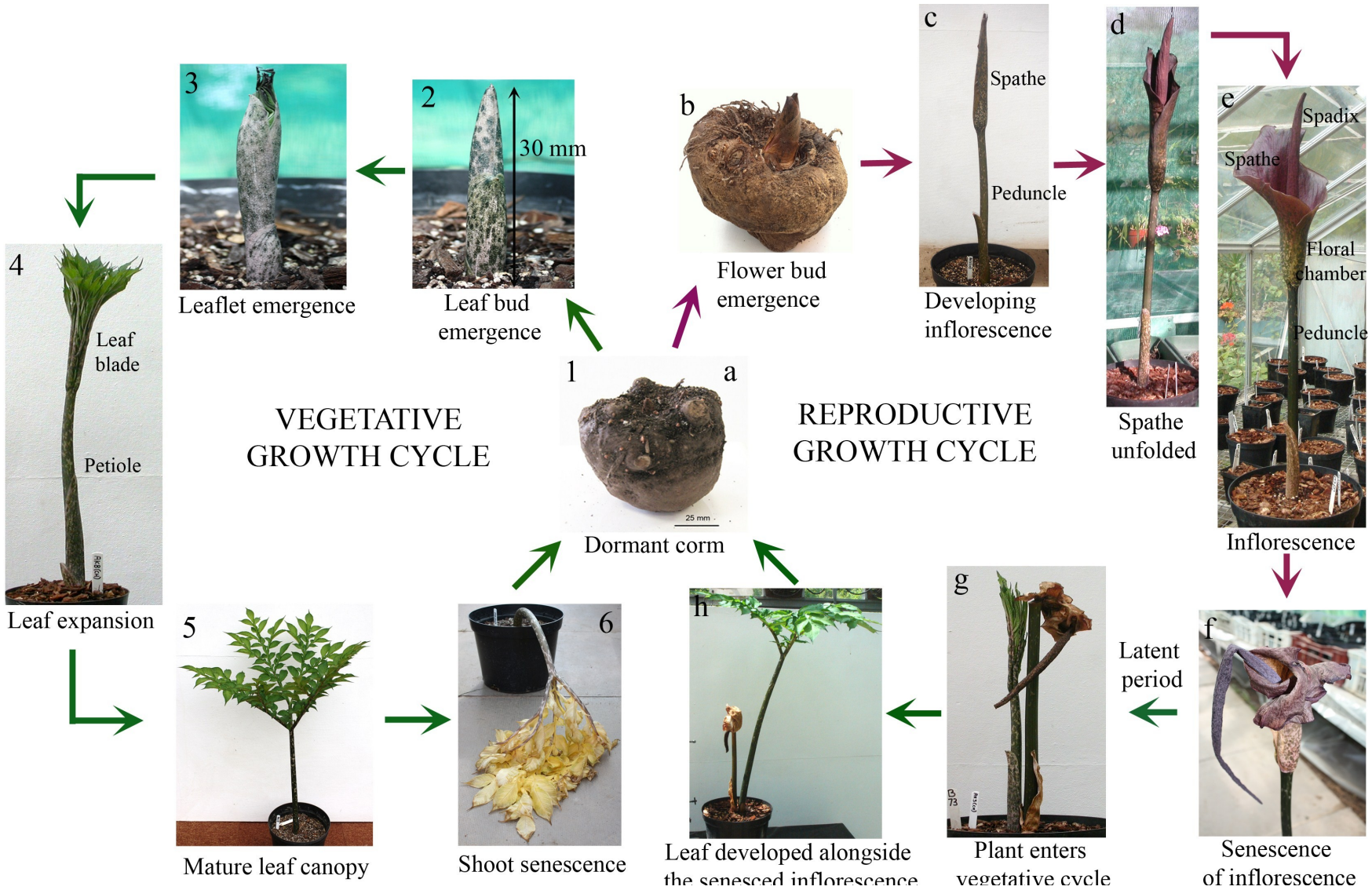
1
a
Dormant corm
2
30 mm
Leaf bud emergence
3
Leaflet emergence
4
Leaf blade
Petiole
Leaf expansion
5
Mature leaf canopy
6
Shoot senescence
b
Flower bud emergence
c
Spathe
Peduncle
Developing inflorescence
d
Spathe unfolded
e
Spadix
Spathe
Floral chamber
Peduncle
Inflorescence
f
Senescence of inflorescence
Latent period
g
Plant enters vegetative cycle
h
Leaf developed alongside the senesced inflorescence
VEGETATIVE GROWTH CYCLE
REPRODUCTIVE GROWTH CYCLE

Figure 2.4 Growth cycles of *A. konjac*. (1 - 6 and g, h) Green arrows indicate the vegetative growth cycle. **(a - f)** Red arrows indicate the reproductive growth cycle. **(1)** Corms entered into the dormant phase at the end of October. **(2)** Leaf buds emerged 8 - 10 weeks after potting (mid to late May). **(3)** Leaflets emerged from the enclosed cataphylls a few days after leaf bud emergence. **(4)** The petiole emerged from the leaf bud, with the formation of leaflets on the unfolded rachis. **(5)** In ~ 10 weeks time (late July to early August), the leaf blade was fully expanded, forming the leaf canopy. **(6)** Shoot senescence occurred 5 - 6 weeks after the development of mature leaf canopy (late September). **(b)** The flower bud emerged during early March. **(c)** The peduncle emerged from the flower bud with the formation of the unfolded spathe. **(d)** The spathe began to unfold ~ 2 weeks after flower bud emergence, with the appearance of a flower-bearing spadix. **(e)** The mature inflorescence was formed ~ 3 weeks after flower bud emergence. **(f)** The spathe and spadix collapsed ~ 10 days after anthesis. **(g and h)** The leaf began to develop alongside the dead inflorescence after a latent period of ~ 2 months.

2.3.2. Observations of the vegetative and reproductive growth cycles of *A. konjac*

The following descriptions of the development of both underground and above ground structures are taken from plants typical of the population grown during the 2009 and 2010 growing seasons. The quantitative relationships may vary between plants (see section 2.3.3), but the patterns of vegetative growth observed are representative for this species grown under the stated conditions.

First I shall describe the dormant phase, then the development of the corm and offset during the vegetative cycle, followed by the above ground morphogenesis during the reproductive cycle, and finally the above ground vegetative development, up to shoot senescence.

2.3.2.1. Morphology of corms of different age during dormancy

The variation in morphology of one to five-year-old corms during dormancy (early March) is shown in Figure 2.5. In general, the corms are globose and have a dorsoventral orientation. The dorsal surface possesses a depression in the central area from which the apical bud develops. The corm size increased with age, ranging from 5 to 11 cm in diameter, with four (AK3) and five-year-old (AK4) corms having a larger central depression. The apical bud, comprised of a leaf bud or flower bud, was enclosed by two or three cataphylls. Distinct differences in morphology were observed between flower and leaf buds. The leaf bud was arrow-shaped and the tip of the cataphyll was at the centre; whilst the flower bud was bell-shaped and the tip of the cataphyll was laterally placed. These differences became more marked as the bud elongated.

At the peripheral regions of the apical bud in all corms, densely-arranged concentric rings, which were the scars of the detached petiole from the previous growing season, can be seen (Figure 2.5: ib - ivb). Outside these regions to the upper corm edge, lateral buds arranged in concentric nodes were observed (Figure 2.6). At each node, one main lateral bud was found associated with many small ones. As shown in Figure 2.6, the main lateral buds were located at the intersection of two contact phyllotaxies, *i.e.* curve rows extending from the centre of corms. They were arranged in a phyllotactic pattern of 3 (clockwise or counter-clockwise directions) plus 5 (counter-clockwise direction), with buds from the first three nodes (1 to 3) surrounding the apical bud. At the ventral side, however, the number of lateral bud was fewer and the corm surface appeared to be smoother compared to the dorsal side.

At the base of some corms, remains of the degenerated corm (indicated by arrows) were observed (Figure 2.5: iia, iiia). Once the degenerated corm was removed, as shown in Figure 2.5 (iic), a scar marking the detachment could be found at the base of the corm.

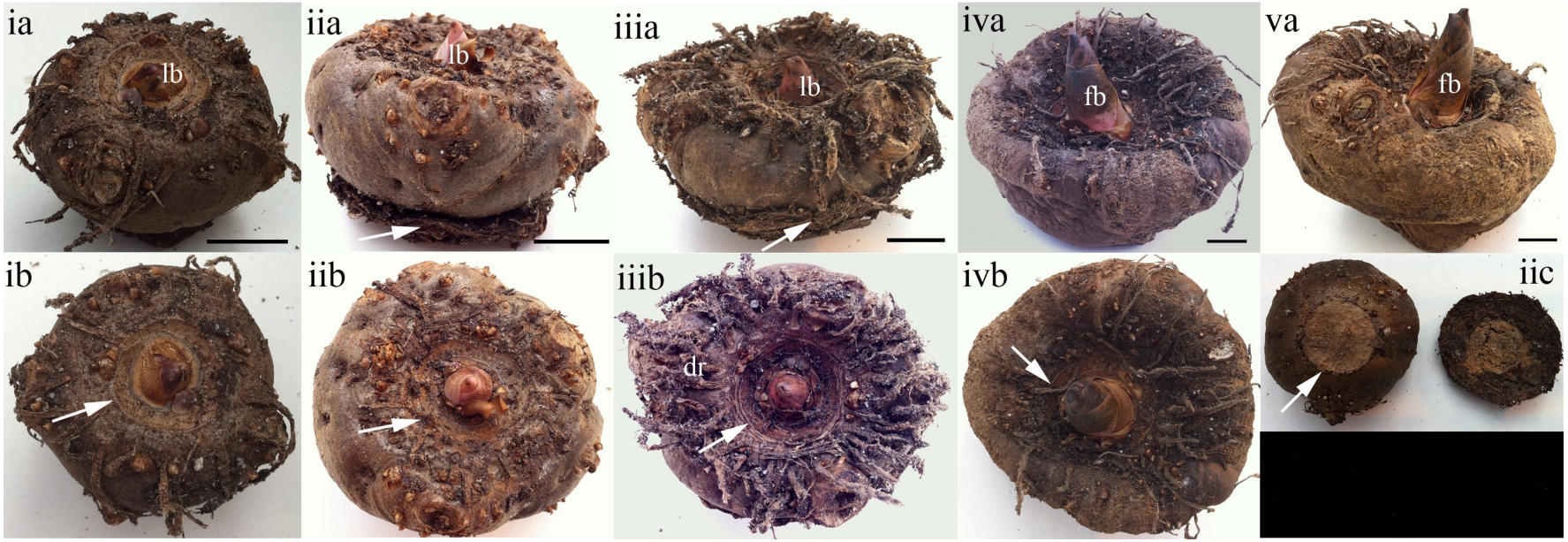

Figure 2.5 Morphology of F0 corms of different age at the end of dormant period (early March). (ia - va) Side view of one (27 g), two (109 g), three (430 g), four (725 g) and five (1092 g)-years-old corms, respectively. **(ib - ivb)** Top view of one to four-year-old corms, showing the scars of the detached petiole (indicated by arrows) from the previous growing season. **(iic)** Base of a two-year-old corm, showing the scar of the detached, degenerated corm (indicated by arrow). *lb* leaf bud, *dr* dried roots, *fb* flower bud. Scale bars = 30 mm.

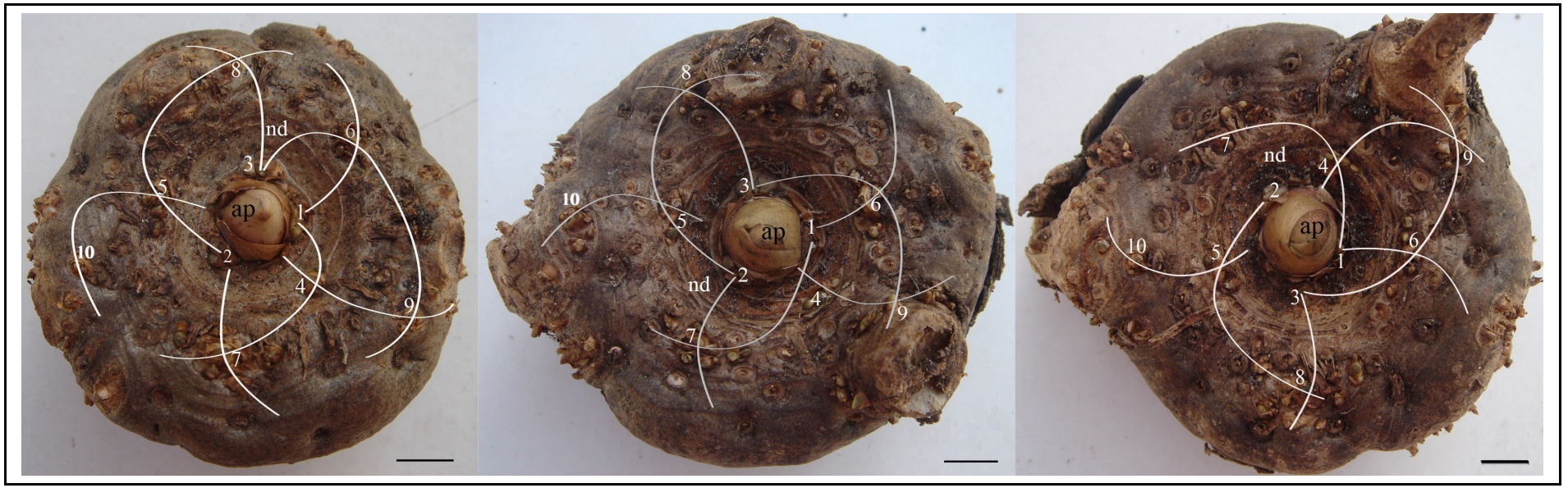

82

Figure 2.6 Positions of apical and lateral buds at the dorsal region of the F0 corms. The main lateral buds (indicated by numbers 1 - 10) were found at the intersection of two contact phyllotaxies (*i.e.* curve rows extending from the centre of corms) and were arranged in a phyllotactic pattern of 3 (clockwise or counter-clockwise directions) plus 5 (counter-clockwise direction). *ap* apical bud, *nd* node. Scales bars = 10 mm.

2.3.2.2. Morphogenesis of corm and offset throughout the vegetative growth cycle

As mentioned in section 2.2.5, during the 2009 growing season, one corm and two offsets of similar weights were harvested at six developmental stages, namely 1) dormancy, 2) leaf bud emergence, 3) leaf bud elongation, 4) leaflet emergence, 5) leaf expansion and 6) shoot senescence, in order to study the morphological changes occurring in the corms and offsets during the vegetative growth of the plant. The gross morphology of the plants developed from corms at each of the selected developmental stages is shown in Figure 2.7.

In the example presented (which was typical of a number of corms observed during the 2009 season), twelve adventitious roots, heavily branched with fibrous roots grew out from the apex of the corm (from the 4^{th} - 7^{th} nodes), when the leaf bud had reached 30 mm in length (Figure 2.7: 2). At this stage, the corm fresh weight was reduced by 10% and as the bud further elongated to a length of 90 mm (Figure 2.7: 3), a 31% reduction in corm fresh weight was recorded (Table 2.5).

Once the petiole (180 mm in length) had emerged from the leaf bud, with the formation of leaflets on the unfolded rachis that extended from the petiole (Figure 2.7: 4i), the corm fresh weight had decreased by 59%. As shown in Figure 2.7 (4ii), the ventral region of the corm was noticeably shrunken by this stage, with a ~ 5 mm reduction in corm diameter, compared to the size at planting.

Throughout the course of leaf expansion, during which petiole length reached 380 mm and leaf width ~ 450 mm (Figure 2.7: 5i), stolons (long etiolated stems) ending with developing offsets at the apices extended from the dorsal region of the corm (Figure 2.7: 5ii). No stolons were formed from the middle and ventral region of the corm. The offsets developed an apical bud and bore a physical resemblance to a cormel, with size ranging from 10 - 15 mm in diameter. Moreover, a mass of roots

were produced near the apex of the corm, as shown in Figure 2.7 (5ii), with a 40% gain in corm fresh weight during this stage.

Towards the end of growing season, during which shoot senescence occurred (Figure 2.7: 6i), there was an increment of 130% and 19 mm in corm fresh weight and diameter, respectively. The stolons remained attached to the corm, with larger offsets (15 - 25 mm in diameter) present at the apex, as compared to the previous developmental stage. As shown in Figure 2.7 (6ii), the roots were dying off at this stage, and upon removal of the withered petiole from the corm, a developing internal bud (for the next growth cycle) was visible at the apical growth point (indicated by arrow).

Table 2.5 Changes in F0 corm fresh weight and diameter throughout the vegetative growth cycle, recorded during the 2009 growing season.

		Fresh weight (g)		Diameter (mm)	
Developmental stage	Date of harvest	at planting	at harvest	at planting	at harvest
1. Dormancy	01/02/2009	-	72.3	-	50
2. Bud emergence	15/05/2009	74.0	60.7	50	45
3. Bud elongation	20/05/2009	74.7	51.4	48	44
4. Leaflet emergence	03/06/2009	73.5	29.8	45	40
5. Leaf expansion	01/09/2009	73.0	102.3	47	59
6. Shoot senescence	25/09/2009	74.2	170.6	51	70

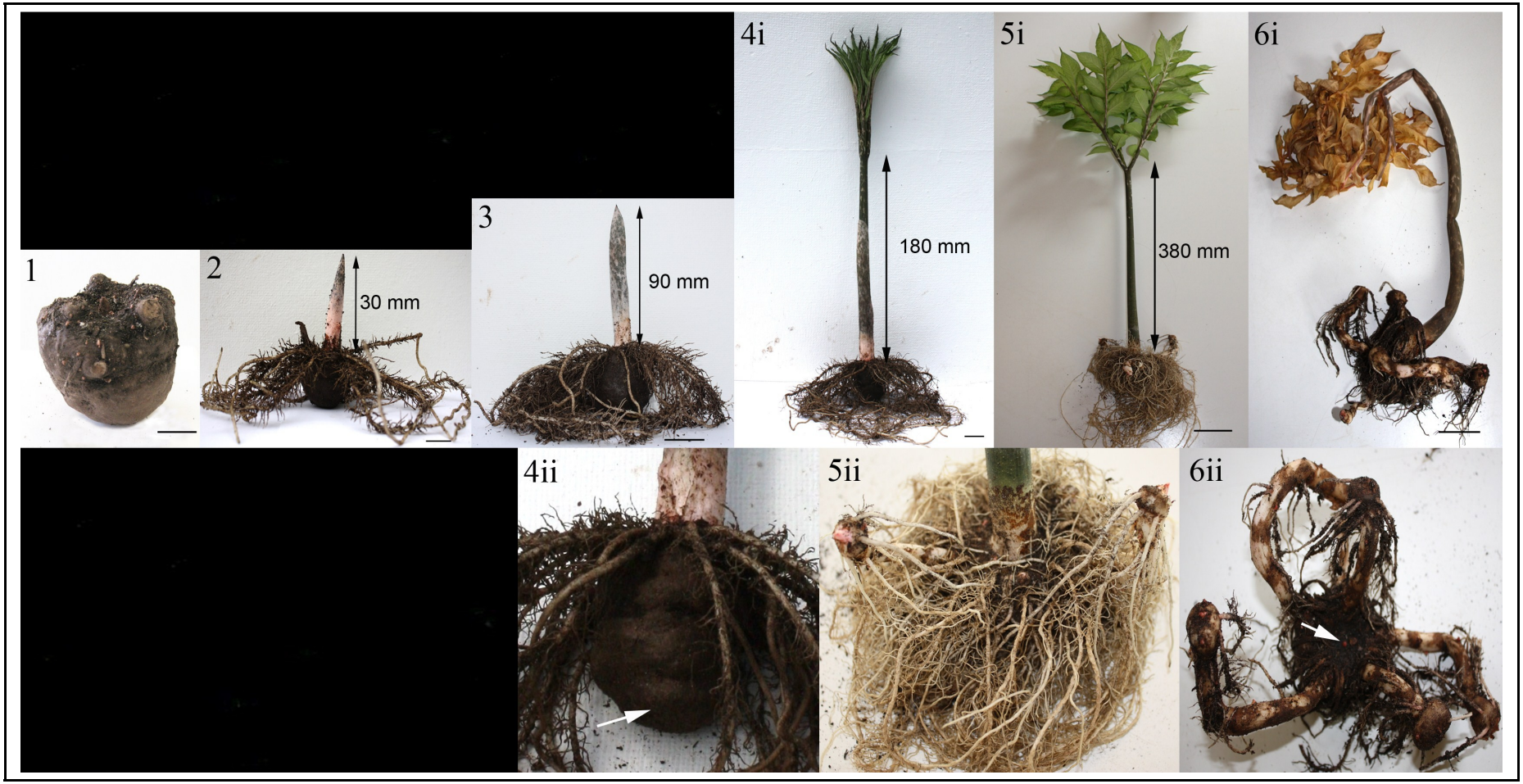

85

Figure 2.7 Selected developmental stages of the konjac vegetative growth cycle. **(1)** Dormancy (November - May). **(2)** Leaf bud emergence (mid May). **(3)** Leaf bud elongation (late May). **(4i)** Leaflet emergence (early June). **(4ii)** Shrinkage of ventral region of corm (indicated by arrow) during leaflet emergence. **(5i)** Leaf expansion (early September). **(5ii)** A mass of roots and stolons ending with developing offsets at the apex produced from the dorsal region of the corm during leaf expansion. **(6i)** Shoot senescence (late September). **(6ii)** The roots were dying off at the stage of shoot senescence, with an internal bud (indicated by arrow) developing for the next growth cycle visible at the apical growth point. Scale bars = 25 mm.

The morphology of plants developed from offsets, $f_0 1(0)$, during each of the selected developmental stages are shown in Figure 2.8. Compared to the F0 generation, offsets had more distinct nodes which were arranged in concentric rings and at each node only one main lateral bud was present (Figure 2.8: 1).

During leaf bud emergence (25 mm in length), 6 to 7 adventitious roots were produced from the base of the bud (Figure 2.8: 2) and the offset fresh weight was reduced by 26% (Table 2.6). As the leaf bud elongated to a length of 70 mm (Figure 2.8: 3), a 39% reduction in offset fresh weight was recorded, followed by a 65% reduction when the petiole (120 mm) had emerged from the bud and the leaflets had formed (Figure 2.8: 4).

During the course of leaf expansion, when petiole length reached 140 mm with a leaf width of ~ 250 mm (Figure 2.8: 5i), a mass of roots were produced from the dorsal region of the corm, with developing offsets ranging from 5 - 20 mm in diameter (Figure 2.8: 5ii). The developing offsets produced an apical bud covered with cataphylls, with a mass of adventitious roots growing out from the middle region (Figure 2.8: 5iii). In addition, remains of the degenerated offset (indicated by arrow) were found attached to the basal region of the corm (Figure 2.8: 5iv). An increment of 397% and 12 mm in fresh weight and diameter, respectively was recorded for the planted offset at this stage.

During shoot senescence (Figure 2.8: 6i), the fresh weight of the planted offset increased progressively by 574%, with a 16 mm gain in diameter. As shown in Figure 2.8 (6ii), the roots and stolons were dying off at this stage and a developing internal bud (for the next growth season), was found at the apical growth point. After ~ 3 weeks, during which time the aerial part of the plant had fully senesced, stolons

bearing offsets at the apices were completely dried out (Figure 2.8: 6iii) and eventually abscised from the corm.

Table 2.6 Changes in offset [$f_0 1(\theta)$] fresh weight and diameter throughout the vegetative growth cycle (n = 2), recorded during the 2009 growing season.

		Fresh weight (g)		Diameter (mm)	
Developmental stage	Date of harvest	at planting	at harvest	at planting	at harvest
1. Dormancy	01/03/2009	-	3.1	-	20
2. Bud emergence	22/05/2009	3.1	2.3	19	16
3. Bud elongation	26/06/2009	3.1	1.9	18	15
4. Leaflet emergence	07/06/2009	3.1	1.1	19	15
5. Leaf expansion	01/09/2009	3.1	15.4	20	32
6. Shoot senescence	21/09/2009	3.1	20.9	20	36

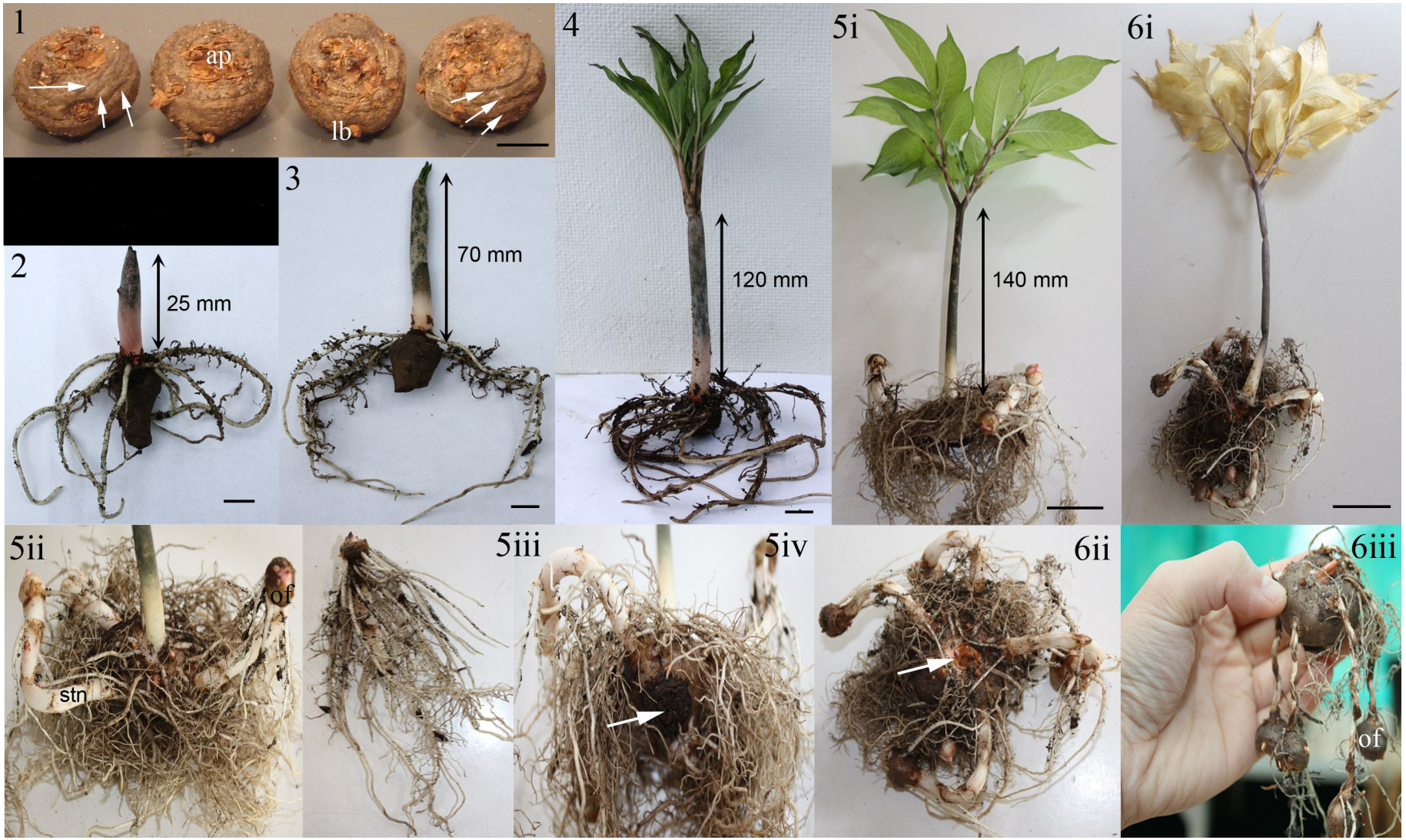
1
ap
lb
2
25 mm
3
70 mm
4
120 mm
5i
140 mm
6i
5ii
of
stn
5iii
5iv
6ii
6iii
of

Figure 2.8 Selected developmental stages of konjac plants developed from offsets throughout a vegetative growth cycle. (1) Dormant (November - May) offsets with distinct nodes arranged in concentric rings (indicated by arrows). **(2)** Leaf bud emergence (late May). **(3)** Leaf bud elongation (late May). **(4)** Leaflet emergence (early June). **(5i)** Leaf expansion (early September). **(5ii)** A mass of roots and stolons ending with developing offsets at the apices produced from the dorsal region of the corm at the stage of leaf expansion. **(5iii)** Roots growing out from the developing offset during leaf expansion. **(5iv)** The remains of the degenerated offset attached to the basal region of the corm during the course of leaf expansion. **(6i)** Shoot senescence (late September). **(6ii)** The roots and stolons were dying off during shoot senescence and an internal bud (developing for the next growth season) (indicated by arrow) was observed at the apical growth point. **(6iii)** The stolons were completely dried out after the leaf had fully senesced. *ap* apical bud, *lb* lateral bud, *stn* stolon, *of* offset. Scale bars = 10 mm.

2.3.2.3. Cellular morphology of corm tissues at selected developmental stages

Figures 2.9 - 2.14 show light micrographs of toluidine blue-stained corm tissues and corresponding tissue maps. Overall, the most abundant cell type observed was thin-walled parenchyma, in which several distinct cell types were embedded, namely amyloplasts, glucomannan idioblasts, calcium oxalate crystal idioblasts and vascular bundles.

The glucomannan idioblasts were single cells, the shape of which varied from circular to elongate (Figure 2.15), with diameters ranging from ~ 150 to 600 µm (up to 15 times larger than the surrounding parenchyma cells). At the early stages of shoot development (Figures 2.10b, 2.11 and 2.12b, c), the majority of glucomannan idioblasts appeared as empty, unstained cells. By contrast, at dormancy (Figure 2.9), and as the corm approached maturity/dormancy, *i.e*. at the stage of leaf expansion (Figure 2.13) and shoot senescence (Figure 2.14); numerous glucomannan idioblasts composed of densely-stained, thin-filmed mucilaginous material closely adhered to the idioblast cell walls were observed. Moreover, some glucomannan idioblasts were shown to contain a sol-like substance, either abundantly throughout the cell (Figures 2.9a and 2.13a), or near the periphery of the cell (Figures 2.10c, 2.11b and 2.13).

In accordance with the occurence of strongly stained glucomannan idioblasts, densely packed starch granules accumulated within amyloplasts were also shown to be abundant throughout the corm tissues at dormancy (Figure 2.9), leaf expansion (Figure 2.13) and shoot senescence (Figure 2.14). A marked decrease in the number of amyloplasts was also observed during the early stages of shoot development (Figures 2.11 and 2.12).

Two forms of calcium oxalate crystal idioblasts were found to be randomly distributed throughout the corm tissues: raphide idioblasts and druse idioblasts.

Raphide idioblasts were observed to be axially elongated and larger than neighbouring parenchyma cells. Each contained a densely-stained crystal bundle which extended almost the entire length of the idioblast and appeared to be surounded by mucilage in the central vacuole of the idioblast. The star-shaped druse crystals, on the other hand, were deposited in cells of similar dimension and appearance to the surrounding parenchyma cells, filling almost the entire idioblast.

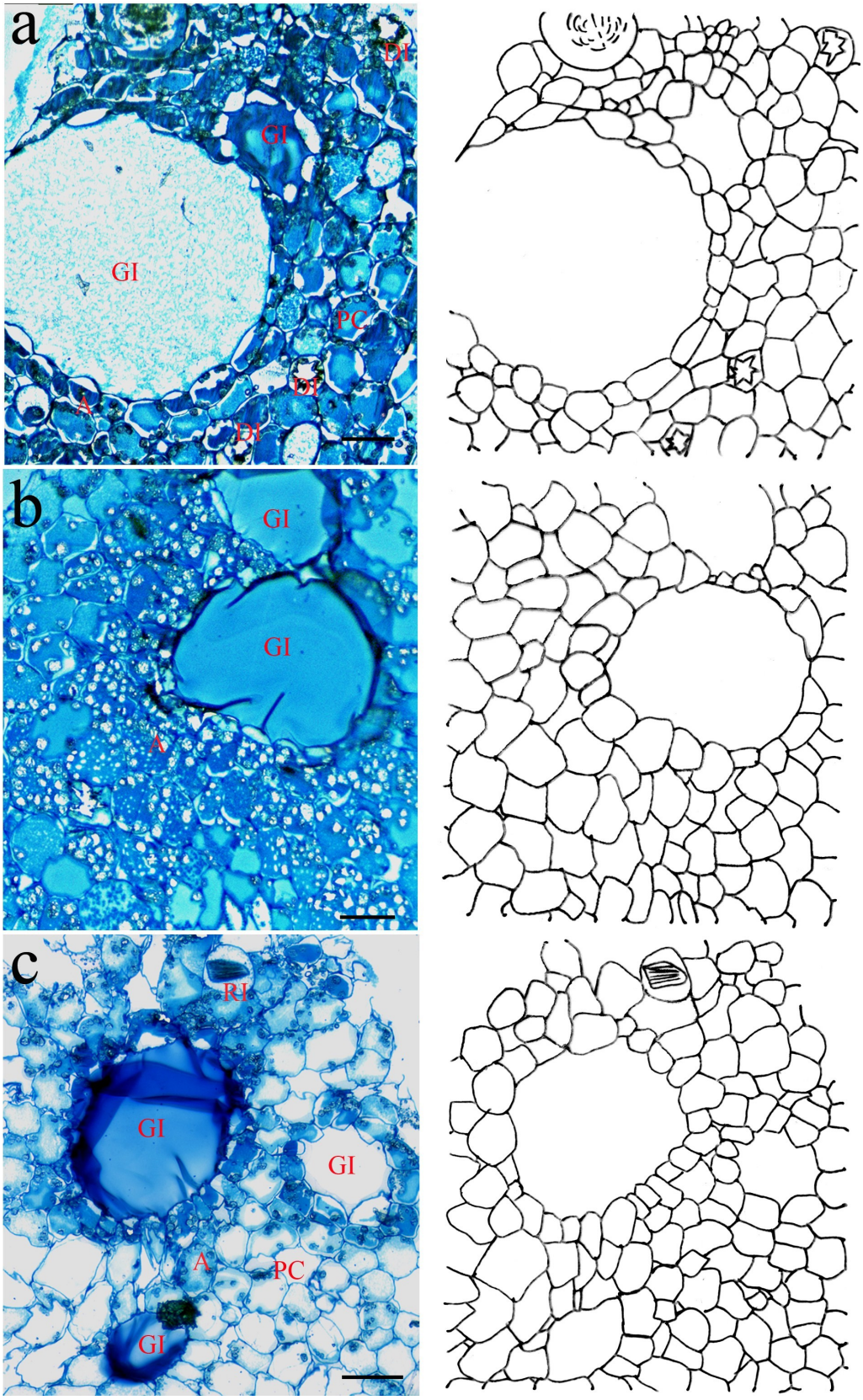

Figure 2.9 Light micrographs and tissue maps of a konjac corm at dormancy (stage 1). L.R. White resin embedded samples stained with toluidine blue at positions a, b and c along the cross section of the corm (Figure 2.3). *A* amyloplast, *DI* druse idioblast, *GI* glucomannan idioblast, *PC* parenchyma cell, *RI* raphide idioblast. Scale bars = 100 µm.

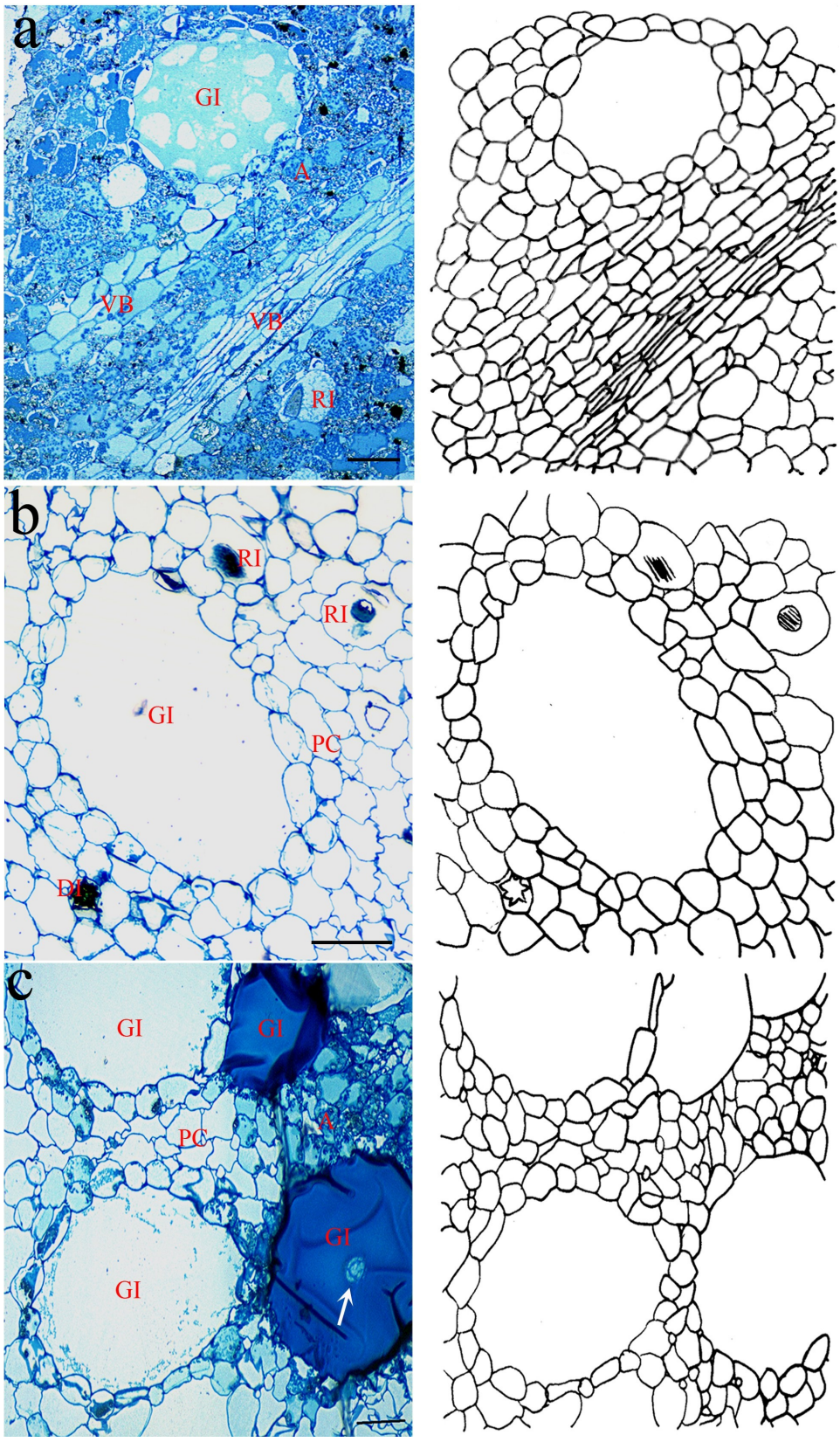

Figure 2.10 Light micrographs and tissue maps of a konjac corm at the stage of leaf bud emergence (stage 2). L.R. White resin embedded samples stained with toluidine blue at positions a, b and c along the cross section of the corm (Figure 2.3). *A* amyloplast, *DI* druse idioblast, *GI* glucomannan idioblast, *PC* parenchyma cell, *VB* vascular bundle, *RI* raphide idioblast. Scale bars = 100 μm.

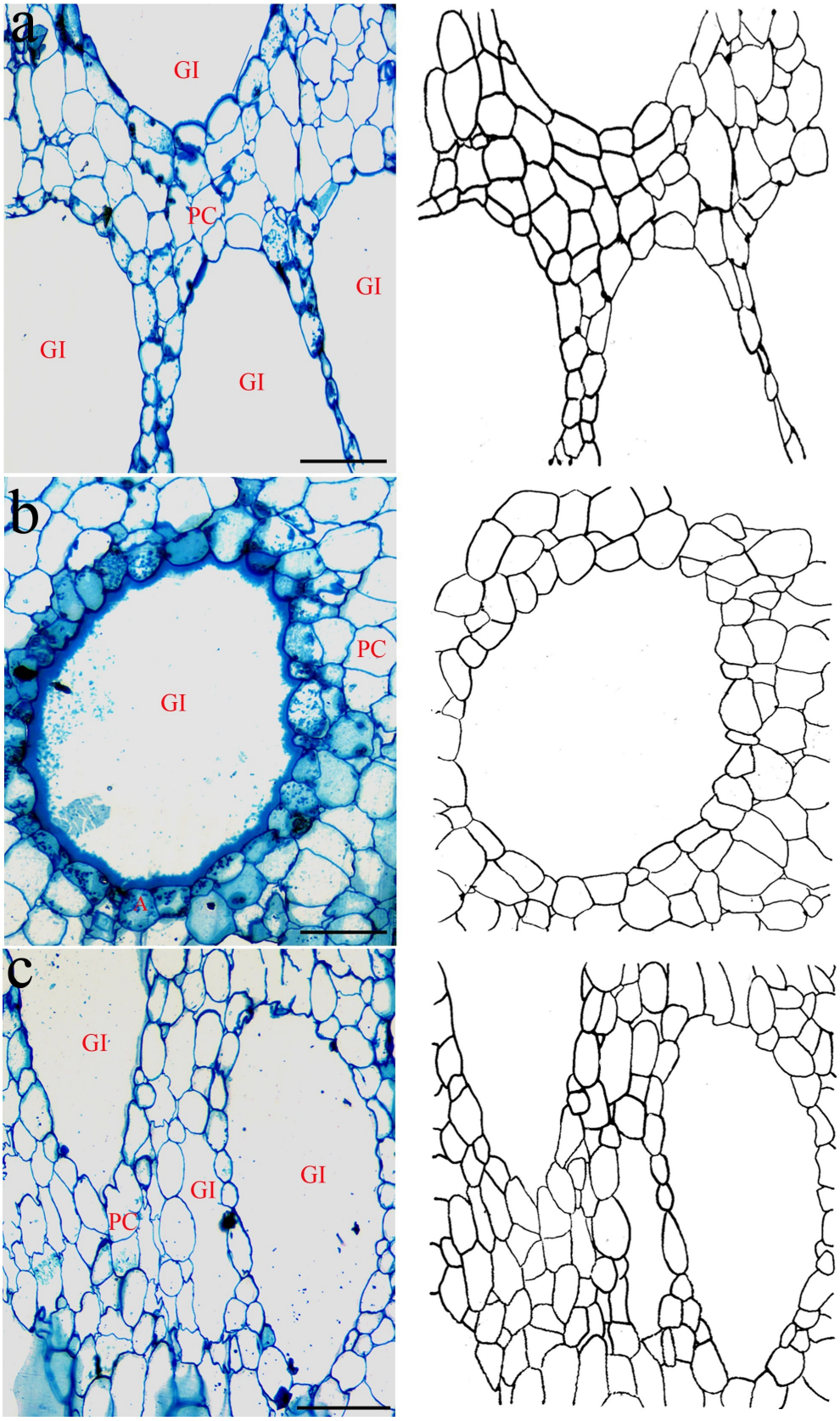

Figure 2.11 Light micrographs and tissue maps of a konjac corm at the stage of leaf bud elongation (stage 3). L.R. White resin embedded samples stained with toluidine blue at positions a, b and c along the cross section of the corm (Figure 2.3). *A* amyloplast, *GI* glucomannan idioblast, *PC* parenchyma cell. Scale bars = 100 µm.

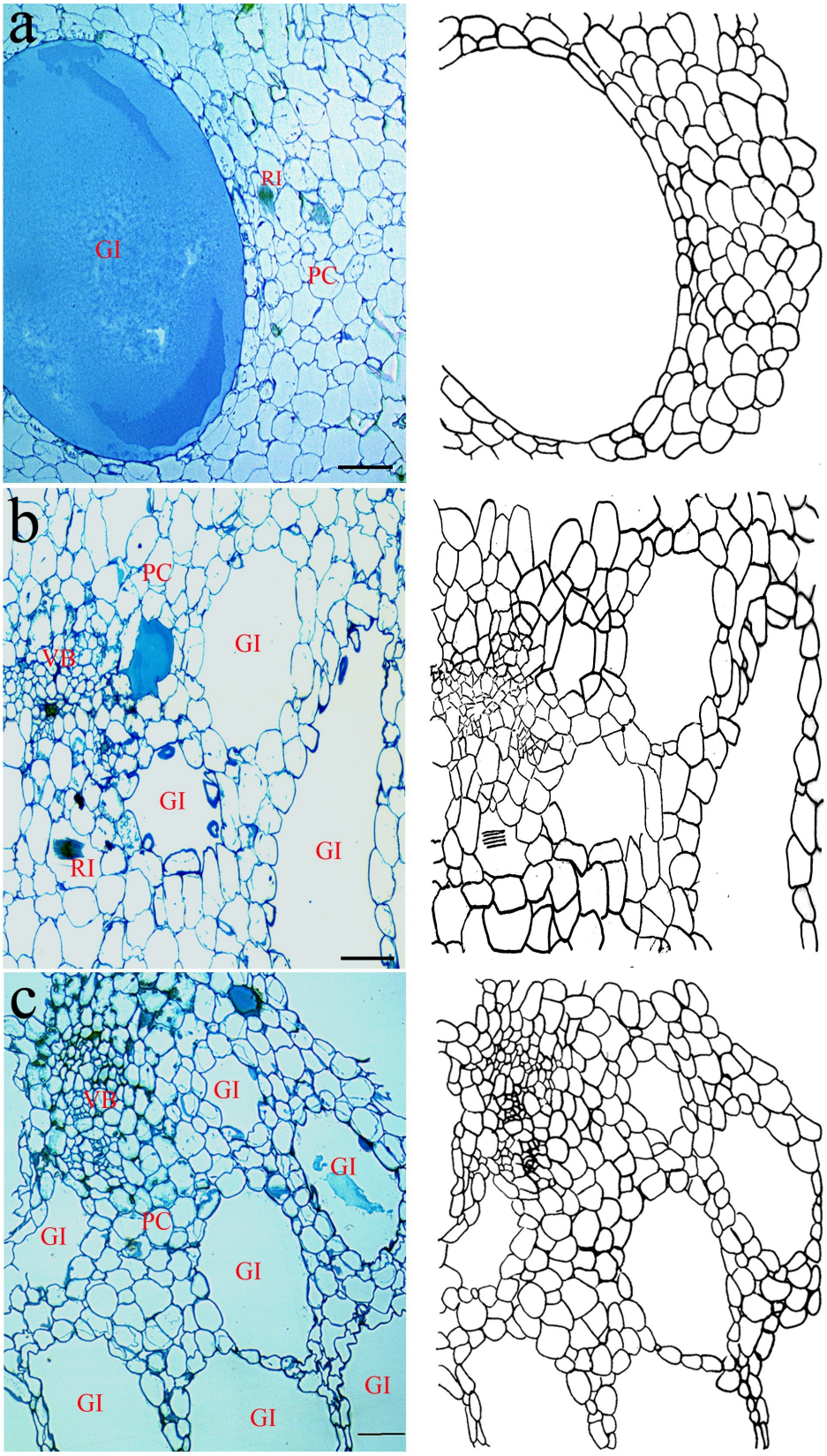

Figure 2.12 Light micrographs and tissue maps of a konjac corm at the stage of leaflet emergence (stage 4). L.R. White resin embedded samples stained with toluidine blue at positions a, b and c along the cross section of the corm (Figure 2.3). *GI* glucomannan idioblast, *PC* parenchyma cell, *VB* vascular bundle, *RI* raphide idioblast. Scale bars = 50 µm.

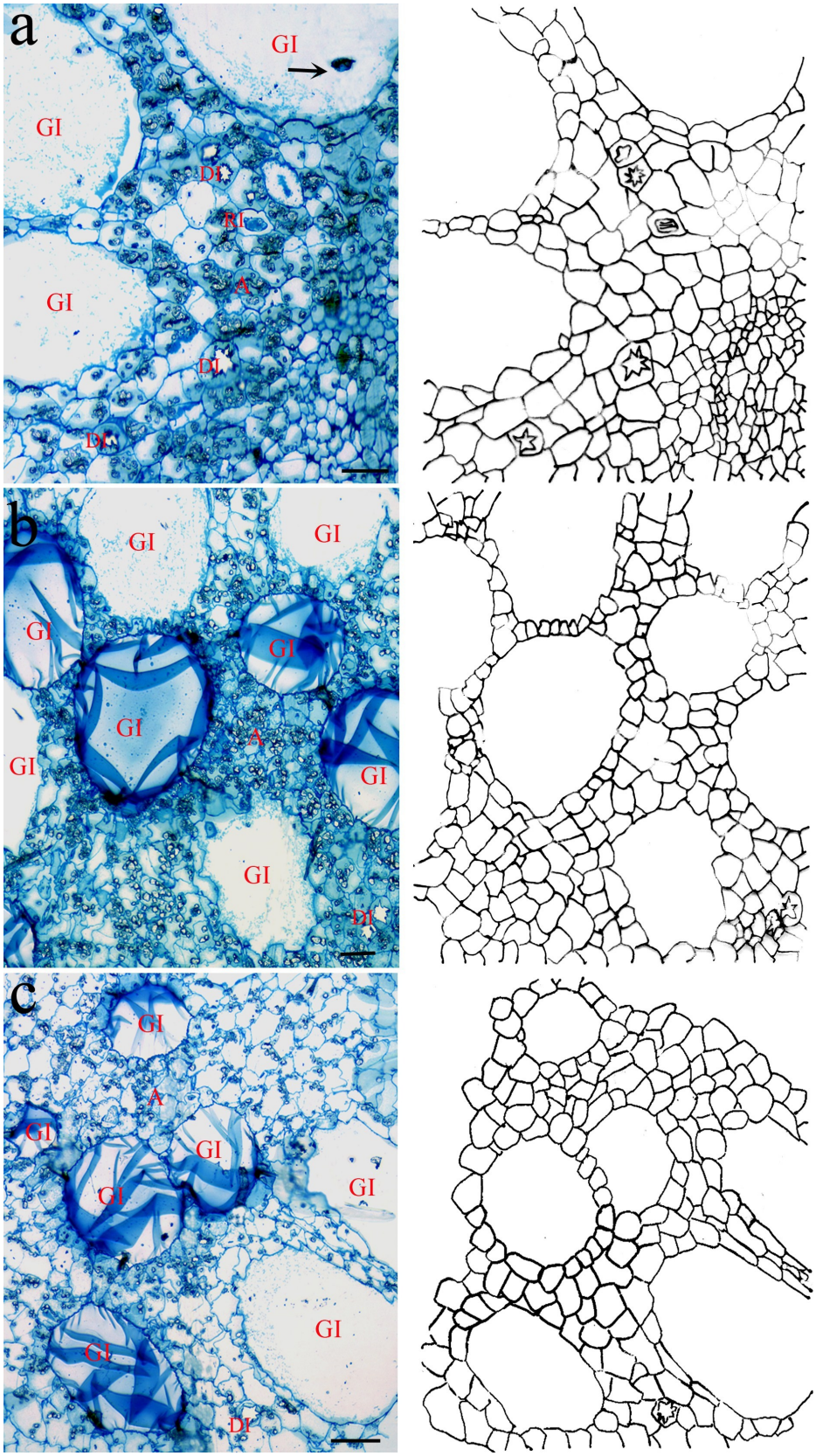

Figure 2.13 Light micrographs and tissue maps of a konjac corm at the stage of leaf expansion (stage 5). L.R. White resin embedded samples stained with toluidine blue at positions a, b and c along the cross section of the corm (Figure 2.3). *A* amyloplast, *DI* druse idioblast, *GI* glucomannan idioblast, *RI* raphide idioblast. Scale bars = 100 µm.

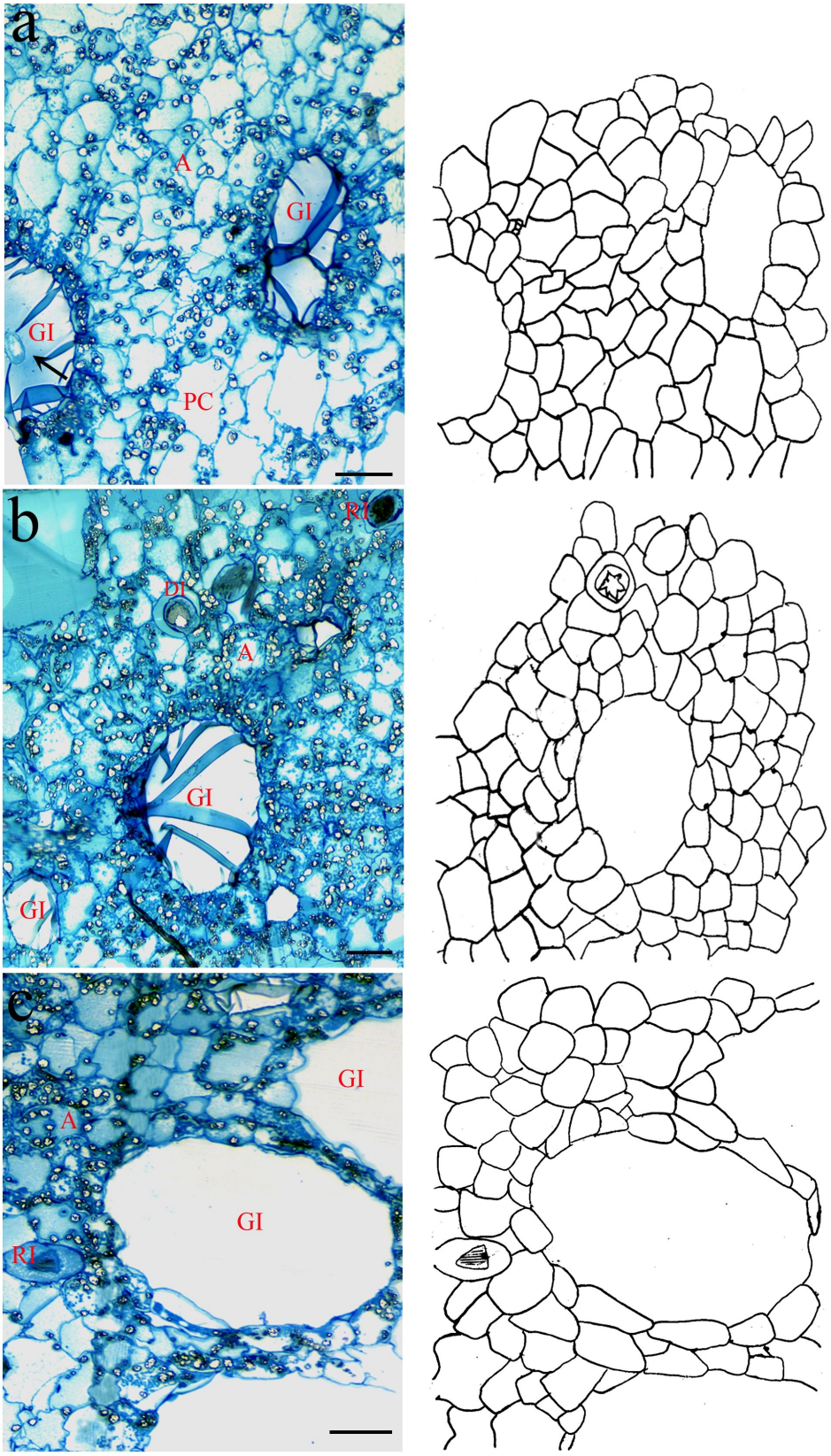

Figure 2.14 Light micrographs and tissue maps of a konjac corm at the stage of shoot senescence (stage 6). L.R. White resin embedded samples stained with toluidine blue at positions a, b and c along the cross sections of the corm (Figure 2.3). *A* amyloplast, *DI* druse idioblast, *GI* glucomannan idioblast, *PC* parenchyma cell, *RI* raphide idioblast. Scale bars = 100 μm.

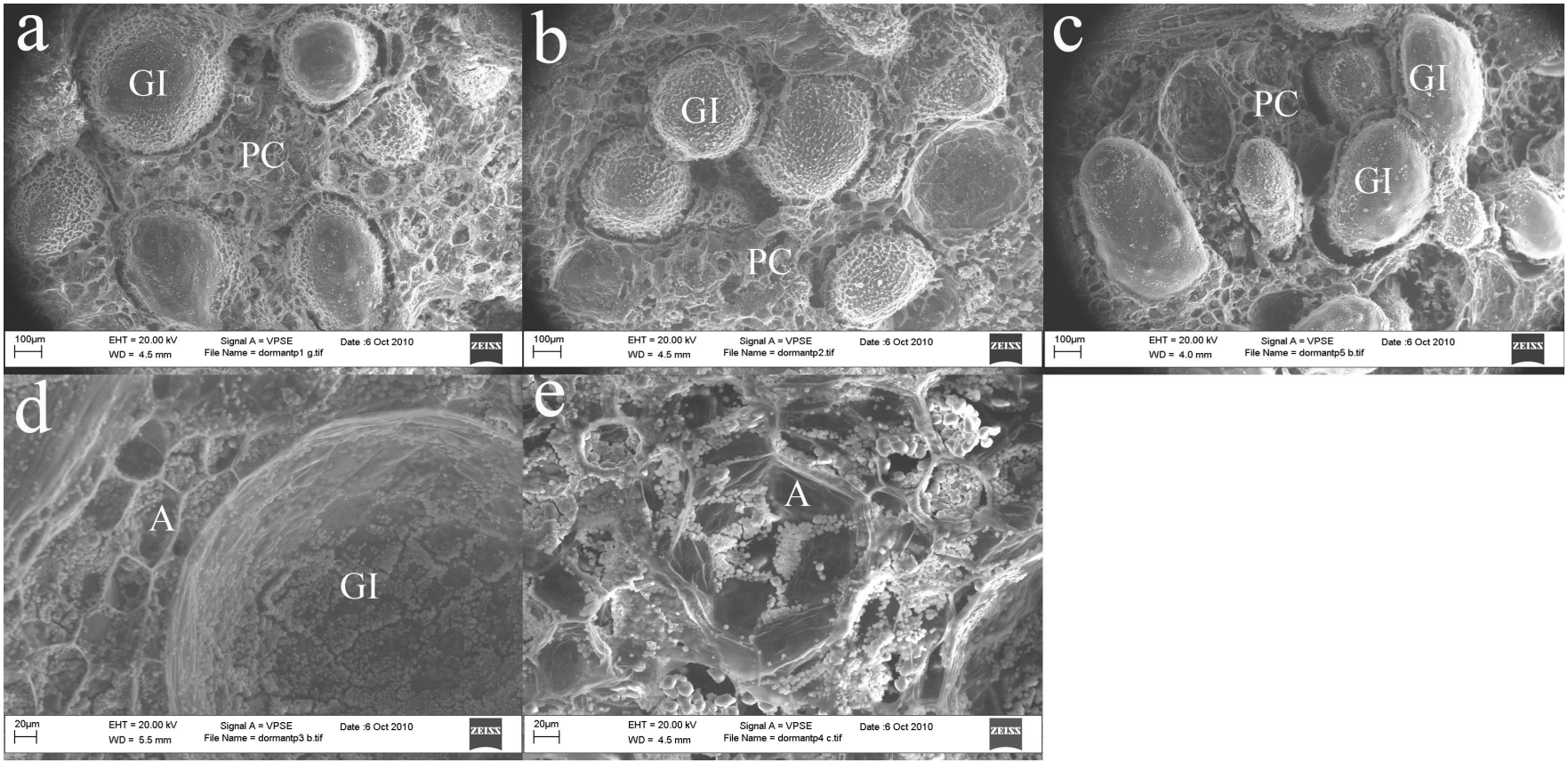

Figure 2.15 Structure of glucomannan idioblasts and amyloplasts of a dormant (stage 1) konjac corm as viewed under the scanning electron microscope. (a, b and c) Structure of glucomannan idioblasts at positions a, b and c along the cross section of a dormant corm (Figure 2.3). **(d)** Higher magnification of the structure of a glucomannan idioblast observed at position b. **(e)** Higher magnification of the surface structure of amyloplasts and starch granules. *A* amyloplast, *GI* glucomannan idioblast, *PC* parenchyma cell. Scale bar = 100 µm (a – c), 20 µm (d, e).

2.3.2.4. Immunolocalisation of mannan epitopes in corm tissues at the light microscope level

Indirect immunofluorescence light microscopy revealed the presence of mannan-containing epitopes at all developmental stages across the width of the corm, including the glucomannan idioblasts, calcium oxalate crystal idioblasts, vascular bundles and parenchyma cell walls (Figure 2.16). The overall semi-quantitative labelling intensity of each cell type (Table 2.7), is indicated by a scale (1 to 4), with 1 indicating little labelling and 4 representing the strongest labelling. *N.B*. The labelling intensity was judged by visual inspection.

Table 2.7 Relative immunofluorescence labelling intensity of different cell types observed in corm tissue using the anti-mannan antisera.

Cell type	Immunofluorescence labelling intensity
Glucomannan idioblast	
• Thin-film mucilage	4
• Sol-like substance	3
• Empty	< 1
Calcium oxalate crystal idioblast	
• Raphide idioblast	4
• Druse idioblast	4
Parenchyma cell wall	1
Tracheid	3.5

N.B. Scale of labelling intensity: 1 → 4 intensity increases.

Glucomannan deposition in the idioblasts was observed to be developmentally regulated. Towards the end of dormancy (stage 1), most of the glucomannan idioblasts were strongly labelled (Figure 2.16: 1a - 1c). One of the idioblasts, containing a sol-like substance at the mid-point (position a) of the corm, demonstrated a slightly weaker expression of mannan epitopes (Figure 2.16: 1a).

Throughout the early stages of shoot development, *i.e.* leaf bud emergence (stage 2), leaf bud elongation (stage 3) and leaflet emergence (stage 4), mannan epitopes present in the glucomannan idioblasts were shown to gradually decrease. At all these stages, mannan epitopes were observed to be rare, or absent in most idioblasts (Figure 2.16: 2b, 2c, 3a - c, 4b, 4c), with the notable exception of idioblasts near the mid-point of the corm (position a), which were strongly labelled (Figure 2.16: 2a, 4a, 4b).

As the corm approached maturity, *i.e*. from leaf expansion (stage 5) until shoot senescence (stage 6), an increase in the label intensity within the glucomannan idioblasts was observed (Figure 2.16: 5a - e, 6a - e). Mannan-containing epitopes were observed to be most abundant in the thin-filmed mucilage of the glucomannan idioblasts, the quantity of which increased as the leaf canopy developed. Moreover, the sol-like substance, with a slightly weaker expression of mannan epitopes, was progressively deposited at the periphery of the glucomannan idioblasts (Figures 2.16: 5a - c and 2.17: K, L).

The expression of mannan-containing epitopes in both the raphide (Figure 2.17: B - D) and druse (Figure 2.17: E, F) idioblasts was strong, regardless of the stage of development. From the immunofluorescence micrographs, it is also of interest to note the presence of densely-labelled raphide crystals in some of the glucomannan idioblasts (Figure 2.17: G - J).

The anti-mannan antiserum also labelled the secondary thickenings of tracheids in the vascular bundles (Figure 2.17: A). Furthermore, mannan-containing epitopes were detected in the majority of thin-walled parenchyma cell walls surrounding the glucomannan idioblasts at all stages of development, but the level of label was very light, suggesting that less mannan-containing polysaccharides are

present in these tissues. No labelling was observed in any of the control sections (in which the primary antibody was omitted) (Figure 2.16: n-1a, n-1b, n-1c).

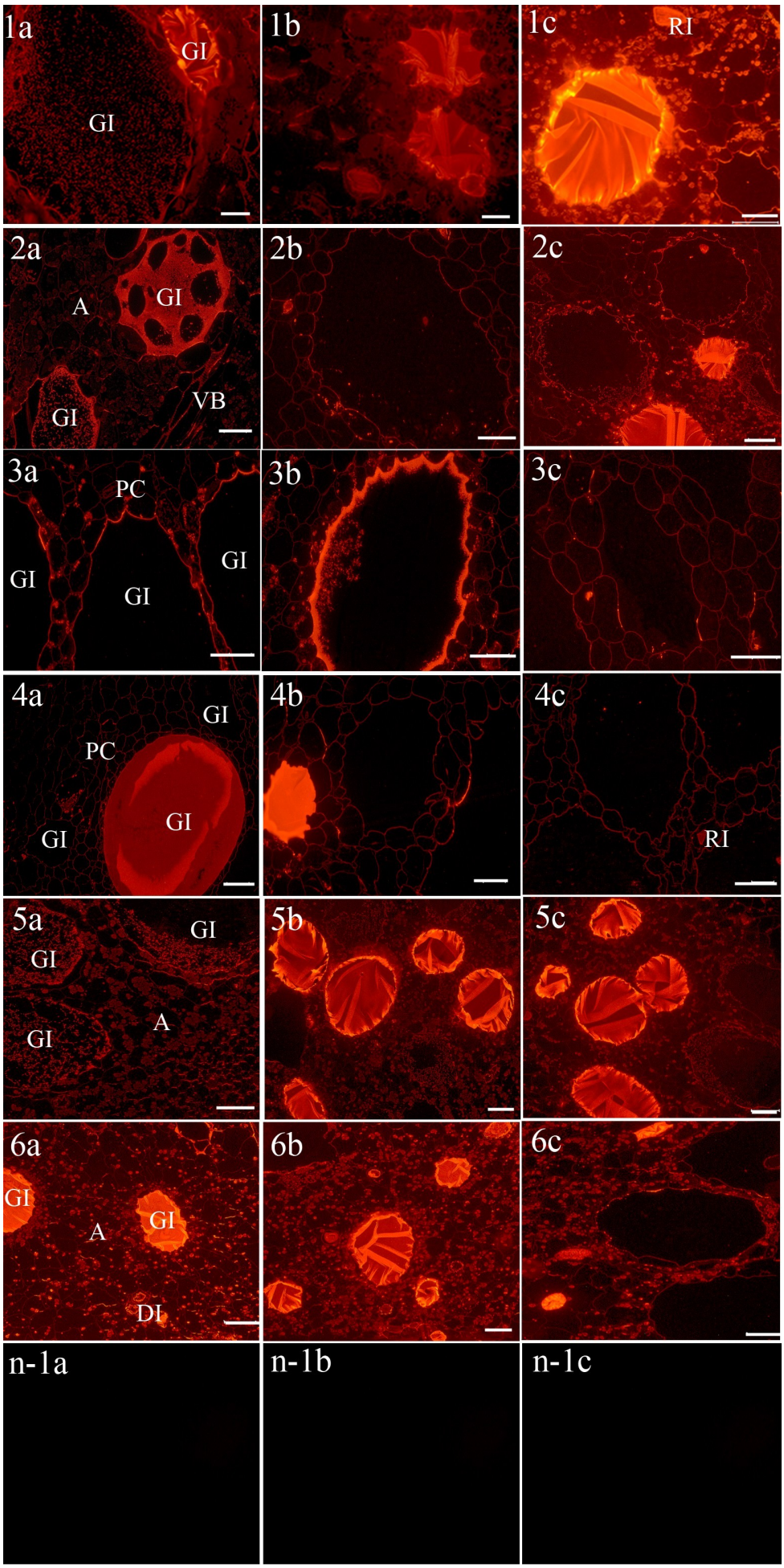
1a
GI
GI
1b
1c
RI
2a
A
GI
GI
VB
2b
2c
3a
PC
GI
GI
GI
3b
3c
4a
GI
PC
GI
GI
4b
4c
RI
5a
GI
GI
GI
A
5b
5c
6a
GI
A
GI
DI
6b
6c
n-1a
n-1b
n-1c

Figure 2.16 Immunolocalisation of mannan epitopes in cross-sections of konjac corm tissue at different stages of development. (1, 2, 3, 4, 5 and 6) The distribution of mannan epitopes at dormancy (early March), leaf bud emergence (mid May), leaf bud elongation (late May), leaflet emergence (early June), leaf expansion (early September) and shoot senescence (late September), respectively. (**a, b and c)** The distribution of mannan epitopes at three positions along the cross section of the corm (see Figure 2.3). (**n-1a, n-1b and n-1c**) Negative controls, sections of (1a, 1b and 1c) not treated with primary antibody. Strongly labelled glucomannan idioblasts (with thin-filmed mucilage) and calcium oxalate crystal idioblasts appear bright red. Cells which contain less mannan epitopes display less red label or cannot be seen. *A* amyloplast, *DI* druse idioblast, *GI* glucomannan idioblast, *PC* parenchyma cell, *RI* raphide idioblast, *VB* vascular bundle. Scale bars = 100 μm.

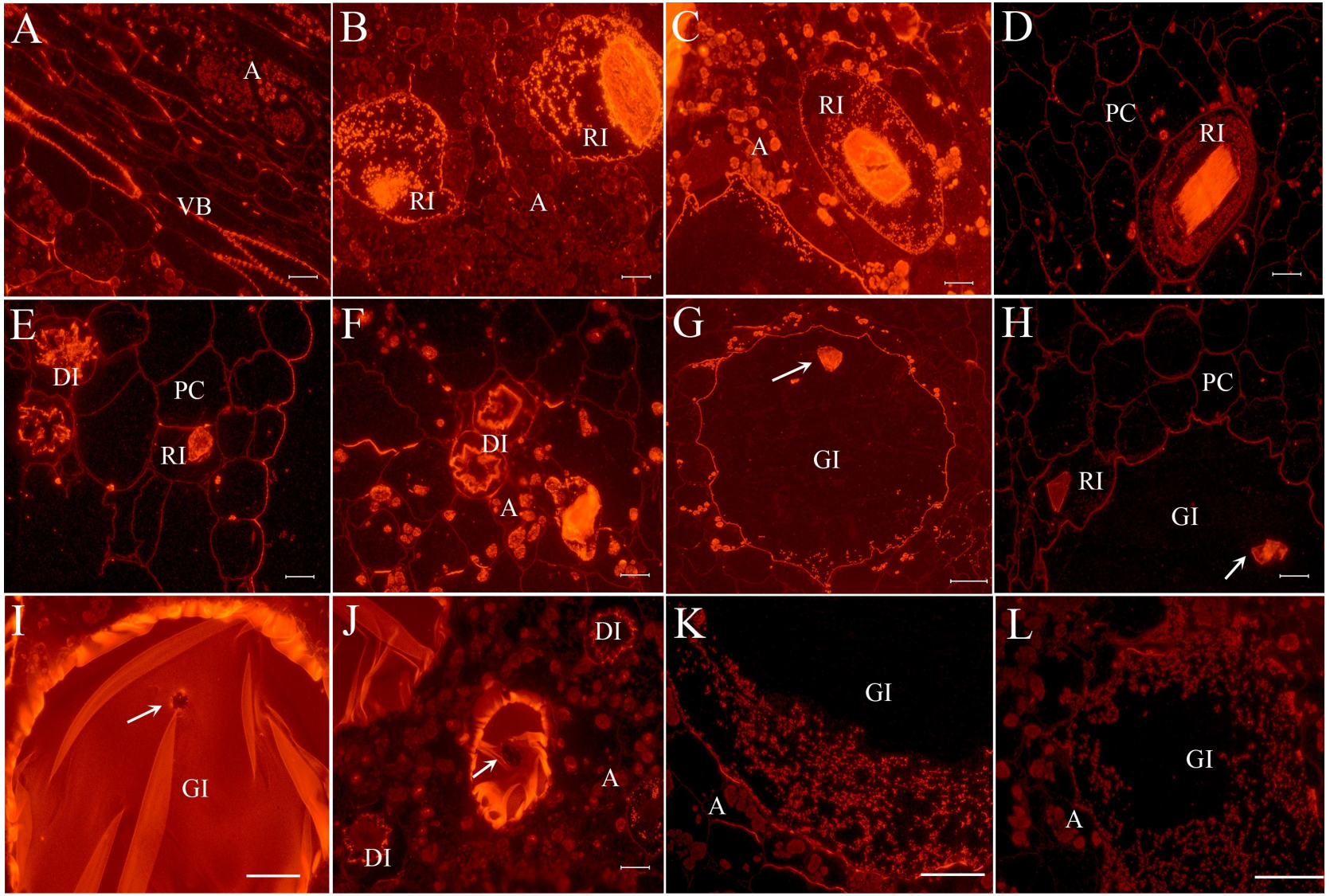
A
A
VB
B
RI
RI
A
C
RI
A
D
PC
RI
E
DI
PC
RI
F
DI
A
G
GI
H
PC
RI
GI
I
GI
J
DI
A
DI
K
GI
A
L
GI
A

Figure 2.17 Higher magnification of images in Figure 2.16. (A) Higher magnification of (2a), showing strong labelling of mannan epitopes in tracheids. **(B, C and D)** Higher magnification of (2a, 2c and 4c), showing strongly labelled raphide crystal idioblasts. **(E and F)** Higher magnification of (2b and 6a), showing strongly labelled druse crystal idioblasts. **(G, H, I and J)** Higher magnification of (2c, 4c, 5b and 6b), indicating the presence of raphide crystals (indicated by arrows) within the glucomannan idioblasts. (**K and L**) Higher magnification of (5a and 5b), showing the deposition of mannan epitopes inwards from the periphery of the glucomannan idioblasts, at the stage of leaf expansion. *A* amyloplast, *DI* druse idioblast, *GI* glucomannan idioblast, *PC* parenchyma cell, *RI* raphide idioblast, *VB* vascular bundle. Scale bars = 45 µm.

2.3.2.5. Immunogold labelling of mannan-containing polysaccharides in corm tissues at the transmission electron microscope level

The location of mannan epitopes in the glucomannan idioblasts was examined in more detail using immunogold electron microscopy (Figure 2.18 - 2.23). Two glucomannan idioblasts present at the mid-point (position a) of the corm were selected and examined for each developmental stage. The results obtained were consistent with the light microscopy.

At dormancy (stage 1), intense labelling indicating an abundance of mannan epitopes, was observed to be evenly distributed throughout both the glucomannan idioblasts examined (Figure 2.18). Fewer immunogold particles were detected in the idioblast which contains the sol-like substance (Figure 2.18: IA, IB), compared to the one with the thin-film mucilage (Figure 2.18: IIA, IIB).

During leaf bud emergence (stage 2), a considerable amount of label was detected in one of the glucomannan idioblasts examined, with more label present in the inner region, than at the periphery of the idioblast (Figure 2.19: IA, IB). The second selected idioblast, however, contained few mannan epitopes (Figure 2.19: IIA, IIB), with most label observed near the periphery of the idioblast.

During leaf bud elongation (stage 3), immunogold particles within both the glucomannan idioblasts examined, were observed to be rare (Figure 2.20). At the stage of leaflet emergence (stage 4), a considerable amount of label was shown to be evenly distributed in one of the glucomannan idioblasts (Figure 2.21: IA, IB), with few immunogold particles visible within the other idioblast (Figure 2.21: IIA, IIB).

During leaf expansion (stage 5), mannan epitopes were deposited at the periphery of one of the glucomannan idioblasts examined, with most label found close to the plasma membrane (Figure 2.22: IA, IB). For the other idioblast,

however, mannan epitopes filled the entire cell and were shown to be more generally distributed (Figure 2.22: IIA, IIB).

As the corm approached maturity, *i.e*. at the stage of shoot senescence (stage 6), labelling became more intense than whilst the foliage was developing and was uniformly distributed throughout both the idioblasts examined (Figure 2.23).

Immunogold labelling confirmed that little mannan epitope was present in the parenchyma cell walls at all stages of development (Figure 2.18 - 2.23).

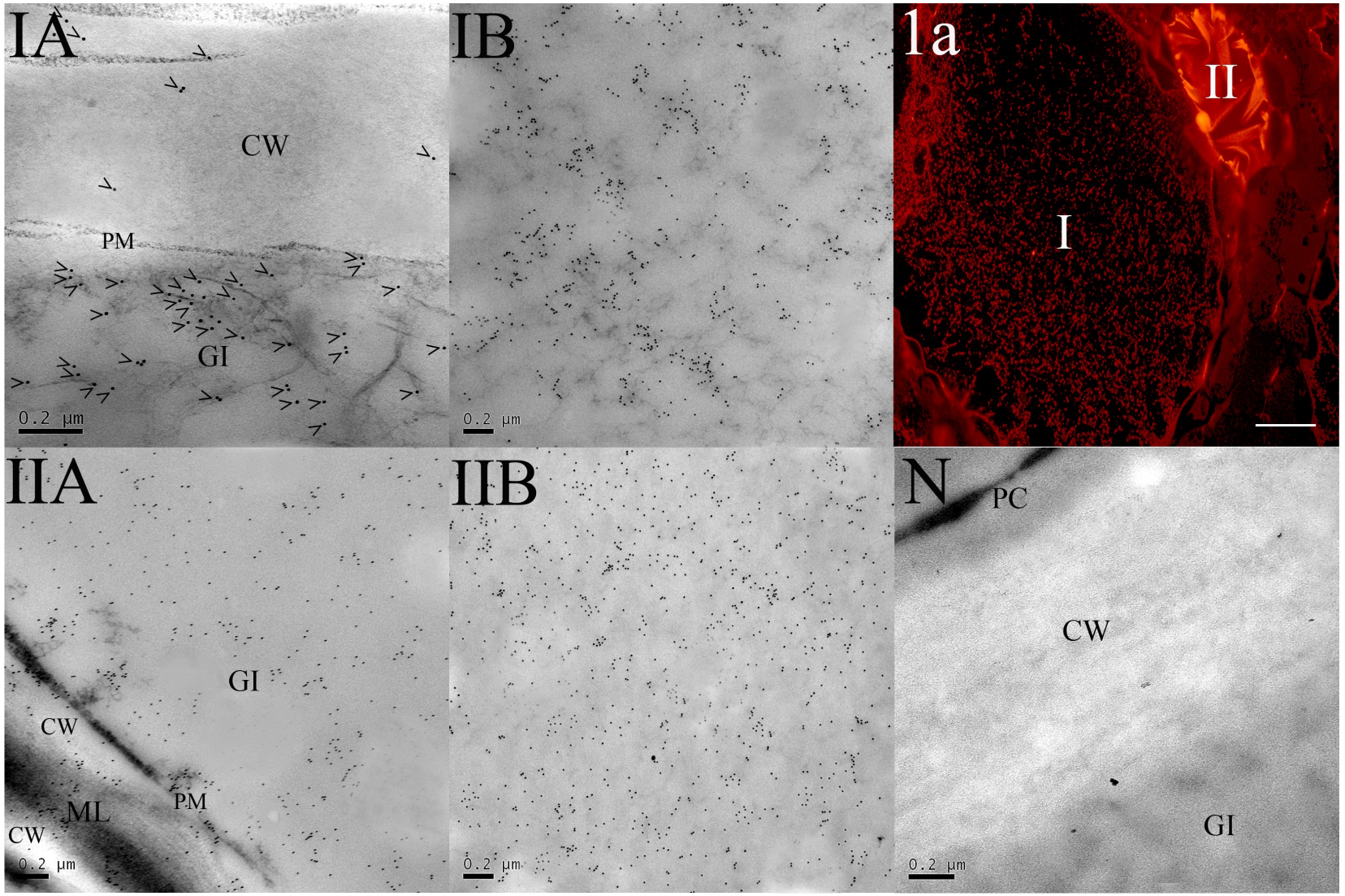
IA
CW
PM
GI
0.2 µm
IB
0.2 µm
1a
II
I
IIA
GI
CW
ML
PM
CW
0.2 µm
IIB
0.2 µm
N
PC
CW
GI
0.2 µm

Figure 2.18 Localisation of mannan epitopes within glucomannan idioblasts from the mid-point (*i.e*. position a, as shown in Figure 2.3) of a corm at dormancy. (IA and IIA) Mannan epitopes at the peripheral region of the selected glucomannan idioblasts (labelled as I and II, respectively in Figure 1a), with immunogold particles (indicated by arrows) detected in the primary cell walls and middle lamella. **(IB and IIB)** Mannan epitopes within the selected glucomannan idioblasts, in the region inward from the area shown in Figure IA and IIA, respectively with many immunogold particles visible. **(1a)** Immunofluorescence labelling of the selected glucomannan idioblasts in cross section from the mid-point of a corm at dormancy with the anti-mannan antiserum (I and II indicate the glucomannan idioblasts represented in Figure I and II). **(N)** Negative control, section 1a not treated with primary antibody. *CW* cell wall, *GI* glucomannan idioblast, *ML* middle lamella, *PM* plasma membrane. Scale bars = 0.2 μm (IA, IB, IIA, IIB, N), 80 μm (1a).

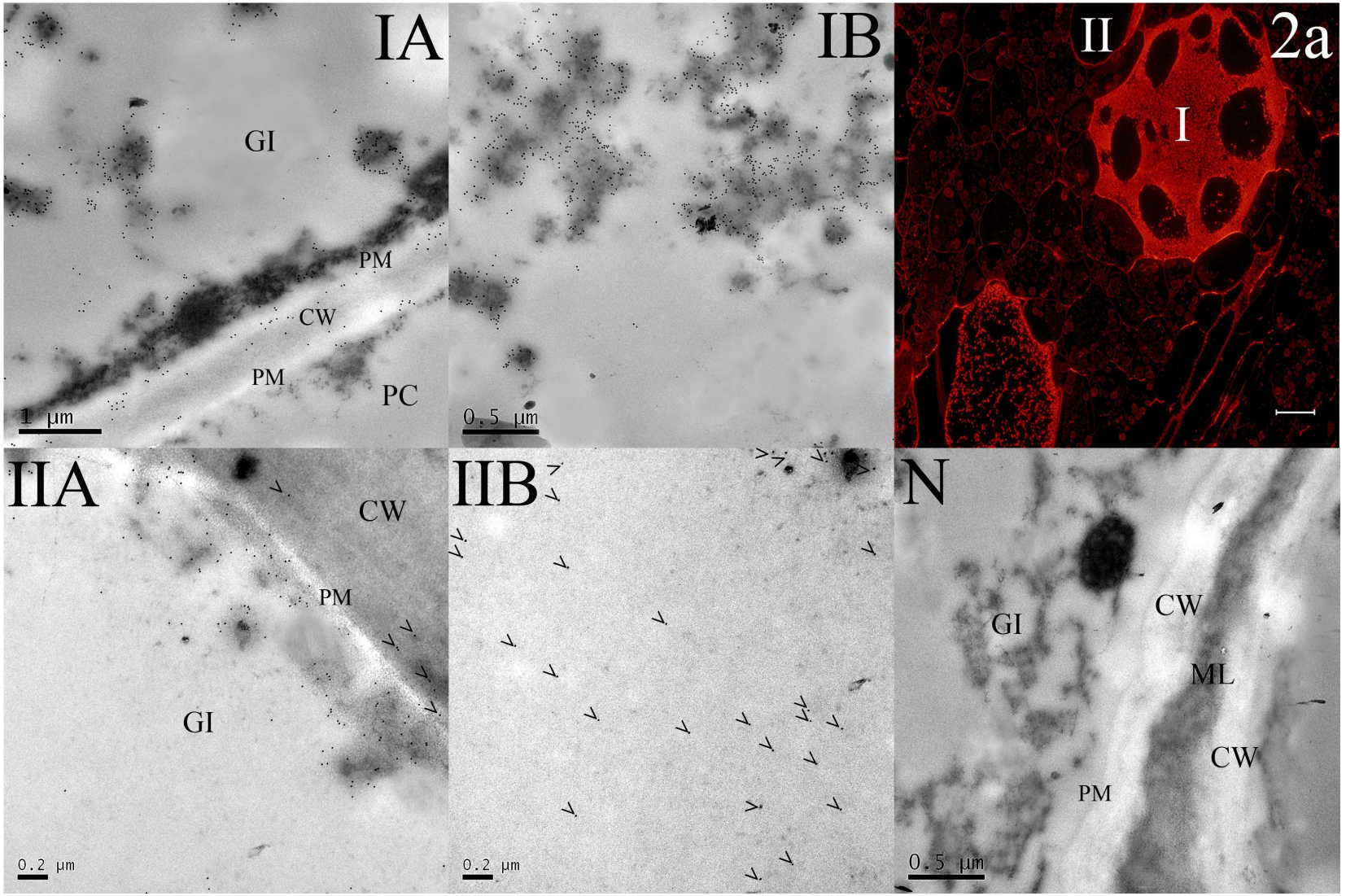
IA
GI
PM
CW
PM
PC
1 µm
IB
0.5 µm
II
2a
I
IIA
CW
PM
GI
0.2 µm
IIB
0.2 µm
N
GI
CW
ML
CW
PM
0.5 µm

Figure 2.19 Localisation of mannan epitopes within glucomannan idioblasts from the mid-point of a corm at the stage of leaf bud emergence. (IA) Mannan epitopes at the peripheral region of the selected glucomannan idioblast (labelled as I in Figure 2a). **(IB)** Mannan epitopes within the glucomannan idioblast, in the region inward from the area shown in Figure IA. Immunogold particles were shown to be unevenly distributed, with more labelling present in the inner region than the periphery of the idioblast. **(IIA)** Mannan epitopes at the periphery of the selected glucomannan idioblast (labelled as II in Figure 2a). **(IIB)** Mannan epitopes within the selected glucomannan idioblast, in the region inward from the area shown in Figure IIA. Less immunogold particles were observed at the inner region than the periphery of the idioblast. **(2a)** Immunofluorescence labelling of the selected glucomannan idioblasts from the mid-point of a corm at the stage of leaf bud emergence with the anti-mannan antiserum (I and II indicate the glucomannan idioblasts represented in Figure I and II). **(N)** Negative control, section 2a not treated with primary antibody. *CW* cell wall, *GI* glucomannan idioblast, *ML* middle lamella, *PM* plasma membrane. Scale bars = 1 μm (IA), 0.5 μm (IB, N), 0.2 μm (IIA, IIB), 60 μm (1a).

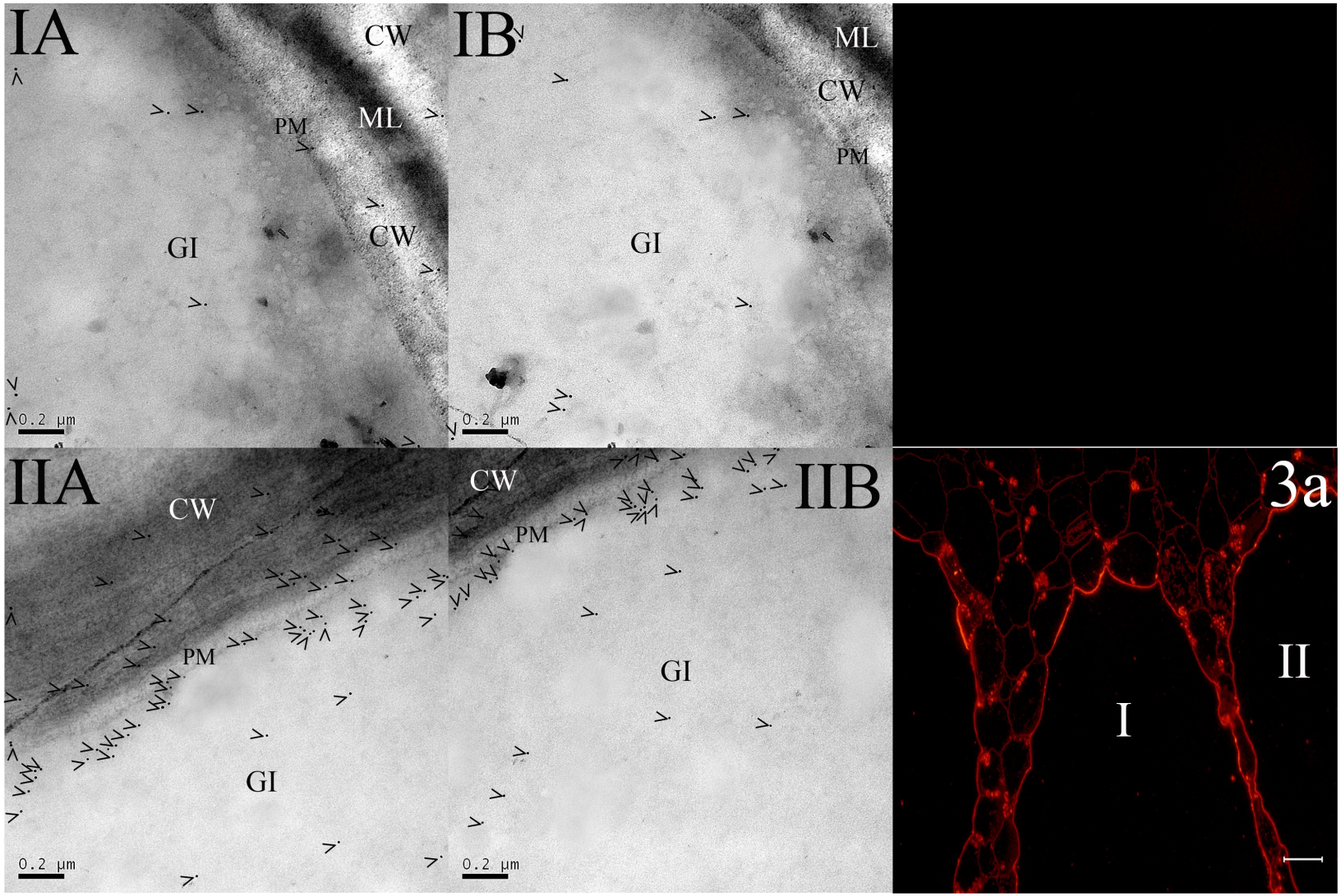
IA
CW
ML
PM
CW
GI
0.2 µm
IB
ML
CW
PM
GI
0.2 µm
IIA
CW
PM
GI
0.2 µm
IIB
CW
PM
GI
0.2 µm
3a
II
I

113

Figure 2.20 Localisation of mannan epitopes within glucomannan idioblasts from the mid-point of a corm at the stage of leaf bud elongation. (IA) Mannan epitopes at the peripheral region of the selected glucomannan idioblast (labelled as I in Figure 3a). **(IB)** Mannan epitopes within the selected glucomannan idioblast, in the region inward from the area shown in Figure IA with few immunogold particles detected. **(IIA)** Mannan epitopes at the periphery of the selected glucomannan idioblast (labelled as II in Figure 3a). **(IIB)** Mannan epitopes within the selected glucomannan idioblast, in the region inward from the area shown in Figure IIA. Less immunogold particles were observed at the inner region than the periphery of the idioblast. **(3a)** Immunofluorescence labelling of the selected glucomannan idioblasts from the mid-point of a corm at the stage of leaf bud elongation with the anti-mannan antiserum (I and II indicate the glucomannan idioblasts represented in Figure I and II). *CW* cell wall, *GI* glucomannan idioblast, *ML* middle lamella, *PM* plasma membrane. Scale bars = 0.2 μm (IA, IB, IIA, IIB), 30 μm (3a).

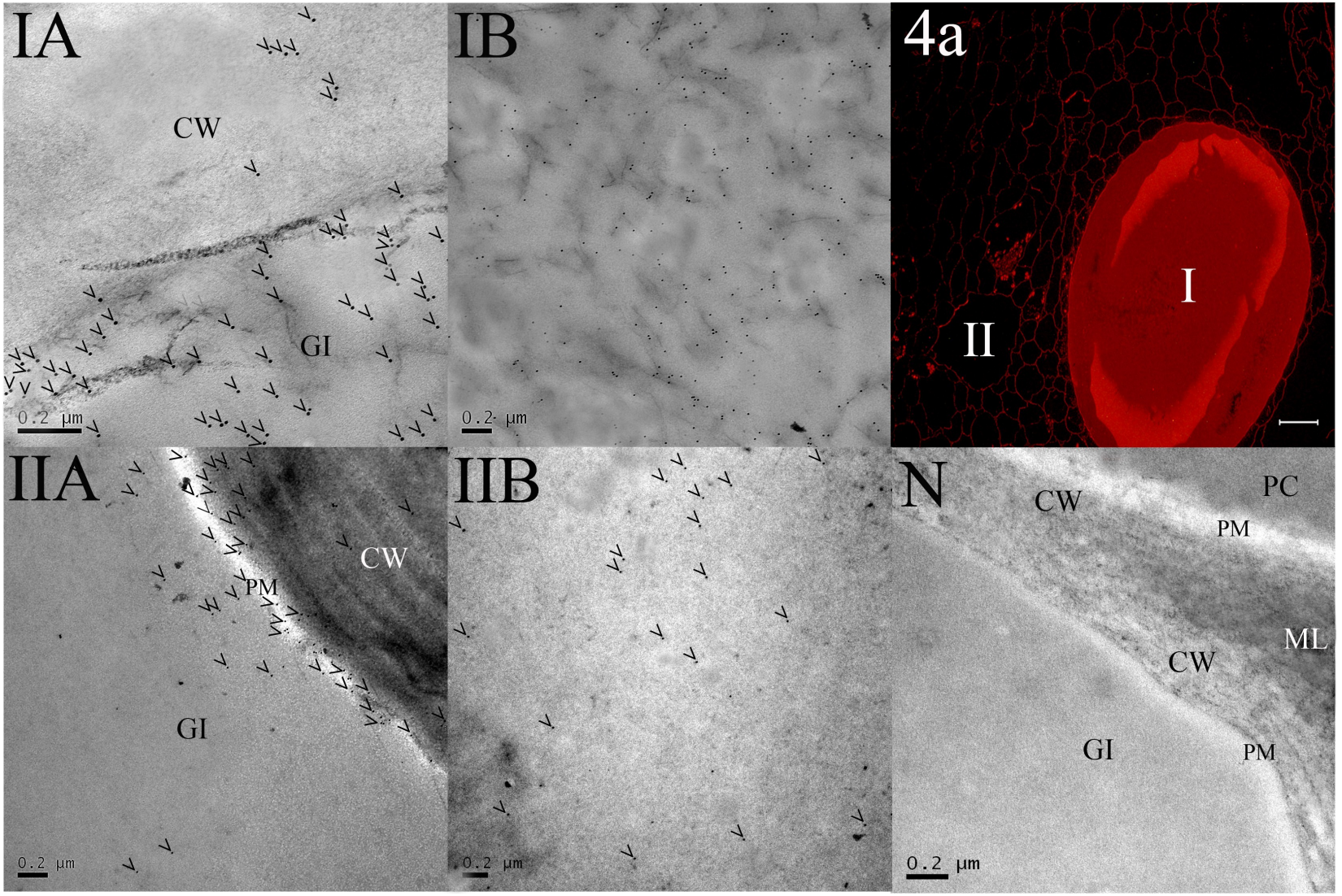
IA
CW
GI
0.2 µm
IB
0.2 µm
4a
I
II
IIA
CW
PM
GI
0.2 µm
IIB
0.2 µm
N
CW
PC
PM
ML
CW
GI
PM
0.2 µm

115

Figure 2.21 Localisation of mannan epitopes within glucomannan idioblasts from the mid-point of a corm at the stage of leaflet emergence. (IA) Mannan epitopes at the peripheral region of the selected glucomannan idioblast (labelled as I in Figure 4a). **(IB)** Mannan epitopes within the selected glucomannan idioblast, in the region inward from the area shown in Figure IA with many immunogold particles detected. **(IIA)** Mannan epitopes at the periphery of the selected glucomannan idioblast (labelled as II in Figure 4a). **(IIB)** Mannan epitopes within the selected glucomannan idioblast, in the region inward from the area shown in Figure IIA with few immunogold particles visible. **(4a)** Immunofluorescence labelling of the selected glucomannan idioblasts from the mid-point of a corm at the stage of leaflet emergence with the anti-mannan antiserum (I and II indicate the glucomannan idioblasts represented in Figure I and II). **(N)** Negative control, section 4a not treated with primary antibody. *CW* cell wall, *GI* glucomannan idioblast, *ML* middle lamella, *PM* plasma membrane. Scale bars = 0.2 μm (IA, IB, IIA, IIB), 50 μm (4a).

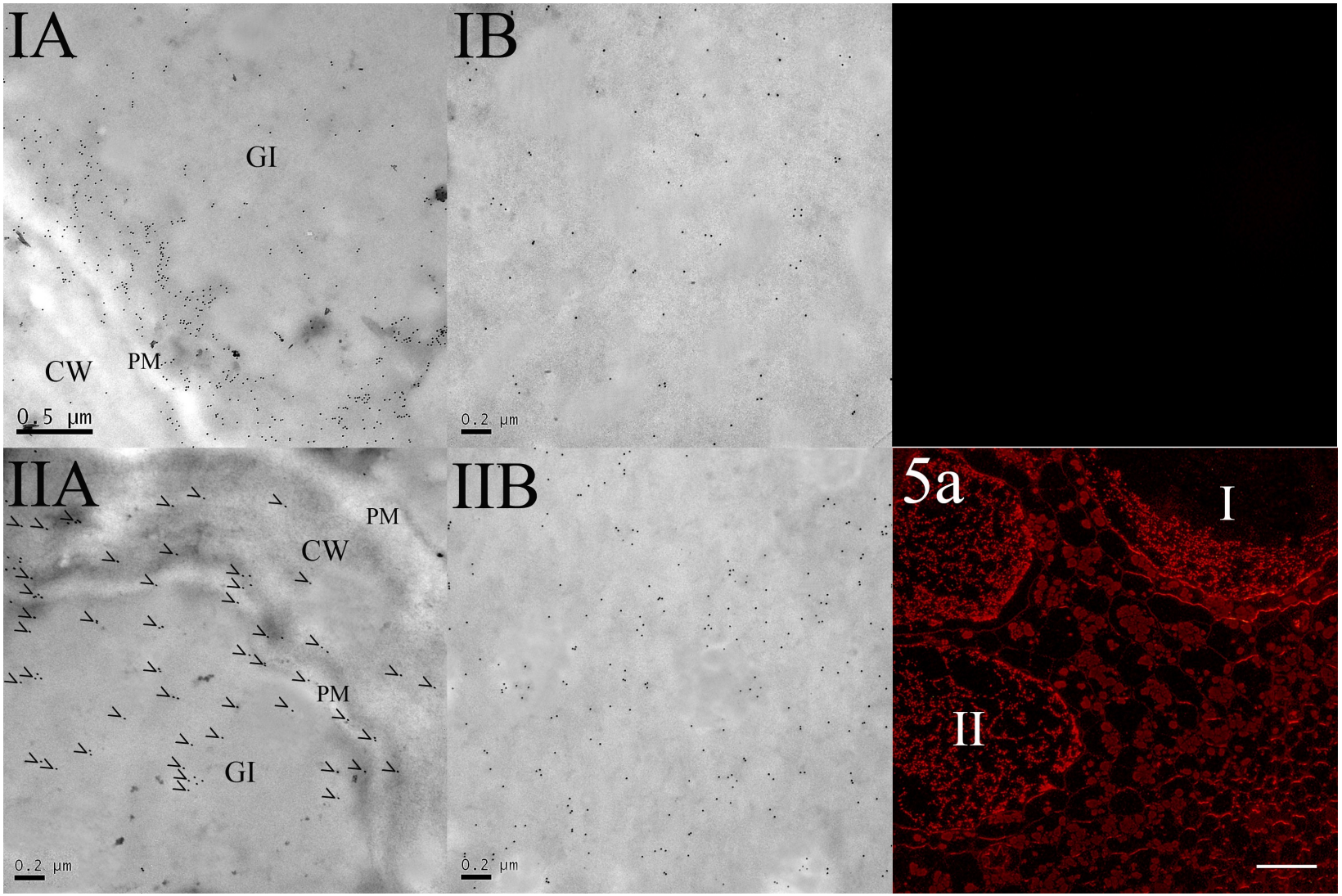
IA
GI
CW
PM
0.5 µm
IB
0.2 µm
IIA
PM
CW
PM
GI
0.2 µm
IIB
0.2 µm
5a
I
II

Figure 2.22 Localisation of mannan epitopes within glucomannan idioblasts from the mid-point (position a) of a corm at the stage of leaf expansion. (IA) Mannan epitopes at the peripheral region of the selected glucomannan idioblast (labelled as I in Figure 5a). **(IB)** Mannan epitopes within the selected glucomannan idioblast, in the region inward from the area shown in Figure IA. More immunogold particles were observed at the periphery of the idioblasts than the inner region. **(IIA)** Mannan epitopes at the periphery of the selected glucomannan idioblast (labelled as II in Figure 5a). **(IIB)** Mannan epitopes within the selected glucomannan idioblast, in the region inward from the area shown in Figure IIA with many immunogold particles evenly distributed in the idioblast. **(5a)** Immunofluorescence labelling of the selected glucomannan idioblasts in cross sections from the mid-point of a corm at the stage of leaf expansion with the anti-mannan antiserum (I and II indicate the glucomannan idioblasts represented in Figure I and II). *CW* cell wall, *GI* glucomannan idioblast, *PM* plasma membrane. Scale bars = 0.5 μm (IA), 0.2 μm (IB, IIA, IIB), 100 μm (5a).

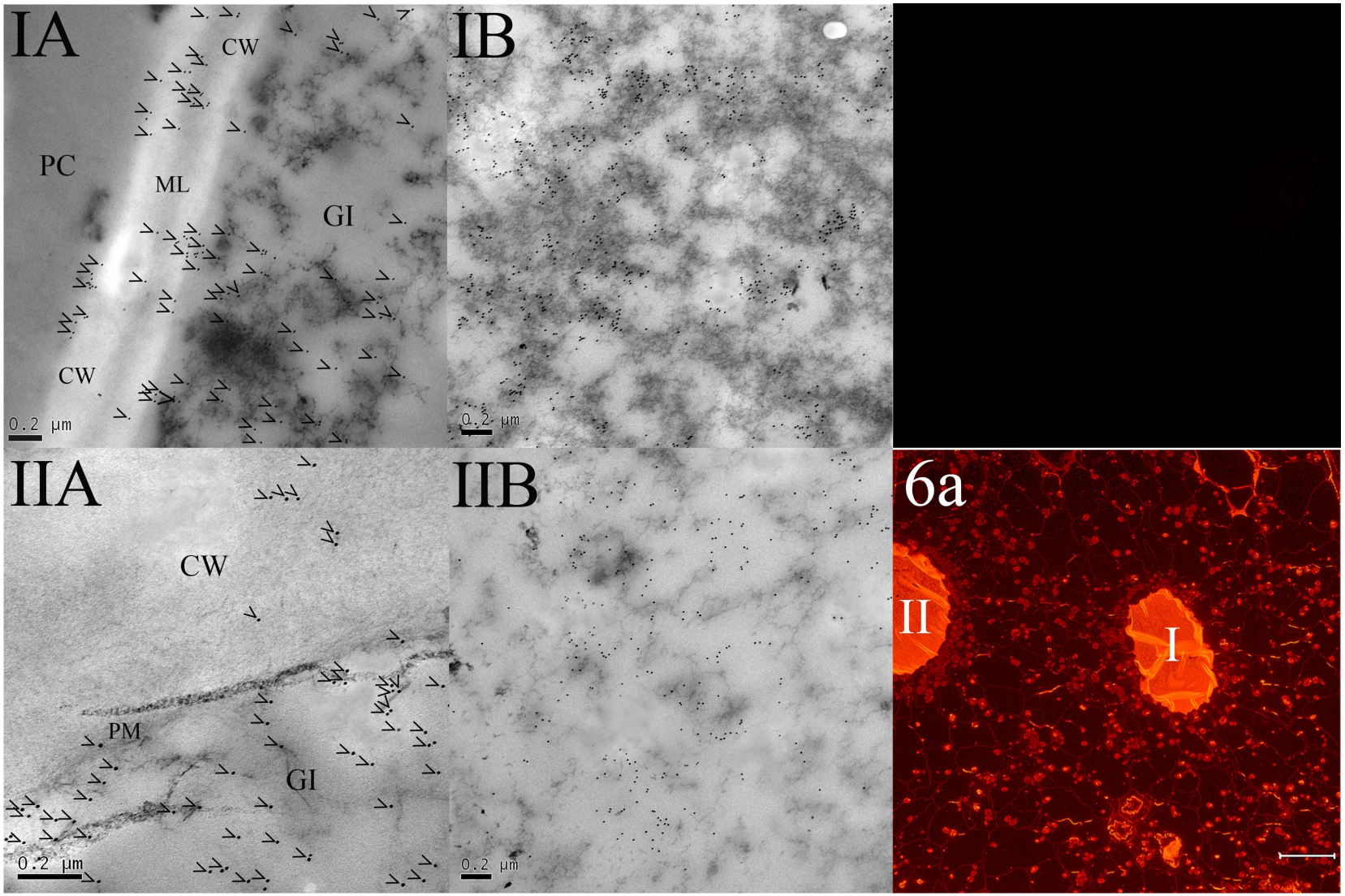
IA
CW
PC
ML
GI
CW
0.2 µm
IB
0.2 µm
IIA
CW
PM
GI
0.2 µm
IIB
0.2 µm
6a
II
I

Figure 2.23 Localisation of mannan epitopes within glucomannan idioblasts from the mid-point of a corm at the stage of shoot senescence. (IA and IIA) Mannan epitopes at the periphery of the selected glucomannan idioblasts (labelled as I and II, respectively in Figure 6a). **(IB and IIB)** Mannan epitopes within the selected glucomannan idioblasts, in the region inward from the area shown in Figure IA and IIA, respectively with plenty of immunogold particles visible. **(6a)** Immunofluorescence labelling of the selected glucomannan idioblasts from the mid-point of a corm at the stage of shoot senescence with the anti-mannan antiserum (I and II indicate the glucomannan idioblasts represented in Figure I and II). *CW* cell wall, *GI* glucomannan idioblast, *ML* middle lamella, *PM* plasma membrane. Scale bars = 0.2 μm (IA, IB, IIA, IIB), 170 μm (6a).

2.3.2.6. Flower bud and inflorescence development in A. konjac

As mentioned in section 2.3.1, AK3 and AK4, the two oldest F0 corms, both produced an inflorescence followed by a leaf within the same growing season (in both 2009 and 2010). The inflorescence growth curves for both AK3 and AK4, with a starting corm weight of 725 and 1092 g, respectively during the 2009 growing season are shown in Figure 2.24. For AK4, the flower bud was first visible on 6th March and the spathe started to unfold 16 days after bud emergence (22nd March), with a floral chamber measuring ~ 120 mm in diameter. Two days later (24th March), the spathe had completely opened and the diameter of floral chamber was ~ 180 mm. The maximum height of the AK4 inflorescence (including peduncle) was 1200 mm, with the peduncle reaching 500 mm in height. The spadix collapsed 9 days after the opening of spathe (31st march) and was completely senesced by mid May.

For AK3, the flower bud was first visible on 10th March 2009 and the spathe started to unfold 19 days after bud emergence (29th March), with a floral chamber measuring ~ 100 mm in diameter. The spathe was completely open after two days (31st March) and the diameter of the floral chamber was recorded as ~ 160 mm. The maximum height (including peduncle) recorded for the AK3 inflorescence was 1020 mm, with the peduncle reaching 48 mm in height. The inflorescence lasted for 10 days and was fully senesced by the end of May.

During the first few hours after anthesis, both AK4 and AK3 plants emitted a foul odour (similar to rotting meat), which gradually faded in the following day. In brief, the time span for the development of the inflorescence in both plants after the emergence of the flower bud was between 18 and 21 days, and the flower lasted for ~ 10 days after the spathe had completely unfolded.

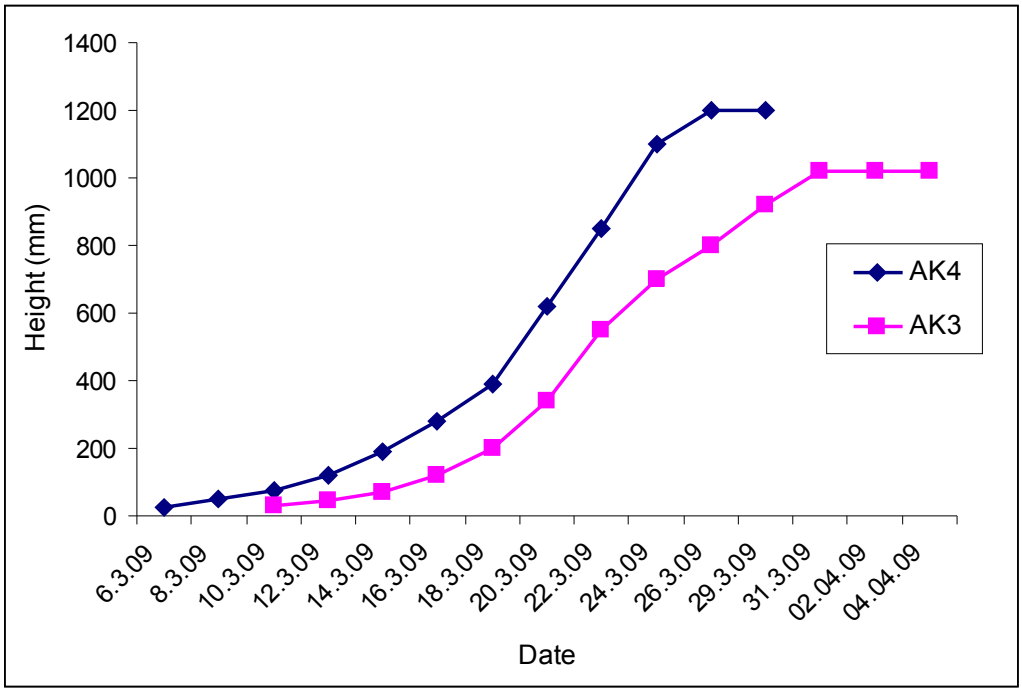

Figure 2.24 Growth curves of inflorescences produced by AK3 and AK4 corms during the 2009 growing season.

2.3.3. Quantitative differences in growth and development of plants produced from F0 corms of different age during the 2009 growing season

2.3.3.1. Timing of leaf bud and leaflet emergence

As shown in Table 2.8, the leaf buds of the two-year-old corms emerged between 59 and 62 days after planting (DAP), with leaflets emerging 8 - 11 days after bud emergence. Compared to two-year-old corms, leaf bud emergence was delayed by 10 - 14 days in one-year-old corms. The delayed shoot growth in both AK3 and AK4 was due to the prior production of an inflorescence by these plants. Moreover, leaf bud emergence and shoot senescence of these post-flowering corms were at approximately the same time, *i.e.* ~ 90 and 216 DAP respectively, with leaflets emerging at 102 DAP.

Table 2.8 Timings (DAP) of the key stages of development (leaf bud emergence, leaflet emergence and shoot senescence) and quantitative differences in growth and development of plants produced from F0 corms of different age during the 2009 growing season.

			Days after planting (DAP)							
					Shoot senescence					
F0	Age	Planting wt. (g)	Leaf bud emergence	Leaflet emergence [§]	Stage 1 [†]	Stage 4	Growth period (days) [ψ]	Max. petiole length (mm)	Max. leaf width (mm)	Max. RChl units
AK4	5	1092.1	88	102	216	244	128	915	1060	41.0
AK3	4	725.2	92	102	216	244	124	840	880	34.9
AK15	2	88.8	59	70	202	226	143	525	620	32.5
AK17	2	113.3	59	70	197	221	138	450	650	35.5
AK18	2	112.9	62	72	197	221	135	445	685	31.1
AK19	2	109.1	62	70	202	221	140	505	670	34.8
AKR1	1	26.7	72	74	216	226	144	355	480	29.9
AKR2	1	35.8	72	74	192	221	144	280	470	26.1

[§] Canopy width: 100 - 150 mm.

[†] Stage 1: leaf chlorosis; stage 4: above ground structures senesced and detached from corm (see Plate 2.2).

[ψ] Defined as the time span from leaf bud emergence to leaf chlorosis.

2.3.3.2. Pattern of petiole growth, leaf expansion and quantitative differences between plants derived from F0 corms of different age

Petiole length (Figure 2.25) and leaf width (Figure 2.26) increased markedly with corm age. These differences are clearly evident in Plate 2.5, where plants at full maturity are compared photographically. The petiole length and leaf width of both one and two-year-old plants increased sharply up to 92 and 84 DAP respectively, and remained almost constant thereafter. The maximum petiole length and leaf width for the one and two-year-old plants were attained at 130 and 160 DAP, respectively.

For AK3 and AK4 plants, petiole length increased gradually during the first month after leaf bud emergence (from 90 - 120 DAP), followed by a sharp increase of 455 mm (from 190 - 645 mm) and 495 mm (245 - 740 mm), respectively within the next 10 days (from 120 - 130 DAP) and thereafter showed a steady increase up to maturity (Figure 2.25). Similarly, the leaf blade expanded rapidly within the 10 days after leaflet emergence (from 105 - 115 DAP), from 270 - 625 mm in AK3 and 265 - 730 mm in AK4, and the maximum leaf width was observed at ~ 180 DAP (Figure 2.26).

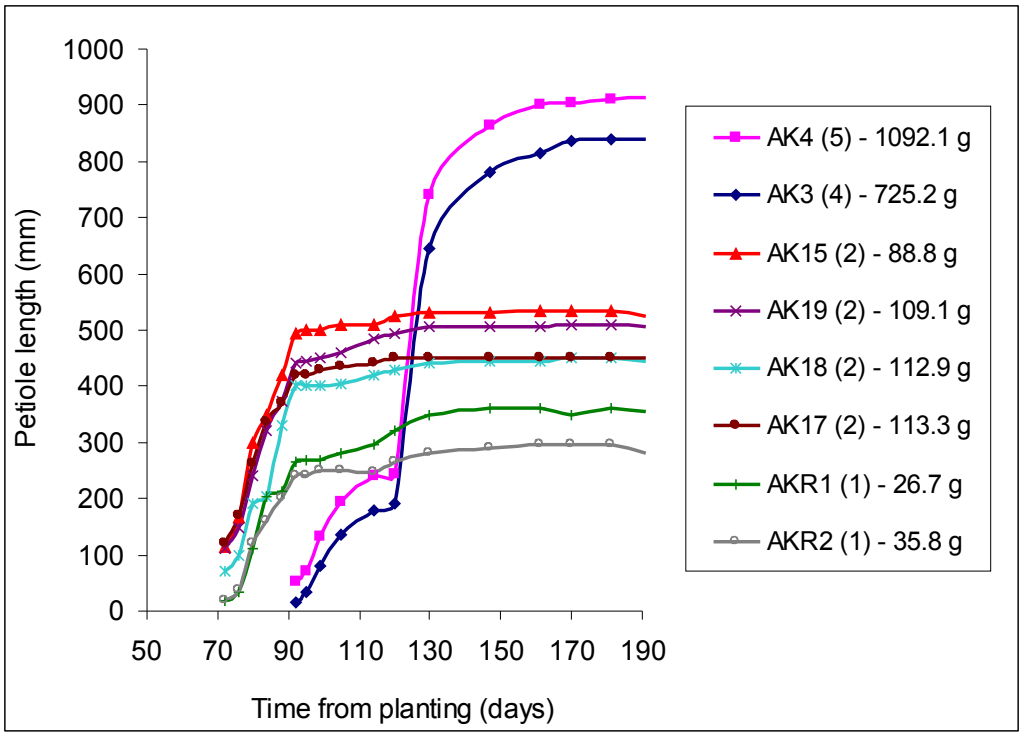

Figure 2.25 Petiole length of plants produced from one, two, four and five-year-old F0 corms. The age of F0 corms in year is shown in parentheses.

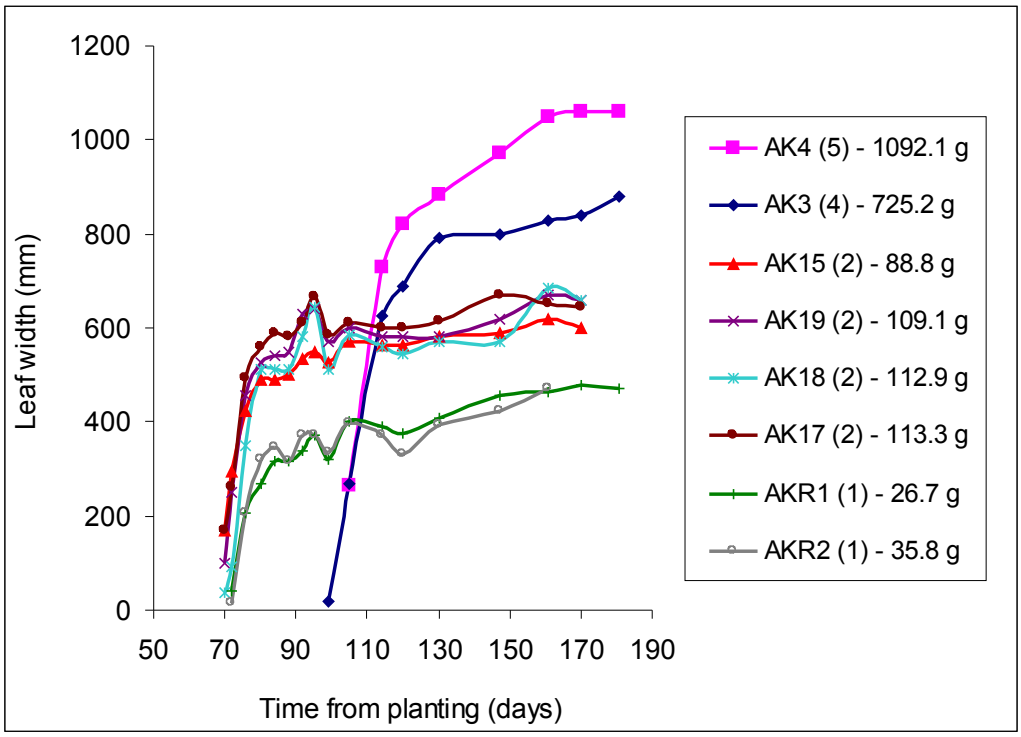

Figure 2.26 Leaf width of plants produced from one, two, four and five-year-old F0 corms. The age of F0 corms in year is shown in parentheses.

Plate 2.5 Morphology of konjac plants produced by corms of varying age. Photograph taken during the 2009 growing season of plants at full maturity. *From left:* offset-derived plant, one-year-old plant, two-year-old plant, four-year-old plant.

2.3.3.3. Pattern of leaf senescence

Leaf senescence was monitored both visually (with photographic records) at key stages of development (Plate 2.2) and by measuring RChl content. The RChl content in F0 plants was estimated non-destructively using a SPAD-502 chlorophyll meter and expressed as RChl units.

Figure 2.27 presents the profiles of leaf greenness measured from 72 DAP, during which the leaflets had emerged (canopy width = 100 - 150 mm). Both one and two-year-old F0 plants showed the highest RChl content at 80 DAP, during the period of vigorous leaf expansion (Figure 2.26), with RChl units ranging between 26.1 and 35.5 (Table 2.8). For two-year-old plants, the time span from leaf bud emergence until complete leaf chlorosis (SPAD reading = 0) ranged from 135 - 143 days.

Fully expanded leaves of AK3 and AK4 plants were noticeably greener than those of younger plants, attaining RChl units of 25.9 and 38.3, respectively. The highest RChl readings for AK3 (34.9) and AK4 (41.0) were recorded at 134 DAP. The senescence of the leaf canopy of these post-flowering plants was initiated with abscises at the base of one part of the rachis, with the petiole staying upright, followed by the two remaining parts of the rachis. The petiole subsequently buckled at its base and collapsed a few days later, with leaflets retained in a fully green state. As shown in Table 2.8, petioles of both AK3 and AK4 plants collapsed at 216 DAP and were completely senesced (aerial part died off and detached from corm) at 244 DAP. They had a shorter growth period (124 and 128 days), compared to younger plants (135 - 144 days). The RChl units recorded for AK3 and AK4 just before the abscission of rachis was 25.9 and 28.8, respectively.

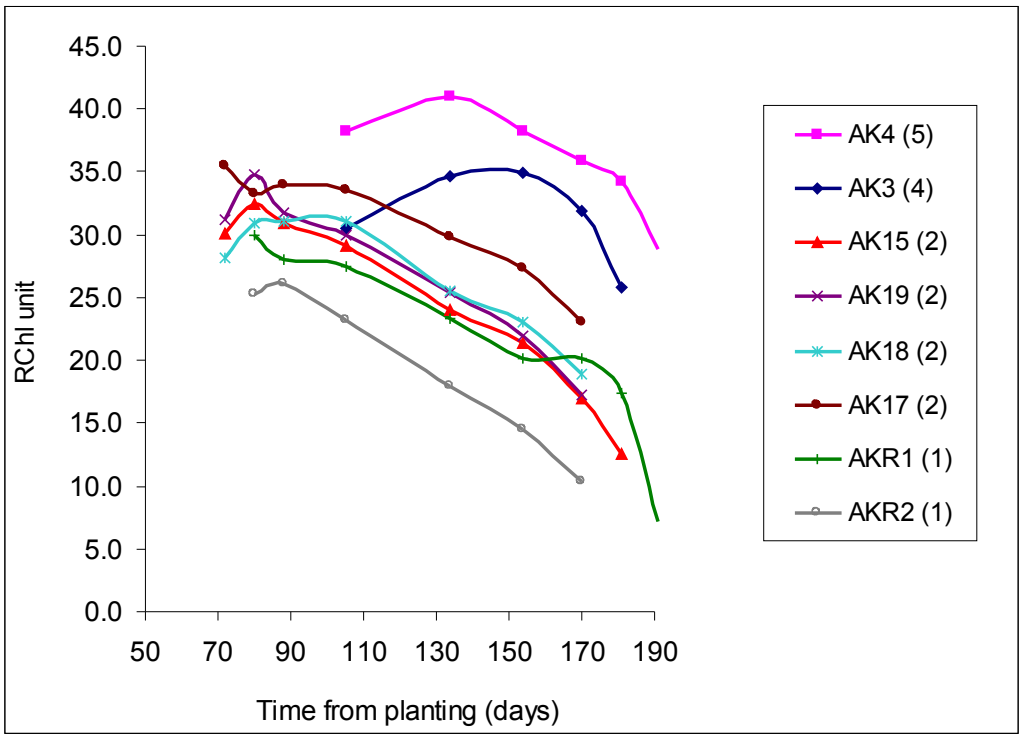

Figure 2.27 Leaf SPAD value of plants produced from one, two, four and five-year-old F0 corms. The age of F0 corms in year is shown in parentheses.

2.3.3.4. Yield of F0 corms

The harvest data for F0 corms during the 2009 growing season is presented in Table 2.9. The two-year-old corms having almost similar planting weight (except AK15) showed a comparable percentage increase in below ground mass (F0 + $F_0$1) over a growing season, ranging from 116 - 135%. By contrast, the older F0, both AK3 and AK4 corms, showed a negative increment of 19% and 31%, respectively. It was also noted that a considerable amount of biomass was allocated to offset materials ($F_0$1) in the younger F0 (except AK15), compared to both AK3 and AK4 corms. The $F_0$1 dry weight ratio of the one and two-year-old F0 ranged from 20 - 32%, compared to 6% and 0.3% in AK3 and AK4 corms, respectively. Moreover, the dry matter content of $F_0$1(*0*) produced by AK3 and AK4 corms was 83% and 77% of the fresh weight respectively, and were lower than those produced by two-year-old corms (85 - 94%).

Table 2.9 Data on plants grown from one, two, four and five-year-old F0 corms during the 2009 growing season (March - October).

(*a*) *Fresh weight at harvest, air-dry weight and number of offset(s) ($F_0$1) produced*

			Fresh wt. at harvest (g)				Air-dried wt. (g)				
F0	Age (year)	Planting wt. (g)	F0	$F_0$1(*0*)	F0 + $F_0$1(*0*)	No. of $F_0$1(*0*) produced	F0	$F_0$1(*0*)	F0 + $F_0$1(*0*)	Above ground	Total
AK4	5	1092.1	897.3	2.8	900.1	2	752.5	2.15	754.7	28.2	782.9
AK3	4	725.2	615.5	44.0	659.5	5	549.6	36.5	586.1	23.0	609.1
AK15	2	88.8	191.4	15.4	206.8	5	176.6	13.1	189.7	13.8	203.5
AK17	2	113.3	220.2	81.3	301.5	7	183.3	76.5	259.8	18.0	277.8
AK18	2	112.9	187.1	93.5	280.6	6	160.0	84.3	244.3	18.4	262.7
AK19	2	109.1	222.2	69.1	291.0	5	196.7	60.5	257.2	20.4	277.6
AKR1	1	26.7	68.6	18.6	87.2	4	56.6	15.5	72.1	5.6	77.7

(*b*) *Percentage increment in weight, dry weight ratio and dry weight/fresh weight ratio*

			% Increment change in wt.		Dry wt. ratio (%)				Dry wt. /fresh wt. ratio (%)	
F0	Age (year)	Planting wt. (g)	F0	F0 + $F_0$1(*0*)	F0	$F_0$1(*0*)	F0 + $F_0$1(*0*)	Above ground	F0	$F_0$1(*0*)
AK4	5	1092.1	-31.1	-30.9	96.1	0.3	96.4	3.6	83.9	76.8
AK3	4	725.2	-24.2	-19.2	90.2	6.0	96.2	3.8	89.3	83.0
AK15	2	88.8	98.9	113.7	86.8	6.4	93.2	6.8	92.3	85.1
AK17	2	113.3	61.8	129.3	66.0	27.5	93.5	6.5	83.2	94.1
AK18	2	112.9	41.7	116.4	60.9	32.1	93.0	7.0	85.5	90.2
AK19	2	109.1	80.3	135.7	70.9	21.8	92.7	7.3	88.5	87.6
AKR1	1	26.7	112.0	170.0	72.8	19.9	92.8	7.2	82.5	83.3

2.3.4. Quantitative differences in growth and development of offsets [$f_0$1(*0*)], produced by F0 corms of varying age during the 2009 growing season

As mentioned in section 2.2.1, offsets, $f_0$1(*0*), were selected for planting on the basis of their "mother" corm age, which was classified into one, two and ≥ four-year-old groups; referred to as group 1, group 2 and group 3 hereafter, for brevity. Each age group comprised of 15 offsets each having mean weight of 2.7 - 3.0 g at planting.

2.3.4.1. Timing of leaf bud and leaflet emergence

As shown in Table 2.10, leaf buds emerged at 72 and 80 DAP in group 1 and 2, respectively. Compared to group 2, leaf bud emergence was significantly delayed by 18 days in group 3. Similarly, leaflets first emerged in both group 1 and 2 (~ 10 days after leaf bud emergence), and was significantly delayed (by 17 days) in group 3.

2.3.4.2. Pattern of petiole growth and leaf expansion

The petiole growth patterns of $f_0$1(*0*) (group 1 to group 3) are presented in Figure 2.28. Similar growth patterns were observed for both group 1 and 2, for which the length of leaf bud (or petiole) rapidly increased during the first month after emergence (80 - 114 and 72 - 105 DAP, respectively). Thereafter, petiole elongation progressively slowed; with maximum petiole length attained at ~ 145 DAP. For group 3, the petiole length gradually increased for ~ 70 days after leaf bud emergence, up to 160 DAP, during which the maximum length was reached. From Table 2.10, the mean petiole length between group 1 (117 mm) and 3 (103 mm) are comparable, while group 2 produced a significantly shorter petiole (88 mm).

Leaf blade expansion occurred concurrently with petiole elongation for all three groups (Figure 2.29), with significantly lower leaf width recorded in group 3, compared to group 1 and 2 (Table 2.10). Both group 1 and 2 showed similar patterns of leaf expansion, *i.e.* leaflets unfurled rapidly (~ 85 - 105 DAP) after emergence, followed by a gradual expansion up to maturity (~ 160 DAP). The slightly different patterns of petiole growth and leaf blade expansion observed in group 3 were due to the large variations in both parameters among the individual plants (n = 15), with a coefficient of variation 0.346 and 0.192, respectively.

2.3.4.3. Pattern of leaf senescence

Figure 2.30 presents the data of the RChl units of $f_0 1(0)$ plants (group 1 to group 3) measured from 88 DAP. Overall, RChl content gradually increased up to 154 DAP, during which all the groups had the highest RChl readings, and thereafter sharply decrease. As presented in Table 2.10, there are no significant differences in the RChl units measured at 154 DAP (ranging from 24.8 - 26.4) between the three groups. However, group 3 had a significantly shorter growth period (104 days), compared to group 1 (119 days) and 2 (113 days).

Table 2.10 Timings (DAP) of the key stages of development (leaf bud emergence, leaflet emergence and shoot senescence) and quantitative differences in growth and development of offsets [$f_0 1(0)$], produced by F0 corms of varying age during the 2009 growing season.

		Days after planting (DAP)							
				Shoot senescence					
F0 age (year)	$f_0 1(0)$ planting wt. (g)	Leaf bud emergence	Leaflet emergence [§]	Stage 1 [†]	Stage 4	Growth period (days) [ψ]	Max. petiole length (mm)	Max. leaf width (mm)	Max. RChl units
1	2.7	80	90	199	220	119	117	269.2	26.4
2	3.0	72	82	185	206	113	88.3	251.5	24.8
≥ 4	2.9	90	107	194	213	104	102.5	227.3	25
LSD (P ≤ 0.05)		11**	16**	6**	5**	9**	18.8**	22.5**	ns

[§] Canopy width: 100 - 150 mm.

[†] Stage 1: leaf chlorosis; stage 4: above ground structures senesced and detached from corm (see plate 2.2).

[ψ] Defined as the time span from leaf bud emergence to leaf chlorosis.

** = highly significant (P ≤ 0.01).

ns = not significant.

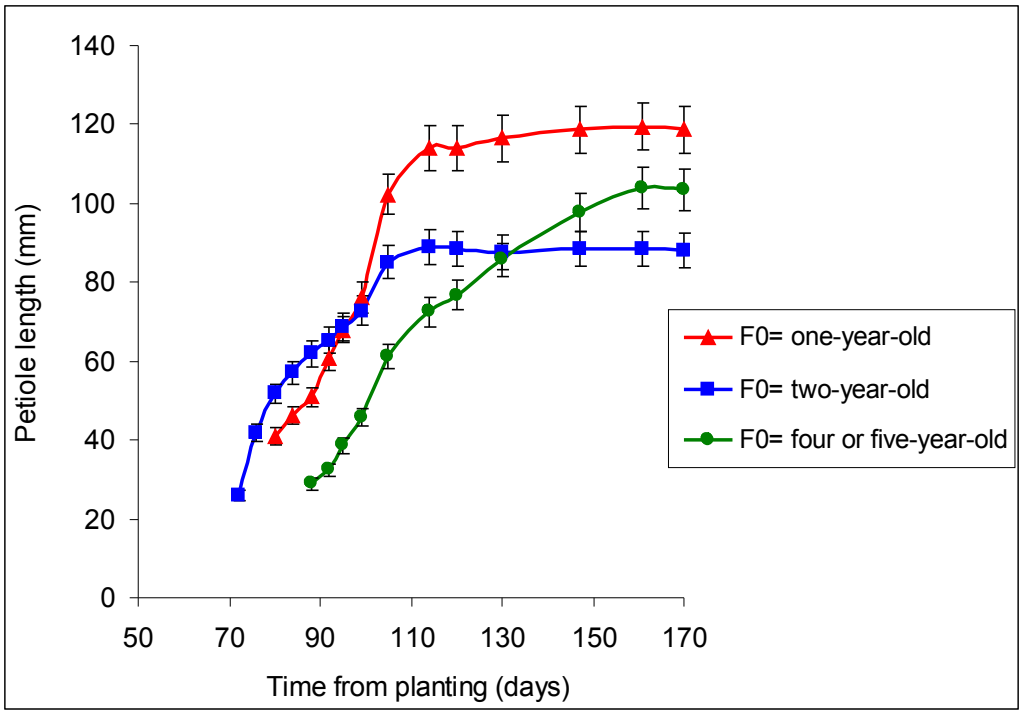

Figure 2.28 Petiole length of $f_0 1(0)$ plants (n = 15). Vertical bars indicate ± 95% confidence intervals.

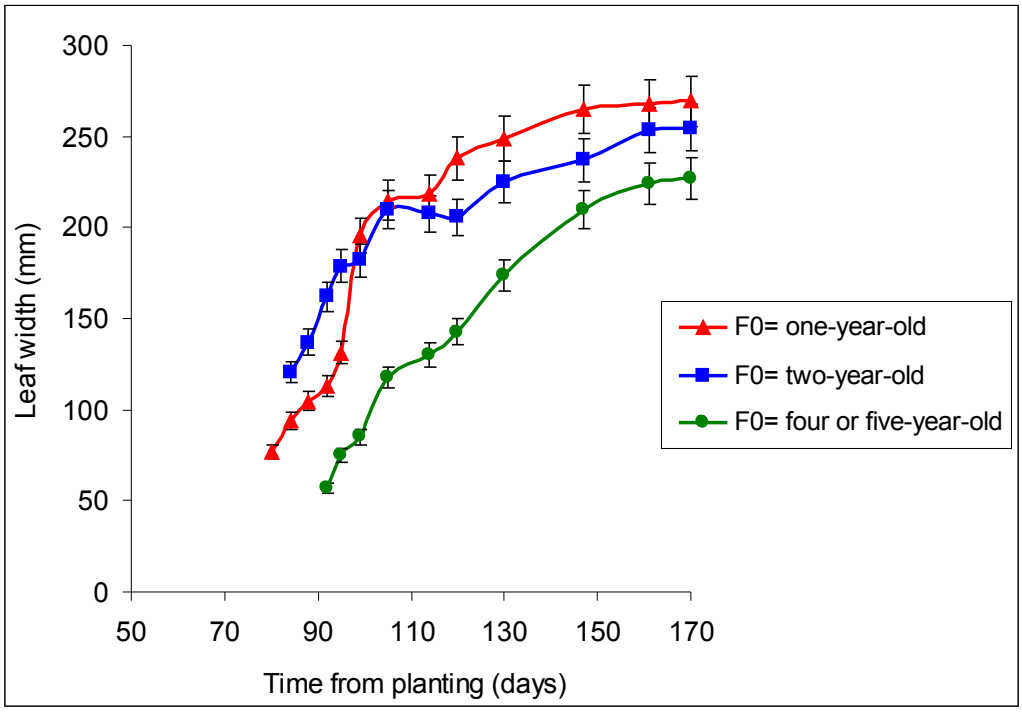

Figure 2.29 Leaf width of $f_0 1(0)$ plants (n = 15). Vertical bars indicate ± 95% confidence intervals.

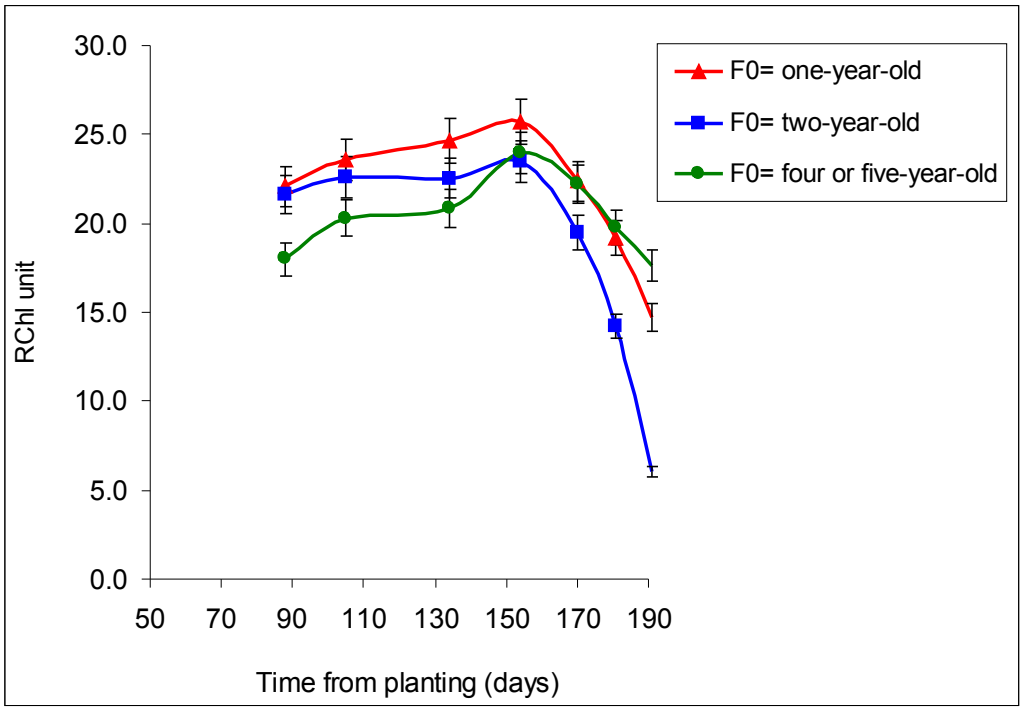

Figure 2.30 Leaf SPAD value of $f_0$1(*0*) plants (*n* = 15). Vertical bars indicate ± 95% confidence intervals.

2.3.4.4. Overall pattern of shoot development in the $f_0$1(0) plants

The overall patterns of shoot development in both group 1 and 2 are summarised and presented in Figure 2.31.

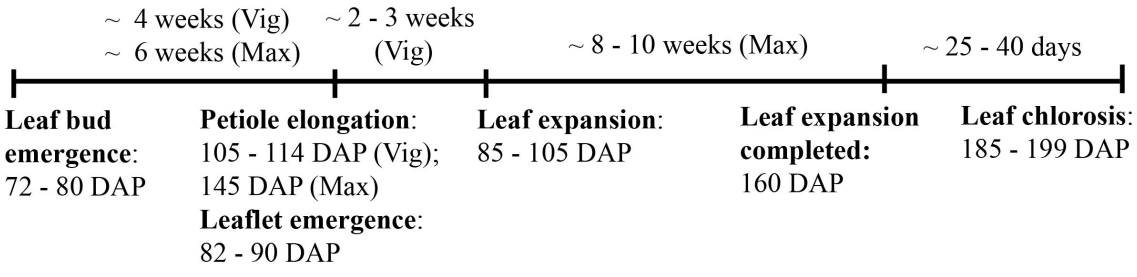

Figure 2.31 Diagrammatical presentation of the growth patterns of shoot produced by offsets [$f_0$1(*0*)] during the 2009 growing season. *DAP* days after planting, *Max* maximum, *Vig* vigorous.

2.3.4.5. Yield of $f_0$1(0) offsets

The harvest data for $f_0$1(*0*) (group 1 to group 3) during the 2009 growing season are presented in Table 2.11. It was noted that below-ground ($f_0$1 + $f_0$2) fresh and air-dry weights of group 3 were significantly lower, compared to both group 1 and 2 (Table 2.11a). The percentage increment in $f_0$1(*0*) weight over a growing season in group 1 (587%) and 2 (602%) were significantly higher than group 3 (452%) (Table 2.11b). Overall, there were no significant differences in most parameters between group 1 and 2, except in the number of offsets ($f_0$2) produced and the dry weight ratios of $f_0$1 and $f_0$2. For group 1, the numbers of $f_0$2 produced (4.5) were approximately 2 and 4 times higher than those produced by group 2 (2.5) and 3 (1.3), respectively. Of the 15 offsets planted from group 3, five corms did not produce any $f_0$2, which significantly lowered offset production in this age group. Despite a significantly higher $f_0$1 dry weight ratio observed for group 3 (87.2%), compared to group 1 (74.4%), there were no significant difference in the overall dry weight ratio of below (~ 95%) and above-ground (~ 5%) materials between these age groups.

Table 2.11 Data on plants (*n* = 15) grown from offsets [$f_0$1(*0*)] produced by one, two and ≥ four-year-old F0 corms during the 2009 growing season (March - October).

(*a*) *Fresh weight at harvest, air-dry weight and number of offset(s) ($f_0$2) produced*

		Fresh wt. at harvest (g)				Air-dry wt.				
F0 age (year)	$f_0$1(*0*) planting wt. (g)	$f_0$1(*1*)	$f_0$2(*0*)	$f_0$1(*1*) + $f_0$2(*0*)	No. of $f_0$2(*0*)	$f_0$1(*1*)	$f_0$2(*0*)	$f_0$1(*1*) + $f_0$2(*0*)	Above ground	Total
1	2.7	22.7	5.7	28.4	4.5	18.8	5	23.8	1.5	25.3
2	3.0	24.4	4.2	28.7	2.5	20.6	3.5	24.1	1.4	25.5
≥ 4	2.9	19.3	2.1	21.4	1.3	15.7	1.7	17.4	1	18.4
LSD (P ≤ 0.05)		4.2*	2.0*	5.4*	0.8**	3.8**	1.9**	4.8**	0.3**	4.8**

(*b*) *Percentage increment in weight, dry weight ratio and dry weight/fresh weight ratio*

		% increment in wt.		Dry wt. ratio (%)				Dry wt. /fresh wt. ratio (%)	
F0 age (year)	$f_0$1(*0*) planting wt. (g)	$f_0$1(*1*)	$f_0$1(*1*) + $f_0$2(*0*)	$f_0$1(*1*)	$f_0$2(*0*)	$f_0$1(*1*) + $f_0$2(*0*)	Above ground	$f_0$1(*1*)	$f_0$2(*0*)
1	2.7	587	770	74.4	19.7	94.1	5.9	82.4	84.1
2	3	602	714	81.6	12.9	94.5	5.5	85.1	76.9
≥ 4	2.9	452	506	87.2	7.1	94.3	5.7	80.3	52.3
LSD (P ≤ 0.05)		101**	89**	6.2**	5.8**	ns	ns	ns	17.8**

* = significant (P ≤ 0.05).
** = highly significant (P ≤ 0.01).
ns = not significant.

2.3.5. Quantitative differences in growth and development of F0 plants during the 2010 growing season

2.3.5.1. Timing of leaf bud and leaflet emergence

For the three-year-old corms, leaf buds emerged at 62 DAP for both growing seasons; whilst leaflet emergence was delayed by 10 - 14 days during the 2010 season (Table 2.12). The time span from leaf bud emergence to leaflet emergence ranged from 18 - 22 days. The delayed shoot emergence in both AK3 and AK4 was again due to the prior production of an inflorescence in each of these plants. The timings of leaf bud and leaflet emergence for the post-flowering plants were almost same, but leaf bud emergence was delayed by 8 and 17 days in AK3 and AK4 respectively, compared to the 2009 growing season.

2.3.5.2. Pattern of petiole growth and leaf expansion

Figures 2.32 and 2.33 clearly show that all F0 plants followed consistent patterns of petiole growth and leaf expansion compared to the previous growing season, and that these parameters increased with corm age. In all the three-year-old plants, rapid growth of petioles was observed from the first month of leaf bud emergence, with the phase of rapid leaf expansion lasting ~ 2 weeks, up to 100 DAP. The maximum petiole length and leaf width were attained at 125 DAP (63 days after leaf bud emergence), ranging from 350 - 645 mm and 435 - 500 mm, respectively. For both AK3 and AK4 plants, a sharp increased in petiole length (495 and 545 mm, respectively) and leaf width (370 and 790 mm, respectively) were recorded between 111 and 133 DAP. The highest value of these parameters were recorded at 163 and 133 DAP in AK3 and AK4, respectively.

2.3.5.3. Pattern of leaf senescence

Profiles of RChl content of F0 plants are shown in Figure 3.34. Overall, RChl content increased with corm age, and the highest RChl unit recorded for the three-year-old and the two older plants (*i.e.* AK3 and AK4) was at 125 and 133 DAP, respectively; during which the leaf had completely expanded. In contrast to the 2009 growing season, both AK3 and AK4 plants had a longer growth period (197 days), compared to the three-year-old plants (163 - 173 days) in the 2010 season (Table 2.12). The maximum RChl units recorded for both AK3 (31.8) and AK4 (42.7) were also comparable to the values obtained from the previous season (31.8 and 42.7, respectively), whilst in case of three-year-old plants, a mean reduction of 25% in RChl unit was observed during the 2010 growing season (Table 2.12).

Table 2.12 Timings (DAP) of the key stages of development (leaf bud emergence, leaflet emergence and shoot senescence) and quantitative differences in growth and development of plants produced from F0 corms during the 2010 growing season.

			Days after planting (DAP)							
					Shoot senescence					
F0	Age (year)	Planting wt. (g)	Leaf bud emergence	Leaflet emergence [§]	Stage 1[†]	Stage 4	Growth period (days) [ψ]	Max. petiole length (mm)	Max. leaf width (mm)	Max. RChl units
AK4	6	752.5	105	111	197	230	92	685	900	42.7
AK3	5	549.6	100	100	197	230	97	590	645	31.8
AK15	3	176.6	62	80	173	215	111	465	435	23.6
AK17	3	183.3	62	84	163	215	101	420	470	26.8
AK18	3	160	62	84	173	215	111	350	460	23.8
AK19	3	196.7	62	80	163	215	111	390	500	25.6
AKR1	2	56.6	84	92	183	220	99	230	355	26.4

[§] Canopy width: 100 - 150 mm.
[†] Stage 1: leaf chlorosis; stage 4: above ground structures senesced and detached from corm (see plate 2.2).
[ψ] Defined as the time span from leaf bud emergence to leaf chlorosis.

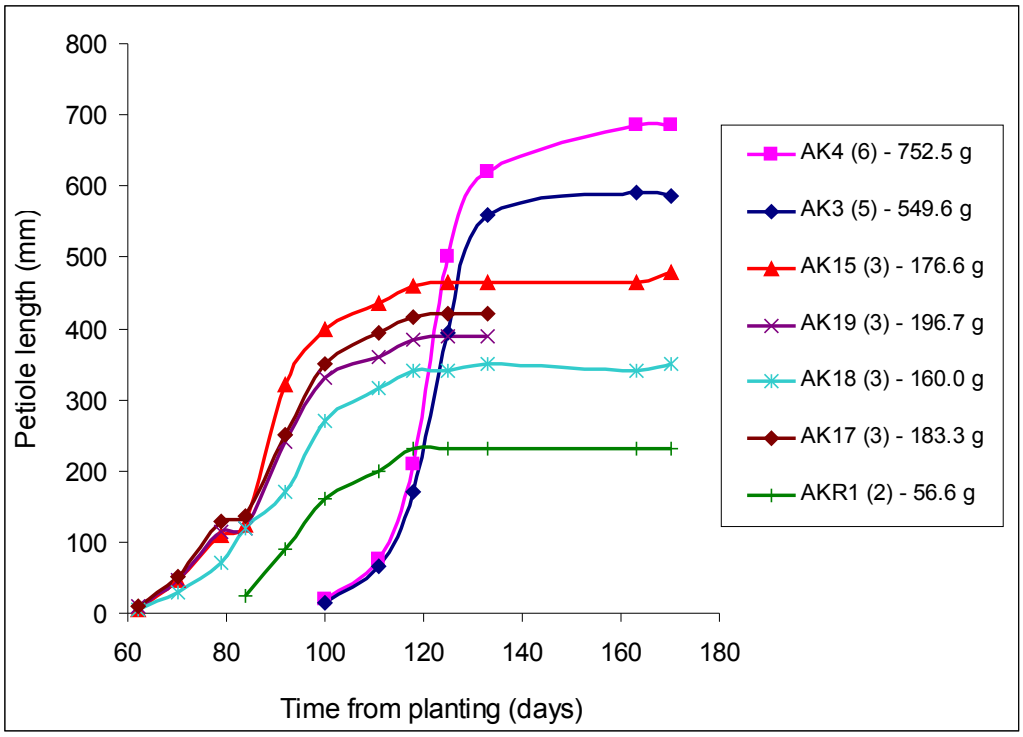

Figure 2.32 Petiole length of plants produced from two, three, five and six-year-old F0 corms. The age of F0 corms in year is shown in parentheses.

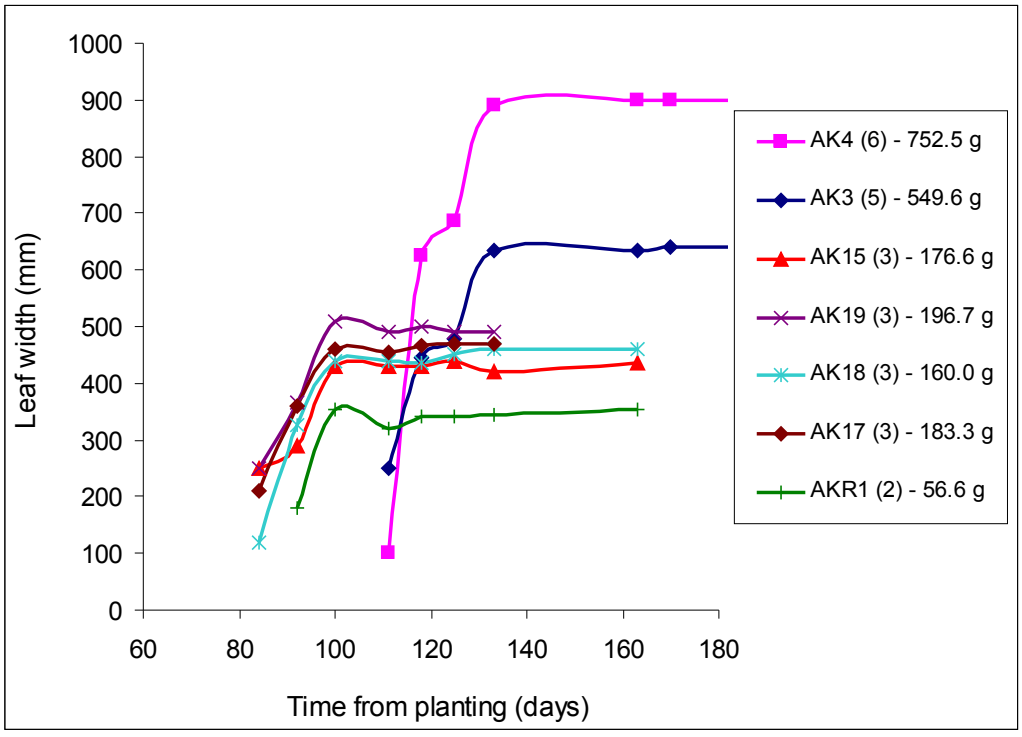

Figure 2.33 Leaf width of plants produced from two, three, five and six-year-old F0 corms. The age of F0 corms in year is shown in parentheses.

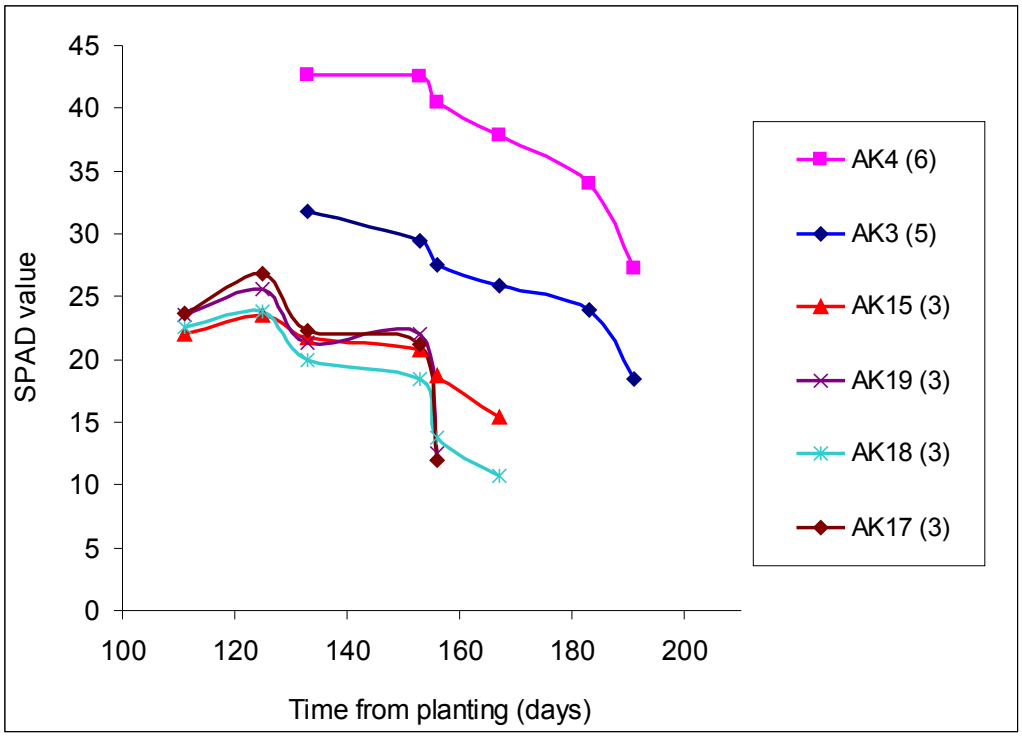

Figure 2.34 Leaf SPAD value of plants produced from two, three, five and six-year-old F0 corms. The age of F0 corms in year is shown in parentheses.

2.3.5.4. Yield of F0 corms

The harvest data for F0 corms during the 2010 growing season is presented in Table 2.13. All F0 showed a negative growth in below ground structures (F0 + $F_0$1), with the highest being recorded in AK3 and AK4 (-51% and -54.6%, respectively). In addition, the three-year-old corms had a comparable growth over the season, ranging from -17.5 to -19.5%. The amount of biomass partitioned to offset ($F_1$1) was reduced in the two and three-year-old F0 (6.0 - 17.1%), compared to the 2009 season, which ranged from 20 - 32%. Moreover, the dry matter contents of $F_1$1 produced by AK3 and AK4 corms (40.4% and 25%, respectively) was 2 - 3 fold lower than those younger F0 (75.2 - 80.3%), similar to the previous growth season. It was also noted that the dry matter content in the oldest corm, AK4 (55.8%), was considerably lower compared to other F0 (72.8 - 82.5%).

Table 2.13 Data on plants grown from two, three, five and six-year old F0 corms during the 2010 growing season (March - October).

(*a*) *Fresh weight at harvest, air-dry weight and number of offset(s) ($F_1$1) produced*

			Fresh wt. at harvest (g)				Air-dried wt. (g)				
F0	Age (year)	Planting wt. (g)	F0	$F_1$1(*0*)	F0 + $F_1$1(*0*)	No. of $F_1$1(*0*) produced	F0	$F_1$1(*0*)	F0 + $F_1$1(*0*)	Above ground	Total
AK4	6	752.5	608.3	8.8	617.1	2	339.6	2.2	341.8	15.4	357.2
AK3	5	549.6	353.4	24.5	377.9	4	258.1	9.9	268	8.7	276.7
AK15	3	176.6	151	10.9	161.9	4	124.5	8.2	132.7	4.2	136.9
AK17	3	183.3	172.7	15.7	188.4	3	139	12.6	151.6	6.6	158.2
AK18	3	160	118.2	19.4	137.6	3	97.1	15.4	112.5	4.5	117
AK19	3	196.7	172.8	22.4	195.2	4	141.2	17.6	158.8	6.2	165
AKR1	2	56.6	53.6	11.3	64.9	3	39	8.5	47.5	2.1	49.6

142

(*b*) *Percentage increment in weight, dry weight ratio and dry weight/fresh weight ratio*

			% Increment change in wt.		Dry wt. ratio (%)				Dry wt. /fresh wt. ratio (%)	
F0	Age (year)	Planting wt. (g)	F0	F0 + $F_1$1(*0*)	F0	$F_1$1(*0*)	F0 + $F_1$1(*0*)	Above ground	F0	$F_1$1(*0*)
AK4	6	752.5	-44.2	-54.6	95.1	0.6	95.7	4.3	55.8	25.0
AK3	5	549.6	-27.0	-51.2	93.3	3.6	96.9	3.1	73.0	40.4
AK15	3	176.6	-17.5	-24.9	90.9	6.0	96.9	3.1	82.5	75.2
AK17	3	183.3	-19.5	-17.3	87.9	8.0	95.8	4.2	80.5	80.3
AK18	3	160	-17.9	-29.7	83	13.2	96.2	3.8	82.1	79.4
AK19	3	196.7	-18.3	-19.3	85.6	10.7	96.2	3.8	81.7	78.6
AKR1	2	56.6	-27.2	-16.1	78.6	17.1	95.8	4.2	72.8	75.2

2.3.6. Quantitative differences in growth and development of $f_0$1(*1*) plants during the 2010 growing season

As shown in Figure 2.2, groups 1, 2 and 3 of the offsets [$f_0$1(*0*)] harvested at the end of the 2009 growing season, which were collectively referred to as $f_0$1(*1*), were used as the one-year-old corm material planted for the 2010 growing season. The corms and offsets harvested at the end of the 2010 were referred as $f_0$1(*2*) and $f_1$1(*0*), respectively.

During the 2010 growing season, the mean planting weight of $f_0$1(*1*) corms for group 1, group 2 and group 3 was 18.8, 20.6 and 15.7 g, respectively.

2.3.6.1. Timing of leaf bud and leaflet emergence

The timings of leaf bud and leaflet emergence for group 1 (88 and 97 DAP, respectively) and 2 (86 and 98 DAP, respectively) were almost the same. Compared to these groups, the leaf bud and leaflet emergence in group 3 were significantly delayed by ~ 13 and 9 days, respectively (Table 2.14). Similar observations were recorded during the 2009 growing season (Table 2.10).

2.3.6.2. Pattern of petiole growth and leaf expansion

As presented in Figure 2.35, the petiole length of group 3 (157 mm) was significantly higher than group 1 (113 mm) and 2 (116 mm), despite its late emergence. For all the three groups, the length of the leaf bud (petiole) increased rapidly during the first month after emergence up to 118 DAP in group 1 and 2, and 139 DAP in group 3; and thereafter remained almost constant, with maximum petiole length attained at ~ 163 DAP. There were no significant differences in the size of leaf canopy between the three groups (Table 2.14 and Figure 2.36).

Table 2.14 Timings (DAP) of the key stages of development (leaf bud emergence, leaflet emergence, shoot senescence) and quantitative differences in growth and development of one-year-old corms [$f_0 1(1)$] originated from F0 corms of varying age during the 2010 growing season (n = 15).

		Days after planting (DAP)							
				Shoot senescence					
F0 age (year)	Planting wt. (g)	Leaf bud emergence	Leaflet emergence [§]	Stage 1 [†]	Stage 4	Growth period (days) [Ψ]	Max. petiole length (mm) [Ψ]	Max. leaf width (mm)	Max. RChl units
1	18.8	88	97	203	226	115	112.7	218.3	16.5
2	20.6	86	98	195	225	109	116.2	222.0	18.8
≥ 4	15.7	99	106	201	227	102	157.0	242.0	20.5
LSD (P ≤ 0.05)		6**	7**	4**	ns	6**	22.4**	ns	1.6**

[§] Canopy width: 100 - 150 mm.
[†] Stage 1: leaf chlorosis; stage 4: above ground structures senesced and detached from corm (see plate 2.2).
[Ψ] Defined as the time span from leaf bud emergence to leaf chlorosis.

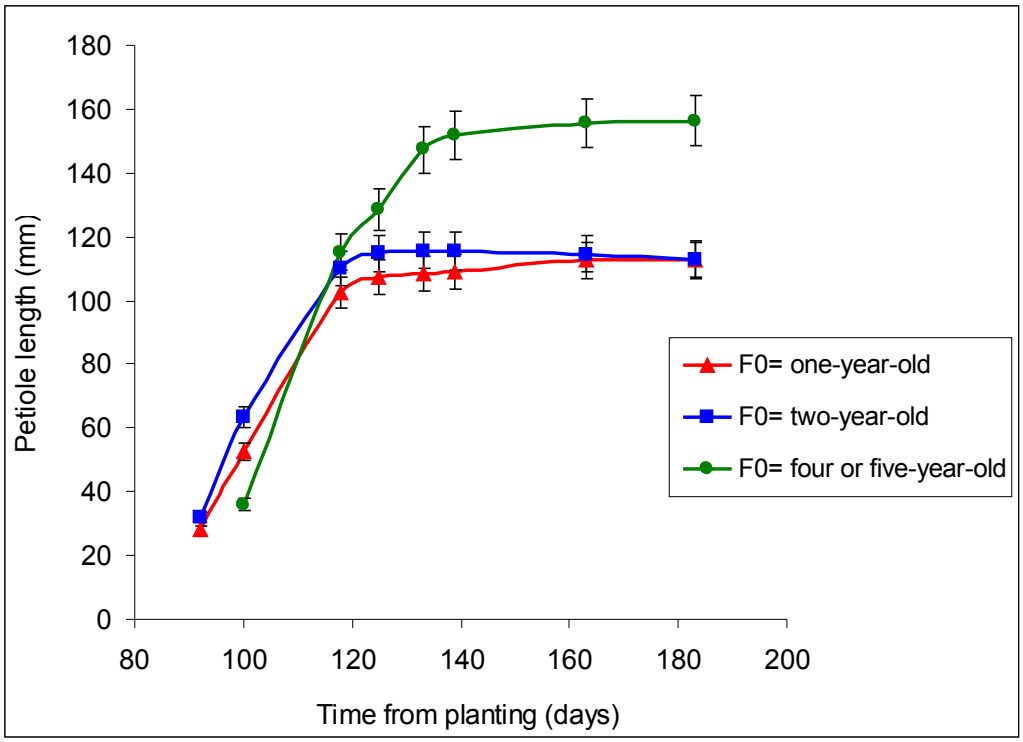

Figure 2.35 Petiole length of $f_0 1(I)$ plants (n = 15). Vertical bars indicate ± 95% confidence intervals.

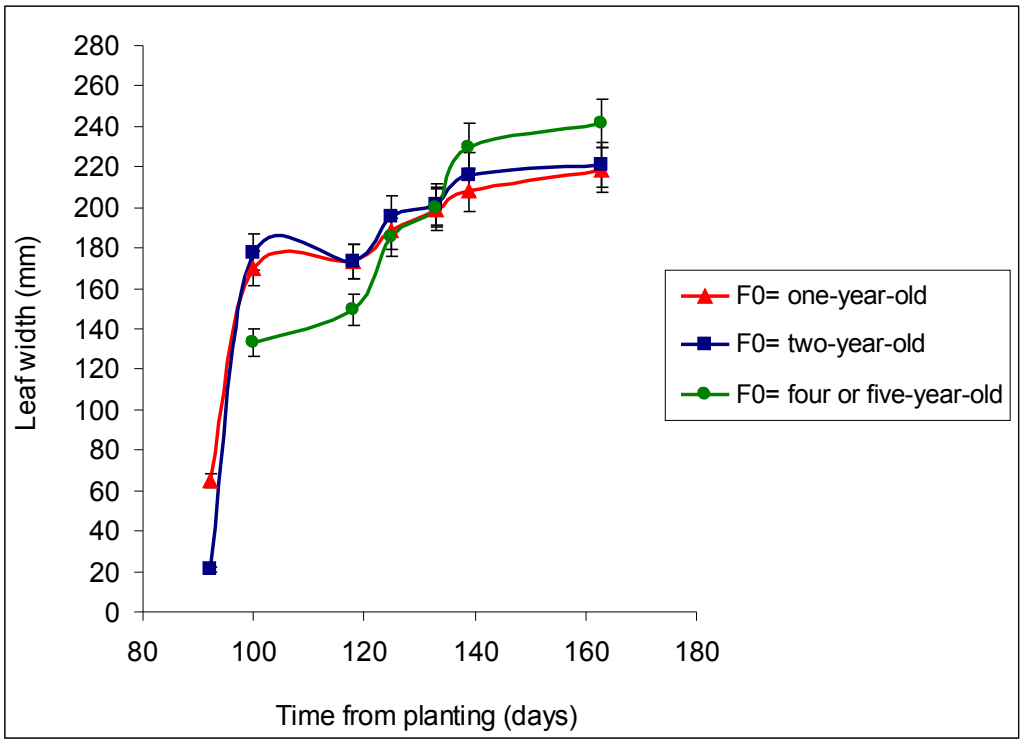

Figure 2.36 Leaf width of $f_0 1(I)$ plants (n = 15). Vertical bars indicate ± 95% confidence intervals.

2.3.6.3. Pattern of leaf senescence

Figure 2.37 presents profiles of RChl units of $f_0$1(*1*) plants measured from 111 DAP. For group 2 and 3, the highest RChl units were recorded at 125 DAP, followed by a sharp decrease in group 2, compared to a more gradual decrease in group 3. A slightly different pattern of leaf senescence was recorded for group 1, with a steady increase in RChl units during the early stages of leaf expansion up to 156 DAP and the highest readings attained later than the other two groups at 167 DAP. These observations correlated with the later occurrence of leaf chlorosis and hence significantly longer growing periods were recorded in group 1, compared to the other two groups (Table 2.14). However, the maximum RChl units recorded for group 1 (16.5), was significantly lower compared to group 2 and 3, which were 18.8 and 20.5, respectively (Table 2.14).

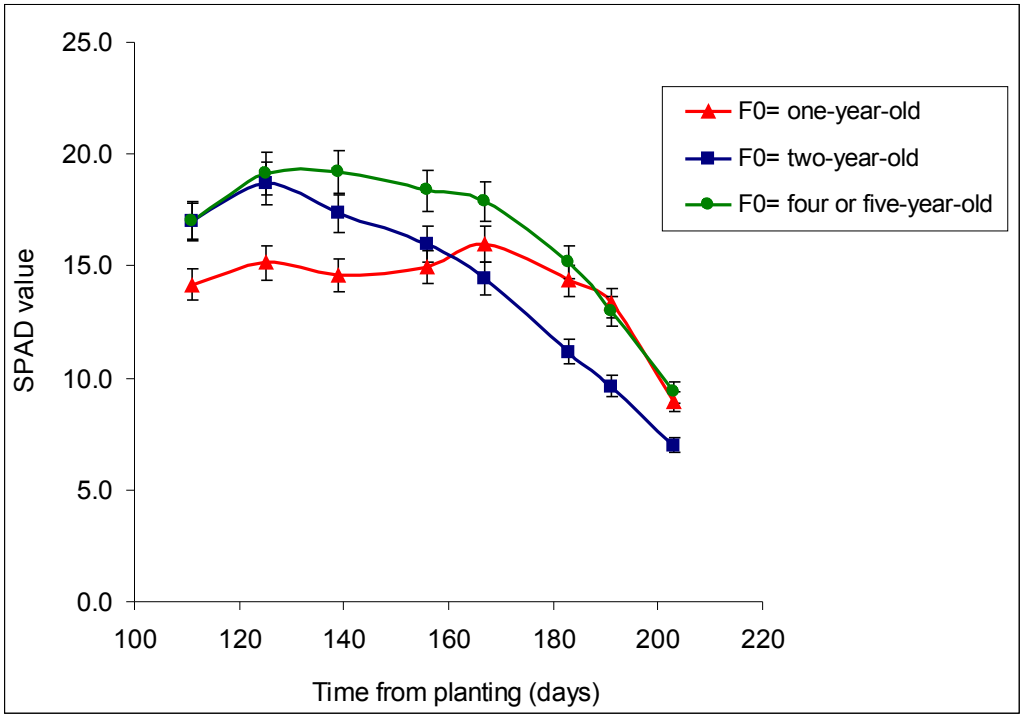

Figure 2.37 Leaf SPAD value of $f_0$1(*1*) plants (*n* = 15). Vertical bars indicate ± 95% confidence intervals.

2.3.6.4. Yield of $f_0$1(1) corms

The harvest data for $f_0$1(*1*) plants during the 2010 growing season are shown in Table 2.15. Overall, there were no significant differences in mean fresh and air-dried weights of both above and below-ground materials between age groups, but the mean number of offsets ($f_1$1) produced in group 1 was significantly higher than the other groups. The highest dry matter content of $f_0$1 and $f_1$1 were produced by group 2 at 62.6% and 66.4%, respectively.

Table 2.15 Data on one-year-old corms [$f_0 1(1)$], originated from one, two and ≥ four-year-old F0 corms during the 2010 growing season (March - October).

(*a*) *Fresh weight at harvest, air-dry weight and number of offset(s) ($f_1 1$) produced*

		Fresh wt. at harvest (g)				Air-dry wt.				
F0 age (year)	$f_0 1(1)$ planting wt. (g)	$f_0 1(2)$	$f_1 1(0)$	$f_0 1(2) + f_1 1(0)$	No. of $f_1 1(0)$	$f_0 1(2)$	$f_1 1(0)$	$f_0 1(2) + f_1 1(0)$	Above ground	Total
1	18.8	29.9	5.2	35.0	2.9	16.6	2.9	19.5	1.2	20.7
2	20.6	27.6	5.4	33.0	1.9	17.3	3.3	20.6	1.0	21.6
≥ 4	15.7	29.1	3.9	33.1	2.0	16.1	2.1	18.2	1.0	19.2
LSD (P ≤ 0.05)		ns	ns	ns	0.71*	ns	ns	ns	ns	ns

(*b*) *Percentage increment in weight, dry weight ratio and dry weight/fresh weight ratio*

		% increment in wt.		Dry wt. ratio (%)				Dry wt. /fresh wt. ratio (%)	
F0 age (year)	$f_0 1(1)$ planting wt. (g)	$f_0 1(2)$	$f_0 1(2) + f_1 1(0)$	$f_0 1(2)$	$f_1 1(0)$	$f_0 1(2) + f_1 1(0)$	Above ground	$f_0 1(2)$	$f_1 1(0)$
1	18.8	-8.5	7.2	80.9	13.4	94.3	5.7	55.4	55.2
2	20.6	-14.8	1.3	79.8	15.6	95.4	4.6	62.6	66.4
≥ 4	15.7	16.4	31.7	84.3	10.5	94.8	5.2	55.7	42.9
LSD (P ≤ 0.05)		ns	ns	ns	ns	ns	ns	4.2**	12.1**

* = significant (P ≤ 0.05).
** = highly significant (P ≤ 0.01).
ns = not significant.

2.3.7. Overall productivity of different aged propagation material

Table 2.16 shows data for the initial planting weight of F0 corms at the beginning of the 2008 growing season, the air-dried (*i.e.* planting) weight of both F0 and $f_0$1 in the subsequent seasons and the annual productivity (harvested corm weight/initial planting weight) of the different aged propagation materials. It was noted that corm productivity decreased with increasing age. During the 2008 growing season (Mar-08 to Oct-08), the productivity of one-year-old corms ranged from 5 - 5.7 and decreased to 1.4 - 2 in the following season (Mar-09 to Oct-10). Moreover, the productivity of older F0, AK3 and AK4, were shown to be ~ 2.5 - 4 times lower than those of younger F0 in 2008 season, with both showing negative growths (*i.e*. productivity < 1) in the 2009 growing season. Over the 2008 and 2009 seasons (Mar-08 to Oct 09), the weight of younger F0 increased 8.4 - 11.1 fold, compared to only 1.2 and 1.6 fold for AK3 and AK4 corms, respectively. Offset materials ($f_0$1), on the other hand, had the highest productivity of 5.4 - 7 in the 2009 season, and was 3 - 5 times higher than those two-year-old F0 corms. As mentioned in section 2.3.4, group 3 (F0 = ≥ four years-old) was the least productive among the three age group of offset material.

In the 2010 growing season, however, all the propagation materials showed negative growth, except for the group 3 offsets, in which no growth was recorded (*i.e*. productivity = 1).

Table 2.16 Summary of the annual production (presented as air-dried weight) and productivity of different-aged propagation material.

	Annual production (air-dried weight) (g)				Productivity			
F0 corm	Mar-08	Mar-09	Mar-10	Mar-11	Mar-08 to Oct-08	Mar-09 to Oct-09	Mar-08 to Oct-09	Mar-10 to Nov-10
AK3	444	725	550	258	1.6 (*3*)	0.8 (*4*)	1.2	0.5 (*5*)
AK4	485	1092	753	340	2.3 (*4*)	0.7 (*5*)	1.6	0.5 (*6*)
AK15	16	89	177	125	5.7 (*1*)	2.0 (*2*)	11.1	0.7 (*3*)
AK17	17	113	183	139	6.6 (*1*)	1.6 (*2*)	10.8	0.8 (*3*)
AK18	19	113	160	97	5.8 (*1*)	1.4 (*2*)	8.4	0.6 (*3*)
AK19	22	109	197	141	5.0 (*1*)	1.8 (*2*)	9.0	0.7 (*3*)
AKR1	-	27	57	39	-	2.1 (*1*)	-	0.7 (*2*)
$f_0$1								
F0 = one year-old (group 1)	-	2.7	18.8	16.6	-	7.0 (*0*)	-	0.9 (*1*)
F0 = two years-old (group 2)	-	3.0	20.6	17.3	-	6.9 (*0*)	-	0.8 (*1*)
F0 ≥ four years-old (group 3)	-	2.9	15.7	16.1	-	5.4 (*0*)	-	1.0 (*1*)

N.B. (i) Annual productivity = harvested corm weight/initial planting weight.
(ii) The age of propagated material in year is shown in parentheses.

2.4. Discussion

2.4.1. Floral development

The size of the underground storage organ of a perennial plant is closely associated with plant age, which in turn determines the energy available for growth and reproduction in the following season (Ehlers and Olesen, 2004). Typically, perennial plants partition energy to the accumulation of reserve carbohydrate until it achieves an optimum underground storage size. At this stage, excess energy produced from photosynthesis is either used in the development of reproductive tissues, or to support secondary growth (Isawa and Cohen, 1989). In the current study, all plants started their seasonal growth by exhibiting vegetative development, except for the two oldest corms, AK3 and AK4. These corms were four and five years-old, respectively during the 2009 growing season and both underwent reproductive growth, with inflorescences produced in two consecutive seasons (2009 and 2010). This suggests that konjac plants grown under glasshouse conditions take at least 4 years to attain sexual maturity, an observation which is in agreement with the literature (Imai and Coleman, 1983; Sun *et al*., 1995; Liu, 2004).

According to Sedayu *et al*. (2010), there are three common types of growth cycles exhibited by mature plants of *Amorphophallus*, corresponding with two major clades of different geographical distributions. For most Asian species, the plants undergo dormancy after flowering for the rest of the growth season with a leaf being produced during the following season. In these species, either an inflorescence or a leaf is developed within a growth season. By contrast, in a few Asian species such as *A. ochroleucus*, *A. coaetaneus* and *A. rhizomatosus*, both leaves and inflorescence are produced in the same growth season, with the leaf appearing first, followed by an

inflorescence several weeks or months later from the same node. For all African species, the growth season starts with the development of an inflorescence, with a leaf produced either simultaneously alongside the inflorescence, or soon after flowering in the same season. Both the inflorescence and leaf develop from different nodes, in which the inflorescence arises on the apical bud from the shoot of the previous season, whilst the leaf develops from a lateral bud, initiating the next sympodial cycle.

In the present study, each of the two oldest corms, AK3 (four-year-old) and AK4 (five-year-old), which produced an inflorescence and a leaf during the same growth season for two consecutive years (2009 and 2010), exhibited a growth cycle similar to that reported for African species of *Amorphophallus* (Sedayu *et al*., 2010). The development of the leaf bud alongside the senescing inflorescence, shown in Figure 2.4g, suggests that the reproductive and vegetative organs of mature plants of *A. konjac* developed from different nodes. Moreover, the shorter period of dormancy observed in both AK3 and AK4 corms indicate that the time period required for differentiation of floral primordia is shorter than for leaf primordia. Working with konjac under glasshouse conditions, Liu (2004) reported that the dormant period for corms of Chinese konjac cultivars with developing flower buds was shortened by 2 months, which is in agreement with our observations. The author did not mention, however, whether a leaf canopy was produced in the same season. The latent period of approximately 2 months after the senescence of the inflorescences in both AK4 and AK3 prior to the initiation of vegetative growth, as recorded in the present study, may be the period required for differentiation of the leaf bud.

To date, little has been published on the flowering pattern of *A. konjac*, compared to *A. titanum*, which has been studied extensively (Hetterscheid *et al*.,

1998; Lobin *et al*., 2007). Researchers from the Botanic Gardens at the University of Bonn in Germany reported that a corm of *A. titanum* which produced inflorescences in three consecutive growth seasons, developed three inflorescences simultaneously during May 2006 (Lobin *et al*., 2007). The development of multiple inflorescences has also been observed by Lobin *et al*. (2007) in konjac plants with the production of three leaves after the flowering events. Hence, it would be interesting to observe if AK3 and AK4 corms could produce multiple inflorescences and leaves over the next two growing seasons. The multiple shoot phenomenon appears to be the result of a reduction in apical dominance once the plant exceeds a critical age which may be due to the reduced ability to synthesize and translocate auxin (Kumar and Knowles, 1993; Davies, 2010), or an increased rate of auxin catabolism in buds from older corms. Furthermore, the inflorescences produced in AK3 and AK4 corms lasted a week longer after anthesis, compared to those observed in *A. titanum* as reported by Lobin *et al*. (2007).

2.4.2. Morphology of corm and offset materials

From the morphological study of corms of different ages, it appears that the konjac corm is a strongly condensed, underground stem. Our observations of the phyllotaxis of the main lateral bud present on each node, agree with data previously reported for *A. paeoniifolius* and *A. variabilis* (Santosa *et al*., 2006). This suggests that lateral buds of *Amorphophallus* species are arranged in a 3 + 5 phyllotactic pattern, similar to that of taro species (*Colocasia esculenta*) (Matsubara and Ishiguro, 1936).

The larger number of lateral buds on the dorsal side simply reflects active cell division in this region which is associated with the lateral growth of offsets and roots.

The absence of lateral growth in the middle and ventral portions, however, may be due to the fact that the number of potential buds per unit surface area was lower compared to the dorsal side. This assumption was based on visual inspection, from which the corm surface at its basal region appeared to be smoother compared to dorsal side. In line with our observations, the dorsal portions of corms have previously been shown to be a better source of propagules for the vegetative propagation of *A. titanum* (Sri Prana, 1997) and *A. paeoniifolius* (Dhua *et al*., 1988; Mondal and Sen, 2004; Ravi *et al*., 2009). In India, the ventral portions of *A. paeoniifolius* corms are treated with chemicals such as thiouarea, potassium nitrate and chlormequat chloride prior to planting, to improve sprouting efficiency (Dhua *et al*., 1988; Kumar *et al*., 1998).

In terms of offset morphology, lateral buds of *A. konjac* developed stolon-like structures with the formation of cormels at their apices, unlike *A. paeoniifolius* and *A. campanulatus* in which cormels are directly attached to the corm surface (Sri Prana, 1997). Liu (2004) reported that offsets produced by Chinese konjac cultivars usually remain inactive throughout the growth season in which they were developed, which is supported by the current data. However, this author also reported that offsets produced by Japanese konjac cultivars may develop shoots during the same growth season after being formed. If substantiated, this suggests a degree of plasticity in the timing of the developmental sequences in konjac, with periods of inactivity or dormancy being facultative rather than obligate. There also appears to be considerable variation of morphogenetic sequences in different cultivars of konjac.

2.4.3. Corm tissue structure

It has been shown previously that glucomannan is stored in a highly hydrated state in the vacuole of highly specialized cells, known as idioblasts, within the vegetative storage organs of many geophytes (Meier and Reid, 1982; Bewley and Reid, 1985; Miller, 1992), including the *A. konjac* (Wakabayashi, 1957; Takigami *et al*., 1997; Shi *et al*., 1998). In the present study, the identification of the cell types observed in the toluidine blue-stained sections of corm tissue were based on earlier observations reported by Takigami and colleagues (Takigami *et al*., 1997), who examined cross sections of two-year-old dormant corm tissues, under both scanning electron and optical microscopes. Their data demonstrated that KGM granules accumulate in large, egg-shaped idioblasts filled with mucilage that are located within the parenchyma and that the size and number of these idioblasts increases with distance from the epidermis. In our study, idioblasts which differed markedly in size and shape from the neighbouring parenchyma cells were also observed throughout the corm tissues at all stages of development (Figure 2.9 - 2.14). Indirect immunofluorescence light microscopy revealed the presence of abundant mannan epitopes in these specialized cells in dormant corms (Figure 2.18), thus confirming the previous observations (Wakabayashi, 1957; Takigami *et al*., 1997; Shi *et al*., 1998). Moreover, the range in diameter (*i.e.* 160 - 650 μm) reported for the glucomannan idioblasts in the literature is comparable with that observed in the current study (~150 - 600 μm). However, no noticeable variation in the number and size of the glucomannan idioblasts was observed at increasing distances from the epidermis in any corm, at any stage of development.

A previous study on the structure and formation of glucomannan idioblasts in corms of konjac and orchid species reported the presence of nuclei in these specialized cells (Wakabayashi, 1957). By contrast, nuclei were not observed in the glucomannan idioblasts (Figure 2.17: G - J) in the current study, which is in agreement with the results reported by other researchers (Takigami *et al*., 1997; Shi *et al*., 1998).

Calcium oxalate crystals, in the form of raphides, styloids, druses, prismatics and crystal sands, occur widely throughout the plant kingdom (Prychid and Rudall, 1999; Franceschi and Nakata, 2005). They perform various biological functions, including herbivore deterrence (Hudgins *et al*., 2003), calcium regulation (Kostman and Franceschi, 2000; Volk *et al*., 2002) and are also associated with heavy metal tolerance (Franceschi and Nakata, 2005). The presence of crystal idioblasts in the leaf (Prychid *et al*., 2008) and underground corm tissues (Wakabayashi, 1957; Takigami *et al*., 1997; Shi *et al*., 1998) of *A. konjac* has been previously reported. In our study, two types of crystal idioblasts, *i.e.* raphide and druse idioblasts, were observed within the parenchyma of the corm tissues. One of the features of the raphide crystal idioblasts observed in the present investigation is the accumulation of mucilage surrounding the crystals in the central vacuoles, similar to some species of the Orchidaceae, Typhaceae, Agavaceae and Actinidaceae (Meier and Reid, 1982; Wang *et al*., 1994). Compositional analysis of the mucilage in the central vacuoles of the idioblasts in leaves of grapes (*Vitis* spp.) showed the presence of an unusual polymer with novel glucuronic acid linkages (Webb *et al*., 1995). Furthermore, linkage analysis indicated the presence of 5-linked arabinans, arabinogalactan (AG) and various mannosyl units, typical of complex carbohydrates attached to proteoglycans and glycoproteins present in the mucilage (Webb *et al*., 1995). Hence,

the strong expression of mannan epitopes in both the raphide and druse crystals and its surrounding mucilage (Figure 2.17: B - F) observed in this study might be due to the presence of arabinogalactan-proteins (AGPs) which may bear terminal mannose residues, mannose-containing hemicelluloses or other mannose-bearing glycoproteins in the crystal idioblasts.

Besides the crystal idioblasts, raphide crystals were also observed within the glucomannan idioblasts (Figure 2.17 G - J), which is in agreement with previous studies (Takigami *et al*., 1997; Shi *et al*., 1998). In the current study, however, not all the glucomannan idioblasts appeared to contain raphide crystals which may be attributed to the fact that most of these crystals are present at the outer surface of the idioblasts (Shi *et al*., 1998), or because resin did not penetrate the crystals (Prychid *et al*., 2008), which resulted in crystals falling out of the corm tissue during sectioning. Hence, precipitation of crystals is seen as an empty hole at the thin-filmed mucilage in some of the glucomannan idioblasts (Figure 2.17: I, J).

2.4.4. Growth and development of corms throughout the vegetative growth cycle

The trends of vegetative growth observed during the 2009 growing season were consistent with those reported for konjac by other workers (Wang and Liu, 1990; Yokoi *et al*., 1991; Hetterscheid and Ittenbach, 1996; Liu *et al*., 1998). The transition from a loss to a gain in corm fresh weight (Table 2.5 and 2.6) has previously been referred to as the "source-sink transition" (Robinson *et al*., 2000; Taiz and Zeiger, 2010). This represents a change in corm function from a source of stored resources for shoot development, to a sink for surplus photosynthate from the mature leaf canopy.

It has been reported previously that reserve carbohydrates and nutrients stored in planted ("mother") corms are metabolised during the initial stages of shoot development leading to the complete degeneration of the "mother" corm (Wang and Liu, 1990; Liu, 2004). As the leaf develops, a "daughter" corm is formed on top of the degenerated "mother" corm and subsequently enlarges through the accumulation of photosynthates. The current observations confirm that the "mother" corm degenerates during early shoot development (Figure 2.8: 5iii). Nevertheless, there was no evidence of complete degeneration of the "mother" corm, as shrinkage was observed at the middle-ventral region of the corm during leaflet emergence (Figure 2.7: 4i). This finding, together with the appearance of vascular bundles (probably connected to the emerging shoot) observed in the central region of the corm tissue during leaf bud emergence (Figure 2.10), suggest the existence of a physiological gradient within the developing corms, such that the direction of reserve carbohydrates and nutrients in the translocation stream to the dorsal side while the corm functioned as a source for apical bud emergence and root development, prior to leaf expansion. Furthermore, as mentioned previously, the growth of corm was more pronounced on the dorsal than on the ventral side, the dorsal region may therefore be functioning as a sink for photosynthates from the leaf canopy.

2.4.5. Developmental regulation of mannan epitopes in corm tissues

Light and transmission electron microscopy of immuno-labelled corm tissues indicated that the expression of mannan epitopes in the glucomannan idioblasts followed a temporally regulated pattern, with increased expression towards the end of the vegetative growth cycle (Figures 2.16, 2.18 - 2.23).

After the dormant period, mannan epitopes in the glucomannan idioblasts were shown to gradually decrease throughout the early stages of shoot development, *i.e.* leaf bud formation (Figures 2.16: 2a - c, 3a – c, 2.19 and 2.20) and leaflet emergence (Figures 2.16: 4a - c and 2.21). From the stage of leaf expansion until shoot senescence, an increase in the intensity of antibody binding in the glucomannan idioblasts was observed (Figures 2.16: 5a - e, 6a - e, 2.22 and 2.23). These observations are associated with the change from loss to gain of both corm fresh weight and diameter (Table 2.5), as recorded at each harvest. This further confirms the occurrence of a source-sink transition in the corm structure during the vegetative growth cycle. Our data (Figure 2.16) suggest that this transition is made in the corm after leaflet emergence, prior to complete expansion of the leaves. Based on our observations of the vegetative growth patterns recorded for all F0 corms (except AK3 and AK4) during the 2009 season, the source-sink transition most probably occurred between 70 and 90 DAP (Figure 2.26). However, since no samples were quantitatively analysed for glucomannan content throughout the growth period, the glucomannan content at the source-sink transition is unknown. However, Wang and Liu (1990), who studied changes in corm composition throughout the vegetative growth period, reported a decrease in glucomannan content (on a fresh weight basis) from 52% to 7% upon the source-sink transition. It is therefore reasonable to assume that this trend of reduction in glucomannan content occurred in corms of plants used in the current study.

During the stages in which the corm functions as a source for early shoot development (stage 2 - 4), mannan epitopes were rare, or absent in most idioblasts (Figure 2.16: 2a - c, 3a - c), except for a few near the mid-point of the corm (*i.e.* position a), which were observed to be strongly labelled (Figures 2.16: 2a, 4a, b;

2.18: IA, IB and 2.20: IA, IB). These observations suggest that the mobilization of glucomannan polysaccharides initiates at the periphery of the corm (*i.e.* from position c and beyond) and proceeds inwards towards the centre of the corm. A similar pattern of reserve carbohydrate mobilization has also been observed in other geophytes, including lily (Matsuo and Mizuno, 1974; Miller, 1992) and taro (Kawasaki *et al*., 2001).

Based on the current observations, we propose that the glucomannan-containing mucilage within the idioblasts degrades and gradually changes to a low-density, sol-like substance, which was shown to produce a weaker expression of mannan epitopes, from the stage of dormancy (Figure 2.16: 1a) throughout the early stages of shoot development (Figure 2.16: 2a - c, 3b). These results were confirmed via immunogold electron microscopy which demonstrated that in dormant corms, fewer immunogold particles were present within idioblasts which contain sol-like substances (Figure 2.18: IA, IB), compared to those with the thin-film mucilage (Figure 2.18: IIA, IIB). In relation to which, Shimahara *et al*. (1975) isolated two β-mannanases from germinating konjac corms and found that both enzymes hydrolyse manno- and glucomanno-oligosaccharides, cleaving β-1,4-linked internal linkages, mainly at the third/fourth position from the non-reducing end *(i.e.* endo-type mechanism). Moreover, high energy production and degradation of starch have been reported previously in tubers of yam (*Dioscorea* spp.) over the pre-sprouting period, during which the development of the shoot apical meristem and foliar primordium were observed (Hariprakash and Nambisan, 1996; Panneerselvam *et al*., 2007). Therefore, initial mobilization of glucomannan reserves observed in the dormant corms in this study may be attributed to these active meristematic activities, prior to leaf bud emergence, by the action of β-mannanases. The presence of empty idioblasts

(Figure 2.16: 2b, 2c, 3a - c, 4b, 4c), indicates that these highly specialized cells function as a temporary reservoir for the glucomannan reserve polysaccharides, which are reabsorbed and replenished periodically over the course of seasonal growth.

During leaf expansion (Figure 2.22: IA), mannan epitopes were observed to be progressively deposited at the periphery of the glucomannan idioblasts, with the majority observed near the plasma membrane (Figures 2.16: 5a – c; 2.17: K, L and 2.22: IA). As mentioned in section 1.4, both Golgi-localised mannan and glucomannan synthases are encoded by the cellulose synthase–like A (*CslA*) gene (Lerouxel *et al*., 2006; Liepman *et al*., 2007; Goubet *et al*., 2009). Expression of this gene has been previously demonstrated in *Arabidopsis thaliana* (Richmond and Somerville, 2000; Scheible *et al*., 2001; Goubet *et al*., 2009), rice (*Oryza sativa*) (Dhugga, 2005), black cottonwood (*Populus trichocarpa*) (Suzuki *et al*., 2006) and in both mono and dicotyledonous angiosperms, as well as a gymnosperm and a bryophyte (Liepman *et al*., 2007). Recently, Gille *et al*. (2011), who studied the biosynthesis of KGM in a developing corm (harvested 17 weeks after planting), reported that the corm produced high level of *CslA* transcript (AKCskA03) with a similar deduced protein sequence and topology to CslA from *A. thaliana* (AtCslA03). The active site of KGM synthase, however, was predicted to face the cytosol, instead of the Golgi lumen, as in *A. thaliana*. Therefore, the increased labelling intensity at the periphery of the glucomannan idioblasts during leaf expansion, as observed in the current study, may be attributed to continuing synthesis of mannan in the Golgi apparatus (Handford *et al*., 2003; Gille *et al*., 2011) and deposition at the idioblast periphery inwards (Figures 2.16: 5a - c and 2.17: K, L).

2.4.6. The growth potential of different aged propagation material and the productivity of offsets produced by F0 corms of different age

Despite the considerable amount of biomass allocated to $F_0$1(*0*) offset structure in the one and two-year-old F0 corms (except AK15) (20 - 32% of the total plant dry wt.), compared to both AK3 and AK4 corms (6% and 0.3% of the total plant dry wt., respectively), there was no discernible difference in the overall partition of biomass to underground structures (F0 + $F_0$1) (*i.e*. harvest index) between the F0 corms (Table 2.9b) with varying age. These observations, together with the decrease in productivity with increasing F0 corm age (Table 2.9b) recorded at the end of the 2009 growing season, are in agreement with earlier results reported by Miura and Watanabe (1985).

The decrease in growth potential observed in the older F0 corms, AK3 and AK4 (Table 2.9b), is evident by their negative growth (-19% and -31%, respectively) recorded over the 2009 growing season. The negative growth of both AK3 and AK4 corms may be attributed to the changes in allocation strategy in these plants with increasing corm age, by partitioning relatively more biomass into floral development after several years of vegetative growth. It may be also due to the fact that both these plants had a shorter growth period, compared to the two-year-old F0 plants (Table 2.8). In our study, the growth period is defined as the time span from leaf bud emergence to the initiation of shoot senescence, during which leaf chlorosis occurred. In contrast to younger plants, it was observed that the senescence of both AK3 and AK4 plants began with the collapse of the aerial part with leaflets retained in a fully green state. This indicates that the whole adult leaf, though resembling a stem plus a leaf, is a structure that can easily lose its rigidity. According to Hejnowicz and Barthlott (2005), the petiole of *Amorphophallus* species is a shell of

compact parenchyma with embedded collenchyma strands surrounding a core filled with aerenchyma. Mechanical stability of this petiole relies entirely on turgor pressure in the parenchyma. Towards the end of growth season, turgor pressure decreases, presumably due to the passive leakage of solutes and the petiole subsequently collapses under axially-directed weight force of the lamina.

Of all the different age propagation material planted in the 2009 growing season, offsets (regardless of the age group of F0 corms) were shown to have the highest productivity. This is in agreement with Yokoi *et al*. (1991), who reported that the productivity of offset plants was 1.4 - 1.7 times higher than both one and two-year-old plants. Among the offsets, it is possible that both group 1 and 2 inherited the greater growth potential from their younger F0 corms, thus producing significantly higher corm yield and number of offsets [$f_0 2(0)$] (Table 2.11), compared to group 3. Typically, the delay in leaf bud emergence and the significantly shorter growth period observed in group 3 (Table 2.10) may be genetically inherited from their older mother corms, AK3 and AK4 (Table 2.8). The significant delay in leaf bud emergence recorded in group 3 for both growing seasons (Table 2.10 and Table 2.14) indicates that this age group had a longer period of dormancy than the other groups.

In the 2010 season, the growth rates from the majority of F0 corms were lower than in 2009. The exceptions were AK3 and AK4, where negative changes in dry weight were shown in both seasons. This suggests that the lower level of fertilisation given in 2010 may have limited growth, but, from the responses of AK3 and AK4, other factors such as developmental age, also contribute to the growth patterns observed over a season. The mean monthly temperatures and humidities recorded in the glasshouse were similar for both seasons (Table 2.2), but other important environmental parameters may have been different, such as incident light intensity

and total sunlight hours, which could not be routinely recorded in this study. The shoots appeared to be less green in 2010 compared to 2009, an observation supported by the differences in relative chlorophyll levels, especially in $f_0$1plants (Figures 2.30 and 2.37). These apparently lower chlorophyll levels were possibly the result of reduced fertiliser inputs and would have lowered the potential assimilation rates in these plants. The involvement of this contributing factor is supported by observations made by the research team, outside the scope of this study, where corms grown during 2011 in compost containing a slow-release high nitrogen fertiliser, have produced much greener leaves and, by visual assessment, more vigorous growth.

Chapter three: A comparative study of methodologies for the extraction and analysis of konjac glucomannan

3.1. Introduction

Konjac glucomannan is the main biologically active constituent of the storage polysaccharide extracted from corm tissues of *A. konjac* (Takigami, 2000; Edison, 2010; Parry, 2010). KGM is composed of a linear chain of β-1,4-linked D-glucose and D-mannose residues in a molar ratio of 1:1.6 (Figure 3.1), with side branches through β-1,6-glucosyl units. The degree of branching is estimated at approximately 3 branches for every 32 sugar residues. The acetyl groups along the KGM backbone are located, on average, every 9 to 19 sugar units at the C-2, C-3 or C-6 position of mannopyranose (Kato and Matsuda, 1969; Shimahara *et al*., 1975; Maeda *et al*., 1980; Parry, 2010).

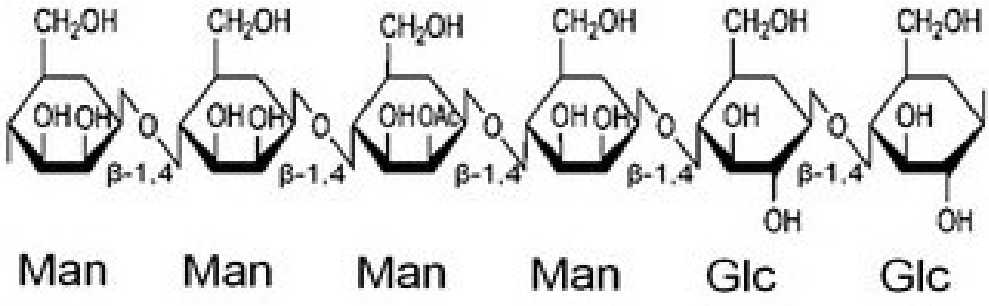

Figure 3.1 Chemical structure of konjac glucomannan (adapted from Gille *et al*., 2011). Man, mannose; Glc, glucose; Ac, acetate.

KGM is water soluble, but is insoluble in organic solvents. It has a remarkable water absorption capacity of up to 100 fold its weight (Koroskenyi and McCarthy, 2001). This solubility characteristic may partly be attributed to the long side chains

which serve to hinder intermolecular association (Williams *et al*., 2000), but is predominantly believed to be associated with the presence of acetyl substituents (Maekaji, 1978; Huang *et al*., 2002; Gao and Nishinari, 2004). Removal of these substituents by alkaline hydrolysis (pH > 12), or heating facilitates gelation (Maekaji, 1978) which is thought to result from cross-linking, mainly through hydrogen-bonding between KGM moieties that are deficient in acetyl groups (Maekaji, 1978; Nishinari *et al.,* 1992). Furthermore, KGM forms a highly viscous solution in the pH range 4 - 7 (Vanderbeek *et al*., 2007) and shows a synergistic interaction with other gelling (agarose and κ-carrageenan) (Miyoshi *et al*., 1997; Penroj *et al*., 2005) and non-gelling polysaccharides (xanthan gum and acetan) (Chandrasekaran *et al*., 2003; Alvarez-Mancenido *et al*., 2008).

To date, konjac corms are the only industrially exploited source of glucomannan (Zhao *et al*., 2009). In recent decades, methods for the extraction and purification of KGM from fresh corm material have been studied and developed (Sugiyama *et al*., 1972; Ogasawara *et al*., 1987; Wu *et al*., 1987; WIPO, 1993; Wootton *et al*., 1993; Takigami, 2000). KGM is extracted either by mechanical means (dry processing), or by wet (chemical) processing methods. The former has traditionally been adopted to prepare konjac flour, and involves slicing and drying of fresh corm material, followed by milling of dried chips into crude konjac flour (CKF), which is subsequently purified via cyclone sifting (Takigami, 2000; Parry, 2010; Zhao *et al*., 2010). Konjac flour produced using such methods is of low purity and is sold as a food commodity at a low price (Zhao *et al*., 2010).

Wet processing methods include the use of lead acetate (Wu *et al*., 1987), salt (aluminium sulphate, calcium phosphate or magnesium phosphate) (WIPO, 1993), 2-propanol coupled with starch hydrolyzing enzymes (Wootton *et al*. 1993) and

ethanol (Sugiyama *et al*. 1972; Ogasawara *et al*., 1987; WIPO, 1993; Zhao *et al*., 2009) to extract KGM from CKF. KGM extracted by lead acetate is not edible, thus limiting its applications in the non-food industries, whilst enzymatic purification, which involves degradation of starch (regarded as an impurity) by hydrolyzing enzymes (α-amylases) is not selective. The latter procedure may result in the depolymerisation of KGM by contaminating β-mannanase, or β-glucanase activity in the starch hydrolyzing enzymes (Gong *et al*., 2002; Zhao *et al*., 2009).

Given the deficiencies mentioned above, to date, the most common konjac flour purification methods involve ethanol extraction of KGM, due to its simplicity and high efficiency (Takigami, 2000; Yunnan Fuyuan Golden Field Agricultural Products Company Ltd., 2008). Considerable success in producing high quality purified konjac flour (PKF) which retains the physicochemical properties of KGM have been reported by Sugiyama *et al*. (1972) and Ogasawara *et al*. (1987), using the ethanol extraction method. Such methods are, however, time-consuming, taking 147 h (Sugiyama's method) to 384 h (Ogasawara's method); and producing low-yields of PKF (WIPO, 1993).

The extraction and purification procedures are therefore crucial as they may affect the quality of PKF in terms of the physicochemical properties of the resultant KGM, which in turn are related to the pharmacological activity (Li *et al*., 2005; Kiriyama *et al*., 2008). The content of glucomannan is a key indicator for evaluating the quality of konjac flour (Byrne, 2001; Liu *et al*., 2002; U.S. Food Chemicals Codex, 2003). Standards for the classification of konjac flour have been established by the Chinese Ministry of Agriculture (CMA) (Liu *et al*., 2002), the European Commission (Bryne, 2001) and the U.S. Food Chemicals Codex (U.S. Food Chemicals Codex, 2003). However, at present there is no globally agreed regulatory

standard for konjac flour. Without such an agreed standard, KGM products are currently introduced to the general public as dietary supplements, functional foods, nutraceuticals or prescription herbal medicines, depending on the licensing policy established by the countries concerned. Therefore, harmonization of monographic standards is needed to assess and ensure the quality of existing KGM products (Chan *et al*., 2009; Chua *et al*., 2010), especially if these products are to be introduced more widely into Western markets.

With this in mind, the objectives of the current study were twofold: Firstly, to develop an improved processing methodology for konjac flour based on the working principles of both Sugiyama's (Sugiyama *et al*., 1972) and Ogasawara's (Ogasawara *et al*., 1987; WIPO, 1993) methods. Two methods with different frequency/duration of ethanol washing and hydration treatments of CKF were established. The yield, glucomannan content, Fourier transform infrared (FTIR) spectra, degree of acetylation (DA), molecular weight distribution and zero shear specific viscosity of the resultant PKFs were compared. Both the starch and protein content of the CKF, before and after purification, were also analysed, as both constituents are regarded as common contaminants in KGM samples. Secondly, to compare three existing methodologies for the quantitative analysis of the glucomannan content in samples of both PKF and CKF to identify the most appropriate assay method, with reference to reproducibility, precision and accuracy. These methods included the 3,5-dinitroscalicylic acid (3,5-DNS) colorimetric assay, which has been adopted by the CMA for the classification of konjac flour (Liu *et al*., 2002); the phenol-sulphuric acid colorimetric assay, which has been used for several decades for the determination of reducing sugars (Dubois *et al*., 1956); and an enzymatic colorimetric assay using a commercially available glucomannan assay kit

(Megazyme International Ireland Limited, Ireland), which has been used in Western food industries for the analysis of KGM content in foodstuffs.

The overall objective was to provide an improved protocol for the extraction, purification and analysis of KGM which could be used in the establishment of GLP for this useful and important foodstuff.

3.2. Materials and methods

Two reference samples were used in the current study. The first was a nutraceutical-grade konjac flour (NKF) (> 99% glucomannan) obtained from M&S Colloid Technology Limited, Hong Kong; the second was a low-viscosity konjac flour (LVKF) (> 98% glucomannan) purchased from Megazyme International Ireland Limited, Ireland. Both samples were used as supplied, without further purification and were oven-dried at 50 °C for 12 h prior to analysis.

3.2.1. Preparation of crude konjac flour from fresh corm material

CKF was prepared from a two-year-old corm (cultivar Yunhua 3) grown under 40% shade at the research farm of Yunnan Agricultural University, Kunming, P.R. China. The corm was weighed, washed, with its epidermis removed and sliced into pieces, 2 - 3 mm in thickness. The corm slices were then immersed in 1% (w/v) sodium bisulphite (anti-browning agent) (Sigma-Aldrich, UK) for 1 min, followed by oven-drying at 120 ºC for 40 min. The drying process was continued at 60 °C until a constant weight was obtained. The dried corm slices were subsequently ground and the resultant flour sieved (425 μm aperture, Fisher Scientific Ltd, Loughborough, U.K.) to produce CKF (Wu *et al*., 2002).

3.2.2. Purification of crude konjac flour

3.2.2.1. Method 1

CKF (2.00 g) was stirred in 50% (v/v) ethanol (200 ml) for 30 min at room temperature in triplicate, followed by centrifugation (5000 g, 30 min, 25 ºC) to remove the aqueous ethanol. This procedure was repeated twice under the same conditions by stirring the pellet obtained in freshly prepared 50% (v/v) ethanol after each centrifugation. Subsequently, the resultant pellet was stirred in deionised (DI) water (200 ml) for 2 h at room temperature, followed by centrifugation (9000 g, 30 min, 25 ºC). This procedure was repeated twice under the same conditions by stirring the insoluble materials obtained in DI water, with the supernatants retained after each centrifugation. The supernatants collected were mixed and the volume was reduced to ~ ⅓ the original volume by rotary evaporation. Glucomannan present in each solution was precipitated overnight with 95% (v/v) ethanol (600 ml) at 4 °C, followed by centrifugation (9000 g, 40 min, 25 ºC). The resultant pellet was washed twice with anhydrous ethanol (dehydration process) and subsequently isolated by vacuum filtration, before being freeze-dried for 48 h. The dried material was ground using a pestle and mortar and sieved to produce PKF (referred to as PKF1 hereafter) which was stored in a desiccator for further analysis.

3.2.2.2. Method 2

CKF (2.00 g) was stirred in 50% (v/v) ethanol (200 ml) for 90 min at room temperature in triplicate, followed by centrifugation (5000 g, 30 min, 25 ˚C) to remove the aqueous ethanol. The resultant pellet was added to DI water (200 ml) and stirred for 3 h at room temperature. Each solution was then diluted to 400 ml with DI water prior to centrifugation (9000 g, 30 min, 25 ºC) to remove the insoluble

materials. Subsequently, rotary evaporation was performed to reduce the volume of each filtrate to ~ ⅓ the original volume. Glucomannan present in each solution was precipitated overnight with 95% (v/v) ethanol (450 ml) at 4 °C, followed by centrifugation (9000 g, 40 min, 25 ºC). The resultant pellet was then washed twice with anhydrous ethanol and subsequently isolated by vacuum filtration before being freeze-dried for 48 h, as described for method 1. The dried material was then ground using a pestle and mortar and sieved to produce PKF (referred to as PKF2 hereafter) which was stored in a desiccator for further analysis.

3.2.3. Comparison of methods for assay of glucomannan content

The reproducibility and accuracy of the 3,5-DNS, phenol-sulphuric acid and enzymatic colorimetric assays were first compared by analysing CKF and LVKF samples in triplicate on different dates under the same experimental conditions. The absorbance readings were determined using a Helios α UV-visible spectrophotometer (Thermo Electron Corp., Rochester). Both glucose and mannose calibration curves were constructed for the 3,5-DNS and phenol-sulphuric acid assays, in order to compare the sensitivity of the assay systems to each of these reducing sugars. The 3,5-DNS method was further validated before being used for the determination of glucomannan content of PKF1, PKF2 and NKF in the later stages of the study.

3.2.3.1. 3,5-DNS colorimetric assay

Preparation of reagents

3,5-DNS reagent was prepared by mixing solutions A and B. Solution A was prepared by mixing phenol (0.70 g; Fisher Scientific Ltd, Loughborough, UK), 10%

(w/w) sodium hydroxide (1.50 ml), DI water (5 ml) and sodium bisulphite (0.70 g; Sigma-Aldrich). Solution B was prepared by mixing potassium sodium tartrate (22.50 g; Sigma-Aldrich), 10% sodium hydroxide (30 ml) and 1% (w/w) 3,5-DNS (88 ml; Sigma-Aldrich).

Formic acid-sodium hydroxide buffer (0.1 mol/L) was prepared by first adding formic acid (1 ml; Sigma-Aldrich) into DI water (60 ml). Sodium hydroxide (0.25 g) was then added into the solution, stirred and was subsequently made up to 250 ml with DI water.

Construction of standard D-glucose and D-mannose calibration curves

D-glucose stock solution was prepared by dissolving D-glucose (0.10 g) in DI water (100 ml) to a concentration of 1 mg/ml (in triplicate). D-glucose stock solution (0.40, 0.80, 1.20, 1.60 and 2.00 ml) and 2.00 ml of DI water (as a blank) were then placed into 25 ml volumetric flasks, respectively. DI water was added to the volume of 2.00 ml, followed by the addition of 3,5-DNS (1.50 ml) to each flask. Each mixture was heated for 5 min in a boiling water bath and cooled to room temperature before being diluted to 25 ml with DI water in a volumetric flask. *N.B.* Pyrex volumetric flasks were pre-tested for any adverse effects arising from the heating process and it was found that provided they were cooled to room temperature after heating, their volumes were indistinguishable (by mass of water contained) from that of an unheated flask. Absorbance readings were then taken at 550 nm and a plot of the measured absorbance against the glucose content (mg) constructed. A D-mannose standard curve was constructed using the procedure as described for glucose.

Preparation of KGM sample solutions

Each sample (0.20 g) was added to a magnetically-stirred formic acid-sodium hydroxide buffer (50 ml) and mixed for 4 h at room temperature. Each mixture was then transferred to a 100 ml volumetric flask and the beaker flushed twice with formic acid-sodium hydroxide buffer (20 ml x 2) to ensure all the sample was transferred into the flask before being made up to 100 ml. KGM sample solutions were obtained after centrifugation (4500 g, 40 min, 25 °C).

Hydrolysis of KGM sample solutions

Each KGM sample solution (5.00 ml) was added to a 25 ml volumetric flask followed by the addition of 3 M sulphuric acid (2.50 ml). The resultant solutions were stirred and hydrolyzed for 90 min in a sealed boiling water bath and allowed to cool to room temperature before the addition of 6 M sodium hydroxide (2.50 ml). Each solution was stirred and cooled to room temperature before being made up to 25 ml with DI water to form the KGM hydrolysate.

Colorimetric reactions (3,5-DNS assay)

KGM sample solution, KGM hydrolysate and DI water (as a blank), 2.00 ml each, were placed into 25 ml volumetric flasks followed by the addition of 3,5-DNS reagent (1.50 ml). The solutions were then stirred and incubated in a sealed boiling water bath for 5 min and allowed to cool to room temperature before being made up to 25 ml with DI water. Absorbance readings were then taken at 550 nm. The glucose content of KGM sample solution and KGM hydrolysate, corresponding to their absorbance readings were determined from the linear regression equation of the

glucose standard curve. The glucomannan content was determined by evaluation of equation 1,

$$\text{Glucomannan content (\%)} = \frac{5000\, f\,(5T - T_0)}{m}$$

of which f = correction factor, T = glucose content of KGM hydrolysate (mg), T_0 = glucose content of KGM sample solution (mg) and m = mass of konjac flour (200 mg).

Method validation study

The precision of the 3,5-DNS colorimetric assay, expressed as the relative standard deviation (RSD), was evaluated by assaying four replicate of the NKF sample (reference sample), each at six different concentrations (0.5, 1.0, 2.5, 5.0, 10.0 and 12.5 mg/ml). Sample stock solution was prepared following the procedures previously described and subsequently placed (0.25, 0.50, 1.25, 2.50, 5.00 and 6.25 ml) into a series of 25 ml volumetric flasks. Formic acid-sodium hydroxide buffer was then added (to the volume of 5.00 ml) prior to hydrolysis following the protocols as described previously. A plot of the mean absorbance for KGM hydrolysate against the concentration of NKF sample solution was then constructed.

Accuracy was assessed by spiking the NKF samples (0.20 g) with a possible interfering substance, *i.e.* starch (potato starch; VWR BDH Prolabo, UK) at three levels: 250, 500 and 750 μg/g (in 4 replications). The recoveries of glucomannan from NKF samples at each spiking level were subsequently evaluated.

3.2.3.2. Phenol-sulphuric acid colorimetric assay

Construction of standard D-glucose and D-mannose calibration curves

A D-glucose stock solution (0.80 mg/ml) was prepared. Subsequently, glucose stock solutions (1.00 ml, 2.00 ml, 3.00 ml, 4.00 ml and 5.00 ml) were added in triplicate into 50 ml volumetric flasks, respectively and diluted to 50 ml with DI water to form the glucose standard solutions. The colorimetric reactions were performed by placing glucose standard solutions and DI water (as a blank) into test tubes (2.00 ml each), followed by the addition of 5.0% (w/w) phenol reagent (1.00 ml). Concentrated sulphuric acid (98% w/w; 5.00 ml) was then delivered rapidly into each tube. The tubes were allowed to stand for 10 min at room temperature and mixed prior to incubation at 25 °C for 20 min. Absorbance was then measured at 490 nm. A calibration plot of the measured absorbance against the glucose concentration (μg/ml) was constructed. A mannose calibration curve was constructed using the procedures as described for glucose.

Preparation of KGM sample solutions

Each sample (0.05 g) was added to magnetically-stirred DI water (40.00 ml) and mixed for 4 h at room temperature. Each solution was then transferred into a 50 ml volumetric flask and the beaker flushed with DI water (10.00 ml) to ensure all the sample was transferred into the flask before being made up to 50 ml. The solutions were centrifuged (4000 g, 40 min, 25 °C) to remove the insoluble fraction and subsequently diluted (3.00 ml made up to 50.00 ml with DI water) to obtain the KGM sample solutions.

Colorimetric reactions (Phenol-sulphuric acid assay)

KGM sample solutions and DI water (as a blank), were added (2.00 ml each) into test tubes, respectively, followed by the addition of 5.0% (w/w) phenol reagent (1.00 ml). Concentrated sulphuric acid (5.00 ml) was then delivered rapidly into each tube. The tubes were allowed to stand for 10 min at room temperature and mixed prior to incubation at 25 °C for 20 min. Absorbance readings were then measured at 490 nm. The concentration of reducing sugar (glucose) in each KGM hydrolysate, corresponding to its absorbance reading was determined from the linear regression equation of the glucose calibration curve. The glucomannan content was determined by evaluation of equation 2,

$$\text{KGM content (\%)} = \frac{100\, f\, C_1}{C_2}$$

of which f = correction factor, C_1 = concentration of reducing sugar (glucose) in the KGM hydrolysate (μg/ml) and C_2 = concentration of KGM sample solution (μg/ml).

3.2.3.3. Enzymatic colorimetric assay

This was performed using a commercial KGM assay kit purchased from the Megazyme International Ireland Limited, Ireland (catalogue number: K-GLUM) which contains the full assay method plus the following reagents in bottles:

1. Sodium acetate buffer (25 ml, 1 M, pH 4.5) plus sodium azide (0.02% w/v).
2. TEA buffer (12.5 ml, 1 M, pH 7.6) plus magnesium chloride (100 mM) and sodium azide (0.02% w/v).
3. $NADP^+$ (150 mg) plus ATP (440 mg).
4. β-mannanase suspension (1.2 ml, 450 U/ml).
5. β-Glucosidase (100 U/ml) plus β-mannosidase (100 U/ml) suspension (1.1 ml).

6. Hexokinase (425 U/ml) plus glucose-6-phosphate dehydrogenase (212 U/ml) suspension (1.1 ml).
7. Phosphoglucose isomerise (1000 U/ml) plus phosphomannose isomerise (1000 U/ml) suspension (1.1 ml).
8. D-glucose plus D-mannose standard solution (0.2 mg/ml each).

Preparation of reagent solutions/suspensions

The contents of bottle 1 were diluted to 450 ml with DI water, followed by adjustment of the pH to 4.5 before being made up to 500 ml with DI water. Two drops of toluene were then added to prevent microbial contamination before being stored at 4 °C. The content of bottle 3 was dissolved in DI water (12 ml) and stored in polypropylene tubes at -20 °C. The contents of bottles 2, 4, 5, 6, 7 and 8 were used as supplied.

Preparation of sample solutions

Konjac flour (0.10 g) was weighed into a glass test tube, followed by the addition of 80% (v/v) aqueous ethanol (5 ml), stirred and incubated at 85 - 90 ˚C for 5 min. Subsequently, 80% (v/v) aqueous ethanol (5 ml) was again added into the solution before being stirred for 10 min on a vortex mixer. The solution was then centrifuged (1500 *g*, 10 min) and the resulting pellet stirred in 80% (v/v) aqueous ethanol (5 ml) for 10 min. Following this, 80% (v/v) aqueous ethanol (5 ml) was added into the solution and stirred for another 5 min prior to centrifugation (1500 *g*, 10 min) to remove the aqueous ethanol.

The resulting pellet was re-suspended in 50 mM sodium acetate buffer (8 ml; pH 4.5) and was stirred vigorously on a vortex mixer to ensure complete dispersion. The tube was subsequently incubated in a boiling water bath for 30 s, followed by

vigorous stirring on a vortex mixer. These heating and stirring procedures were then repeated. Following this, the tube was incubated in a boiling water bath for 4 min to ensure full hydration of the glucomannan and stirred vigorously on a vortex mixer before being incubated continuously at 40 ºC for 5 min. β-mannanase suspension (20 µl) was then added and stirred vigorously on a vortex mixer for 30 s prior to incubation at 40 ºC for 60 min.

After incubation, the solution was quantitatively transferred into a 200 ml beaker and made up to approximately 70 ml with DI water. The pH of the solution was then adjusted to approximately 12.5 via drop wise addition of 1 M sodium hydroxide, followed by incubation at room temperature for 10 min. Subsequently, 200 mM sodium phosphate buffer (20 ml; pH 6.5) was added and the pH adjusted to 6.5 by drop wise addition of 1 M hydrochloric acid. The solution was then quantitatively transferred to a 100 ml volumetric flask and adjusted to volume using DI water.

Enzymatic colorimetric reactions

Sample solution (500 µl) and suspension 5 (20 µl) was pipetted into a 1 cm light path plastic cuvette and mixed by gentle swirling before being incubated at 35 °C for 20 min. The blank was prepared by omitting suspension 5 (substituted with DI water). Subsequently, DI water (2 ml), solution 2 (200 µl) and solution 3 (100 µl) were added into both the sample and blank solutions before being incubated at ~ 25-30 °C. After 3 min of incubation, the absorbance of both solutions were measured at 340 nm (referred to as A1). This was followed by the addition of suspension 6 (20 µl) and the absorbance of both solutions were measured at 340 nm after 5 min incubation. Absorbance readings were then taken every 2 min until constant readings

(referred to as A2) were obtained. Subsequently, suspension 7 (20 µl) was added into both solutions, followed by the measurement of absorbance at 340 nm after 20 min. This was continued at 2 min intervals until constant readings (referred to as A3) were obtained. For each of the reactions mentioned above, sample solution and the suspension added were mixed by gentle inversion after sealing the cuvette with Parafilm. The glucomannan content (% w/w) was determined by evaluation of equation 3,

$$\text{KGM content (\%)} = \frac{\Delta A_{GM}}{6300} \times \frac{V}{1000} \times MW \times \frac{FEV}{v} \times \frac{100}{w} \times F$$

of which ΔA_{GM} = (A3 – A1) sample – (A3 – A1) blank; V = final volume in assay cuvette (2.86 ml); MW = molecular weight of anhydro-D-glucose/D-mannose (162.14); FEV = final extraction volume (100 ml); v = volume of sample added to the cuvette (0.5 ml); w = weight of sample analysed (0.100 g) and F = dilution factor (1).

N.B. This experiment was carried out during 2007, following the procedures cited in the kit instruction booklet (K-GLUM 10/04; see Appendix 1). Unfortunately, an error in the final extraction volume (FEV) for the KGM content calculation (in page 8 of instruction booklet) was noted. It was observed that the FEV value used in the given protocol (*i.e.* 100 ml) was not correlated with the value (*i.e.* 250 ml) employed in the final calculation of KGM content (in page 11 of instruction booklet). We have contacted the managing director of the Megazyme International Ireland Limited (Dr. Barry McCleary) to clarify this matter and the company has recently responded by issuing a revised instruction booklet (K-GLUM 08/10; see Appendix 2) for this kit; with the FEV being amended to 250 ml in the protocol. The results presented in the current study were therefore based upon 100 ml of FEV, and the deviation in results obtained due to the possible use of an incorrect multiplier is discussed.

3.2.4. Determination of starch content

This was performed by using the total starch assay kit purchased from the Megazyme International Ireland Limited, Ireland (catalogue number: K-TSTA) which contains the full assay method (amyloglucosidase/α-amylase method) plus the following reagents in bottles:

1. Thermostable α-amylase (10 ml, 3300 U/ml on Ceralpha reagent at pH 6.5).
2. Amyloglucosidase (10 ml, 3300 U/ml on soluble starch at pH 4.5).
3. Glucose oxidase/peroxidase (GOPOD) reagent buffer.
4. GOPOD reagent enzymes.
5. D-glucose standard solution (5 ml; 1.0 mg/ml) in 0.2% (w/v) benzoic acid.

Preparation of reagent solutions/suspensions

The content of bottle 1 (1.0 ml) was diluted to 30 ml with 100 mM sodium acetate buffer, pH 5.0. The content of bottle 3 was diluted to 1 L with DI water (solution 3). The content of bottle 4 was dissolved in solution 3 (20 ml) and subsequently transferred to the bottle containing the remainder of solution 3 to form the GOPOD reagent. The contents of bottles 2 and 5 were used as supplied.

Starch colorimetric assay

Konjac flour (0.10 g) was weighed into a glass centrifuge tube, followed by the addition of 80% (v/v) aqueous ethanol (5 ml), stirred and incubated at 85 - 90 ˚C for 5 min. Subsequently, 80% (v/v) aqueous ethanol (5 ml) was added into the solution before being centrifuged (1800 *g*, 10 min). The resulting pellet was re-suspended in

80% (v/v) aqueous ethanol (10 ml) and stirred. Following this, the solution was centrifuged (1800 *g*, 10 min) to remove the aqueous ethanol before the addition of thermostable α-amylase (3 ml). The tube was then incubated in a boiling water bath for 6 min (the tube was vigorously stirred after 2, 4 and 6 min) and continued at 50 °C for 30 min after the addition of amyloglucosidase (0.1 ml). The entire contents of the tube were then transferred to a 100 ml volumetric flask and adjusted to volume with DI water, followed by centrifugation (1800 *g*, 10 min) to remove the insoluble material. For samples containing 10 - 100% starch (*i.e*. CKF), an aliquot (1 ml) of the supernatant was diluted to 10 ml with DI water before being transferred (0.1 ml) in duplicate to the bottom of glass test tubes. Subsequently, GOPOD reagent (3 ml) was added to each tube (including the D-glucose controls and reagent blanks) and incubated at 50 °C for 20 min. The absorbance of each sample and the D-glucose control were then read against the reagent blank at 510 nm. The starch content (% w/w) was determined by evaluation of equation 4,

$$\text{Starch content (\%)} = \Delta A \times F \times \frac{FV}{0.1} \times \frac{1}{1000} \times \frac{100}{W} \times \frac{162}{180}$$

of which ΔA = absorbance (reaction) read against the reagent blank; F = conversion from absorbance to µg (100 µg of D-glucose)/absorbance for 100 µg of glucose); FV = final volume (10 or 100 ml); W = weight of sample analysed (100 mg).

3.2.5. Determination of nitrogen/protein content

Nitrogen analysis was undertaken in collaboration with Professor P.A. Williams at the Centre for Water Soluble Polymers at Glyndwr University using the Kjeldahl method. The protein content was calculated by applying the nitrogen conversion factor of 5.7 as proposed by the U.S. Food Chemicals Codex and

European Commission (Byrne, 2001; U.S. Food Chemicals Codex, 2003; Parry, 2010).

3.2.6. Determination of the degree of acetylation (DA)

DA, defined as the wt. % of acetyl-substituted residues in the KGM backbone (Huang *et al*., 2002; Gao and Nishinari, 2004) was determined by a back-titration method. Two solutions were used in the analysis: Solution A (~ 0.45 M NaOH) and Solution B (~ 0.2 M HCl). Potassium hydrogen phthalate (PHP, FSA Laboratory Supplies, Loughborough, UK) was used as the primary standard for all solutions. The standardisation procedure, used throughout, is as follows: Firstly, PHP (1.00 g) was dissolved in DI water and titrated with solution A, using phenolphthalein indicator. The titre was recorded as V_a (ml) and the mass of PHP as m_{PHP} (g). Secondly, Solution B (10.00 ml) was titrated with Solution A using phenolphthalein indicator and the titre was recorded as V_b (ml). Thirdly, the KGM sample (m_{KGM} = 1.00 g) was stirred in DI water (250 ml) for 3 h at room temperature and 2 drops of phenolphthalein indicator added. The solution was titrated with approximately 0.1 M sodium hydroxide to a permanent pink colour (pre-neutralization). Solution A (10.00 ml) was then added and the mixture stirred for 3 h at room temperature. The remaining alkali was back titrated with Solution B (phenolphthalein indicator) and the titre recorded V_c (ml). Duplicate analyses were performed for each sample (PKF1, PKF2, LVKF and NKF). The DA was determined by evaluation of equation 5,

$$DA = \frac{4300\, m_{PHP}(100 - V_c V_b)}{2042.3\, V_a\, m_{KGM}}$$

3.2.7. Fourier transform infrared (FTIR) spectral analyses

IR spectra of CKF, PKF1, PKF2 and LVKF were generated directly from the powdered samples using a Mattson Genesis II spectrometer (Thermo Electron Corp., Madison, Wisconsin) at room temperature, using an attenuated total reflectance (ATR) stage.

3.2.8. Determination of the molecular mass distribution by aqueous gel permeation chromatography (GPC)

Preparation of sample solutions

Konjac flour (0.10 g) was stirred (in duplicate) in DI water (99.90 g) for 30 min at room temperature and continued at 80 °C for 2 h in a loosely covered vessel. The solutions were allowed to cool followed by the addition of DI water to compensate for the evaporative loss before being centrifuged (2500 rpm, 30 min, 25 °C) to remove the insoluble fraction. KGM sample solution (20.00 g) was then loaded into a microwave bomb (model 4782; Parr Instrument Company, Moline, IL) and heated for 30 s in a Powerwave 800 W microwave oven (Proline, Korea) operated at 90% full power prior to measurement. Ratcliffe *et al*. (2005) have previously shown that this procedure is important since it disrupts molecular aggregates, but under the conditions adopted does not cause KGM depolymerisation and subsequent reduction in molecular weight.

GPC apparatus and conditions

The GPC system comprised of a 3215α degasser (ERC Inc., Saitama, Japan), a Constametric 3200 pump (Thermo Seperation Products, San Jose, CA), a Rheodyne 7125 injection valve (Rheodyne Inc., Cotati, CA) fitted with a 200 µl loop, a

suprema guard column and suprema 100, 3000 and 30 000 columns (PSS, Germany). The column eluent was monitored by multi angle laser light scattering (MALLS) detector (Wyatt Technology, Santa Barbara, CA) in conjunction with the Optilab refractive index (RI) detector (Wyatt Technology). RI provides an accurate concentration profile for the eluting species and MALLS enables their absolute molecular mass to be determined.

The eluent employed was 0.1 M sodium chloride delivered at 0.5 mL/min. 0.005% (w/w) sodium azide (acts as a bacteriostatic) was added (1 ml per 1000 ml eluent) into the eluent and filtered through a 0.22 μm membrane filter under reduced pressure before being placed into a covered solvent reservoir. Samples were filtered through a 5 μm membrane filter before injection onto the column.

Interpretation of light scattering data

Data were processed using the ASTRA 4.50 software package (Wyatt Technology). According to Anderson *et al*. (2003), the ideal way to obtain the molar mass by light scattering would be to use the scattered intensity at 0° scattering angle where the relationship between the molar mass, concentration and intensity of scattered light is simple. However, this is impossible as the scattered intensity at 0° is not experimentally measurable. By GPC-MALLS, measurements were made at many angles > 0° and the intensity at 0° estimated by extrapolation from the higher angle data in a Debye plot (Anderson *et al*., 2003). To minimize the effect of possible errors in low-angle data, Debye plots constructed using the Zimm method were first evaluated and data points that deviated from the plots were subsequently excluded before extrapolation using the Berry method with a linear fit (first polynomial) (Anderson *et al*., 2003; Ratcliffe *et al*., 2005). The Berry method relies on

constructing a plot of $\sqrt{Kc/R_\theta}$ against $\sin^2(\theta/2)$, where K is an optical constant, c is the polymer concentration, R_θ is the Rayleigh ratio and θ is the light scattering angle. The refractive index increment, *dn/dc* employed in the determination of *Kc* was 0.14 g/mol (Ratcliffe *et al*., 2005). Data extrapolated using the first to fourth polynomial fit of the Zimm, Debye and Berry models were also compared.

3.2.9. Determination of the zero shear specific viscosity (η_0)

Shear flow measurements were performed using AR500 and AR2000 rheometers (TA Instruments, New Castle, DE) at 25 °C. Stock solutions of PKF1, PKF2 and NKF (2% w/w each) were prepared by adding each sample (2.00 g) to the vortex of DI water (98.00 g) created by an overhead electric stirrer. After 30 min mixing at room temperature, the samples were stirred for 2 h in a 80 °C water bath, followed by the addition of DI water to compensate for evaporative loss. To appropriate aliquots of the 2% (w/w) stock solutions, DI water was added to achieve concentrations of 0.2%, 0.3%, 0.4%, 0.5%, 0.75%, 1.25%, 1.5% and 1.75% (w/w). The diluted solutions were mixed on a roller mixer overnight and allowed to equilibrate to room temperature for 30 min before measurement. Sample concentrations of 0.2 - 0.75% were measured on a AR2000 rheometer using single concentric cylinder geometry, whilst sample concentrations of 1 - 2% were measured on a AR500 rheometer using 4 cm diameter cone geometry, typically in the shear rate range of 1 - 1000 s^{-1}. Zero shear viscosity was determined using the Cross model based on equation 6,

$$\eta = \eta_\infty + \left[\frac{\eta_0 - \eta_\infty}{1 + (C\gamma)^m}\right]$$

of which η = viscosity at a given shear rate ($\dot{\gamma}$); η_0 = zero shear viscosity, η_∞ = infinite shear-rate viscosity; C = arbitrary constant and m = power law exponent.

3.2.10. Statistical analysis

Data were analysed by a paired T-test at 5% level of probability ($P < 0.05$) using the "SPSS 16.0" computer software.

3.3. Results

3.3.1. The yield of crude konjac flour from the fresh corm materials

As shown in Table 3.1, 58.5 g of CKF was produced from the fresh corm material (fresh weight = 372.1 g), giving a yield of 15.7% (w/w).

Table 3.1 Fresh and dry weight (g) of corm used for the preparation of CKF.

Corm material	Weight (g)
Fresh corm	372.1
Fresh corm with epidermis removed	368.3
Dried corm slices	59.4
Crude konjac flour	58.5

3.3.2. The yield of purified konjac flour from crude konjac flour

Both PKF1 and PKF2 were odourless, white and fluffy in appearance, compared to the CKF, which is brownish in colour and emits a strong fishy smell (Figure 3.2). A 38 ± 2% (0.76 ± 0.03 g) and 53 ± 4% (1.06 ± 0.08 g) yield of PKF was obtained from the CKF (2.0 g) using purification methods 1 and 2, respectively.

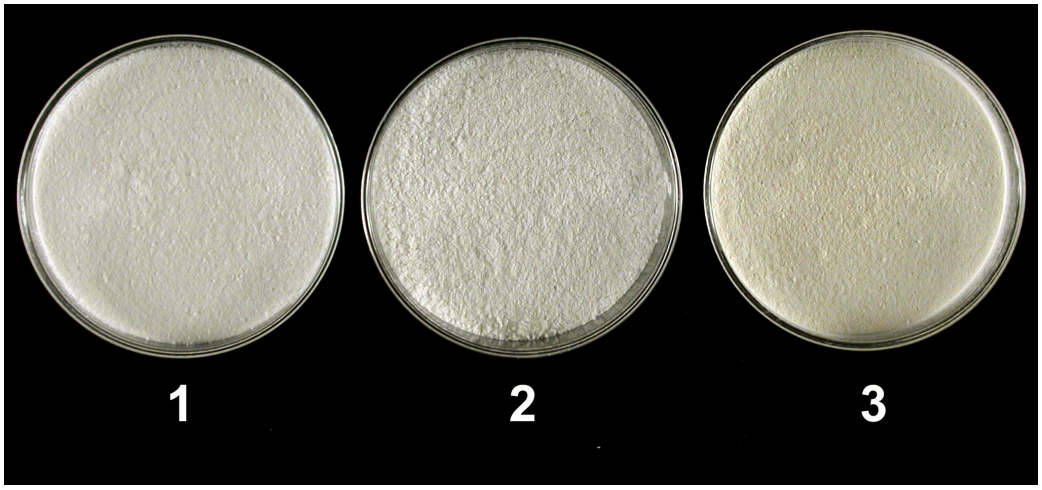

Figure 3.2 Physical appearance of konjac flour. (1) PKF, **(2)** PKF2, **(3)** CKF.

3.3.3. Comparison of glucomannan assay methods

3.3.3.1. Mannose and glucose calibration curves

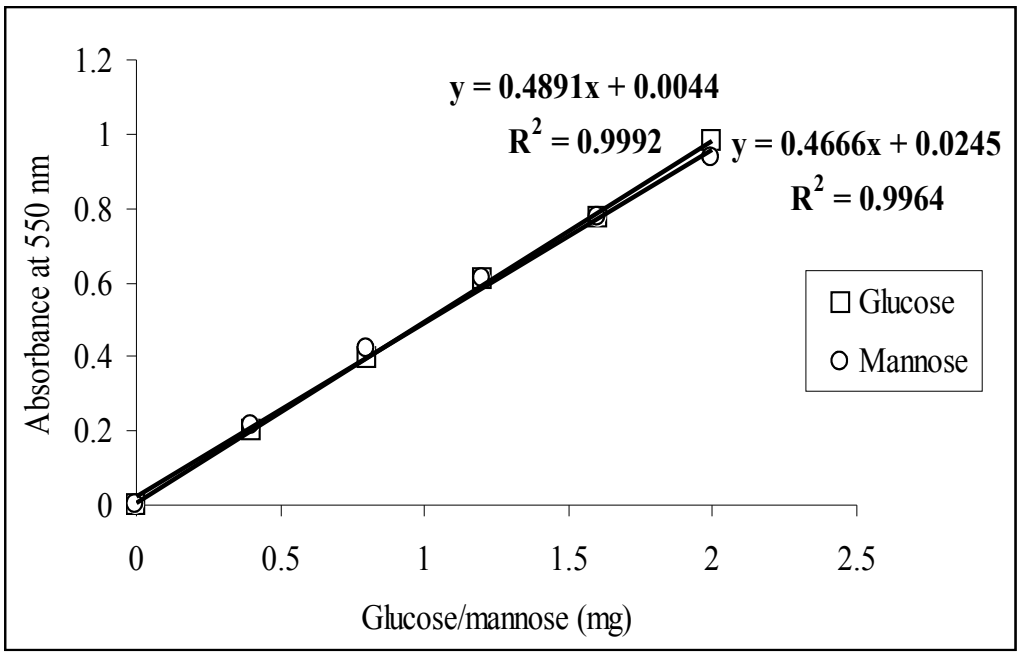

Figure 3.3 Glucose and mannose standard calibration curves for the 3,5-DNS colorimetric assays (*n* = 3). Linear regression equations: glucose, y = 0.4891x + 0.0044 (R^2 = 0.9992); mannose, y = 0.4666x + 0.0245 (R^2 = 0.9964).

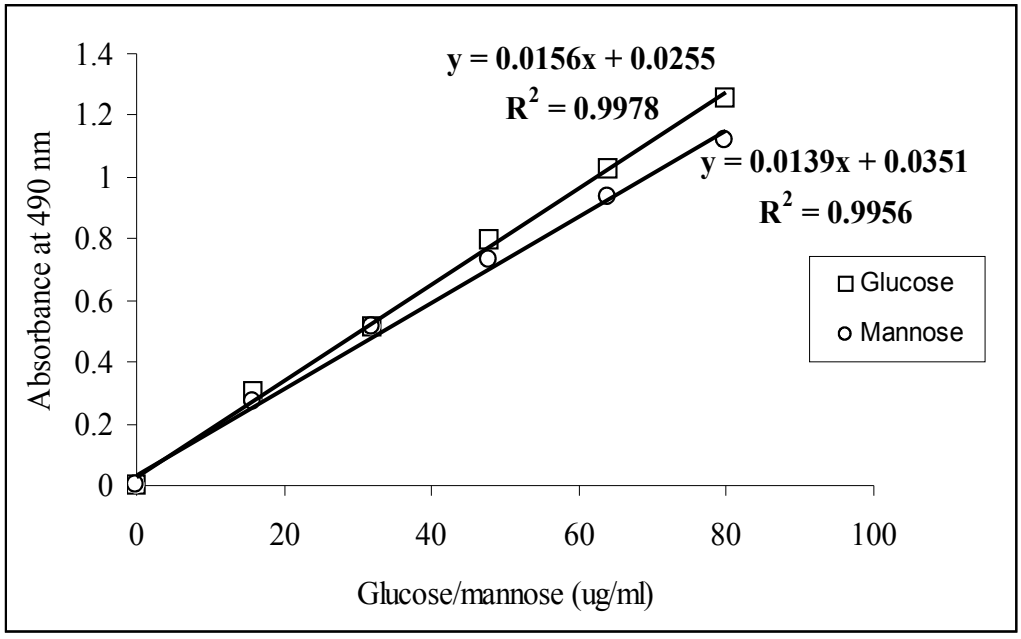

Figure 3.4 Glucose and mannose standard calibration curves for the phenol-sulphuric acid colorimetric assays (*n* = 3). Linear regression equations: glucose, y = 0.0156x + 0.0255 (R^2 = 0.9978); mannose, y = 0.0139x + 0.0351 (R^2 = 0.9956).

Both the D-glucose and D-mannose calibration curves for the 3,5-DNS (Figure 3.3) and phenol-sulphuric acid (Figure 3.4) colorimetric assays were linear, with a correlation coefficient between 0.996 to 0.999. From the gradient of the calibration curves, it was shown that mannose has a slightly lower sensitivity compared to glucose in both assay systems. A correction factor of 1.03 [1/2.6 + (1.6/2.6 x 0.4891/0.4666)] and 1.07 [1/2.6 + (1.6/2.6 x 0.0156/0.0139)] was hence determined and subsequently employed in equations 1 and 2 to determine the glucomannan content in the konjac flour samples. These correction factors were derived from the glucose to mannose ratio (1:1.6) reported in KGM (Kato and Matsuda, 1969; Shimahara *et al*., 1975; Maeda *et al*., 1980) and from the gradient of the calibration curves for each sugar.

3.3.3.2. The reproducibility and accuracy of the 3,5-DNS, phenol-sulphuric acid and enzymatic colorimetric assays

Table 3.2 shows the glucomannan content of CKF and LVKF analysed at two different dates under identical experimental conditions. The glucomannan content of both samples as determined by the 3,5-DNS, phenol-sulphuric acid and enzymatic colorimetric assays, ranged from 50.9 - 53.9% (CKF) and 89.9% - 97.9% (LVKF); 45.4 - 59.2% (CKF) and 84.5 - 99.6% (LVKF); and 28.7 - 31.6% (CKF) and 41.1 - 45.4% (LVKF), respectively. There were no significant differences in the mean glucomannan values obtained from each of the 3,5-DNS and enzymatic colorimetric assays between the two occasions, indicating that both assay methods are more reproducible compared to the phenol-sulphuric acid colorimetric assay. However, the glucomannan values obtained for both CKF and LVKF using the enzymatic colorimetric assay were considerably lower than those recorded using the 3,5-DNS assay.

Table 3.2 Glucomannan content (%) of CKF and LVKF determined by the 3,5-DNS, phenol-sulphuric acid and the enzymatic colorimetric assays on two occasions (n = 3).

	3,5-DNS colorimetry		Phenol-sulphuric acid colorimetry		Enzymatic colorimetry	
	CKF	LVKF	CKF	LVKF	CKF	LVKF
Replicate 1	53.7	89.9	51.4	85.6	30.3	45.4
	52.1	93.2	55.6	95.2	31.5	42.4
Replicate 2	52.5	90.0	45.4	91.7	28.7	43.2
	50.9	97.9	59.2	97.9	30.2	41.7
Replicate 3	53.9	90.6	53.2	84.5	31.6	41.7
	53.2	95.5	58.7	99.6	30.2	41.1
Mean ± SE	53.4±0.4[a]	90.2±0.2[a]	50.0±2.4[a]	83.9±2.3[a]	30.2±0.9[a]	43.4±1.1[a]
	52.1±0.7[a]	95.5±1.4[a]	57.8±1.2[b]	97.7±1.4[b]	30.6±0.5[a]	41.7±0.4[a]

[a] Different letters following mean values within the same column indicate significant differences at the $P < 0.05$ level.

3.3.3.3. Method validation study of the 3,5-DNS colorimetric assay

A plot of mean absorbance against the NKF concentrations, as shown in Figure 3.5, was linearly dependent on the concentration in the range from 0.5 - 12.5 mg/ml with a correlation coefficient of 0.997 and RSD ranging from 0.6 - 10.2% (Table 3.3). These data demonstrate a high precision of results obtained using the 3,5-DNS colorimetric assay.

The overall recoveries for glucomannan were found to be between 97 and 103% across the three spiking levels (250, 500 and 750 µg/g) of starch, with RSD ranged from 5.6 - 8.1% (Table 3.4).

Table 3.3 Repeatability of the 3,5-DNS colorimetric assay at six NKF concentrations, ranging from 0.5 – 12.5 mg/ml (*n* = 4).

NKF (mg/ml)	Minimum	Median	Maximum	Mean	SD	RSD (%)
0.5	0.006	0.007	0.007	0.007	0.001	8.9
1.0	0.013	0.015	0.016	0.015	0.002	10.2
2.5	0.056	0.069	0.071	0.065	0.006	9.9
5.0	0.162	0.165	0.172	0.166	0.004	2.6
10.0	0.364	0.367	0.368	0.366	0.002	0.6
12.5	0.420	0.428	0.438	0.429	0.008	1.8

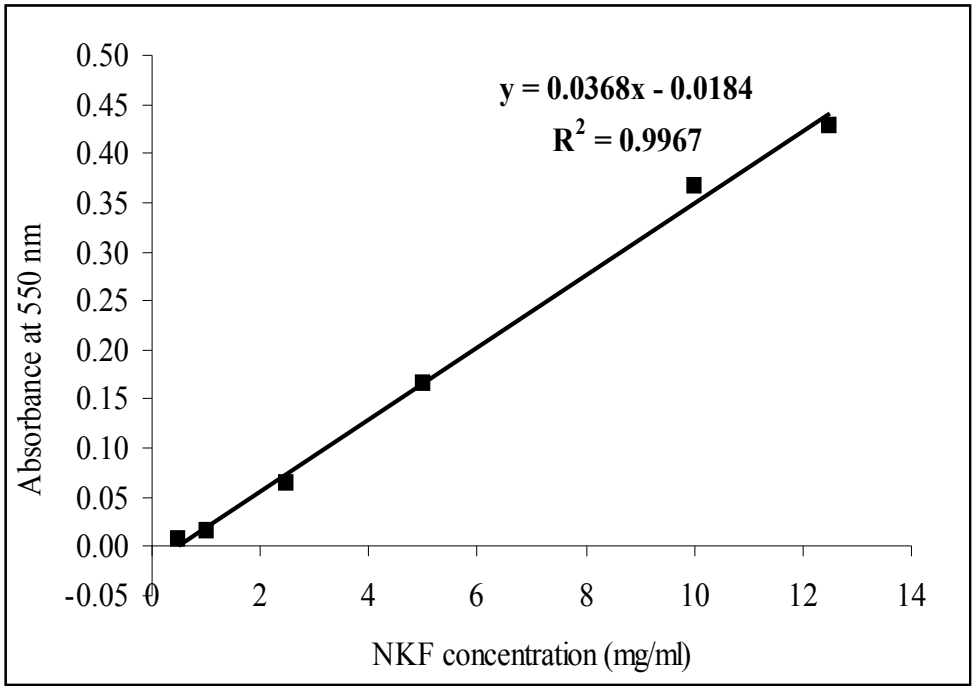

Figure 3.5 Linearity of 3,5-DNS colorimetric assay at six NKF concentrations, ranging from 0.5 – 12.5 mg/ml (*n* = 4).

Table 3.4 Recoveries of glucomannan (in NKF) across the three spiking levels (250, 500 and 750 µg/g) of starch (*n* = 4).

	Glucomannan content (%)				
Spike level (µg/g)	Minimum	Median	Maximum	Recovery (%)*	RSD (%)
250	63.1	72.1	75.4	98	8.1
500	42.2	46	48.3	97	5.6
750	21	22.7	24.6	103	6.9

* The percentage of recovery was calculated on the basis of the mean glucomannan content of NKF (97%) determined in the current study using the 3,5-DNS colorimetric assay. However, by assuming 100% purity of the NKF, the recovery at spiking level of 250, 500 and 750 µg/g is 94, 91 and 92%, respectively.

3.3.4. Overall analytical data of konjac flour samples: crude konjac flour (CKF), purified konjac flour 1 (PKF1), purified konjac flour 2 (PKF2), low-viscosity konjac flour (LVKF) and nutraceutical-grade konjac flour (NKF).

Table 3.5 The glucomannan content [ψ], starch content, protein content, molecular mass distribution [†], polydispersity index (PDI), zero shear specific viscosity (η_0)[*] and the degree of acetylation (DA) of five konjac flour samples.

Sample	Glucomannan (%)	Starch (%)	Protein (%)	M_n (g mol^{-1})	M_w (g mol^{-1})	M_z (g mol^{-1})	PDI (M_w /M_n)	η_0 (Pa s)	DA (%)
CKF	52.7 ± 0.5 [a]	35.7 [a]	7.5	-	-	-	-	-	-
PKF1	90.3 ± 0.7 [b]	0.6 [b]	4.4	4.4 ± 1.1 x 10^5	9.1 ± 0.6 x 10^5 [a]	1.4 ± 1.3 x 10^6	2.1 [a]	702.6	2.4 [a]
PKF2	91.4 ± 0.5 [b]	0.9 [b]	3.8	8.2 ± 0.8 x 10^5	9.5 ± 0.6 x 10^5 [a]	1.1 ± 1.2 x 10^6	1.2 [b]	815.6	2.8 [a]
LVKF	92.9 ± 1.3 [b]	0.8 [b]	0.4	1.3 ± 1.8 x 10^4	5.5 ± 0.8 x 10^4 [b]	1.6 ± 1.9 x 10^4	4.2 [c]	-	1.8 [a]
NKF	96.9 ± 1.3 [b]	0.5 [b]	0.4	1.4 ± 0.4 x 10^6	1.4 ± 0.4 x 10^6 [a]	1.5 ± 0.9 x 10^6	1.0 [b]	886.9	2.0 [a]

[ψ] Determined by 3,5-DNS colorimetric assay (mean ± SE).
[†] Mean ± percentage relative error; number-average (M_n), weight-average (M_w), z-average (M_z) molecular weights.
[*] Sample solution = 2% (w/w).
[a-b-c] Different letters following mean values within the same column indicate significant differences at the $P < 0.05$ level.

3.3.4.1. Glucomannan content

As can be seen from Table 3.5, there is a significant difference ($P < 0.05$) in glucomannan content between the CKF and all the other samples (PKF1, PKF2, LVKF and NKF). The glucomannan content of PKF1 and PKF2 has increased to ~ 91% and ~ 91%, respectively after purification and were comparable to the glucomannan content of both reference samples, LVKF and NKF.

3.3.4.2. Starch content

The starch content of CKF is 35.7% and was reduced to 0.6% and 0.9%, in PKF1 and PKF2, respectively. The latter have comparable starch contents to both LVKF (0.8%) and NKF (0.5%).

3.3.4.3. Protein content

The protein content of CKF is 7.5% and was reduced by 41% (to 4.4%) and 49% (to 3.8%) after purification using method 1 and 2, respectively (Table 3.6). Compared with the reference samples, LVKF and NKF, the protein content of both PKFs is approximately 10 fold higher.

Table 3.6 Protein content (%) of CKF, PKF1, PKF2, LVKF and NKF samples.

Sample	Total nitrogen (%)	Protein content (%)*
CKF	1.31	7.5
PKF1	0.77	4.4
PKF2	0.66	3.8
LVKF	0.07	0.4
NKF	0.07	0.4

* Nitrogen conversion factor of 5.7 was applied.

3.3.4.4. Degree of acetylation (DA)

The data in Table 3.5 indicates that there are no significant differences in the degree of acetylation between PKF1 (2.4%), PKF2 (2.8%), LVKF (1.8%) and NKF (2.0%).

3.3.4.5. FTIR spectra

The spectra obtained for PKF1 and PKF2 are in agreement with the reference sample (LVKF) (Figure 3.6). For PKF1, PKF2 and LVKF, the broad peak at ~ 3300 cm^{-1} results from the stretching vibration of O-H groups. The peaks at ~ 2900 cm^{-1}, ~ 1370 cm^{-1} and ~ 1050 cm^{-1} are assigned to -CH_2- stretching vibration, and two C-H bending modes, respectively. The small peak at ~ 1730 cm^{-1} is due to C=O stretching vibration, presumably arising from the ester carbonyl stretch in acetylated residues. The peaks at ~ 1150 cm^{-1} and ~ 1030 cm^{-1} are usually cited as C-O-C stretching modes from ether groups in the pyranose rings. Peaks attributed to β-glucosidic and β-mannosidic linkages are observed at ~ 870 cm^{-1} and ~ 800 cm^{-1}.

The most striking difference between the PKFs and the CKF is the dramatic increase in the intensity of the whole IR spectrum as a result of the purification process. There is also a significant reduction in the intensity of the band in the region 1623 - 1644 cm^{-1} which is consistent with a fall in protein content after purification. This band can be sensibly attributed to the amide C=O stretch of protein backbone, with LVKF having the lowest intensity band and the lowest protein content.

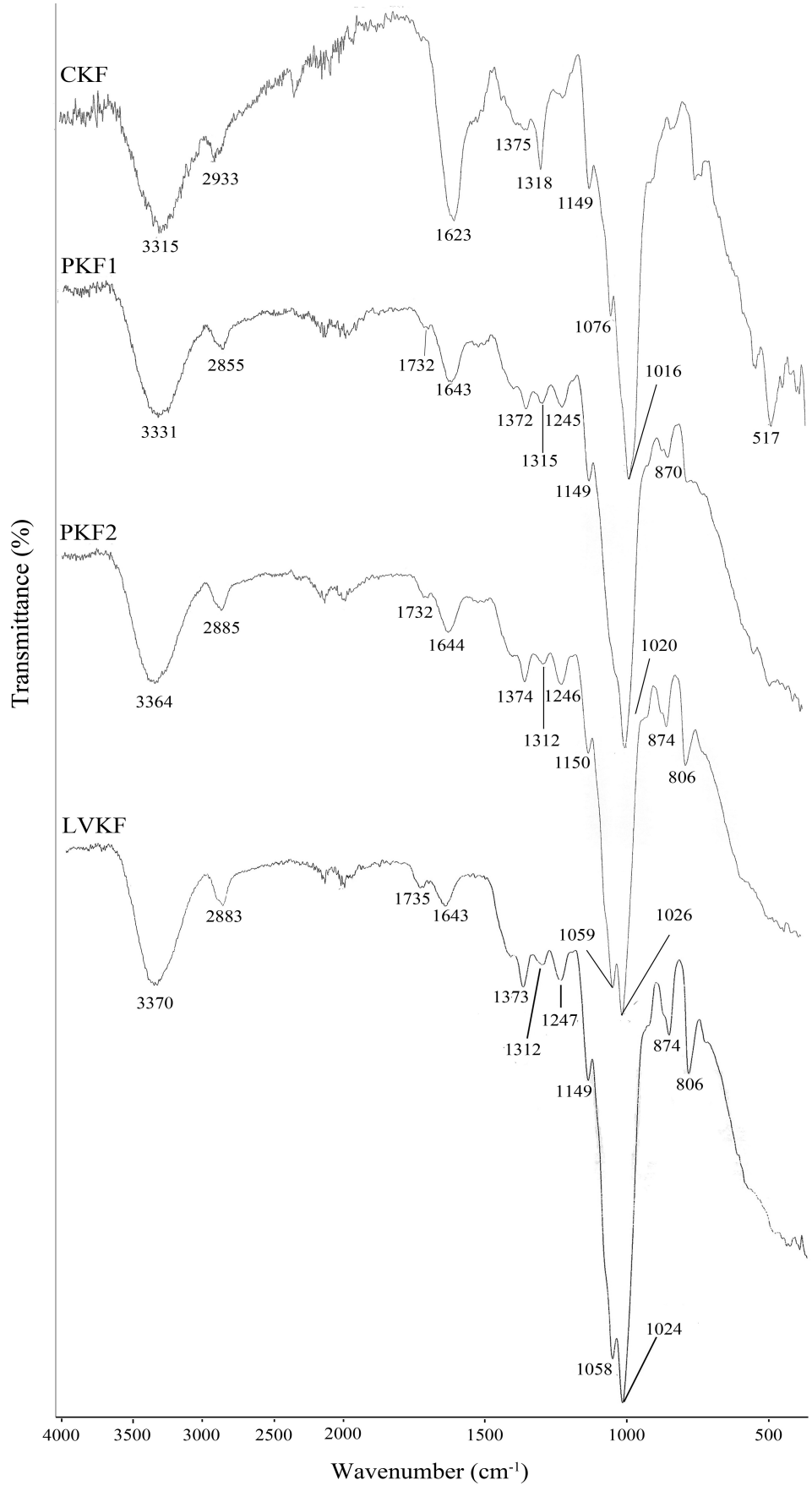

Figure 3.6 FTIR spectra of CKF, PKF1, PKF2 and LVKF samples. **O-H groups:** ~ 3300 cm^{-1}, **CH_2 groups:** ~ 2900 cm^{-1}, **C=O groups:** ~ 1730 cm^{-1}, **C-H groups:** ~ 1370 cm^{-1}, **C-O-C groups:** ~ 1150 and ~ 1030 cm^{-1}, **β-glucosidic and β-mannosidic linkages:** ~ 870 and ~ 800 cm^{-1}.

3.3.4.6. Molecular mass distribution

Table 3.7 presents the data for molecular mass distribution of both PKF1 (*a*) and PKF2 (*b*) generated from GPC-MALLS analysis processed using the first to fourth polynomial fits of the Zimm, Debye and Berry models. It was shown that application of all three transformations for each of the experimental data sets produced different results. For both samples, the weight average molecular weight (M_w) obtained using the Berry method with a linear fit (first polynomial) (*in bold*: 8.9 ± 0.6 x 10^5 and 9.0 ± 0.6 x 10^5) are comparable to those obtained by a second polynomial Debye treatment (*in bold*: 8.0 ± 0.7 x 10^5 and 8.6 ± 0.6 x 10^5).

Table 3.7 Comparison of data (± percentage relative error) generated from GPC-MALLS analysis of PKF1 (*a*) and PKF2 (*b*) processed using the first to fourth polynomial fits of the Zimm, Debye and Berry models through ASTRA software.

(a) PKF1

Parameter	Zimm	Debye	Berry
First polynomial			
M_n	5.5 ± 1.0 x 10^5	2.8 ± 1.2 x 10^5	4.4 ± 1.1 x 10^5
M_w	9.9 ± 0.5 x 10^5	7.3 ± 0.8 x 10^5	**8.9 ± 0.6 x 10^5**
M_z	1.4 ± 1.0 x 10^6	1.1 ± 1.9 x 10^6	1.3 ± 1.3 x 10^6
Second polynomial			
M_n	5.5 ± 1.0 x 10^5	4.6 ± 1.2 x 10^5	5.7 ± 1.0 x 10^5
M_w	1.0 ± 0.5 x 10^6	**8.0 ± 0.7 x 10^5**	9.5 ± 0.5 x 10^5
M_z	1.4 ± 1.1 x 10^6	1.1 ± 1.4 x 10^6	1.3 ± 1.0 x 10^6
Third polynomial			
M_n	8.1 ± 0.9 x 10^5	7.5 ± 0.9 x 10^5	8.1 ± 0.9 x 10^5
M_w	1.1 ± 0.5 x 10^6	9.9 ± 0.5 x 10^5	1.1 ± 0.5 x 10^6
M_z	1.3 ± 1.1 x 10^6	1.2 ± 1.0 x 10^6	1.3 ± 1.1 x 10^6
Fourth polynomial			
M_n	6.0 ± 1.2 x 10^5	7.2 ± 0.8 x 10^5	6.5 ± 1.0 x 10^5
M_w	9.2 ± 0.6 x 10^5	9.7 ± 0.4 x 10^5	9.5 ± 0.5 x 10^5
M_z	1.2 ± 1.3 x 10^6	1.2 ± 0.9 x 10^6	1.2 ± 1.1 x 10^6

(b) PKF2

Parameter	Zimm	Debye	Berry
First polynomial			
M_n	9.5 ± 0.6 x 10^5	5.2 ± 1.4 x 10^5	7.9 ± 0.9 x 10^5
M_w	1.1 ± 0.4 x 10^6	6.9 ± 1.0 x 10^5	**9.0 ± 0.6 x 10^5**
M_z	1.2 ± 0.9 x 10^6	8.1 ± 2.1 x 10^5	9.9 ± 1.3 x 10^5
Second polynomial			
M_n	1.0 ± 0.6 x 10^6	7.6 ± 0.8 x 10^5	9.6 ± 0.6 x 10^5
M_w	1.1 ± 0.4 x 10^6	**8.6 ± 0.6 x 10^5**	1.1 ± 0.4 x 10^6
M_z	1.2 ± 0.9 x 10^6	9.3 ± 1.3 x 10^5	1.2 ± 0.8 x 10^6
Third polynomial			
M_n	1.1 ± 0.8 x 10^6	1.0 ± 0.5 x 10^6	1.1 ± 0.6 x 10^6
M_w	1.2 ± 0.5 x 10^6	1.1 ± 0.4 x 10^6	1.2 ± 0.4 x 10^6
M_z	1.3 ± 1.1 x 10^6	1.1 ± 0.8 x 10^6	1.3 ± 0.8 x 10^6
Fourth polynomial			
M_n	9.4 ± 0.7 x 10^5	9.8 ± 0.6 x 10^5	9.9 ± 0.6 x 10^5
M_w	1.0 ± 0.5 x 10^6	1.1 ± 0.4 x 10^6	1.1 ± 0.4 x 10^6
M_z	1.1 ± 1.0 x 10^6	1.1 ± 0.8 x 10^6	1.1 ± 0.9 x 10^6

Figure 3.7 shows the molecular mass and RI elution profiles of the konjac flour samples generated from GPC analysis using MALLS and RI detectors. The RI profiles of all samples were found to consist of a sharp peak which appears at elution volumes of ~ 22 ml, except for the LVKF which generates two peaks, with the major peak (indicated as peak 2) eluting at ~ 24 ml, and the minor peak (peak 1) at ~ 20 ml. MALLS indicates that the materials eluting at peak 1 and peak 2 has a molecular mass of ~ 1 - 2 x 10^5 and ~ 2 - 4 x 10^4, respectively. From Table 3.5, the M_w of LVKF (5.5 x 10^4) is significantly lower than both PKFs and NKF, with no significant differences between PKF1 (9.1 x 10^5 g mol^{-1}), PKF2 (9.5 x 10^5 g mol^{-1}) and NKF (1.4 x 10^6 g mol^{-1}). LVKF also has the highest polydispersity index (denoted as M_w/M_n), followed by PKF1 which showed a polydispersity value of almost double that of both PKF2 and NKF, despite having a comparable M_w to these samples.

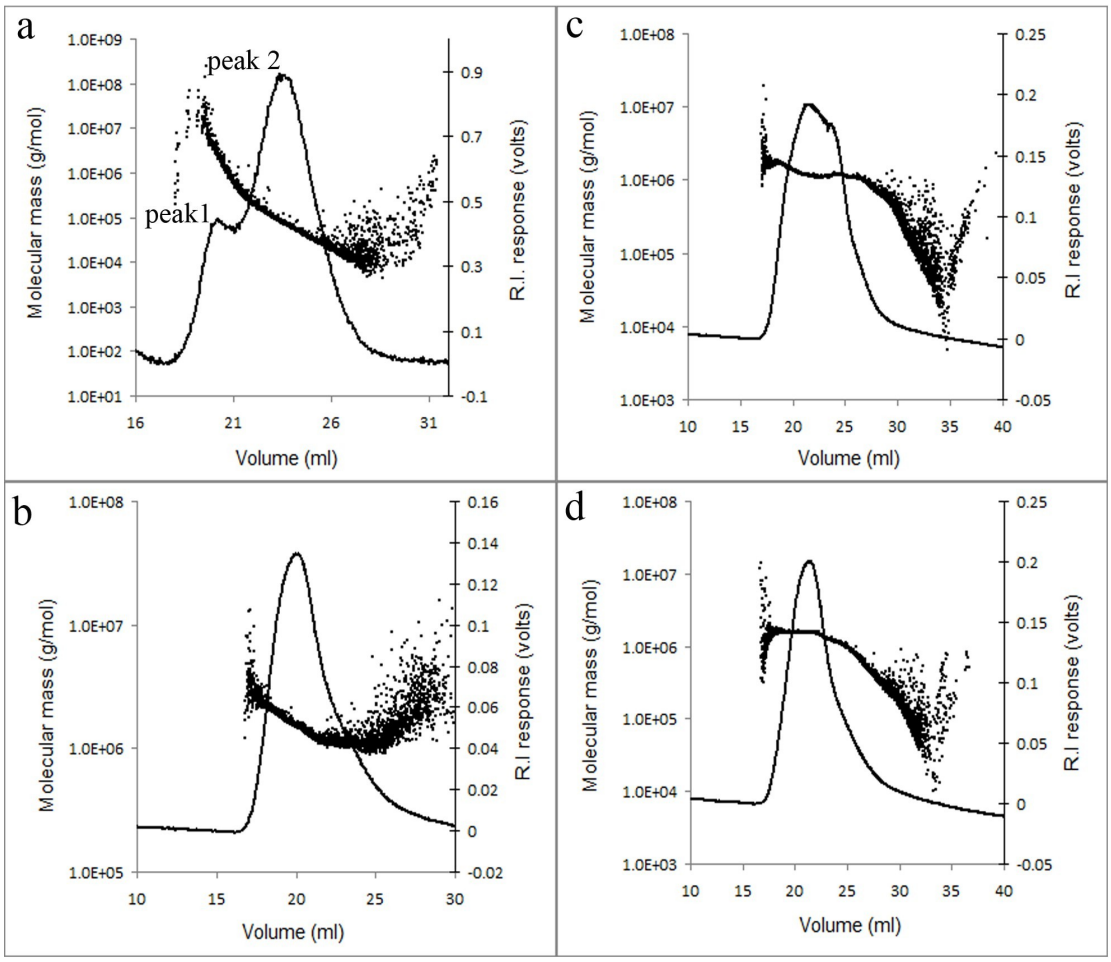

Figure 3.7 Molecular mass and refractive index elution profiles of (*a*) LVKF, (*b*) NKF, (*c*) PKF1 and (*d*) PKF2 generated by GPC-MALLS.

3.3.4.7. Zero shear specific viscosity (η_0)

A double logarithmic plot of sample concentration against the zero shear specific viscosity for NKF, PKF1 and PKF2 are shown in Figure 3.8. Collectively, the η_0 increased linearly with increasing sample concentration, ranging from 0.2 - 2% (w/w). At 2%, the zero-shear viscosity of NKF, PKF1 and PKF2 is 886.9 Pa s, 702.6 Pa s and 815.2 Pa s, respectively.

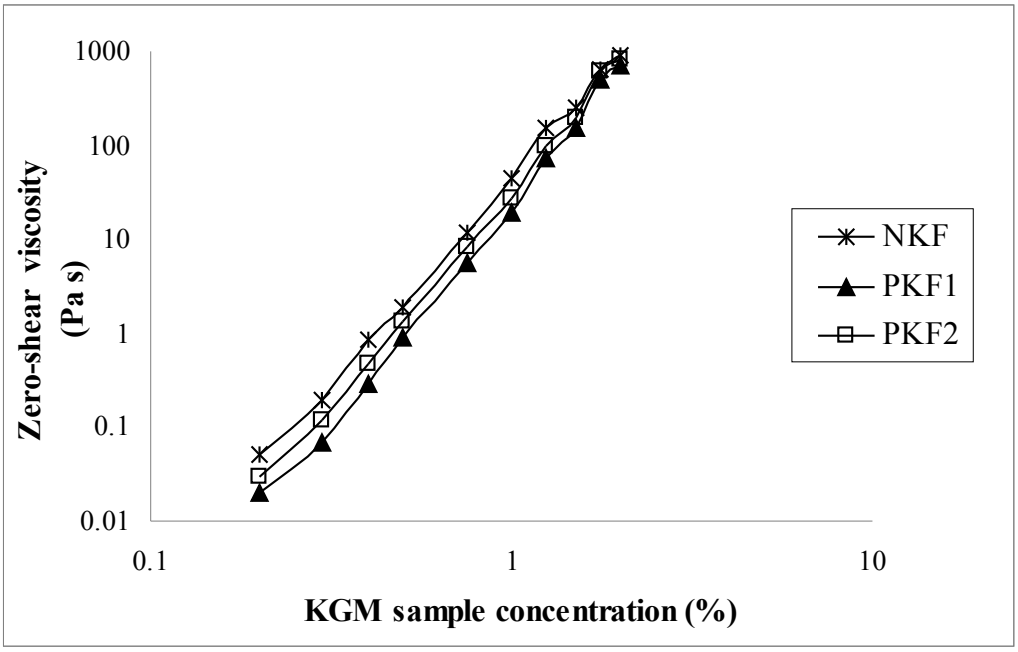

Figure 3.8 Double logarithmic plot of the zero shear specific viscosity (η_0) and the concentration of KGM sample solutions.

As can been seen from Figure 3.9, all sample solutions (0.2 - 2% w/w) exhibited a typical non-Newtonian, shear-thinning (pseudoplastic) behaviour, *i.e.* decreasing viscosity with increasing shear rate, which became progressively more pronounced as the sample concentration increased.

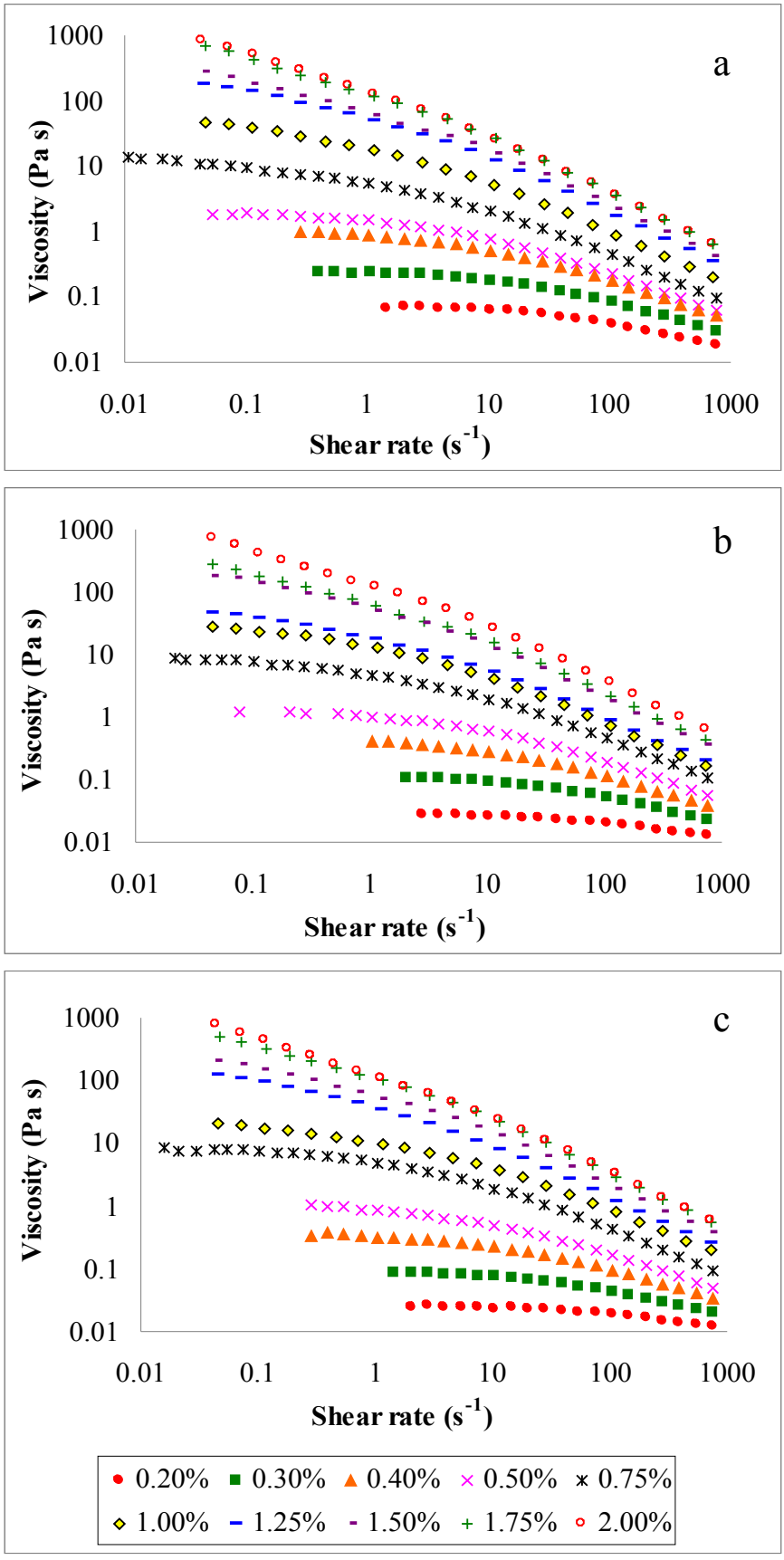

Figure 3.9 Viscosity-shear rate profiles for different concentrations of sample solutions at 25 °C. (a) NKF, **(b)** PKF1, **(c)** PKF2.

3.4. Discussion

3.4.1. Oven-drying conditions for CKF

In general, the purification of konjac flour starts by slicing and drying of fresh corm material. The dried chips are subsequently ground into a powder, commonly known as CKF, which is the starting material for the extraction and purification of KGM. It has previously been reported that use of a high drying temperature for corm slices for extended periods of time in production of CKF should be avoided, as this can significantly reduce the viscosity of resultant PKF (Zhao *et al*., 2010). Drying the corm slices at 120 - 150 °C for 40 min prior to incubation at 60 °C until constant weight was obtained has been shown to accelerate the drying process without affecting the quality of resultant CKF (Wu *et al*., 2002), and hence this drying condition was adopted in the current study.

3.4.2. Purification of CKF

The working principle and procedures involved in both Ogasawara's and Sugiyama's methods for the extraction and purification of KGM are similar (Sugiyama *et al*., 1972; Ogasawara *et al*., 1987; WIPO, 1993), with differences in the duration of ethanol extraction and hydration treatment of CKF. In both methods, the CKF was stirred continuously (3 - 10 days) in different ethanol concentrations ranging from 50 - 100% (v/v) to remove soluble starch and low molecular weight sugars (D-fructose and D-mannose), followed by oven-drying (60 - 90 °C) of the resultant flour before being hydrated (3 - 12 h) to form a sol. As the sol produced was highly viscous, it was diluted up to 10 fold before being dialysed (72 h). The dialyzed solution was subsequently freeze-dried to form the PKF. As mentioned

previously, although the resultant flour produced by both methods was found to retain the physicochemical properties of KGM, these methods are, however, time consuming and produce low yields of PKF.

Since it is important to employ a method that ensures proper purification without compromising the yield of the purified flour, two methods with different frequency/duration of ethanol washing and hydration treatments were hence established in the current study. Both methods are characterized by consecutive steps of: (1) ethanol (50% v/v) washings to remove soluble starch and low molecular weight sugars; (2) dispersing the flour in water with agitation to extract the KGM; (3) coagulating the KGM by addition of a water-miscible coagulant (ethanol) and (4) drying and grinding the KGM coagulate. Method 2 comprised of an ethanol washing treatment (90 min) and a water extraction step (3 h), and is less laborious compared to method 1 which involved three ethanol washing (30 min each) and three water extraction steps (2 h each).

A 38 ± 2% and 53 ± 4% yield of PKF was obtained from the CKF using purification method 1 and 2, respectively. The yield of PKF from both methods is considerably higher than those reported in Ogasawara's (22%) and Sugiyama's (35%) methods (Sugiyama *et al*., 1972; Ogasawara *et al*., 1987; WIPO, 1993). The lower yield of PKF using method 1 is expected as more ethanol washing and hydration steps were involved, which may result in the production of PKF of higher purity, but a concomitant lower yield.

3.4.3. Comparison of assays to determine glucomannan content in KGM samples

Determination of the glucomannan (or reducing sugar) content using the 3,5-DNS (Miller, 1959; Lindsay, 1973; Farhoosh and Riazi, 2007), phenol-sulphuric acid (Dubois *et al*., 1956; Cuesta *et al*., 2003; Yi *et al*., 2006) and enzymatic (Tekinsen and Guner, 2010) colorimetric assays have been previously reported in the literature. The current study compared the reproducibility and accuracy of these three methods, followed by further validation studies to determine the best assay method for quantification of the glucomannan content of KGM samples.

The experimental conditions employed in the colorimetric reactions of 3,5-DNS and phenol-sulphuric acid assay previously reported by the CMA (Liu *et al*., 2002) and Dubois *et al*. (1956) were followed in the current study. In both methods, KGMs were subjected to acid hydrolysis to produce the reducing sugars, D-glucose and D-mannose, which subsequently react with 3,5-DNS under alkaline conditions to form a brownish red amino compound in the 3,5-DNS assay, and an orange-yellow colour compound in the phenol-sulphuric acid assay. The colour intensity of the compounds was then measured spectrophotometrically and the amount of reducing sugar present was determined by reference to a standard calibration curve. Both glucose and mannose standard curves were constructed for each method (Figures 3.3 and 3.4) in order to compare the sensitivity of the assay systems to each sugar. It was shown that mannose has a slightly lower sensitivity compared to glucose in both assay systems, so a correction factor for mannose sugar was determined for each method, based upon the gradient of the constructed standard curves for both sugars and the typical mannose to glucose ratio (1.6:1) reported in KGM (Kato and Matsuda, 1969; Shimahara *et al*., 1975; Maeda *et al*., 1980).

The reproducibility and accuracy of the 3,5-DNS, phenol-sulphuric acid and enzymatic colorimetric assays were compared by first analysing CKF (previously shown to contain 49 - 60% glucomannan) (Li *et al*., 2005) and LVKF (> 98% glucomannan) in triplicate, on two occasions, under the same experimental conditions. The data presented in Table 3.2 indicates that the 3,5-DNS and the enzymatic colorimetric assays are more reproducible than the phenol-sulphuric acid colorimetric assay. Cuesta *et al*. (2003) has previously reported that the reproducibility of the phenol-sulphuric acid assay is highly dependent on the modality of sulphuric acid addition, either directly over the liquid surface or over the side of the tube. It was shown that the sensitivity of phenol-sulphuric acid reaction was 70% lower when the acid was added over the side of the tube. This is mainly related to the differences in the rate of heat dissipation upon acid addition. Furthermore, the speed of acid addition has also been shown to be critical. Saha and Brewer (1994) demonstrated that rapid addition of acid generates sufficient heat to break all the glycosidic bonds in complex carbohydrates. Clearly, the reproducibility of this method is an issue given the difficulty in the precise addition of the acid to produce consistent results, as shown in the current study, which was performed according to Dubois's protocol.

In terms of accuracy, the glucomannan contents of both CKF and LVKF determined by the 3,5-DNS and phenol-sulphuric acid assays were in reasonable agreement to the previously reported values for both samples, compared to the enzymatic colorimetric assay which yielded a considerable lower result for LVKF (~ 43%), despite its high reproducibility. As mentioned previously in section 3.2.3.3, an error for the FEV value involved in the final calculation of glucomannan content using the glucomannan assay kit was encountered in the current study. If the

incorrect FEV value (*i.e*. 250 ml), as cited in the kit instruction booklet was applied to our data, the resultant glucomannan content will be 2.5 fold (*i.e*. around 100%) higher than the current results. The reason for the low results obtained using this assay kit is unclear, and it is possible that the enzymatic reactions involved were incomplete, and therefore, further studies are needed to investigate and optimise the experimental conditions employed in this assay method.

In addition, prior to colorimetric reactions in both 3,5-DNS and phenol-sulphuric acid assays, konjac flour samples were magnetically stirred in formic acid-sodium hydroxide buffer or DI water for 4 h at room temperature to remove any insoluble substances such as starch and cellulose. The resultant solutions (referred to as KGM sample solutions) were then hydrolysed and the amount of reducing sugars (glucose and mannose) determined. In the 3,5-DNS assay, however, the amount of reducing sugars in KGM sample solutions before hydrolysis was also determined and was subsequently subtracted from the amount present after hydrolysis. This prevents overestimation of glucomannan content by free reducing sugars from other sources such as starch in the test sample.

Based upon the analysis as mentioned above, it was hence concluded that the 3,5-DNS colorimetric assay was the most reproducible and accurate among the three methods used and further validation studies were performed subsequently to investigate its accuracy and precision in more depth. As can be seen from the validation data obtained (Tables 3.3, 3,4 and Figure 3.5), it was confirmed that the 3,5-DNS colorimetric assay was the method of choice both in terms of reproducibility, accuracy and precision for the determination of the glucomannan content of KGM samples in the later stages of the study.

3.4.4. Glucomannan content of PKF1 and PKF2 determined by the 3,5-DNS assay

Glucomannan content is a key parameter used in the classification of konjac flour and KGM. According to the CMA, European Commission and the U.S. Food Chemicals Codex, the acceptance limit of glucomannan content for konjac flour is between 70 - 90%, and for KGM is between 90 - 100% (Byrne, 2001; Liu *et al*., 2002; U.S. Food Chemicals Codex, 2003). As can be seen from Table 3.5, the glucomannan content of both PKF1 (90.3%) and PKF2 (91.4%) fall within the acceptance limits for KGM, but are slightly lower compared to the total reducing sugar content (determined by the Bertrand method) of the PKF produced by the Sugiyama's method (Sugiyama *et al*., 1972), which was shown to be 95% as D-glucose.

3.4.5. Starch content

Starch, constituting 10 - 30% of the dry matter of fresh corm (Li *et al*., 2005), is regarded as the common impurity of KGM samples. The starch content of both PKF1 and PKF2 (0.6% and 0.9% of the dry weight, respectively) fall within the European standards for both konjac flour and KGM, *i.e.* < 3% and < 1%, respectively (Byrne, 2001).

3.4.6. Protein content

Nitrogen determination is the most commonly used procedure to assay protein content and it has been the basis for various official and conventional methods currently in use for expressing total protein content of organic materials. The most commonly used nitrogen determination methods include various versions of Kjeldahl

(AOAC, 1999a) and Dumas (AOAC, 1999b) methods. As it is assumed that a mixture of pure proteins contain 16% nitrogen; the protein content of a sample is calculated from the determined nitrogen content by multiplying by a nitrogen-to-protein conversion factor, 6.25 (*i.e.* 100/16). This conversion factor is used for most foodstuffs as their non-protein nitrogen content is negligible. However, a specific conversion factor is determined for some foodstuffs (Mariotti *et al*., 2008), including konjac flour, *i.e.* 5.70 according to the U.S. Food Chemicals Codex and European Commission (Byrne, 2001; U.S. Food Chemicals Codex, 2003; Parry, 2010) which was applied in the current study.

The acceptance limit of protein for konjac flour established by the U.S. Food Chemicals Codex is < 8% (U.S. Food Chemicals Codex, 2003), whilst the standard for konjac flour and KGM established by the European Commission is < 3% and < 1.5%, respectively (Byrne, 2001). The protein content of both PKFs (4.4% and 3.8% of the dry weight) fall within the U.S. acceptance limit, but is slightly higher under the European standards for both konjac flour and KGM. However, the percentage reduction of protein content achieved after purification using method 1 (41.2%) and method 2 (49.7%) was comparable to those reported by Takigami (47 - 50%), who compared the composition of commercial konjac flour produced from the Japanese and Chinese konjac cultivars, before and after purification using the ethanol extraction method (Takigami, 2000). As the protein content of CKF in the current study is ~ 3 times higher than those reported by Takigami (2000), this indicates that an additional deproteinization procedure needs to be performed during the extraction and purification process if konjac cultivars with high protein content are used for the KGM production.

3.4.7. Degree of acetylation (DA)

The DA determined for the PKF1, PKF2, LVKF and NKF (Table 3.5) are similar to previously reported values: 1.6% (Huang *et al*., 2002), 1.98% (Maekaji, 1978) and 3.7% (Dea *et al*., 1977), the observed differences may be due to the purity of sample used and differences in the origin and genotype of the starting material. The DA values for both PKF1 and PKF2 indicate that a significant proportion of acetyl-substituted residues, which are believed to confer solubility of KGM in aqueous solution (Maekaji, 1978; Huang *et al*., 2002; Gao and Nishinari, 2004), have not been removed from the polymer chain during the extraction and purification process.

3.4.8. FTIR analysis

The spectra obtained for PKF1 and PKF2 are in agreement with the reference sample (LVKF) (Figure 3.6) and with those previously reported (Takigami, 2000; Xiao *et al*., 2001; Yu *et al*. 2007; Alvarez-Mancenido *et al*. 2008). The dramatic increase in the intensity of the whole IR spectrum as a result of the purification process indicates that the majority of common impurities are broadly IR inactive, suggesting that impurities such as starch and protein are present at low levels.

3.4.9. Choice of processing model for GPC-MALLS analyses

The molecular mass distribution of the various konjac flour samples were analysed by the GPC-MALLS. The intensity of scattered light were measured at multiple scattering angles of > 0°, from which the intensity at 0° was obtained by extrapolation from the higher angle data, as mentioned in section 3.2.8. This extrapolation is commonly performed in a Debye plot (by linear or polynomial curve

fitting to all data points) where R_θ/Kc is plotted as a function of $\sin^2(\theta/2)$ using three different mathematical transformations of the light scattering function, referred to as the Debye, Zimm or Berry method (Anderson *et al*., 2003). According to Anderson *et al*. (2003) who present a rigorous exposition of the applicability of each method, the relative extrapolation error in molar mass of small molecules (radii < 50 nm) was less than 1% independent of the method used; whilst for larger molecules, the Berry method gives better accuracy (for a given polynomial order). It was also shown that as the size of polymer increases, an increase in the degree of polynomial fit to the data increases the accuracy of the molar mass determination. However, the better curve fit (to the erroneous data point) by using higher polynomials results in high relative errors compared to a first-order (linear) fit, as the latter is more robust toward erroneous data. The current procedures employed were hence to first construct a Debye plot using the linear Zimm fit, as the Zimm method was shown to be more useful in revealing erroneous data in the Debye plot, from a visual inspection of the character of the curvature. This was then followed by the exclusion of deviating data points from the Debye plot and subsequently extrapolated using the Berry method with a linear fit to minimize the effect of possible errors in low-angle data. As can be seen from Table 3.7, the comparable M_w obtained using the Berry method with a linear fit to those obtained by a second polynomial Debye treatment for both PKF1 and PKF2 indicated that the latter processing model can also be used in KGM analysis without affecting the accuracy of the final results.

3.4.10. Molecular mass distributions

The M_w of PKF1 ($9.1 \pm 0.6 \times 10^5$ g/mol) and PKF2 ($9.5 \pm 0.6 \times 10^5$ g/mol) are in close agreement with those determined by Ratcliffe *et al*. (2005) (8.5×10^5 g/mol)

for similar samples and show reasonable agreement with those reported by Kohyama *et al*. (1993) (6.9 x 10^5 g/mol). The polydispersity index of PKF2 (1.2) is comparable to the reference sample, NKF (1.0) and to the values previously reported by Ratcliffe *et al*. (2005), ranging from 1.1 - 1.5. The higher polydispersity index recorded for PKF1 (2.1), compared to both PKF2 and NKF, was due to its low M_n value, suggesting that degradation of KGM polymer chains had occurred during the 6 h hydration treatment to which the CKF was subjected using purification method 1. In relation to which, Shimahara *et al*. (1975) isolated two β-mannanases from germinating konjac corms and other workers have reported on the enzymatic or bacterial degradation of KGM during storage (Nishinari *et al*., 1992). Therefore, degradation of KGM polymer chains during the hydration treatment may be attributed to mannanases present in the corm and/or the action of bacteria.

In the case of LVKF, the differences observed in molecular weight parameters including the lower M_w and wider polydispersity compared to other konjac flour samples were expected, and these differences were most probably due to the processing method(s) employed to degrade/hydrolyze the KGM polymer chains during the preparation of the konjac flour sample.

3.4.11. Steady shear properties

One of the important criteria for the quality of konjac flour is its viscosity in aqueous solution (Byrne, 2001; Liu *et al*., 2002; U.S. Food Chemicals Codex, 2003). In the present study, the zero shear specific viscosities of NKF, PKF1 and PKF2 samples were determined from shear flow measurements over a range of concentrations (0.2 - 2.0% w/w); in the shear rate range 1 - 1000 s^{-1}.

The trend in the data presented in Figure 3.9, essentially a shift in the onset of shear thinning to lower shear rates with increasing sample concentration, is consistent with the literature for KGM (Wientjes *et al*., 2000) and other polysaccharides such as galactomannans and chitosan (Miyoshi and Nishinari, 1999; Huang and Shin, 2000; Oblonsek *et al*., 2003). When the shear rate is increasing, the rate of disentanglement becomes greater than the rate of re-entanglement of long chain molecules, resulting in less intermolecular resistance to flow (Morris, 1989; Bhandari *et al*., 2002), and hence exhibiting the shear-thinning (or pseudoplastic) behaviour, as observed for the samples analysed. However, in dilute solutions of polymers, viscosity most often shows lower shear rate dependence, due to the molecules being widely separated and the polymer chains being not in contact with each other. As the concentration increases, a point is reached during which the polymer chains begin to overlap and this physical contact subsequently changes the flow behaviour (Kaur *et al*., 2009).

The rheological properties of hydrocolloids, including KGM, are closely associated with their molecular weight distribution, (Takigami, 2000; Zhang *et al*., 2001). The lower value of zero-shear specific viscosity at 2% (w/w) observed for PKF1 is correlated with its wider polydispersity compared to PKF2.

Chapter four: General discussion

4.1. Main findings

From the general introduction (chapter 1), it is clear that fundamental research on the biology and chemistry of *A. konjac*, leading to enhanced commercial applications, is required to address questions relating to the improvement of corm productivity, KGM biosynthesis, extraction, purification and assay of KGM and subsequent product safety and efficacy. Therefore, the main objectives of the current study were to provide further insight into the morphogenesis, growth, propagation efficiency and extraction and analysis of KGM. In addition, a preliminary immunocytochemical investigation of the deposition and metabolism of KGM was also performed. This research led not only to a better understanding of the biology and cultivation of *A. konjac*, but also provides the basis for an improved GLP for the commercial extraction and analysis of KGM. In the following paragraphs, the main findings of the research reported in this thesis will be discussed in relation to other published work, followed by suggestions for future study.

An understanding of the growth and development of *A. konjac* is an essential prerequisite for the investigation and improvement of the productivity of this crop. The current study provides the most detailed information to date on both the vegetative and reproductive growth cycles of *A. konjac* (Figure 2.4). Overall, both one and two-year-old corms entered into the dormant phase at the end of October. Corms were then over-wintered and replanted in March, subsequent to which leaf buds emerged in mid to late May. Between late July and early August, the foliage developed, followed by leaf senescence which occurred 5 - 6 weeks after the development of a mature leaf canopy (late September). Of particular interest, is the

observation that mature corms (four years-old and above) started their seasonal growth 2 to 3 months earlier, by first initiating a reproductive cycle, followed by a vegetative cycle, with a leaf bud being produced 2 months after the senescence of the inflorescence (section 2.3.1). The time span for the development of the inflorescence after the emergence of the flower bud was recorded as approximately 21 days and lasted for approximately 10 days after the spathe had completely unfolded (section 2.3.2.6). This finding is of future use in predicting anthesis (flower opening), which could be of use in botanical gardens that wish to exhibit *A. konjac*. With the exception of an earlier report by Lobin *et al*. (2007) on glasshouse grown plants, our data is only the second record of this growth sequence in *A. konjac*, and leads us to the conclusion that this species behaves (under the stated conditions) in a similar way to African species of *Amorphophallus* (Sedayu *et al*., 2010), despite originating from Asia. Once the corm reaches maturity at four years-old, both an inflorescence and a leaf can be produced within the same growing season. Flowering, which has no yield value, will detract from corm yield, and therefore, mature corms are not used in agricultural production in China or Japan. Depending on the size and quality of planted corms, they are usually harvested for commercial processing after 2 – 3 growing seasons (Bown, 2000; Douglas *et al*., 2005; Douglas *et al*., 2006; Takigami, 2000; WFS, 2003).

With respect to offsets (referred to as 0-year-old plants in this thesis), the leaf buds emerged 2 - 3 weeks later than from one and two-year-old corms, *i.e.* between late May and early June. The foliage was fully developed and mature by late August, with leaf senescence initiated by mid September and early October (Figure 2.31).

This thesis represents the first detailed study of the morphogenesis of *A. konjac* corm at various stages of vegetative development in a Western University.

These data demonstrate a morphological and functional separation between the ventral and dorsal regions of the corm. As mentioned in section 2.4.4, our results do not fully agree with earlier observations reported by Wang and Liu, (1990) that the planted ("mother") corm was completely degenerated in order to produce a shoot, and that a "daughter" corm was formed on top of the degenerating "mother" corm as the leaf/shoot developed. These authors concluded that the degenerated "mother" corm became detached from the newly formed "daughter" corm which was enlarged towards the end of the growing season. On the basis of the current observations (Figures 2.7 and 2.8), we propose that the carbohydrate reserves stored in the central and ventral regions (acting as a source) of the planted corm are mobilised for early shoot initiation and subsequently degenerate during leaf expansion. Then, as the mature leaf canopy develops, photosynthates are partitioned into the dorsal region (acting as a sink) of the corm, leading to the enlargement of both this corm region and the developing rhizomatous offsets. The so called "daughter" corm, therefore, is interpreted as the retention of the dorsal portion of the planted corm. A hypothetical model of corm morphogenesis during vegetative growth in *A. konjac* is schematically presented in Figure 4.1. While this does not give a complete picture of the developmental processes in corms of this species, the current data has refined our understanding of the developmental sequences and mechanisms involved.

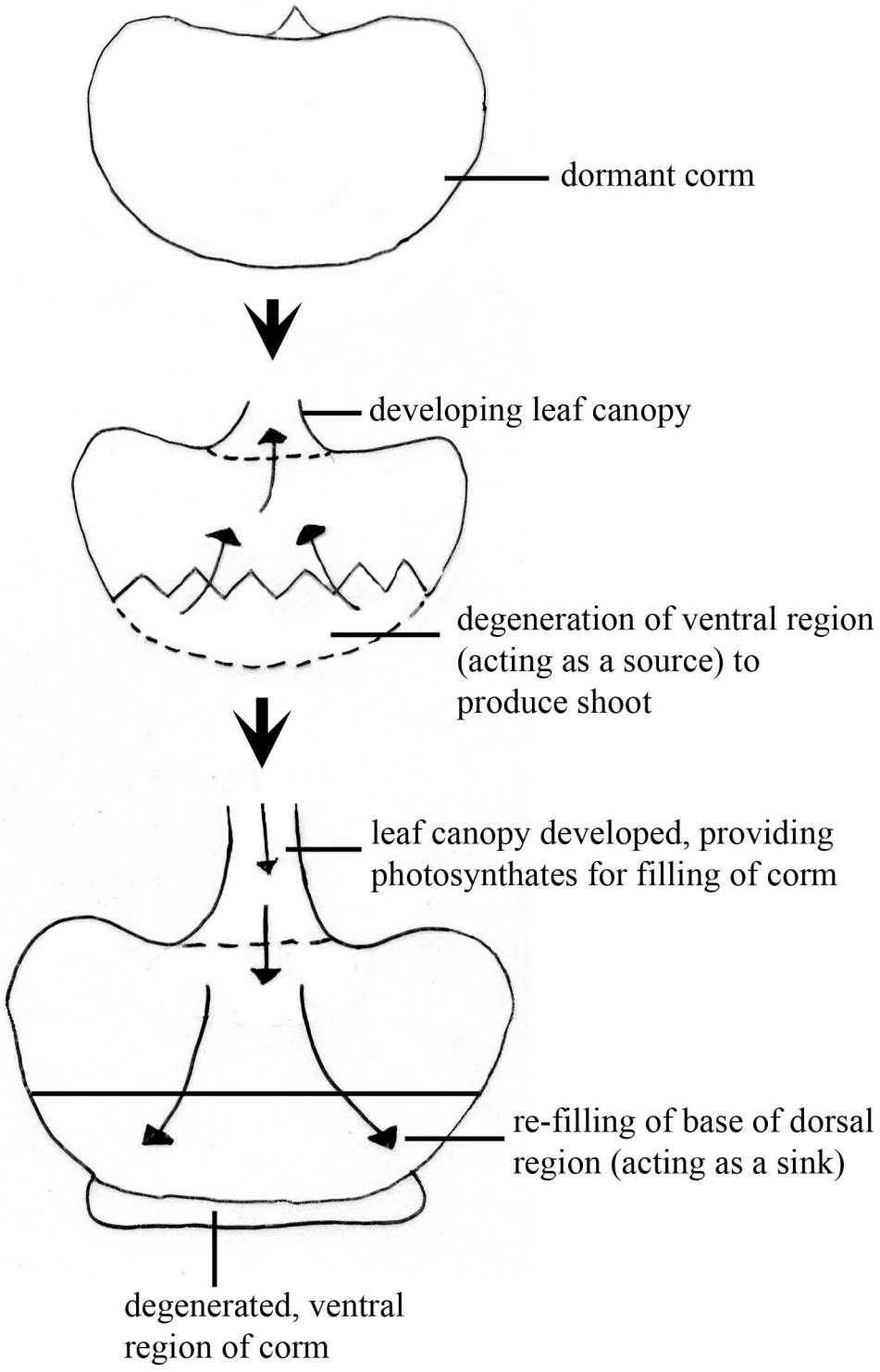

Figure 2.38 Diagrammatical presentation of the morphogenesis of *A. konjac* corm during the vegetative growth.

The present study has also demonstrated that the transitions between phases of growth and dormancy constitute major events in the morphogenesis of *A. konjac*, and that these changes were reflected in the corm tissues (section 2.3.2.3). On the basis of our results, and those of Takigami *et al*. (1997) and Shi *et al*. (1998), it is possible to conclude that the KGM is stored in a hydrated state within the vacuole of highly specialized cells (referred to as glucomannan idioblasts in this thesis) in the corm tissues, and that KGM deposition in the idioblasts is developmentally regulated. Mannan epitopes were shown to be absent/rare during early shoot development and increased as the mature leaf canopy developed. Immunocytochemical investigation at both the LM and TEM level (sections 2.3.2.4 and 2.3.2.5) revealed the occurrence of a source-sink transition in the corm, which was shown to occur after leaflet emergence (*i.e*. 70 to 90 DAP), prior to complete expansion of the leaves.

In addition, by comparing the intensity of antibody binding within the glucomannan idioblasts at three different positions along the cross section of the corm (Figure 2.3) during the stages in which the corm functions as a source for early shoot development; it can be suggested that the mobilization of glucomannan initiates at the periphery and proceeds inwards towards the centre of the corm. Since there have been no previous studies on the reserve carbohydrate mobilization and deposition in corms of *A. konjac*, it is therefore useful to compare our data with those obtained in previous studies performed on other geophytes, such as yam (*Dioscorea* spp.) and taro (*Colocasia* spp.). Kawasaki *et al*. (2001) observed that the mucilage present in the mucilage duct in taro corms and the starch granules within the amyloplasts in yam tubers decomposed to a low-density material, from the periphery and proceeds inwards towards the centre of the cells during shoot initiation. According to these authors, the initiation of starch decomposition at the periphery of

the amyloplasts in yam tubers could be due to the physical fragility of the starch granules near the amyloplast envelope, and/or the actions of starch hydrolyzing enzymes located in the stroma between the starch granules and the amyloplast envelope. Judging from these reports and the previous demonstration of the localisation of mannan (or KGM) synthesis in the Golgi apparatus (Handford *et al*., 2003), we speculate that the patterns of glucomannan mobilization and deposition within the idioblasts are similar to those reported for yam tubers, *i.e*. initiate at the periphery inwards. However, without detailed information on the physiological and biochemical status of the corms at each developmental stage, it is hard to draw any conclusions on the endogenous control of glucomannan metabolism and biosynthesis.

Regarding formation of calcium oxalate crystals, it has previously been described as a complex, dynamic process and that the pre-crystal idioblasts are highly active metabolically throughout the course of cell differentiation and crystal deposition (Sunell and Healey, 1979; Wang *et al*., 1994; Kawasaki *et al*., 2004; Prychid *et al*., 2008). The raphide crystals observed within the glucomannan idioblasts in the current study, therefore, may be ergastic products resulting from metabolic processes associated with cell division. Since many edible geophytes, including *A. konjac* are acrid, which is believed to be associated with the presence of raphide crystals (Sunell and Healey, 1979; O'Hair and Asokan, 1986; Kawasaki *et al*., 2004), the elucidation of the mechanism of crystal formation, as well as identifying the composition(s) and biological function(s) of the surrounding mucilage are essential prerequisites for improving the processing and quality of edible geophytes.

In addition to analyzing the growth patterns of *A. konjac* plants under semi-controlled conditions, the crop establishment potential of different aged propagation materials was also assessed. As mentioned in section 1.5, under modern cultural practice, offsets are planted at a high planting density for one year in order to establish propagation material for the subsequent growing season (Douglas *et al*., 2005). This highlights the importance of offset material in determining the subsequent corm yield. Hence, the current investigation has focused primarily on the productivity of offsets produced by corms of different ages. It has previously been shown that the number of offsets produced is positively correlated with the fresh corm weight at planting (Miura and Watanabe, 1985; Douglas *et al*., 2006). In the current study, however, such a correlation was not observed among the F0 corms in both growing seasons (Tables 2.9 and 2.13) and as the number of F0 corms involved in this study was small, the significance of the quantitative differences between these plants could not be assessed with a high degree of confidence. Nevertheless, the data recorded for F0 corms provide some insight into the quantitative relationship between the $f_0$1 offsets produced by F0 corms with varying age. In the 2009 season, it was found that the $f_0$1 offsets produced by both one and two-year-old F0 corms (referred to as group 1 and 2, respectively in this thesis) have a significantly higher productivity than those by ≥ four-year-old corms (referred to as group 3 in this thesis), indicating that the age of the corm is an important determinant of the quality of offsets produced. The lower productivity observed in group 3 may be correlated with the physiological (*i.e.* more biomass could be partitioned for floral development) and physical (*i.e.* having mechanically unstable aerial structure composed of a long petiole and a large, expanded leaf blade that can easily collapse) constraints of their older mother corms/plants, which resulted in a slowing down or

early termination of photosynthesis. This would, in turn, limit the amount of biomass partitioned into the attached offsets (Table 2.9). Based on the current results, it is also possible that plants in group 3 had genetically inherited physiological traits such as timings of leaf bud emergence and dormancy from their older "mother" corms. In this respect, Passam *et al*. (1982) have proposed that yam dormancy is under strong genetic, constitutive or endogenous control that may be regulated by a biological clock, rather than being under an environmental control. On the other hand, as suggested by Burton *et al*. (1992) for potato, environmental conditions that influence tuber formation and growth may influence the duration of dormancy. Thus, further research is needed to fully separate out developmental and environmental influences in relation to the growth patterns of *A. konjac*.

Turning to our studies on chemical analysis of KGM, we have reported a comparison of commonly used methodologies for the extraction and quantification of KGM. The data presented have shown that purification of CKF using method 2 not only produced PKF with a high glucomannan content (91.4 ± 1.3%) and physicochemical properties consistent with the literature, but also generated a higher yield of PKF (53% w/w) than that reported elsewhere (Sugiyama *et al*., 1972; Ogasawara *et al*., 1987; WIPO, 1993).

Although the glucomannan content of PKF1 was comparable to that of PKF2, the higher polydispersity index observed for PKF1 indicates that increasing the frequency of ethanol washing and hydration treatments during purification may degrade the resultant KGM polymer chains. It is hence proposed that the quality of KGM-derived products should not be evaluated by glucomannan content alone. The molecular weight distribution, viscosity, chain length and structure (e.g. degree of acetylation) of KGM should also be evaluated.

Our comparison of three existing methodologies for the quantitative analysis of the KGM content of the PKF, namely 3,5-DNS, phenol-sulphuric acid and enzymatic colorimetric assays, indicated that the 3,5-DNS colorimetric assay was the most reproducible and accurate method of choice with which to monitor the glucomannan content present in KGM-derived products. This method showed a linear correlation coefficient of 0.997 for samples ranging from 0.5 - 12.5 mg/ml, and recoveries between 97% and 103% across three spiking levels (250, 500 and 750 μg/g) of starch (section 3.3.3.3).

In conclusion, we have described the vegetative and reproductive growth cycles, the morphological changes in both corms and offsets at various developmental stages and the growth pattern of different-aged plants. These data, together with the results presented for the immunocytochemical investigation, constitute a first step towards an understanding of the mechanisms involved in the physiological and biochemical control of KGM biosynthesis, partitioning, storage and re-mobilisation. This information is essential for further improvement of the yield and productivity of this crop. We have also shown that offsets produced by one and two-year-old corms have higher productivity when compared to those produced from older corms.

Given the increasing demand for KGM in the food industry and in the treatment of various medical conditions, the methodologies outlined for the purification and assay of KGM may assist in the establishment of monographic standards for this multifunctional natural polymer.

4.2. Further work

This section will outline some of the ways in which the experiments in the present study could be expanded.

The hypothetical model of corm morphogenesis during the vegetative growth presented in Figure 4.1 could be further tested by examining and comparing the developmental anatomy and carbohydrate content of longitudinal sections (*i.e.* the dorsal, central and ventral regions of corm on the vertical axis of the apical bud) of corm tissues throughout the key stages of growth and development. The key aspect of this morphogenesis is the development of vascular tissue into the emerging shoot. However, how the vascular tissues connect to the emerging shoot and the route via which sugars are transported to the developing bud are unclear and future work is needed to answer these questions.

As limited numbers of F0 corms were collected during the 2008 growing season, we could not perform destructive analyses to investigate the physiology of shoot and corm development and processes including photosynthesis and partitioning of carbohydrate during various stages of plant development. Therefore, future studies could focus on the investigation of photosynthesis and assimilate production, followed by an analysis of assimilate partitioning, location of polymer synthesis, temporary and permanent storage and re-mobilisation. In conjunction with the physiological studies, monitoring the activities of enzymes such as β-mannanases and the expression of Golgi-localised *CslA* genes within corm tissues throughout the growing period could be useful in addressing question relating to the endogenous control of KGM metabolism and biosynthesis.

The strong labeling of mannan epitopes detected in the mucilage within the raphide crystal idioblasts (Figure 2.17B - D) was thought to be due to the presence of AG/AGPs which may bear terminal mannose residues or these may be present on other glycoproteins or proteoglycans present in the mucilage. This assumption could be investigated further by probing the corm tissues with anti-AG/AGP antibodies (Knox, 1995, 1997) to observe if there is any overlap of mannan-bearing epitopes with the epitopes recognized by the anti-AG/AGP antibodies, within the crystal idioblasts.

As the results presented for the quantitative analysis of offsets in the current study were based on glasshouse conditions, it would clearly be sensible to re-assess the productivity of offsets produced by one and two-year-old corms under field conditions, to examine if they can deliver growth rates that would be acceptable for agricultural production. Moreover, the results presented for the 2010 growing season (sections 2.3.5 and 2.3.6) have also demonstrated the importance of fertilizer in determining the corm yield and productivity. Hence, more studies are needed to devise the fertilizer regime required for konjac cultivation based upon previous investigations (Lee *et al*., 1992; Douglas *et al*., 2005).

The feasibility of the current purification protocol (*i.e.* method 2) for industrial KGM production could also be tested. To further optimize the purification methodology, we think that an additional deproteinization treatment of CKF, e.g. via Sevag method or alkaline protease (Peng and Zhang, 2003; Wang *et al*., 2007), could also be included in the protocol. Moreover, since the physical properties of KGM, such as storage and loss moduli, microstructure and particle size, play extremely important roles in its functionality during food processing and bioabsorption, it would be useful to study these properties in the PKF obtained.

References

Albersheim, P., Darvill, A., Roberts, K., Sederoff, R. and Staehelin, A. (2010) *Plant cell walls*. New York: Garland Science.

Al-Ghazzewi, F.H., Khanna, S., Tester, R.F. and Piggott, J. (2007) The potential use of hydrolysed konjac glucomannan as a prebiotic. *Journal of the Science of Food and Agriculture*, **87**, pp. 1758–66.

Alonso-Sande, M., Teijeiro-Osorio, D., Remunan-Lopez, C. and Alonso, M.J. (2009) Glucomannan, a promising polysaccharide for biopharmaceutical purposes. *European Journal of Pharmaceutics and Biopharmaceutics*, **72**, pp. 453–62.

Alvarez-Mancenido, F., Landin, M., Lacik, I. and Martinez-Pacheco, R. (2008) Konjac glucomannan and konjac glucomannan/xanthan gum mixtures as excipients for controlled drug delivery system. Diffusion of small drugs. *International Journal of Pharmaceutics*, **349**, pp. 11–18.

Anderson, M., Wittgren, B. and Wahlund, K. (2003) Accuracy in multiangle light scattering measurements for molar mass and radius estimations. Model calculations and experiments. *Analytical Chemistry*, **75**, pp. 4279-91.

Association of Analytical Communities (AOAC) (1999a) *Official methods of analysis method 988.05*. Gaithersburg, Maryland: AOAC International.

Association of Analytical Communities (AOAC) (1999b) *Official methods of analysis method 968.06*. Gaithersburg, Maryland: AOAC International.

Bacic, A., Harris, P.J. and Stone, B.A. (1988) Structure and function of plant cell walls. in Preiss, J. (ed.) *The biochemistry of plants*. New York: Academic Press, pp. 297-371.

Bewley, J.D. and Reid, J.S.G. (1985) Mannans and glucomannans. in Dey, P.M. and Dixon, R.A. (eds.) *Biochemistry of storage carbohydrates in green plants*. New York: Academic Press.

Bhandari, P.N., Singhal, R.S. and Kale, D.D. (2002) Effect of succinylation on the rheological profile of starch pastes. *Carbohydrate Polymers*, **47**, pp. 365-71.

Bown, D. (2000) *Aroids, Plants of the Arum Family*. Portland, Oregon: Timber Press.

Boyce, P. (1993) *The Genus Arum.* London: The Royal Botanic Gardens, Kew.

Brett, C.T. and Waldron, K.W. (1996) *Physiology and biochemistry of plant cell walls*. 2nd ed. London: Chapman & Hall.

Brown, D.M., Zeef, L.A.H., Ellis, J. and Turner, S.R. (2005) Identification of novel genes in *Arabidopsis* involved in secondary cell wall formation using expression profiling and reverse genetics. *Plant Cell*, **17**, pp. 2281–95.

Burton, R.A., Shirley, N.J., King, B.J., Harvey, A.J. and Fincher, G.B. (2004) The CesA gene family of barley. Quantitative analysis of transcripts reveals two groups of co-expressed genes. *Plant Physiology*, **134**, pp. 224-36.

Burton, W.G., van Es, A. and Hartmans, K.J. (1992) The physics and physiology of storage. in Harris, P.M. (ed.) *The potato crop*. London: Chapman & Hall, pp. 608-727.

Byrne, D. (2001) *Commission directive 2001/30/EC of 2001, amending Directive 96/77/EC laying down specific purity criteria on food additives other than colours and sweeteners* [online]. Brussels: European Commission. [Accessed 9 August 2011]. Available at: <http://eurlex.europa.eu/LexUriServ/LexUriServ.do?uri=OJ:L:2001:146:0001:0023:EN:PDF>.

Carpita, N.C., Defernez, M., Findlay, K., Wells, B., Shoue, D.A., Catchpole, G.,Wilson, R.H., and McCann, M.C. (2001) Cell Wall Architecture of the Elongating Maize Coleoptile. *Plant Physiology*, **127**, pp. 551-65.

Cartier, N., Chambat, G. and Joseleau, J.P. (1988) Cell wall and extracellular galactoglucomannans from suspension-cultured *Rubus fruticosus* cells. *Phytochemistry*, **27**, pp. 1361-4.

Chandrasekaran, R., Janaswami, S. and Morris, V.J. (2003) Acetan-glucomannan interactions- a modeling study. *Carbohydrate Research*, **338**, pp. 2889-98.

Chan, K., Leung, K.S. and Zhao, S.S. (2009) Harmonization of monographic standards is needed to ensure the quality of Chinese medicinal materials. *Chinese Medicine*, **4**, pp. 18-22.

Chen, H.L., Fan, Y.H., Chen, M.E. and Chan, Y. (2005) Unhydrolyzed and hydrolyzed konjac glucomannans modulated cecal and fecal microflora in Balb/c mice. *Nutrition*, **21**, pp. 1059–64.

Chen, H.L., Cheng, H.C., Liu, Y.J., Liu, S.Y. and Wu, W.T. (2006) Konjac acts as a natural laxative by increasing stool bulk and improving colonic ecology in healthy adults. *Nutrition*, **22**, pp. 1112–19.

Chen, H.L., Cheng, H.C., Wu, W.T., Liu, Y.J. and Liu, S.Y. (2008) Supplementation of konjac glucomannan into a low-fibre Chinese diet promoted bowel movement and improved colonic ecology in constipated adults: a placebo-controlled, diet controlled trial. *Journal of the American College of Nutrition*, **27**, pp. 102–8.

Chen, J. and Meeuse, B.J.D. (1971) Production of free indole by some aroids. *Acta Botanica Neerlandica*, **20**, pp. 627–35.

Chen, W, Stoddard, F.L. and Baldwin, T.C. (2006) Development regulation of mannan, arabinogalactan-protein and pectic epitopes in pistils of *Vicia faba* (faba bean). *International Journal of Plant Sciences*, **167**, pp. 919-32.

Cheung, A.Y., Wu, H-M., Di Stilio, V., Glaven, R., Chen, C., Wong, E., Ogdahl, J. and Estavillo, A. (2000) Pollen-pistil interactions in *Nicotiana tabacum*. *Annals of Botany*, **85**, pp. 29-37.

Chua, M., Baldwin, T.C., Hocking, T.J. and Chan, K. (2010) Traditional uses and potential health benefits of *Amorphophallus konjac* K. Koch ex N.E.Br. *Journal of Ethnopharmacol*ogy, **128**, pp. 268-78.

Cuesta, G., Suarez, N., Bessio, M.I., Ferreira, F. and Massalsi, H. (2003) Quantitative determination of pneumococcal capsular polysaccharide serotype 14 using a modification of phenol-sulphuric acid method. *Journal of Microbiological Methods,* **52**, pp. 69-73.

Davies, P.J. (ed.) (2010) *Plant Hormones: Biosynthesis, Signal Transduction, Action!* The Netherlands: Springer, Dordrecht.

Dea, I.C.M., Morris, E.R., Rees, D.A., Welsh, E.J., Barnes, H.A. and Price, J. (1977). Associations of like and unlike polysaccharides: Mechanism and specificity in galactomannans, interacting bacterial polysaccharides, and related systems. *Carbohydrate research*, **57**, pp. 249-72.

Dhua, R.S., Ghosh, S.K., Biswas, J., Mitra, S.K. and Sen, H. (1988) Effect of some chemicals on sprouting, growth and corm yield of *Amorphophallus campanulatus*. *Journal of Root Crops*, **14**, pp. 47-9.

Dhugga, K.S. (2001) Building the wall: genes and enzyme complexes for polysaccharide synthases. *Current Opinion in Plant Biology*, **4**, pp. 488-93.

Dhugga, K.S. (2005) Plant Golgi cell wall synthesis: from genes to enzyme activities. *The Proceedings of the National Academy of Sciences*, **102**, pp. 1815–16.

Douglas, J.A., Follett, J.M. and Waller, J.E. (2005) Research on konjac (*Amorphophallus konjac*) production in New Zealand. *Acta Horticulturae,* **670,** pp. 173-80.

Douglas, J.A., Follett, J.M. and Waller, J.E. (2006) Effect of three plant densities on the corm yield of konjac (*Amorphophallus konjac*) grown for 1 or 2 years. *New Zealand Journal of Crop and Horticultural Science,* **34**, pp. 139-44.

Dubois, M., Gilles, K.A., Hamilton, J.K., Rebers, P.A. and Smith, F. (1956) Colorimetric method for determination of sugars and related substances. *Analytical Chemistry,* **28**, pp. 350-56.

Edison, S. (2010) Konjac [online]. in Fajardo, J., Lutaladio, N., Larinde, M., Rosell, C., Barker, I., Roca, W. And Chujoy, E. (eds.) *Quality declared planting material: Protocols and standards for vegetatively propagated crops*. Rome: Food and Agriculture Organization of the United Nations (FAO), pp. 65-9. [Accessed 12 August 2011]. Available at: <http://www.fao.org/docrep/013/i1195e/i1195e00.pdf>.

Edwards, M.E., Choo T.S., Dickson, C.A., Scott, C., Gidley, M.J. and Reid, J.S.G. (2004) The seeds of Lotus japonicus Lines transformed with sense and sense/antisense galactomannan galactosyltrasferase constructs have structurally altered galactomannans in their endosperm cell walls. *Plant Physiology*, **134**, pp. 1153-62.

Ehlers, B.K. and Olesen, J.M. (2004) Flower production in relation to individual plant age and leaf production among different patches of *Corydalis intermedia*. *Plant Ecology*, **174**, pp. 71-8.

Elamir, A.A., Tester, R.F., Al-Ghazzewi, F.H., Kaal, H.Y., Ghalbon, A.A., Elmegrahai, N.A. and Piggott, J.R. (2008) Effects of konjac glucomannan hydrolysates on the gut microflora of mice. *Nutrition and Food Science*, **38**, pp. 422–29.

En, S.C. (2008) Current production of konjac: problems and strategies. *Journal of Anhui Agricultural Science*, **36**, pp. 14792–93 [in Chinese].

Farhoosh, R. and Riazi, A. (2007) A compositional study on two current types of salep in Iran and their rheological properties as a function of concentration and temperature. *Food Hydrocolloids*, **21**, pp. 660-66.

Follett, J.M. and Douglas, J.A. (2002) Konjac production in Japan and potential for New Zealand. *Combined Proceedings International Plant Propagators' Society*, **52**, pp. 186-90.

Franceschi, V.R. and Nakata, P.A. (2005) Calcium oxalate in plants: formation and function. *Annual Review of Plant Biology*, **56**, pp. 41-71.

Frei, E. and Preston, R.D. (1968) Non-cellulosic structural polysaccharides in algal cell walls. III. Mannan in siphoneous green algae. *Proceedings of the Royal Society B: Biological Sciences*, **169**, pp. 127–45.

Freshour, G., Bonin, C.P., Reiter, W.D., Albersheim, P., Darvill, A.G. and Hahn, M.G. (2003) Distribution of fucose-containing xyloglucans in cell walls of the *mur1* mutant of Arabidopsis. *Plant Physiology*, **131**, pp. 1602-12.

FSA (Food Standards Agency) (2007) *Current EU approved additives and their E numbers* [online]. [Accessed 11 August 2011]. Available at: <http://www.food.gov.uk/safereating/chemsafe/additivesbranch/enumberlist> .

Gallaher, C.M., Munion, J., Hesslink, R., Wise, J. and Gallaher, D.D. (2000) Cholesterol reduction by glucomannan and chitosan is mediated by changes

in cholesterol absorption and bile acid and fat excretion in rats. *The Journal of Nutrition*, **130**, pp. 2753–2759.

Gao, S. and Nishinari, K. (2004) Effect of degree of acetylation on gelation of konjac glucomannan. *Biomacromolecules*, **5**, pp. 175-85.

Gille, S., Cheng, K., Wilkerson, C. and Pauly, M. (2011) Deep sequencing of Voodoo Lily (*Amorphophallus konjac*): an approach to identify relevant genes involved in the synthesis of the hemicellulose glucomannan. *Planta*, **234**, pp. 515-26.

Gong, X.M., Yan, R.W., Xu, H.Y., Li, C., Guang, S.Y. and Fang, M. (2002) Study of the extraction methods and properties of konjac glucomannan. *Fine Chemicals,* **19**, pp. 486-88 [in Chinese].

Goubet, F., Barton, C.J., Mortimer, J.C., Yu, X., Zhang, Z., Miles, G.P., Richens, J., Liepman, A.H., Seffen, K. and Dupree, P. (2009) Cell wall glucomannan in Arabidopsis is synthesised by CSLA glycosyltransferases, and influences the progression of embryogenesis. *The Plant Journal*, **60**, pp. 527-38.

Handford, M.G., Baldwin, T.C., Goubet, F., Prime, T.A., Miles, J., Yu, X.L. and Dupree, P. (2003) Localisation and characterisation of cell wall mannan polysaccharides in *Arabidopsis thaliana*. *Planta*, **218**, pp. 27-36.

Harholt, J., Jensen, J.K., Sorensen, S.O., Orfila, C., Pauly, M. and Scheller, H.V. (2006) ARABINAN DEFICIENT 1 is a putative arabinosyltransferase involved in biosynthesis of pectic arabinan in *Arabidopsis*. *Plant Physiology*, **140**, pp. 49-58.

Hariprakash, C.S. and Nambisan, B. (1996) Carbohydrate metabolism during dormancy and sprouting in yam (*Dioscorea*) tubers. Changes in carbohydrate constituents in yam (*Dioscorea*) tuber during dormancy and sprouting. *Journal of Agricultural and Food Chemistry*, **44**, pp. 3066-9.

Hazen, S., Scott-Craig, J.S. and Walton, J.D. (2002) Cellulose synthase-like genes of rice. *Plant Physiology*, **128**, pp. 336–40.

Hejnowicz, Z. and Barthlott, W. (2005) Structural and mechanical peculiarities of the petioles of giant leaves of *Amorphophallus* (Araceae). *American Journal of Botany*, **92**, pp. 391-403.

Hetterscheid, W.L.A. (1994) Notes on the genus *Amorphophallus* (Araceae). 2. New species from tropical Asia. *Blumea*, **39**, pp. 237-81.

Hetterscheid, W.L.A. and Ittenbach, S. (1996) Everything you always wanted to know about *Amorphophallus* but were afraid to stick your nose into. *Aroideana*, **19**, pp. 7–129.

Hetterscheid, W.L.A., Koenen, M., Lobin, W., Ittenbach, S. and Neumann, M. (1998) Cultivation. in Barthlott, W. and Lobin, W. (eds.) *Amorphophallus titanum – Tropische und Subtrop*. *Pflanzenwelt*, **99**, pp. 198-205.

Holland, N., Holland, D., Helentjaris, T., Dhugga, K.S., Xoconostle-Cazares, B. and Delmer, D.P. (2000) A comparative analysis of the plant cellulose synthase (*CesA*) gene family. *Plant Physiology*, **123**, pp. 1313-23.

Holliday, R.J. (1960) Plant population and crop yield. *Nature*, **186**, pp. 22.

Huang, J.K. and Shin, H.H. (2000) Rheological properties of chitosan solutions. *Korea-Australia Rheology Journal,* **12**, pp. 175-9.

Huang, L., Takahashi, R., Kobayashi, S., Kawase, T. and Nishinari, K. (2002) Gelation behaviour of native and acetylated konjac glucomannan. *Biomacromolecules,* **3**, pp. 1296-1303.

Hudgins, J.W., Krekling, T. and Franceschi, V.R. (2003) Distribution of calcium oxalate crystals in the conifers: a constitutive defense mechanism? *New Phytologist*, **159**, pp. 677-90.

Imai, K. and Coleman, D.F. (1983) Elevated atmospheric partial pressure of carbon dioxide and dry matter production of konjac (*Amorphophallus konjac* K. Koch). *Photosynthesis Research*, **4**, pp. 331-6.

Inaba, K. (1984) Effect of shading on leaf anatomy in konjac plant. *Japanese Journal of Crop Science*, **53**, pp. 243-48 [in Japanese with English abstract].

Inaba, K. and Chonan, N. (1984) The effect of light intensity on ultrastructure of chloroplasts in konjac (*Amorphophallus konjac* K. Koch). *Japanese Journal of Crop Science*, **53**, pp. 503-9 [in Japanese with English abstract].

Isawa, Y. and Cohen, D. (1989) Optimal growth schedule of a perennial plant. *The American Naturalist*, **133**, pp. 480-505.

Kato, K. and Matsuda, K. (1969) Studies on the chemical structure of konjac mannan. Part I: Isolation and characterization of oligosaccharides from the partial acid hydrolyzate of the mannan. *Agricultural and Biological Chemistry*, **33**, pp. 1446–53.

Kaur, L., Singh, J. and Singh, H. (2009) Characterization of gum ghatti (*Anogeissus latifolia*): a structural and rheological approach**. *Journal of Food Science*, 74, E328-32.**

Kawasaki, M., Matsuda, T., Miyake, H., Taniguchi, M. and Nitta, Y. (2001) Morphological studies on the mobilization of reserves in Japanese yam (*Dioscorea japonica* Thunb.) seed tuber and eddo (*Colocasia esculenta* Schott var. *antiquorum* Hubbard & Rehder) seed corm on and after sprouting. *Plant Production Science*, **4**, pp. 304-10.

Kawasaki, M., Taniguchi, M. and Miyake, H. (2004) Structural changes and fate of crystalloplastids during growth of calcium oxalate crystal idioblasts in Japanese yam (*Dioscorea japonica* Thunb.) tubers. *Plant Production Science*, **7**, pp. 283-91.

Keithley, J. and Swanson, B. (2005) Glucomannan and obesity: a critical review. *Alternative Therapies in Health and Medicine,* **11**, pp. 30-4.

Kim, S., Mollet, J.C., Dong, J., Zhang, K.L., Park, S.Y. and Lord, E.M. (2003) Chemocyanin, a small basic protein from the lily stigma, induces pollen tube chemotropism. *Proceedings of the National Academy of Sciences of the United States of America*, **100**, pp. 16125-30.

Kiriyama, S., Ichihara, Y., Enishi, A. and Yoshida, A. (2008) Effect of purification and cellulase treatment on the hypocholesterolemic activity of crude konjac mannan. *Journal of Nutrition*, **102**, pp. 1689-97.

Kite, C.G. and Hetterscheid, W.L.A. (1997) Inflorescence odours of *Amorphophallus* and *Pseudodracontium* (Araceae). *Phytochemistry*, **46**, pp. 71-5.

Kite, C.G., Hetterscheid, W.L.A., Lewis, M.J., Boyce, P.C., Ollerton, J., Cocklin, E., Diaz, A. and Simmonds, M.J. (1998) Inflorescence odours and pollinators of *Arum* and *Amorphophallus* (Araceae). in: Owens, S.J. and Rudall, P.J. (eds.) *Reproductive Biology*. London: Royal Botanic Gardens, Kew, pp. 295-315.

Knox, J.P. (1995) Developmentally regulated proteoglycans and glycoproteins of the plant cell surface. *The FASEB Journal*, **9**, pp. 1004-12.

Knox, J.P. (1997) The use of antibodies to study the architecture and developmental regulation of plant cell walls. *International Review of Cytology,* **171**, pp.79-120.

Kohyama, K., Iida, H. and Nishinari, K. (1993) A mixed system composed of different molecular weights konjac glucomannan and kappa-carrageenan: large deformation and dynamic viscoelastic study. *Food Hydrocolloids*, **7**, pp. 213-26.

Kok, M.S., Abdelhameed, A.S., Ang, S., Morris, G.A. and Harding, S.E. (2009) A novel global hydrodynamic analysis of the molecular flexibility of the dietary fibre polysaccharide konjac glucomannan. *Food Hydrocolloids*, **23**, pp. 1910–17.

Konishi, T., Takeda, T., Miyazaki, Y., Ohnishi-Kameyama, M., Hayashi, T., O'Neill, M.A. and Ishii, T. (2007) A plant mutase that interconverts UDP-arabinofuranose and UDP-arabinopyranose. *Glycobiology*, **17**, pp. 345-54.

Koroskenyi, B. and McCarthy, S.P. (2001) Synthesis of acetylated konjac glucomannan and effect of degree of acetylation on water absorbency. *Biomacromolecules*, **2**, pp. 824-6.

Kostman, T.A. and Franceschi, V.R. (2000) Cell and calcium oxalate crystal growth is coordinated to achieve high-capacity calcium regulation in plants. *Protoplasma*, **214**, pp. 166-79.

Kraemer, W.J., Vingren, J.L., Silvestre, R., Spiering, B.A., Hatfield, D.L., Ho, J.Y., Fragala, M.S., Maresh, C.M. and Volek, J.S. (2007) Effect of adding exercise to a diet containing glucomannan. *Metabolism Clinical and Experimental*, **56**, pp. 1149-58.

Kumar, D.A., Indira, P. and Nambisan, B. (1998) Effect of light and growth regulators on sprouting of *Amorphophallus* tubers. *Tropical Science*, **38**, pp. 187-9.

Kumar, G.N.M. and Knowles, N.R. (1993) Involvement of auxin in the loss of apical dominance and plant growth potential accompanying aging of potato seed tubers. ***Canadian Journal of Botany***, **71**, pp. 541-50.

Kurihara, H. (1979) Trends and problems of konjac (*Amorphophallus konjac*) cultivation in Japan. *Japan Agricultural Research Quarterly,* **13,** pp. 174-9.

Lee, H.D., Rho, T.H. and Choi, C.Y. (1992) Fertilizer and row-spacing effects on growth and yield of *Amorphophallus konjac* K. *Korean Journal of Crop Science*, **37**, pp. 22-7 [In Korean with English abstract].

Leeds, T. (2010) Obesity: the walking financial time bomb [online]. London: BBC News. [Accessed 10 August 2011]. Available at: <http://news.bbc.co.uk/1/hi/health/8646677.stm>.

Lerouxel, O., Cavalier, D. M., Liepman, A. H. and Keegstra, K. (2006) Biosynthesis of plant cell wall polysaccharides: a complex process. *Current Opinion in Plant Biology,* **9**, pp. 621-30.

Li, B., Xia, J., Wang, Y. and Xie, B.J. (2005) Grain-size effect on the structure and antiobesity activity of konjac flour. *Journal of Agricultural and Food Chemistry*, **53**, pp. 7404-7.

Liepman, A. H., Nairn, C. J., Willats, W. G. T., Sorensen, I., Roberts, A. W. and Keegstra, K. (2007) Functional genomic analysis supports conservation of function among cellulose synthase-like A gene family members and suggests diverse roles of mannans in plants. *Plant Physiology,* **143**, pp. 1881-93.

Lindsay, H. (1973) A colorimetric estimation of reducing sugars in potatoes with 3,5-dinitrosalicylic acid. *Potato Research*, **16**, pp. 176-9.

Liu, P.Y., Lin, Z.S. and Guo, Z.X. (1998) Research and Utilization of *Amorphophallus* in China. *Acta Botanica Yunnanica*, **Suppl. X**, pp. 48-61.

Liu, P.Y., Zhang, S.L., Zhu, G.H., Chen, Y., Ouyang, H.X., Han, M., Wang, Z.F., Xiong, W. and Peng, H.Y. (2002) *Professional standard for the classification, requirements and test methods of konjac flour*; *Technical*

Report NY/T 494 [online]. Sichuan: Chinese Ministry of Agriculture. [Accessed 10 August 2011]. Available at: <http://www.konjacfoods.com/pdf/NY494-cn.pdf>.

Liu, P.Y. (2004) *Konjac*. Beijing: China Agricultural Press [in Chinese].

Lobin, W., Neumann, M., Radscheit, M. and Barthlott, W. (2007) The cultivation of *Titan arum* (*Amorphophallus titanum*) – a flagship species for botanic gardens. *The Journal of Botanic Garden Horticulture*, **5**, 69-86.

Long, C.L. (1998) Ethnobotany of *Amorphophallus* of China. *Acta Botanica Yunnanica*, **Suppl. X**, pp. 89-92.

Maeda, M., Shimahara, H. and Sugiyama, N. (1980) Detailed examination of the branched structure of konjac glucomannan. *Agricultural and Biological Chemistry*, **44**, pp. 245-52.

Maeda, Y., Awano, T., Takabe, K. and Fujita, M. (2000) Immunolocalisation of glucomannans in the cell wall of differentiating tracheids in *Chamaecyparis obtusa*. *Protoplasma*, **213**, pp. 148-56.

Maekaji, K. (1978) Determination of acidic component of konjac mannan. *Agricultural and Biological Chemistry*, **42**, pp. 177-8.

Mariotti, F., Tome, D. and Mirand, P.P. (2008) Converting nitrogen into protein-beyond 6.25 and Jones' factor. *Critical Reviews in Food Science and Nutrition*, **48**, pp. 177-84.

Matheson, N.K. (1990) Mannose-based polysaccharides. in Dey, P.M. (ed.) *Methods in plant biochemistry*, *volume 2, carbohydrates*. London: Academic Press, pp. 371-413.

Matsubara, S. and Ishiguro, J. (1936) Pattern of cormel formation in Japanese taro. *Journal of the Okitsu Horticultural Society*, **32**, pp. 102-5.

Matsuo, T. and Mizuno, T. (1974) Changes in the amounts of two kinds of reserve glucose-containing polysaccharides during germination of the Easter lily bulb. *Plant Cell Physiology*. **15**, pp. 555-8.

Mayo, S.J., Bogner, J. and Boyce, P.C. (1997) *The genera of Araceae*. London: Royal Botanic Gardens, Kew.

McCleary, B.V. (2003) Dietary fibre analysis. *Proceedings of the Nutrition Society*, **62**, pp. 3–9.

Meier, H. and Reid, J.S.G. (1982) Reserve polysaccharides other than starch in higher plants. in Loewus, F.A. and Tanner, W. (eds.) *The encyclopedia of plant physiology*. Berlin: Springer Verlag, Vol. 12A.

Miller, G.L. (1959) Use of dinitrosalicylic acid reagent for determination of reducing sugar. *Analytical Chemistry*, **31**, pp. 426-8.

Miller, W.B. (1992) A review of carbohydrate metabolism in geophytes. *Acta Horticulturae*, **325**, pp. 239-46.

Miura, K. and Osada, A. (1981) Effect of shading on photosynthesis, respiration, leaf area and corm weight in konjac plants (*Amorphophallus konjac* K. Koch). *Japanese Journal of Crop Science*, **50**, pp. 553-9.

Miura, K. and Watanabe, K. (1985) Effect of seed corm age and weight on the efficiency of corm tuberization in konjac plants (*Amorphophallus konjac* K. Koch). *Japanese Journal of Crop Science*, **54**, pp. 1-7 [in Japanese with English abstract].

Miyoshi, E., Takaya, T., Williams, P.A. and Nishinari, K. (1997) Rheological and DSC studies of mixtures of gellan gum and konjac glucomannan. *Macromolecular Symposia*, **120**, pp. 271-80.

Miyoshi, E. and Nishinari, K. (1999) Rheological and thermal properties near the sol–gel transition of gellan gum aqueous solutions. *Progress in Colloid and Polymers Science*, **114**, pp. 68–82.

Mondel, S. and Sen, H. (2004) Seed corm production of elephant foot yam through agronomical manipulation. *Journal of root Crops*, **30**, pp. 115-9.

Moreira, L.R.S. and Filho, E.X.F. (2008) An overview of mannan structure and mannan-degrading enzyme systems. *Applied Microbiology and Biotechnology*, **79**, pp. 165-78.

Morris, E.R. (1989) Polysaccharide solution properties: origin, rheological characterization and implications for food systems. in Millane, R.P., BeMiller, J.N. and Chandrasekaran, R. (eds.) *Frontier in carbohydrate research-1: Food applications*. New York: Elsevier Applied Science, pp. 145-8.

Nishinari, K., Williams, P.A. and Phillips, G.O. (1992) Review of the physico-chemical characteristics and properties of konjac mannan. *Food Hydrocolloids*, **6**, pp. 199-222.

Niwa, T., Etoh, H., Shimizu, A. and Shimizu, Y. (2000) Cis-N-(p-Coumaroyl) serotonin from Konnyaku, *Amorphophallus konjac* K. Koch. *Bioscience, Biotechnology and Biochemistry*, **64**, pp. 2269-71.

Oblonsek, M., Sostar-Turk, S. and Lapasin, R. (2003) Rheological studies of concentrated guar gum. *Rheologica Acta*, **42**, pp. 491-9.

Ogasawara, S., Yamazaki, H. and Nunomura, W. (1987) Electrophoresis on konjac mannan gel. *Seibutsu Butsuri Kagaku*, **31**, pp. 155-8 [in Japanese].

O'Hair, S.K. and Asokan, M.P. (1986) Edible aroids: botany and horticulture. in Janick, J. (ed.) *Horticultural reviews*. Hoboken, New Jersey: John Wiley & Sons, Inc., pp. 43-99.

Ohtsuki, T. (1968) Studies on reserve carbohydrates of flour *Amorphophallus* species with special reference to mannan. *Botanical Magazine Tokyo*, **81**, pp. 119-26.

Onishi, N., Kawamoto, S., Suzuki, H., Santo, H., Aki, T., Shigeta, S., Hashimoto, K., Hide, M. and Ono, K. (2007a) Dietary pulverized konjac glucomannan suppresses scratching behaviour and skin inflammatory immune responses in NC/Nga mice. *International Archives of Allergy and Immunology*, **144**, pp. 95–104.

Onishi, N., Kawamoto, S., Ueda, K., Yamanaka, Y., Katayama, A., Suzuki, H., Aki, T., Hashimoto, K., Hide, M. and Ono, K. (2007b) Dietary pulverized konjac glucomannan prevents the development of allergic rhinitis-like symptoms and IgE response in mice. *Bioscience, Biotechnology and Biochemistry*, **71**, pp. 2551–6.

Panneerselvam, R., Abdul Jaleel, C., Somasundaram, R., Sridharan, R. and Gomathinayagam, M. (2007) Carbohydrate metabolism in *Dioscorea esculenta* (Lour.) Burk. tubers and *Curcuma longa* L. rhizomes during two phases of dormancy. *Colloids and Surfaces B: Biointerfaces*, **59**, pp. 59-66.

Parry, J. (2010) Konjac glucomannan. in Imeson, A. (ed.) *Food stabilisers, thickeners and gelling agents*. Singapore: Blackwell Publishing Ltd., pp. 198-215.

Passam, H.C., Wickham, L.D. and Wilson, L.A. (1982) A note on the relationship between maturity and dormancy in tubers of *Dioscorea alata* L. *Tropical Science*, **24**, pp. 47-51.

Pear, J.P., Kawagoe, Y., Schreckengost, W.E., Delmer, D.P. and Stalker, D.M. (1996) Higher plants contain homologs of the bacterial *celA* genes encoding the catalytic subunit of cellulose synthase. *Proceedings of the National Academy of Sciences of the United States of America*, **93**, pp. 12637-42.

Peng, Y.F. and Zhang, L.N. (2003) Characterization of a polysaccharide protein complex from *Ganoderma tsugae* mycelium by size exclusion chromatography combined with laser light scattering. *Journal of Biochemical and Biophysical Methods*, **56**, pp. 243-52.

Penroj, P., Mitchell, J.R., Hill, S.E. and Ganjanagunchorn, W. (2005) Effect of konjac glucomannan deacetylation on the properties of gels formed from mixtures of kappa carrageenan and konjac glucomannan. *Carbohydrate Polymers*, **59**, pp. 367-76.

Pettolino, F.A., Hoogenraad, N.J., Ferguson, C., Bacic, A., Johnson, E. and Stone, B.A. (2001) A (1,4)-β-mannan-specific monoclonal antibody and its use in the immunocytochemical location of galactomannans. *Planta*, **214**, pp. 235-42.

Preston, R.D. (1968) Plants without cellulose. *Scientific American*, **216**, pp. 102-8.

Prychid, C.J. and Rudall, P. (1999) Calcium oxalate crystals in monocotyledons: a review of their structure and systematics. *Annals of Botany*, **84**, pp. 725-9.

Prychid, C.J., Jabaily, R.S. and Rudall, P.J. (2008) Cellular ultrastructure and crystal development in *Amorphophallus* (Areceae). *Annals of Botany*, **101**, pp. 983-95.

Ratcliffe, I., Williams, P.A., Viebke, C. and Meadows, J. (2005) Physicochemical characterization of konjac glucomannan. *Biomacromolecules*, **6**, pp. 1977–86.

Ravi, V., Ravindran, C.S. and Suja, G. (2009) Growth and productivity of elephant foot yam (*Amorphophallus paeoniifolius* (Dennst. Nicolson); an overview. *Journal of Root Crops*, **35**, pp. 131-42.

Reid, J.S.G. and Bewley, J.D. (1979) A dual role for the endosperm and its galactomannan reserves in the germinative physiology of fenugreek (*Trigonella foenum-graecum* L.) an endospermic legume seed. *Planta*, **147**, pp. 145-50.

Reid, J.S.G. (1985) Cell wall storage carbohydrates in seeds.Biochemistry of the seed "gums" and "hemicelluloses". *Advances in Botanical Research*, **11**, pp. 125-55.

Reid, J.S.G. and Edwards, M.E. (1995) Galactomannans and other cell wall storage polysaccharides in seeds. in Stephen, A.M. (ed.) *Food polysaccharides and their applications*. New York, Basel and Hong Kong: Marcel Dekker, pp. 155-86.

Reiter, W.D. (2008) Biochemical genetics of nucleotide sugar interconversion reactions. *Current Opinion in Plant Biology*, **11**, pp. 236-43.

Reyes, F. and Orellana, A. (2008) Golgi transporters: opening the gate to cell wall polysaccharide biosynthesis. *Current Opinion in Plant Biology*, **11**, pp. 244-51.

Richmond, T.A. and Somerville, C.R. (2000) The Cellulose Synthase Superfamily. *Plant Physiology*, **124**, pp. 495-8.

Robinson, A., Clark, C.J. and Clemens, J. (2000) Using ^{1}H magnetic resonance imaging and complementary analytical techniques to characterize developmental changes in the *Zantedeschia* Spreng. tuber. *Journal of Experimental Botany*, **51**, pp. 2009-20.

Rose, J.K.C. (2003) *The plant cell wall*. Oxford: Blackwell Publishers.

Saha, A.K. and Brewer, C.F. (1994) Determination of the concentrations of oligosaccharides, complex type carbohydrates, and glycoproteins using the phenol-sulfuric acid method. *Carbohydrate Research*, **254**, pp. 157-67.

Samuels, A.L., Rensing, K.H., Douglas, C.J., Mansfield, S.D., Dharmawardhana, D.P. and Ellis, B.E. (2002) Cellular machinery of wood production: differentiation of secondary xylem in *Pinus contorta* var. latifolia. *Planta*, **216**, pp. 72-82.

Santosa, E., Sugiyama, N., Lee, O.N. and Nakata, M. (2006) Arrangement of cormels on the corms of edible *Amorphophallus* species in Indonesia. *Japanese Journal of Tropical Agriculture*, **50**, pp. 92-4.

Scheible, W.R., Eshed, R., Richmond, T., Delmer, D. and Somerville, C. (2001) Modifications of cellulose synthase confer resistance to isoxaben and thiazolidinone herbicides in *Arabidopsis Ixr1* mutants. *Proceeding of National Academy of Sciences of the United States of America*, **98**, pp. 10079-84.

Schröder, R., Nicolas, P., Vincent, S. J. F., Fischer, M., Reymond, S. and Redgwell, R. J. (2001) Purification and characterization of a galactoglucomannan from kiwifruit (*Actinidia deliciosa*). *Carbohydrate Research*, **331**, pp. 291-306.

Sedayu, A., Eurlings, M.C.M., Gravendeel, B. and Hetterscheid, W.L.A. (2010) Morphological character evolution of *Amorphophallus* (Araceae) based on a combined phylogenetic analysis of *trn*L, *rbc*L and *LEAFY* second intron sequences. *Botanical Studies*, **51**, pp. 473-90.

Seifert, G.J. (2004) Nucleotide sugar interconversions and cell wall biosynthesis: how to bring the inside to the outside. *Current Opinion in Plant Science*, **7**, pp. 277-84.

Sims, I.M. and Bacic, A. (1995) Extracellular polysaccharides from suspension-cultures of *Nicotiana plumbaginifolia*. *Phytochemistry*, **38**, pp. 1397-1405.

Seo, G.S., Lee, J.Y., Song, N.H., Sin, B.W. and Lee, H.D. (1988) Effect of shading and mulching materials on the characteristics and yield of elephant foot (*Amorphophallus konjac*). *Research Reports of the Rural Development Administration, Upland and Industrial Crops*, **30**, pp. 74-8 [in Korean with English abstract].

Shi, Y., Tao, Y., Lu, Y. and Fei, X. (1998) Development and structure of mannan granules in corms of *Amorphophallus konjac*. *Journal of Tropical and Subtropical Botany*, **6**, pp. 75-77 [in Chinese].

Shimahara, H., Suzuki, H., Sugiyama, N. and Nishizawa, K. (1975) Isolation and characterization of oligosaccharides from an enzymic hydrolysate of konjac glucomannan. *Agricultural and Biological Chemistry*, **39**, pp. 293-9.

Sood, N., Baker, W.L. and Coleman, C.I. (2008) Effect of glucomannan on plasma lipid and glucose concentrations, body weight and blood pressure: systemic review and meta-analysis. *American Journal of Clinical Nutrition*, **88**, pp. 1167–75.

Sri Prana, M. (1997) Vegetative propagation of giant elephant foot yam (*Amorphophallus titanum* Becc.). *Annales Bogorienses*, **5**, pp. 63-8.

Sugiyama, N., Shimahara, H. and Andoh, T. (1972) Studies on mannan and related compounds. I. The purification of konjac mannan. *Bulletin of the Chemical Society of Japan,* **45**, pp. 561-3.

Sumner, J.B. (1925) A more specific reagent for the determination of sugar in urine. *Journal of Biological Chemistry*, **65**, pp. 393-5.

Sumner, J.B. and Howell, S.F. (1935) A method for determination of saccharase activity. *Journal of Biological Chemistry,* **108**, pp. 51-4.

Sun, Y.M., Liu, P.Y., Liu, C.G., Su, C.G. and Li, Q.M. (1995) Studies of the dormancy of mature konjac corms. *Journal of South West Agricultural University*, **17**, pp. 118-21 [in Chinese].

Sunell, L.A. and Healey, P.L. (1979) Distribution of calcium oxalate crystal idioblasts in corms of taro (*Colocasia esculenta*). *American Journal of Botany*, **66**, pp. 1029-32.

Suzuki, S., Li, L.G., Sun, Y.H. and Chiang, V. L. (2006) The cellulose synthase gene superfamily and biochemical functions of xylem-specific cellulose synthase-like genes in *Populus trichocarpa*. *Plant Physiology*, **142**, pp. 1233-45.

Taiz, L. and Zeiger, E. (2010) *Plant physiology*. 5th ed. Sunderland, Massachusetts: Sinauer Associates.

Takigami, S. and Phillips, G.O. (1996) The production and quality of konjac mannan. in Phillips, G.O., Williams, P.A. and Wedlock, D.J. (eds.) *Gums and Stabilisers*. Oxford: IRL Press, pp. 385-91.

Takigami, S., Takiguchi, T. and Phillips, G.O. (1997) Microscopical studies of the tissue structure of konjac tubers. *Food Hydrocolloids*, **11**, pp. 479–84.

Takigami, S. (2000) Konjac mannan. in Phillips, G.O. and Williams, P.A. (eds.) *Handbook of Hydrocolloids*. Florida: CRC Press, pp. 413-24.

Tekinsen, K.K. and Guner, A. (2010) Chemical composition and physicochemical properties of tubera salep produced from some *Orchidaceae* species. *Food Chemistry*, **121**, pp. 468-71.

U.S. Botanic Garden (2003) *USBG's Titan Arum on Display in 2003* [online]. [Accessed 11 August 2011]. Available at: <http://www.usbg.gov/your-visit/Titan-Day-1.cfm>.

USDA (U.S. Department of Agriculture) (2004) *Dr. Duke's phytochemical and ethnobotanical databases* [online]. [Accessed 23 August 2011]. Available at: <http://www.sugarwise.net/pdf/20070110144717.pdf>.

U.S. Food Chemicals Codex, Food and Nutrition Board (2003) *Food Chemicals Codex*. 5th ed. Washington: U.S. National Academy of Sciences, pp. 238-9.

Vanderbeek, P.B., Fasano, C., O'Malley, G. and Hornstein, J. (2007) Esophageal obstruction from a hygroscopic pharmacobezoar containing glucomannan. *Clinical Toxicology*, **45**, pp. 80-2.

Vasques, C.A.R., Rossetto, S., Halmenschlager, G., Linden, R., Heckler, E., Fernandez, M.S.P. and Alonso, J.L.L. (2008) Evaluation of the pharmacotherapeutic efficacy of *Garcia cambogia* plus *Amorphophallus konjac* for the treatment of obesity. *Phytotheraphy Research*, **22**, pp. 1135-40.

Volk, G.M., Lynch-Holm, V.M., Kostman, T.A., Goss, L.J. and Franceschi, V.R. (2002) The role of druse and raphide calcium oxalate crystals in tissue calcium regulation in *Pistia stratiotes* leaves. *Plant Biology*, **4**, pp. 34-45.

Vuksan, V., Jenkins, D. J. A., Spadafora, P., Sievenpiper, J. L., Owen, R., Vidgen, E., Brighenti, F., Josse, R., Leiter, L. A. and Bruce-Thompson, C. (1999) Konjac-mannan (Glucomannan) improves glycemia and other associated risk factors for coronary heart disease in type 2 diabetes. *Diabetes Care,* **22**, pp. 913-9.

Vuksan, V., Sievenpiper, J. L., Owen, R., Swilley, J. A., SpadaforaA, P., Jenkins, D. J. A., Vidgen, E., Brighenti, F., Josse, R. G., Leiter, L. A., Xu, Z. and Novokmet, R. (2000) Beneficial effects of viscous dietery fiber from konjac-mannan in subjects with the insulin resistance syndrome. *Diabetes Care,* **23**, pp. 9-14.

Vuksan, V., Sievenpiper, J. L., Xu, Z., Wong, E. Y. Y., Jenkins, A. L., Zdravkovic, U. B., Leiter, L. A., Josse, R. G. and Stavro, M. P. (2001) Konjac-mannan and American ginsing: emerging alternative therapies for type 2 diabetes mellitus. *Journal of the American College of Nutrition,* **20**, 370S-380S.

Wakabayashi, S. (1957) Studies on the structure and the formation of mucilage cells in corms of *Amorphophallus konjac*. *Journal of Japanese Botany*, **32**, pp. 337-46 [in Japanese with English abstract].

Wang, C.H., Lai, P., Chen, M.E. and Chen, H.L. (2008) Antioxidative capacity produced by *Bifidobacterium* and *Lactobacillus acidophilus*-mediated fermentations of konjac glucomannan and glucomannan oligosaccharides. *Journal of the Science of Food and Agriculture*, **88**, pp. 1294-300.

Wang, X., Yuan, Y., Wang, K., Zhang, D., Yang, Z. and Xu, P. (2007) Deproteinization of gellan gum produced by *Sphingomonas paucimobilis* ATCC 31461. *Journal of Biotechnology*, **128**, pp. 403-7.

Wang, Y.L. and Liu, P.Y. (1990) Studies of the changes in constituents of konjac corms during growth. *Journal of the South West Agricultural University*, **12**, pp. 471-4 [in Chinese].

Wang, Z.F., Zhang, S.L. and Liu, P.Y. (2001) Study on the method of weighing mannose-hydrazone for determining content of glucomannan in konjac powder. *Food and Fermentation Industries*, **27**, pp. 53-6 [in Chinese].

Wang, Z.Y., Gould, K.S. and Patterson, K.J. (1994) Structure and development of mucilage-crystal idioblasts in the roots of five *Actinidia* species. *International Journal of Plant Science*, **155**, pp. 342-9.

Webb, M.A., Cavaletto, J.M., Carpitan, N.C., Lopez, L.E., Arnott, H.J. (1995) The intravacuolar organic matrix associated with calcium oxalate crystals in leaves of *Vitis*. *Plant Journal*, **7**, pp. 633-48.

WFS (World of Food Science) (2003) *Part II: konjac- a program to help reduce poverty in northern Guangdong, China* [online]. [Accessed 11 August 2011]. Available at: <http://www.worldfoodscience.org/cms/?pid=1003561>.

Wientjes, R.H.W., Duits, M.H.G., Jongschaap, R.J.J. and Mellema, J. (2000) Linear rheology of guar gum solutions. *Macromolecules*, **33**, pp. 9594-605.

Williams, M.A., Foster, T.J., Martin, D.R., Norton, I.T., Yoshimura, M. and Nishinari, K. (2000) A molecular description of the gelation mechanism of konjac mannan. *Biomacromolecules*, **1**, pp. 440-50.

WIPO (World Intellectual Property Organization) (1993) *Clarified konjac glucomannan* [online]. Geneva, Switzerland: WIPO. [Accessed 11 July 2011]. Available at: <http://www.sumobrain.com/patents/wipo/Clarified-konjac-glucomannan/WO1993003047A1.pdf>.

Wootton, A. J., Luker-Brown, M., Westcott, R. J. and Cheetham, P. S. J. (1993) The extraction of a glucomannan polysaccharide from konjac corms (Elephant Yam, *Amorphophallus rivierii*). *Journal of the Science of Food and Agriculture,* **61**, pp. 429-33.

Wu, J.C., Liang, C.J. and Guo, S.Y. (1987) Studies of the extraction, analysis and application of konjac glucomannan. *Food Science*, **3**, pp. 20-2 [in Chinese].

Wu, Y.J., Meng, W.N., Chai, J.T. and Wang, J.F. (2002) Extraction of glucommanan from *Amorphophallus konjac*. *Science and Technology of Food Industry*, **23**, pp. 41-3 [in Chinese].

Xiao, C., Lu, Y. and Zhang, L. (2001) Preparation and physical properties of konjac glucomannan-polyacrylamide blend films. *Journal of Applied Polymer Science*, **81**, pp. 882-8.

Xu, L., Xu, H.H., Huang, T.S., Du, T.F., He, X.R. and Shen, L.H. (2001) *New techniques of cultivation for good agricultural practice (GAP) and*

industrializing development of the Chinese rare-medicinal herbs. Beijing: Xie He Medical University [in Chinese].

Yi, C.Y., Li, J.F., Yu, A.N., Shao, Y., Wang, X.P., Wu, Y.R., Chen, J.Y. and Huang J. J. (2006) Determination of glucommanan content in *Amorphophallus konjac*. *Science and Technology of Food Industry,* **27**, pp. 177-81 [in Chinese].

Yokoi, Y., Kimura, M. and Nomoto, N. (1991) Growth and reproduction of asexual konjac plants (*Amorphophallus konjac* K. Koch) I. Analysis of growth and reproduction of different-aged plants. *The Botanical* Magazine, *Tokyo*, **104**, pp. 145-55.

Yu, H., Huang, Y., Ying, H. and Xiao, C. (2007) Preparation and characterization of a quaternary ammonium derivative of konjac glucomannan. *Carbohydrate Polymers*, **69**, pp. 29-40.

Yunnan Fuyuan Golden Field Agricultural Products Company Ltd. (2008) [online]. [Accessed 11 August 2011]. Available at: <www.jty.cn> [in Chinese].

Zhang, H., Yoshimura, M., Nishinari, K., Williams, M.A.K., Foster, T.J. and Norton, I.T. (2001) Gelation behaviour of konjac glucomannan with different molecular weights. *Biopolymers*, **59**, pp. 38-50.

Zhang, Y.Q., Xie, B.J. and Gan, X. (2005) Advance in the applications of konjac glucomannan and its derivatives. *Carbohydrate Polymers*, **60**, pp. 27–31.

Zhang, Y.Q. (2009) *Responses of shade cultivation to growth and leaf senescence in Amorphophallus konjac*. Ph.D. Thesis, Yunnan Agricultural University, P.R. China [in Chinese].

Zhao J., Zhang D., Srzednicki, G., Kanlayanarat, S. and Borompichaichartkul, C. (2009) A simplified method of purifying konjac glucomannan. *Acta Horticulturae*, **837**, pp. 345-50.

Zhao, J., Zhang, D., Srzednicki, G., Kanlayanarat, S. and Borompichaichartkul, C. (2010) Development of a low-cost two-stage technique for production of low-sulphur purified konjac flour. *International Food Research Journal*, **17**, pp. 1113-24.

Zhong, R., Pena, M.J., Zhou, G.K., Nairn, C.J., Wood-Jones, A., Richardson, E.A., Morrison, W.H., Darvill, A.G., York, W.S. and Ye, Z.H. (2005) *Arabidopsis* fragile fiber8, which encodes a putative glucuronyltransferase, is essential for normal secondary wall synthesis. *Plant Cell*, **17**, pp. 3390–408.

Appendix 1

Megazyme glucomannan assay procedure (K-GLUM 10/04).

Appendix 2

Megazyme glucomannan assay procedure (K-GLUM 08/10).

Appendix 3

Chua, M., Baldwin, T.C., Hocking, T.J. and Chan, K. (2010) Traditional uses and potential health benefits of *Amorphophallus konjac* K. Koch ex N.E.Br. *Journal of Ethnopharmacology*, **128**, pp. 268-78.

Appendix 4

Chua, M., Chan, K., Hocking, T.J., Williams, P.A., Perry, C.J. and Baldwin, T.C. (2012) Methodologies for the extraction and analysis of konjac glucomannan from corms of *Amorphophallus konjac* K. Koch. *Carbohydrate Polymers*, **87**, pp. 2202-10.